Physics and Design of
High intensity circular accelerators

Jie Wei, Alexei Fedotov (BNL)

Yannis Papaphilippou (ESRF)

June 28 – July 2, 2004

Preface

- This is a collection of notes presented at the US Particle Accelerator School at Madison, Wisconsin, in the summer of 2004. The year 2004 class was titled "Spallation Neutron Source II: Ring and Transports" given by J. Wei and Y. Papaphilippou. A large portion of the preparation was based on the year 2001 class titled "Physics and Design of High Intensity Circular Accelerators" given by J. Wei, A. Fedotov, and Y. Papaphilippou.

Course description (2001)

- High-intensity synchrotrons and accumulator rings are essential elements for new-generation accelerator facilities including spallation neutron sources, neutrino factories, and multi-functional applications. This course is to introduce design principle and procedure, beam physics and technology for the high-intensity frontier machines. We will start from the design philosophy and basic functions of the ring and the transport lines, and study machine lattice and optimization, injection and extraction options, and machine aperture determination. We then will emphasize on beam dynamics subjects including space charge, transverse phase space painting, longitudinal beam confinement with single and dual harmonic radio-frequency systems, magnetic nonlinearity and fringe field, and beam collimation. In computer simulation sessions we will study basic tracking and mapping techniques, tune spread and resonance analysis techniques, and statistical accuracy. Finally, we will discuss more advanced topics like transition crossing, intra-beam Coulomb scattering, beam-in-gap cleaning, chromatic and resonance correction, electron cloud effects and instabilities.
- Prerequisites: Accelerator fundamentals or Accelerator physics

Course description (2004)

- The Spallation Neutron Source (SNS) is a new-generation, high-power accelerator complex that delivers a proton beam power above 1 MW for pulsed neutron applications. The complex consists of a H- ion source and front end, a superconducting RF linac, a full-energy accumulator ring, and a mercury target. The SNS accumulator ring and the transport lines are designed to handle a record intensity of 2 x 10^14 protons at a repetition rate of 60 Hz. This course is to introduce design principle and procedure, beam physics and technology for this high-intensity frontier machine. We will start with the design philosophy and the basic layout and functions of the ring and transport lines. Among beam dynamics subjects are machine lattice design and aperture selection, beam loss mechanisms, single-particle topics including kinematic nonlinearity, sextupole effects, magnetic imperfection and nonlinearity, magnet fringe field, resonance analysis, and dynamic apertures, and multi-particle topics including space charge, coupling impedance, instabilities, and electron-cloud effects. Among accelerator system subjects are magnet, power-supply, vacuum, injection, extraction, collimation, RF, and diagnostics. Finally, we will review basic beam commissioning procedures.
- Prerequisites: Accelerator fundamentals or Accelerator physics

Acknowledgements

- It would not have been possible to complete this work without the generous help from the author's colleagues and friends. In particular, the authors would like to thank G. Arduini, R. Baartman, A. Browman, R. Cappi, M. Chanel, W. Chou, A. Fedotov, M. Furman, C. Gardner, I. Gardner, R. Garoby, O. Groebner, I. Hofmann, Y. Irie, S. Ivanov, M. Kinsho, T. Linnecar, H. Ludewig, R. Macek, S. Machida, Y. Mori, M. Pivi, M. Plum, C. Prior, G. Rees, T. Roser, F. Ruggiero, H. Schonauer, E. Shaposhnikova, K. Takayama, P. Thieberger, P. Wanderer, L. Wang, C.M. Warsop, R. Webber, and the SNS team for generously providing information. The authors also would like to thank J. Galambos, H. Hahn, S. Koscielniak, T. Linnecar, R. Ma, Y. Papaphilippou, C. Prior, G. Rees, A. M. Sessler, A. Woodhead, and B. Zotter for carefully reading and correcting the manuscript, and thank A. Aleksandrov, J. Beebe-Wang, M. Blaskiewicz, J. Brodowski, A. Chao, P. Cameron, N. Catalan-Lasheras, E. D. Courant, S. Cousineau, G. Danby, V. Danilov, D. Davino, A. Fedotov, D. Finley, R. Gluckstern, M. Hemmer, S. Henderson, J. Holmes, H. Hseuh, J. Jackson, A. Jain, S. Kim, R. Lambiase, Y. Y. Lee, D. Lowenstein, N. Malitsky, W. Meng, J. Mi, G. Parzen, S. Peggs, D. Raparia, J. Sandberg, K. Schindl, R. Siemann, N. Simos, R. Talman, S. Tepikian, D. Trbojevic, N. Tsoupas, J. Tuozzolo, W. T. Weng, S. Y. Zhang, and F. Zimmermann for many useful discussions. This work was performed under the auspices of the U.S. Department of Energy. The Spallation Neutron Source Project is managed by UT-Battelle, LLC, under contract DE-AC05-00OR22725 for the U.S. Department of Energy. SNS is a partnership of six national laboratories: Argonne, Brookhaven, Jefferson, Lawrence Berkeley, Los Alamos, and Oak Ridge.

Group photo (2004)

Spallation Neutron Source II

Accumulator Ring & Transports

Jie Wei (BNL)

Yannis Papaphilippou (ESRF)

June 28 – July 2, 2004

Course Schedule

	Monday	Tuesday	Wednesday	Thursday	Friday
1	Overview	Lattice Matching	Problem solving 1,2,4,5	Problem solving 8,9,3	Diagnostics
2	Parameters	Tune spread Work point	Injection	RF & Longitudinal dynamics	Commissioning
3	Layout & Function	Field errors Compensation Correction	Extraction	Vacuum & Electron cloud	Problem solving 6,10, (7) Summary
4	Aperture Acceptance	Magnet	Computer lab	Space charge	
5	Beam loss Collimation	Power supply	Computer lab	Impedance & Instability	
	Problems 1,2	Problems 4,5	Problems 3,8,9	Problems 6,10, (7)	

Problem 1

- Two identical, vertically stacked rapid-cycling synchrotrons are housed in the same tunnel. The circumference is 300 m. The proton beams are injected at 400 MeV, and extracted at 2 GeV. The repetition rate is 30 Hz for each ring. The pulse in each ring contains 10^{14} particles. The RF system operates at harmonic h=2, and that the pulse contains two bunches.
  - What is the total output beam power? What is the total average current of the facility?
  - What is the tolerable fractional uncontrolled beam loss in each ring?
  - What is the range of RF frequency swing?
  - The beam gap reserved for extraction kicker rise is a minimum 200 ns. Assuming that the bunch density distribution is parabolic. What is the maximum bunching factor? What is the average and peak current in the ring?

Problem 2

- Let E be the total energy, E_k be the kinetic energy, and p be the momentum. Assume that the deviation in kinetic energy is much smaller than the kinetic energy. Prove that

$$\frac{\Delta E}{E} \approx \beta^2 \frac{\Delta p}{p} \qquad\qquad \frac{\Delta p}{p} \approx \frac{\gamma}{1+\gamma}\frac{\Delta E_k}{E_k}$$

where β and γ are the relativistic factors. For a proton beam of 1 GeV kinetic energy with a +/-1% spread in $\Delta p/p$, how accurate are these relations?

Problem 3

- A ring consists of 4 bending arcs, each a horizontal achromat consisting of 4 identical FODO cells of π/2 phase advance. The dispersion is suppressed. Evaluate the value and location of peak dispersion of the ring in terms of cell length, and compare it with the minimum achievable peak dispersion of a matched FODO cell.
- Repeat this exercise by flipping the polarity or the quadrupoles, i.e. DOFO instead of FODO.
- Replace the dispersion suppression method by the missing-dipole (half-field) scheme. Evaluate the minimum achievable peak dispersion in terms of cell length.
- Compare the advantage and disadvantage of the above three schemes

Problem 4

1) Assume that the betatron phase advance from location s_1 to s_2 is Δμ. Prove that the transfer matrix for (x,x′) can be written as:

$$M(s_2 \mid s_1) = \begin{bmatrix} \sqrt{\dfrac{\beta_2}{\beta_1}}(\cos\Delta\mu + \alpha_1 \sin\Delta\mu) & \sqrt{\beta_1\beta_2}\sin\Delta\mu \\ -\dfrac{1}{\sqrt{\beta_1\beta_2}}\left[(1+\alpha_1\alpha_2)\sin\Delta\mu + (\alpha_2-\alpha_1)\cos\Delta\mu\right] & \sqrt{\dfrac{\beta_1}{\beta_2}}(\cos\Delta\mu - \alpha_2\sin\Delta\mu) \end{bmatrix}$$

2) Using the result of 1), prove that the condition for realizing a closed orbit bump from s_1 to s_3 using three dipole magnets is

$$\frac{\theta_1\sqrt{\beta_1}}{\sin(\Delta\mu_{32})} = \frac{\theta_2\sqrt{\beta_2}}{\sin(\Delta\mu_{13})} = \frac{\theta_3\sqrt{\beta_3}}{\sin(\Delta\mu_{21})}$$

Here, θ_i is the dipole kick at location s_i, $\Delta\mu_{ij}$ is the phase advance between s_i and s_j.

Problem 5

- Prove that in terms of variable $\mu(s) = \int^s \frac{ds'}{\beta(s')}$, the normalized displacement $X \equiv \frac{x}{\sqrt{\beta_x}}$ obeys simply harmonic motion
- With two-stage betatron betatron collimation consisting of a scraper and two collectors, prove that when the conditions

  $$\mu_1 = \cos^{-1}\left(\frac{A}{A+H}\right) \qquad \mu_2 = \pi - \mu_1$$

  are satisfied, minimum number of secondary particles escape the collimation process. Here, the scraper radius A and the collector radius A+H are both defined in terms of the normalized variables
- Express the above phase-advance conditions in terms of the physical apertures

Problem 6

- Consider beam density distribution in the normalized phase space during multi-turn injection. Define $\rho^2 \equiv X^2 + X'^2$ and the quantity $\lambda(\rho)\rho d\rho$ is the number of particle populated within the phase-space circle of radius ρ and width dρ.
  - What is the closed-orbit function with time to realize a uniform distribution in phase space with a constant density $\lambda(\rho)$ within a radius R during a total injection time of $t_{\max}$?
  - Prove that the closed-orbit function to realize a Gaussian distribution

    $$\lambda(\rho) = \frac{2N_0}{\sigma^2}\exp\left(-\frac{\rho^2}{2\sigma^2}\right)$$

    is approximately $X_C(t) = \sqrt{2}\sigma\sqrt{-\ln\left(1 - t/t_{\max}\right)}$

    where the injection is performed during a time $0 < t < t_{\max}$

Problem 7

- Upon multi-turn injection of a beam with emittance ε_i, and Courant-Snyder parameters β_i and α_i, injecting with input beam center $(\bar{x}, \bar{x}')$ relative to instantaneous injection orbit bump. The ring beam emittance is ε, and ring Courant-Snyder parameters β and α at injection.
  - Prove that in the normalized phase space of the ring

$$X \equiv \frac{x}{\sqrt{\beta}} \qquad X' \equiv \frac{dX}{d\mu} = \frac{\alpha x + \beta x'}{\sqrt{\beta}}$$

the injecting beam ellipse becomes upright and the injection position is optimized when

$$\frac{\alpha_i}{\beta_i} = \frac{\alpha}{\beta} = -\frac{\bar{x}'}{\bar{x}}$$

the injecting beam ellipse can be described as

$$\frac{\beta_i}{\beta} X'^2 + \frac{\beta}{\beta_i} X^2 \leq \varepsilon_i$$

Problem 7 (continue)

- Let X_C be the injection closed orbit center relative to ring beam origin in the normalized phase space of the ring. The ring emittance circle corresponding to the injecting beam ellipse can be parameterized as

$$\varepsilon(\theta) = \left(X_C + \sqrt{\frac{\beta_i}{\beta}\varepsilon_i} \cos\theta \right)^2 + \frac{\beta}{\beta_i}\varepsilon_i \sin^2\theta$$

Assume that $\varepsilon_i << \varepsilon$

show that when the condition

$$\frac{\beta_i}{\beta} \approx \left(\frac{\varepsilon_i}{\varepsilon} \right)^{1/3}$$

is satisfied, the injecting beam ellipses will all be contained by the emittance circle $\varepsilon(\theta = 0)$ (i.e. minimum phase-space dilution after injection), while the width of the injecting beam is minimum.

Problem 8

- Prove that for a quadrupole magnet, the magnetic errors that are allowed by the quadrupole symmetry are quadrupole, 12-pole, 20-pole, and so on.

Problem 9

- A C-dipole magnet is designed to operate at a field of 1 T. The magnet has a width of 0.8 m, height 0.6 m. The iron material has a relative permeability of 2500. The gap height is 18 cm. The maximum current is 5000 Amp. How many turns of coil is needed for the top and bottom pole?

Problem 10

- A H^- beam of 1 GeV kinetic energy is transported through an achromat of 90 degree bend before the ring injection. Suppose that the magnetic stripping loss criteria is for the fractional beam loss to be below 10^{-7} per meter. Use the following mean decay path length (in meters in the laboratory frame)

$$\lambda_s = \frac{A_{s1}}{B} \exp \frac{A_{s2}}{\beta\gamma B}, \qquad A_{s1} = (2.47 \pm 0.09) \times 10^{-6} \text{ Tm, and } A_{s2} = 15.0 \pm 0.03 \text{ T}$$

  - Estimate the maximum magnetic field that can be used to transport the beam under the loss criteria
  - The achromat consists of 4 FODO cells, each containing 2 dipoles and 2 quadrupoles. What is the minimum length of the dipole?
  - The beam trajectory has a maximum transverse orbit deviation of 2 cm from the magnet center in the quadrupoles. What is the maximum gradient of the quadrupole that can be used under the loss criteria?
  - Estimate the maximum dipole field when the loss criteria is 10^{-6} per meter instead
  - Estimate the minimum dipole length when the H^- beam is injected at 8 GeV kinetic energy, and the loss criteria is 10^{-5} per meter

Spallation Neutron Source II
Accumulator ring & transports

Overview

Jie Wei (BNL)
Yannis Papaphilippou (ESRF)
June 28 – July 2, 2004

Outline

- What is SNS?
- Comparison of high-power accelerator facilities
  - SNS, J-PARC, ISIS, PSR
- Accumulator vs. Rapid-cycling synchrotrons
- Beam loss, radio-activation, collimation and protection
- Design philosophy
- Rest part of the accelerator facility
  - Ion source, linac, target, instruments
- Challenges and design debates

What is the SNS Project?

- A US Department of Energy user facility under construction
- A US$1.4 billion, 7-year construction project due June 2006
- Collaborated by six national laboratories, built at Oak Ridge
  - Argonne, Brookhaven, Jefferson, Berkeley, Los Alamos, Oak Ridge
- A model for the construction of future US large-scale projects?

The Spallation Neutron Source, currently being built at Oak Ridge National Laboratory, will provide the most intense pulsed neutron beams in the world for scientific research and industrial development. Construction will be completed in 2006.

Layout

- At 1.4 Mega Watt power, it will be ~ 8 times ISIS, RAL (UK) the world's leading pulsed spallation source
- The peak neutron flux will be ~20-100 times ILL reactor (France)
- SNS is a short drive from HFIR, a reactor source with a flux comparable to the ILL

Why a 1 GeV machine costs $1.4B?

- High beam power (> 1 MW, > 1 mA average linac current)
- Pulsed beam structure of high peak intensity (> 10^{14} ppp, ~ 100 A)
- A 1 GeV full-energy, super-conducting linac for H^- beam
  - One-klystron-per-cavity RF control
- Stringent limit on beam loss: < 10^{-4} fractional uncontrolled beam loss
- A mercury target of nuclear facility safety standard
  - Previous nuclear reactor proposal at ORNL ~ $10B
- A green-field start-up with 6 collaborating laboratories

Estimate-at-Complete cost breakdown

WBS	Description	November 2003 Review Baseline ($M)	Net Forecast Changes ($M)	Management EAC ($M)	
1.2	Project Support	75.6	0.3	75.9	
1.3	Front End Systems	20.8	-	20.8	
1.4	Linac Systems	313.2	1.4	314.6	
1.5	Ring and Transfer Systems	141.2	0.9	142.1	
1.6	Target Systems	106.5	1.6	108.1	
1.7	Instrument Systems	63.3	0.0	63.3	
1.8	Conventional Facilities	367.5	9.4	376.9	
1.9	Integrated Controls	59.6	(0.0)	59.6	
BAC		1,147.9	13.5	1,161.4	
Total Contingency		44.8		31.3	21.8%*
	TEC	1,192.7		1,192.7	
	OPC	219.0		219.0	
	TPC	1,411.7		1,411.7	

* based on estimated costs and awards through October 2003

Evolution of the beam-power front

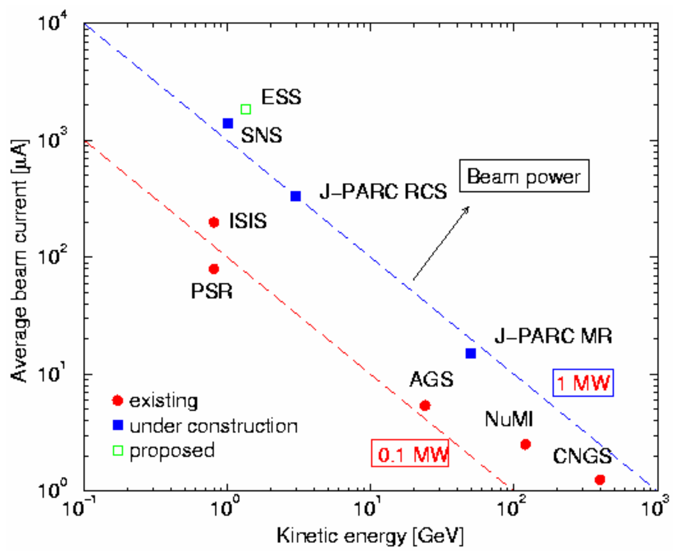

Mega Watt accelerator applications

- Spallation Neutron Sources (SNS; J-PARC; …)
- Accelerator Production of Tritium (APT; TRISPAL; …)
- Nuclear Transmutation (ADTW; ATW; …)
- Energy Amplifier (CERN EA; …)
- Neutrino factory proton driver (J-PARC, BNL, FNAL, CERN/RAL …)
- Muon-collider proton driver (BNL; FNAL; CERN; …)

Mega-Watt project examples

	Energy [GeV]	Current [mA]	Rep.-rate [Hz]	Ave. power [MW]	Type
SNS	1	1.5	60	1.4	AR
J-PARC	3	0.33	25	1	RCS
CERN PD	2	2	100	4	AR
RAL PD	5	0.4	25	2	RCS
FNAL PD	16	0.25	15	2	RCS
EA	1	10 -- 20	CW	10 -- 20	cyclotron
APT	1.03	100	CW	103	linac
TRISPAL	0.6	40	CW	24	linac
ADTW	0.6 – 1.2	20 -- 50	CW	> 20	linac
μ-collider driver	30	0.25	15	7.0	RCS

Spallation Neutron Sources

Machine	Energy [GeV]	Intensity [ppp]	Rep-rate [Hz]	Power ave.[MW]	Type
Existing:					
LANSCE (LANL)	0.8	2.3×10^{13}	20	0.07	AR
ISIS (UK)	0.8	2.5×10^{13}	50	0.2	RCS
Proposed:					
JPARC (Japan)	3.0	8.0×10^{13}	25	1.0	RCS
SNS (US)	1.0	2.1×10^{14}	60	2.0	AR
ESS (Europe)	1.334	2.3×10^{14}	50	2.5	AR

Features of high-power facilities

- Non-pulsed (CW) applications:
  - Use cyclotron or linear accelerator
  - Use proton source
  - Often use superconducting technology
  - Final beam power 10 – 100 MW
- Pulsed applications:
  - Use linear accelerator and ring (synchrotron or accumulator)
  - Use H- source
  - Final beam power 1 – 5 MW

J-PARC schematic layout

Japan Proton Accelerator Research Complex

- Similar cost, similar schedule (due 2006 ~ 2007)
- Ring clusters with expandable energy range; multipurpose

(Courtesy J-PARC)

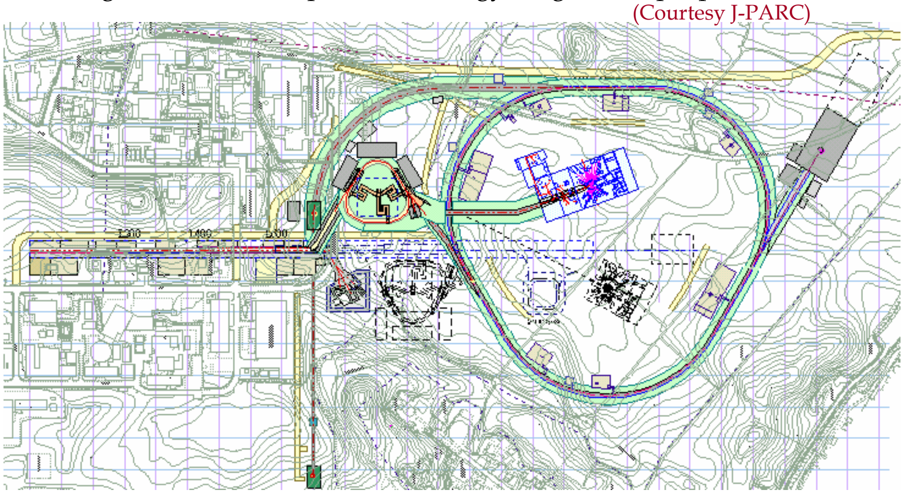

SNS schematic layout

- Built on top of the ridge, only expandable with a 2nd target
- Extra long linac tunnel is reserved for future energy/power upgrade; ring capacity reserved

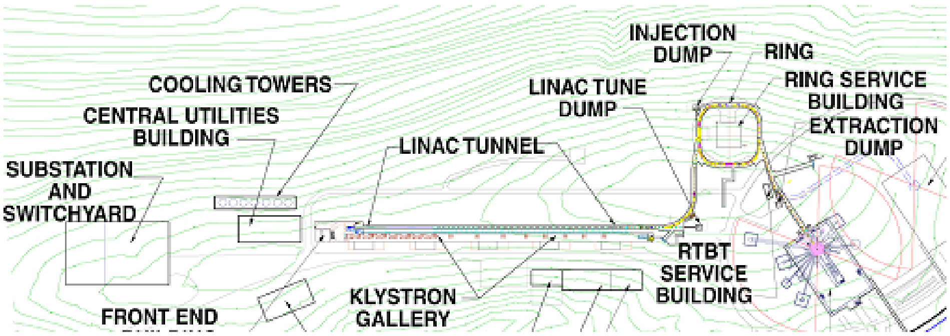

Pulsed Accelerator Options:

- Full energy linac & accumulator ring
  - Simpler ring design, no magnet ramping, better field quality
  - Shorter ring storage time, less instability, lower beam loss
  - Not compatible to energy/power upgrade
  - Longer, more expensive linac
- Low energy linac & rapid cycling synchrotron
  - Easy on energy/power upgrade with additional RCSs
  - Less overall cost for facilities of lower (<1 MW) beam power
  - More RF, higher magnet strength for ring
  - Difficult to control beam loss

SNS versus J-PARC

- SNS:
  - Single-purpose: neutron spallation
  - A long linac for full-energy (1 GeV) acceleration
  - Ring "conservatively" designed and built for success
  - Linac uses superconducting technology
  - Future upgrades: increasing power to 2-4 MW (extending the linac & run the ring at 1.3 GeV) & adding the 2nd target
- J-PARC:
  - Multipurpose: neutron spallation, waste transmutation, high-energy experiments, and neutrino factory
  - A short room-temperature linac (400 MeV)
  - A challenging ring design (rapid-cycling-synchrotron) with many R&D items (high-gradient RF cavity, braided coil …)
  - Flexible energy range (linac 186 MeV, 400 MeV, 600 MeV; Main ring 30 – 50 GeV)

Evolution of ring beam intensity

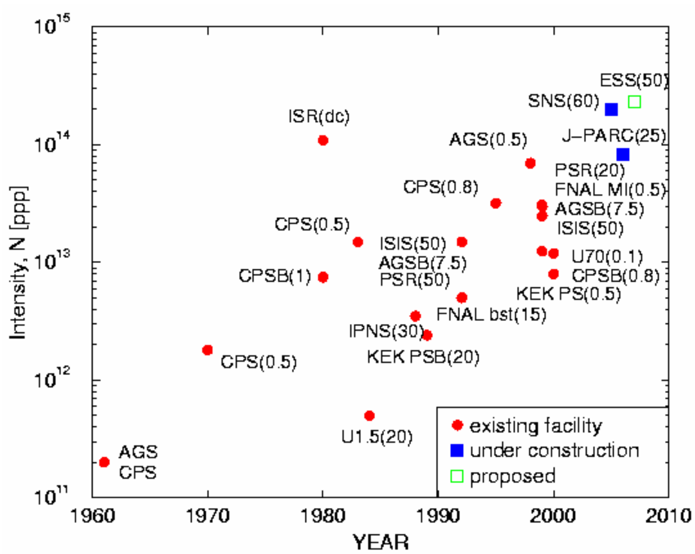

Intensity evolution of BNL AGS

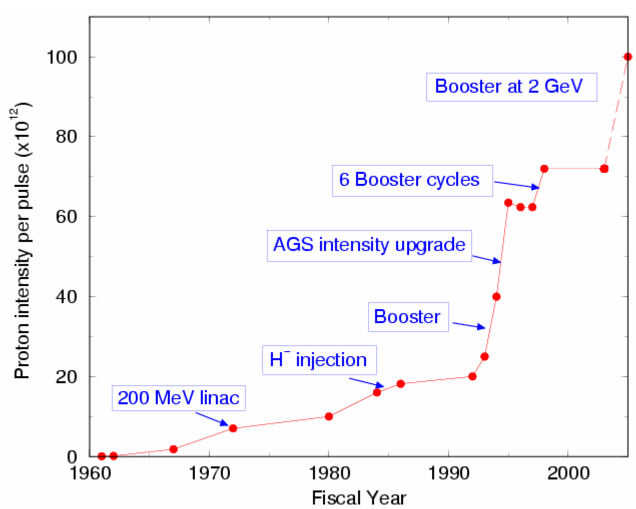

History (what made it possible?)

- 1945 (E.M. McMillan, V.Veksler):
  Synchrotron
- 1950 – 1952 (E.D. Courant, M.S. Livingston, H.S. Snyder, N.C. Christofilos):
  Alternating-Gradient focusing
- Development of intense H^- and H^+ source
- 1970 (I.M. Kapchinskii, V.A. Teplyakov):
  Radio Frequency Quadrupole
- Linac development:
  - Permanent magnet quad for DTL, super-conducting RF, etc.

ISIS at Rutherford Appleton Lab

- 0.16 MW beam power
- 70 – 800 MeV proton
- Typical ~10% beam loss

(C. Warsop's talk)

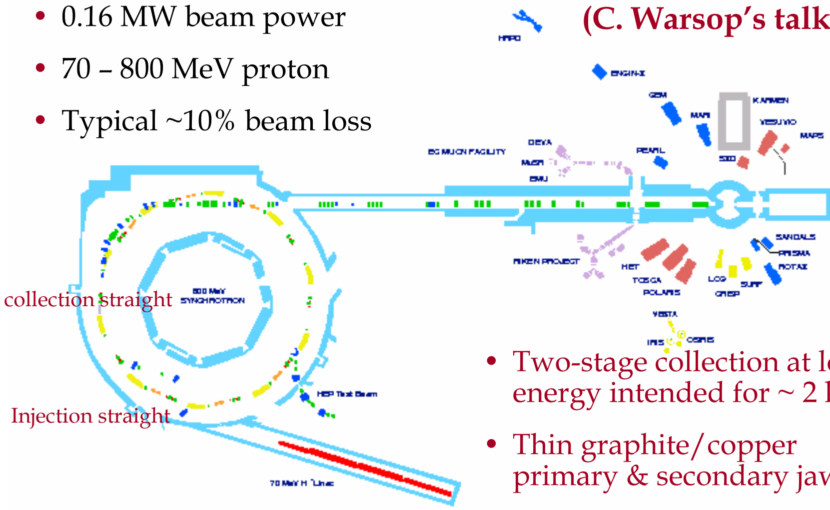

- Two-stage collection at low energy intended for ~ 2 kW
- Thin graphite/copper primary & secondary jaws
- Transverse & momentum

Proton Storage Ring

Shown are the ratios of electron line density (striking the chamber wall) to average proton beam line density, f_e , for 5.5 μC of stored protons

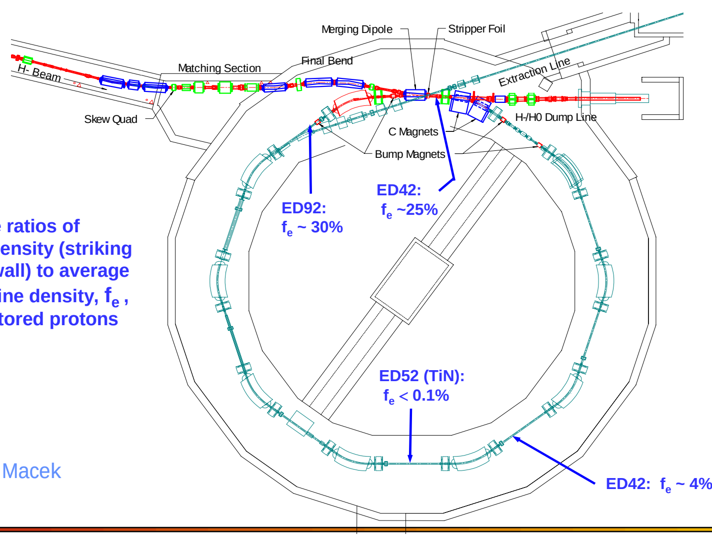

courtesy R. Macek

European Spallation Source

ESS layout courtesy RAL

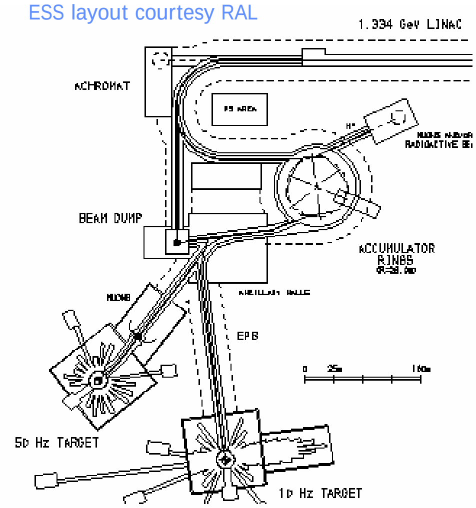

- Linac halo: adjustable foil scraper in HEBT
- Linac energy tail: scraping at high-dispersion location in HEBT
- Linac gap residual: beam-in-gap kicker or momentum collection during initial ramping
- Linac malfunction: scraper in HEBT
- Ring halo: two-stage collimation

Primary concern: *Radio-activation*

- High radio-activation at injection, extraction,collection
  - AGS: up to 10 mSv/hour at localized area
- High beam loss
  - FNAL Booster (15 - 40%): ramp tracking, debunching-recapturing, transition, aperture!
  - AGS/Booster (20 – 30%): pushing record intensity
  - ISIS (~15%): injection capture, initial ramp
  - PSR (0.3% Full energy accumulation): injection loss
- Injection, initial ramping, transition, instability
- 1 – 2 mSv / hour average activation (30 cm, 4h cool)
- 1 – 2 Watt / meter average beam power loss: ~10^{-4} needed

Significance of exposure to radiation

- 1 Sv = 100 Rem
- US occupational limit 5 Rem per year
- DOE laboratory guideline 1.25 Rem per year
- Hands-on maintenance:
  - 100 mrem/hour
  - 50 hours of work per year

Exposure	Significance
3.5 Sv	50% chance of survival
> Sv	Serious to lethal
> 50 mSv	Requiring medical checks
50 $mSv.y^{-1}$	Occupational dose limit
15 – 50 $mSv.y^{-1}$	Strict dose control necessary
5 - 15 $mSv.y^{-1}$	Professional exposure
< 5 $mSv.y^{-1}$	Minimum control necessary
1 $mSv.y^{-1}$	Natural background
10 $\mu Sv.y^{-1}$	Insignificant

SNS expected beam-loss distribution

- Hands-on maintenance: no more than 1 mSv/h (100 mrem/hour) residual activation (4 h cool down, 30 cm from surface)
- 1 Watt/m uncontrolled beam loss
- Less than 10^{-6} fractional beam loss per tunnel meter at 1 MW operation
- Less than 10^{-4} uncontrolled beam loss in the ring

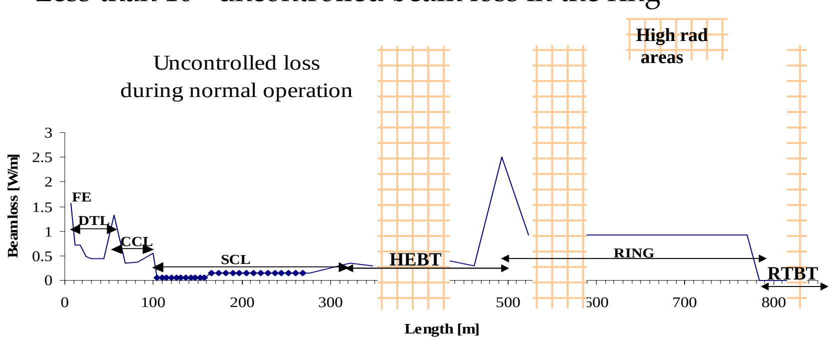

Source of uncontrolled beam loss

- Linac structure & lattice change: mismatches
- Space charge resonances: envelope, parametric halo, non-equipartitioning, tune shift & tune spread
- Physical aperture & momentum aperture limitation: dispersion, injection/extraction channel, chicane perturbation
- Ring injection loss: premature H^- and H^0 stripping, foil hits
- Ring magnet errors: dipole-quad tracking; eddy-current & saturation, fringe field
- Instabilities: envelope, head-tail, microwave, coupled bunch, electron cloud
- Accidental loss: ion source and linac malfunction, extraction kicker failure

Low-loss design philosophy

- Localize beam loss to shielded area
  - 2-stage collimation, 3-step beam-gap chopping/cleaning
- A low-loss design
  - Proper lattice design with adequate aperture & acceptance $A/\varepsilon>2$
  - Injection painting; Injection & space-charge optimization $\Delta Q<0.2$
  - Resonance minimization; Magnet field compensation & correction
  - Impedance & instability control
- Flexibility
  - Adjustable energy, tunes; Flexible injection; Adjustable collimation
  - Foil & spare interchange
- Engineering reliability: heat & radiation resistant
- Accidental prevention: Immune to front end, linac & kicker fault

Beam-loss localization

- "Sacrifice" collimation region for the rest
- Two-stage system, efficiency above 90%
- Needs a large vacuum-pipe aperture and a long straight section

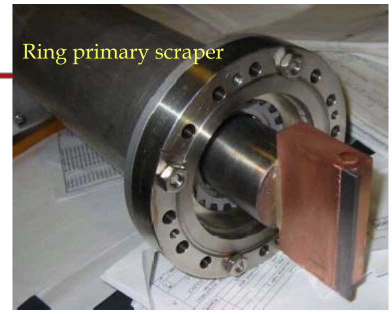

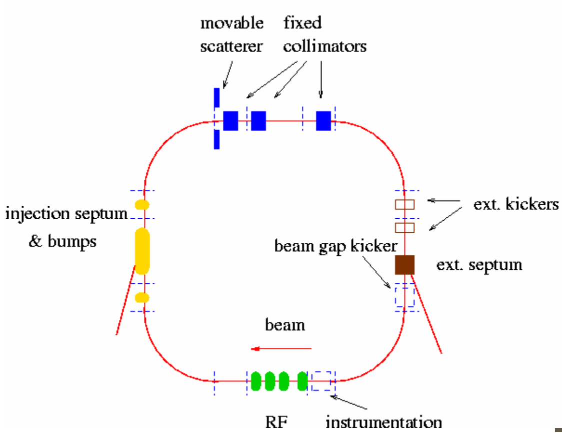

(Courtesy H. Ludewig et al)

Secondary collector design

- Length enough to stop primary protons (~ 1 m for 1 GeV beam)
- Layered structure (stainless steel particle bed in borated water, stainless steel blocks) to shield the secondary (neutron, γ)
- Fixed, enclosing elliptical-shaped wall for operational reliability
- Double-wall Inconel filled with He gas for leak detection

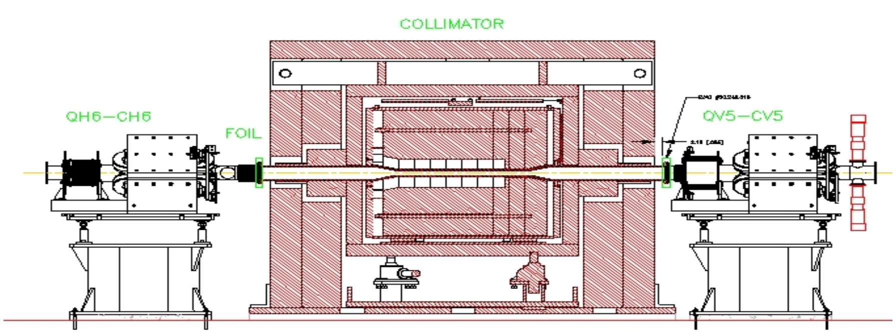

Remote handling

- Overhead, around-the-ring crane
- Quick handling fixtures incorporated into shielding/absorber design
- Remote vacuum clamps; remote water fittings
- Passive dump window & change mechanism

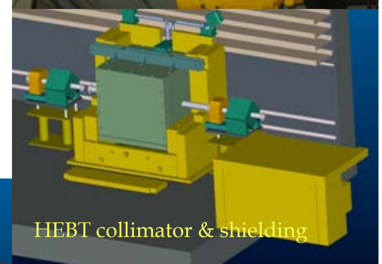

HEBT collimator & shielding

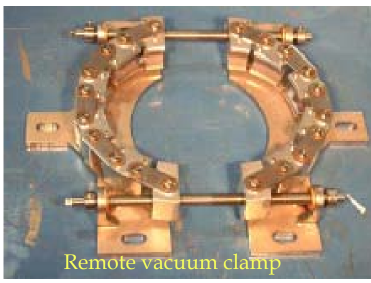

Remote vacuum clamp

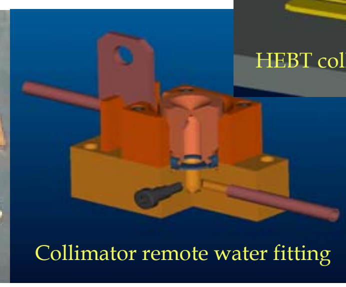

Collimator remote water fitting

(Courtesy G. Murdoch et al)

SNS ion source, LEBT, RFQ, MEBT

- Source/RFQ commissioned at LBL and ORNL
- Beam accelerated to ~ 40 MeV energy in April 2004
- RFQ mysteriously detuned by ~ 400 kHz; re-tuned in 2 weeks with re-machined tuning rods

Parameter	Baseline Design	Achieved
Peak Current	38 mA	40 mA
Pulse Length	1.0 msec	1.0 msec
H^- ions per macropulse	$1.6x10^{14}$ $1.1x10^{13}$ (CD-4)	$1.3x10^{14}$
Emittance	0.3 π μm	~ 0.3 π μm
Duty Factor	6%	4%

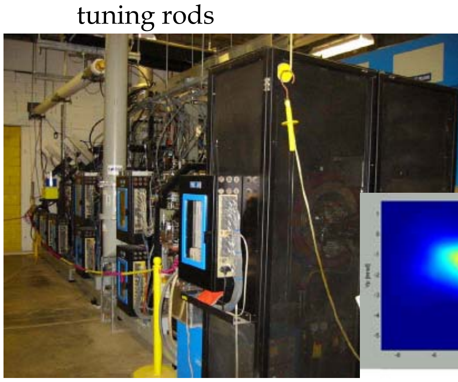

(Courtesy ORNL/LBNL)

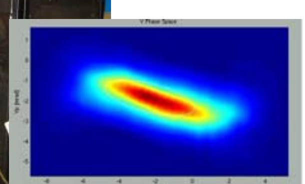

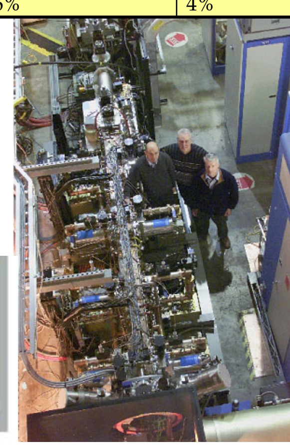

Linac Choice: *Superconducting RF*

- Adopting superconducting RF technology (186 – 1000 MeV)
- 2 types of cavity (β=0.61 and β=0.81) for economic savings & future energy upgrade
- One-cavity-per-klystron independent RF control of Lorentz detuning, microphonics, beam transients, injection offsets
- Motivation: … reliability, flexibility, cost (?), … technology of future

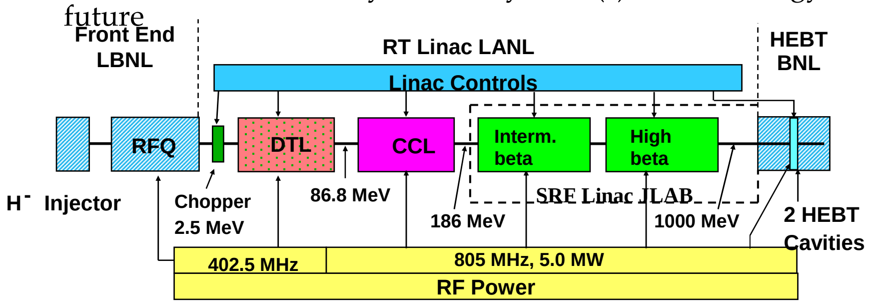

Linac Structure

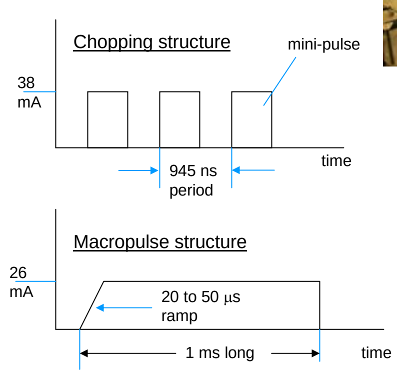

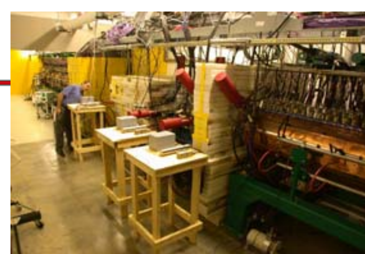

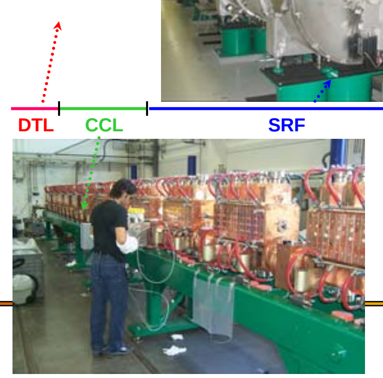

Ring / HEBT

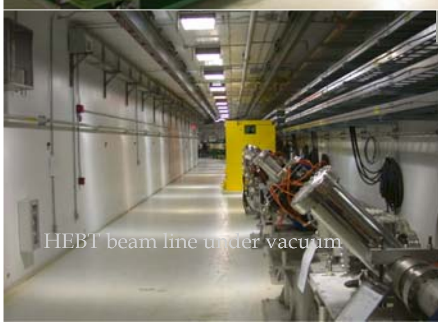

- HEBT beamline partly under vacuum (10^{-9} Torr)
- 26 (total 32) ring arc half cells delivered; all installed in tunnel
- Ring straight section doublet assembly started

Target pitting issue

- Pitting/cavitation on liquid Hg container inner surface due to pulsed energy deposition; strong function of beam power
- Surface treatment (kolstersing) helps
- Further tests at JAERI and ESS

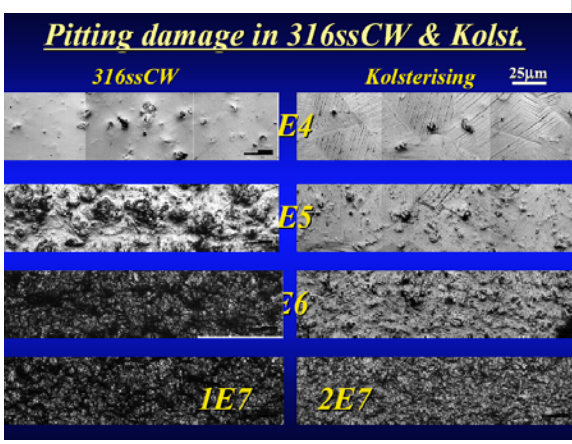

(Courtesy ORNL)

Effective neutron flux

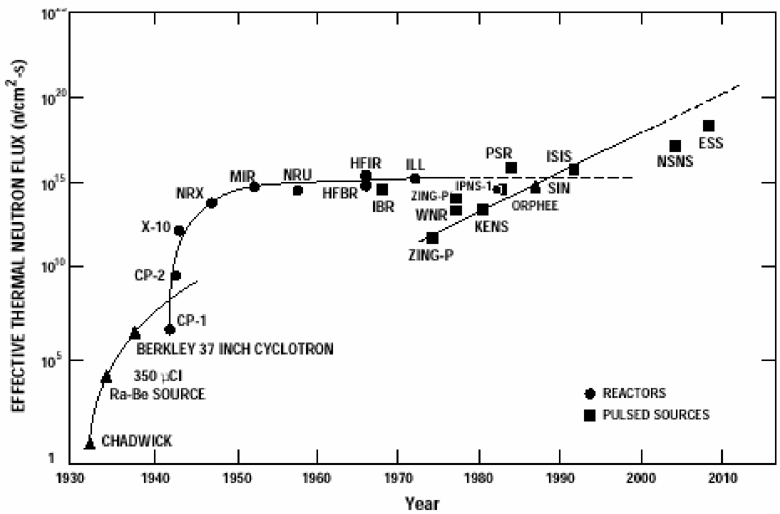

Instruments – Five Funded by the Project

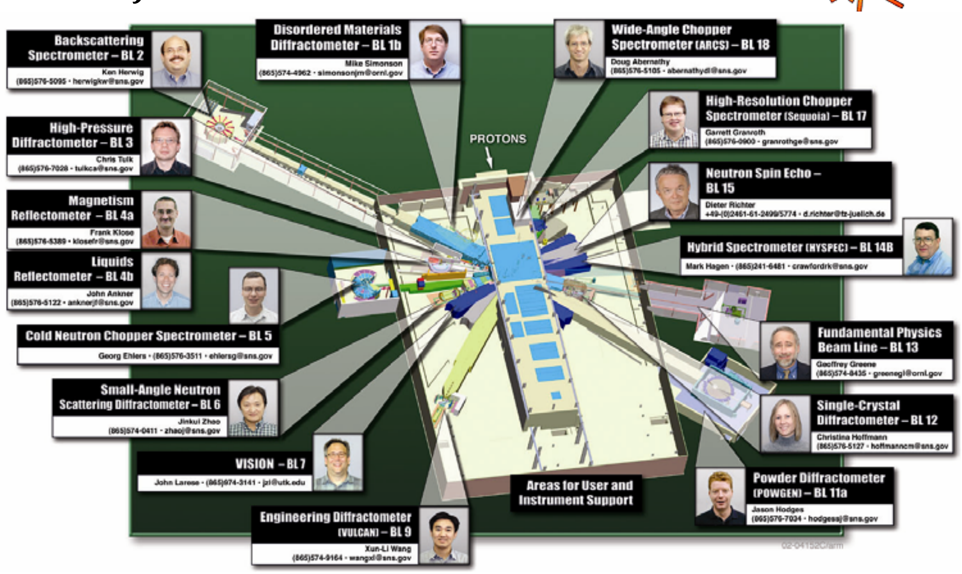

Linac physical challenges

- Output energy within +/- 5% window (H^0 stripping loss)
  - SCL gradient? Extra linac tunnel space as a back-pocket plan
- Transverse emittance and jitter
  - Ring foil miss 1-2%; total emittance growth in linac < (2 x); compared with, e.g., 5 –8 times growth at LANSCE), identified transverse jitter as main issue
- Momentum spread and jitter
  - Facilitate longitudinal painting with a narrow "brush" +/- 0.3%
  - Further correct phase-error at corrector with feed-forward
- Beam-loss, cleaning, diagnostics, machine protection
  - Lower than 1 W/m; adjustable scrapers in med.-energy transport
  - Fast loss monitor as part of machine protection
- RF power & overhead for RF control
  - Active Lorentz-force compensation with piezo tuners

Linac-design debates

- Warm vs. superconducting RF linac?
  - SRF provides higher gradient (11~16 MV/m); tolerable to cavity/klystron failure; better vacuum & reliability
- Linac RF control: how many cavities per klystron?
  - SRF requires careful RF control on injection energy offset, Lorentz detuning, microphonics, beam loading/transient effects
  - One-klystron-per-cavity individual RF control for SNS linac
- How many types of cold cavity?
  - two cavity beta type: flexible for gradient upgrade, but large phase-slip requires detailed error-sensitivity analysis
  - Constant gradient & continuous focusing: maximizing field strength but compromising equipartition law
- How big should be the warm linac bore size (*)?
  - CCL bore diameter reduced from 4 to 3 cm, now aperture bottle-neck due to CCL-to-SCL lattice (FODO to doublet) matching

Ring physical challenges

- Guaranteed beam-density on target
  - Immune to kicker misfiring, protected against malfunctions
- Electron cloud & other instabilities
  - Electron collection & control: electron-cloud generated at injection, collimators, and due to multipacting
  - Impedance from kicker ferrite module in the beam pipe
- Magnet field variation, correction, alignment
  - Field uniformity ~ 10^{-4} for main magnets; shimming needed for solid-core magnets
  - Non-trivial design on C-type, septum to reach 10^{-3}
- Loss control
  - Control of injection field to reduce H- and H0 loss
  - Facilitate two-stage collimation and beam-in-gap cleaning
- Diagnostics: e.g., ionization or luminescence profile monitor?

Ring-design debates

- Accumulator or rapid-cycling synchrotron?
  - Loss-power comparison: PSR loss 0.3%; usual RCS loss ~10%
  - RF, power supply, beam-pipe shielding, magnetic & track errors
- FODO-doublet lattice or all-FODO lattice?
  - Long, matched straight section: injection independent of tuning; collimation efficiency from ~ 80% to 95%
- Do we need sextupoles? Energy corrector & spreaders?
  - Four-family chromatic sextupole for tune-spread control & match
  - Energy correctors & spreaders for longitudinal painting
- Can we use permanent magnets? Certainly not for a cold linac!
- Should the aperture be reduced? No, aperture is everything!
- Solid-core or laminated-core magnets (*)?
  - Large field variation in a solid-core magnet (although lower cost)

Lessons learned

- Permanent-magnet quadrupole in Drift-Tube-Linac
  - Possible lack of tuning capability
  - Complications on the manufacture of drift tubes
- Reduction of Coupled-Cavity-Linac aperture
  - Cost savings: CCL bore diameter reduced from 4 to 3 cm
  - Become an aperture bottle-neck when linac becomes super-conducting (from FODO to doublet lattice)
- Ring solid-steel magnets
  - Instead of laminated steel, solid steel was chosen for cost savings
  - Individual magnet satisfactory
  - Magnetic field varies from magnet to magnet – lack of shuffling
  - A big effort in measuring and shimming these magnets

Spallation Neutron Source II
Accumulator ring & transports

Parameters

Jie Wei (BNL)

Yannis Papaphilippou (ESRF)

June 28 – July 2, 2004

Outline

- Primary parameters
  - Ion species; Kinetic energy
  - Repetition rate
  - Pulse intensity; Bunch length
  - Emittances
- Beam evolution parameters
- Beam loss budget
  - Controlled loss, uncontrolled loss
- Ring system parameters

Major SNS parameters

Proton beam power on target	1.4 MW
Proton beam kinetic energy on target	1.0 GeV
Average beam current on target	1.4 mA
Pulse repetition rate	60 Hz
Protons per pulse on target	1.5×10^{14} protons
Charge per pulse on target	24 μC
Energy per pulse on target	24 kJ
Proton pulse length on target	695 ns
Ion type (Front end, Linac, HEBT)	H minus
Average linac macropulse H- current	26 mA
Linac beam macropulse duty factor	6 %
Front end length	7.5 m
Linac length	331 m
HEBT length	170 m
Ring circumference	248 m
RTBT length	150 m
Ion type (Ring, RTBT, Target)	proton
Ring filling time	1.0 ms
Ring revolution frequency	1.058 MHz
Number of injected turns	1060
Ring filling fraction	68 %
Ring extraction beam gap	250 ns
Maximum uncontrolled beam loss	1 W/m
Target material	Hg
Number of ambient / cold moderators	1/3
Number of neutron beam shutters	18
Initial number of instruments	5

Time structure (before injection)

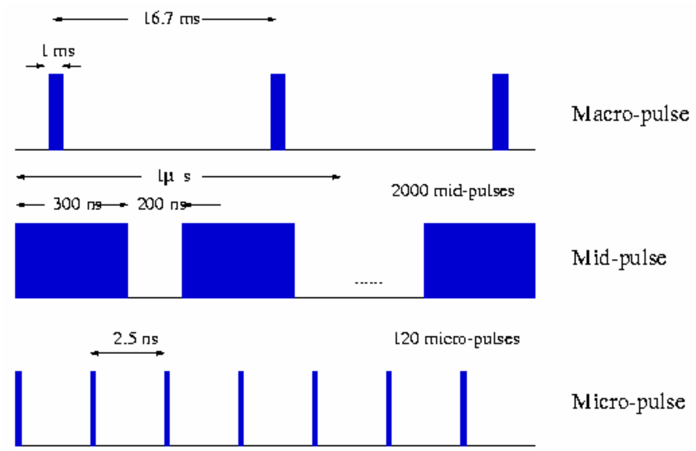

Time structure (after extraction)

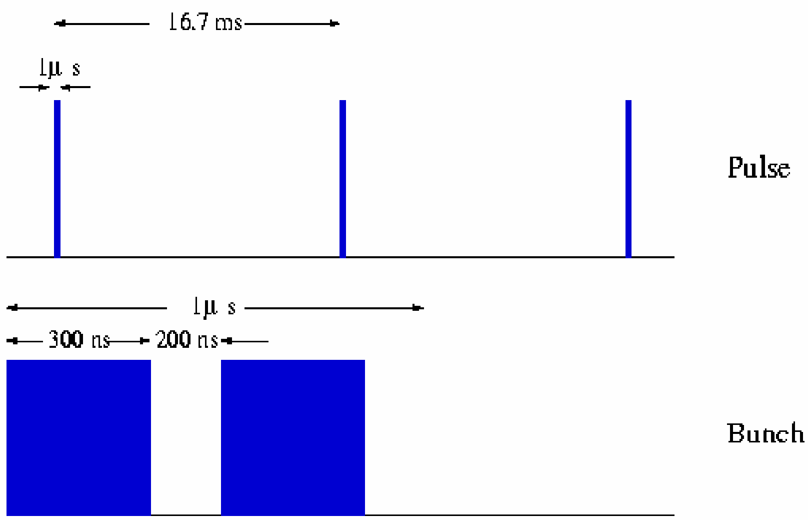

Beam power

- Characterizing the "power" of a high-intensity accelerator

$$\langle P \rangle = E_k \langle I \rangle$$

energy & average current

- Average current of "facility"

$$\langle I \rangle = f_N N_p e$$

  - Repetition rate
  - Number of particles per pulse
- Raise energy, increase repetition rate, increase pulse intensity

Key specs: power, energy, current

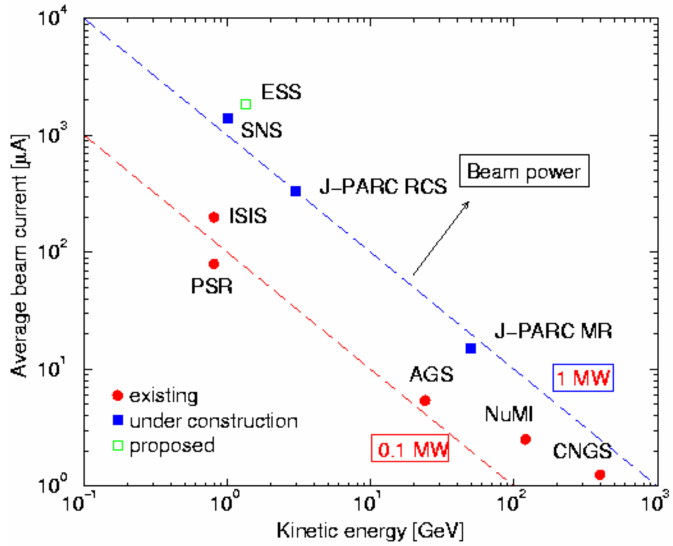

Ion species

- H^- ion in comparison with proton beam
  - Allows multi-turn accumulation to enhance pulse intensity
  - Controls beam profile
  - Demands a powerful H^- ion source
  - Complication with electron stripping under gas scattering and under magnetic field
    - » Gas scattering: requiring relatively high vacuum
    - » Magnetic stripping: limits maximum magnetic field
- Proton beam is usually used for high-intensity dc applications in the absence of rings

Kinetic energy

- Range largely determined by applications & experiments
  - E.g. 0.8 – 5 GeV for neutron spallation
- Within a given range, a higher output energy implies
  - a higher output beam power, relatively "cheap" to achieve for a RCS (linearly proportional)
  - alleviated heating on target due to longer stopping length
  - higher magnet field, higher ramping power, more difficult field quality control
- A higher injection energy implies
  - reduced space-charge effects due to electro-magnetic force cancellation
  - more probably magnetic stripping demanding lower field, longer magnet, more injection space
  - higher cost of the injector accelerator

Repetition rate

- Proportional to output beam power - as high as possible
- Rapid-Cycling Synchrotrons: crucial & demanding
  - Demands a strong power supply
  - Demands a high radio-frequency (RF) voltage
  - Demands RF shielding to avoid heating on vacuum chamber while allowing image charge to circulate (impedance control)
  - Demands lamination to avoid heating in magnets
- Accumulators: less demanding
  - More demanding on the pre-injector (ion source output, linac klystron power …)
  - Injection and extraction kicker power supply (shorter charging period)
  - RF power load and beam loading

Pulse intensity

- Proportional to output beam power – as high as possible
- Usually limited by space charge constraints, instability threshold, instability growth
- Ring average current $\bar{I} = Nef_s$
- Ring peak current $\hat{I}$

  parabolic: $\hat{I} = \frac{3\pi}{2\hat{\phi}}\bar{I}$ Gaussian: $\hat{I} = \frac{1}{\sqrt{2\pi}\sigma_\phi}\bar{I}$
- Bunching factor

$$B = \bar{I}/\hat{I} \leq 1$$

  parabolic: $B = \frac{C - L_{gap}}{C}\frac{2}{3}$ Gaussian: $B \approx \frac{\sqrt{2\pi}}{6} \approx 0.42$

  Empirically: ~0.5 (accumulator); ~0.35 (RCS)

Bunch length

- Range largely determined by applications & experiments
  - E.g. ~ 1 ns for neutrino factory proton drivers
- Beam gap needed for beam extraction; maintained by the RF system
  - For low harmonic number: control bunch area/bucket area ratio
  - For high harmonic number: missing bunches
- Choice of RF harmonic number
  - Hardware availability at a particular RF frequency
  - Consideration of possible coupled-bunch instability
  - Needs for beam-gap cleaning

Emittances

- Transverse emittance

  constant of acceleration: $\oint x dp_x \qquad p_x \sim \beta\gamma x'$

  – Preservation of normalized emittance often needed for downstream applications; damping usually not practical
  – Controlled emittance enlargement is sometimes used to alleviate space-charge effects; constraints from magnet aperture and power supply

- Longitudinal emittance

  constant of acceleration: $\oint \phi dW \qquad W \equiv \frac{\Delta E}{h\omega_s}; \quad \frac{\Delta E}{E} = \beta^2 \frac{\Delta p}{p}$

  – Often limited by the available momentum acceptance

SNS beam evolution parameters

	Front End			Linac					Ring		
	IS/LEBT	RFQ	MEBT	DTL	CCL	SCL (1)	SCL (2)	HEBT	Ring	RTBT	Unit
Output Energy	0.065	2.5	2.5	86.8	185.6	391.4	1000	1000	1000	1000	MeV
Relativistic factor β	0.0118	0.0728	0.0728	0.4026	0.5503	0.7084	0.875	0.875	0.875	0.875	
Relativistic factor γ	1.00007	1.0027	1.0027	1.0924	1.1977	1.4167	2.066	2.066	2.066	2.066	
Peak current	47	38	38	38	38	38	38	38	9×10^4	9×10^4	mA
Minimum horizontal acceptance			250	38	19	57	50	26	480	480	πmm mr
Output H emittance (unnorm., rms)	17	2.9	3.7	0.75	0.59	0.41	0.23	0.26	24	24	πmm mr
Minimum vertical acceptance			51	42	18	55	39	26	480	400	πmm mr
Output V emittance (unnorm., rms)	17	2.9	3.7	0.75	0.59	0.41	0.23	0.26	24	24	πmm mr
Minimum longitudinal acceptance			4.7E-05	2.4E-05	7.4E-05	7.2E-05	1.8E-04		19/π		πeVs
Output longitudinal rms emittance		7.6E-07	1.0E-06	1.2E-06	1.4E-06	1.7E-06	2.3E-06		2/π		πeVs
Controlled beam loss; expected	0.05[a]	N/A	0.2[b]	N/A	N/A	N/A	N/A	5[c]	62[d]	58[e]	kW
uncontrolled beam loss; expected	70	100[f]	2	1	1	0.2	0.2	<1	1	<1	W/m
Output H emittance (norm., rms)	0.2	0.21	0.27	0.33	0.39	0.41	0.41	0.46	44	44	πmm mr
Output V emittance (norm., rms)	0.2	0.21	0.27	0.33	0.39	0.41	0.41	0.46	44	44	πmm mr

Note a) corresponding to 27% chopped beam
b) corresponding to 5% chopped beam
c) beam loss on the transverse and momentum collimators
d) including total 4% of beam escaping foil and 0.2% beam loss on collimators
e) including 4% beam scattered on the target window
f) corresponding to 20% beam loss averaged over RFQ length

Ring primary parameters

Ring circumference	248.0 m
HEBT, RTBT length	169, 151 m
Proton beam energy	1 GeV
Average beam power	1.5 MW
Repetition rate	60 Hz
Number of protons per pulse	1.6×10^{14}
Peak RF voltage ($h = 1, 2$)	(40, 20) kV
No. of RF station (ring, HEBT, RTBT)	4, 2, 0
Unnorm. emittance ($\epsilon_x + \epsilon_y$, 99%)	240 $\pi\mu$m
Betatron acceptance	480 $\pi\mu$m
RF momentum acceptance	$\pm$ 1 %
Transverse tunes (ν_x, ν_y)	6.23, 6.20
Transition energy, γ_T	5.23
No. of lattice super-periods	4
No. of dipole (ring, HEBT, RTBT)	39, 9, 1
Ring dipole field	0.7406 T
Ring dipole gap height	170 mm
No. of quad (ring, HEBT, RTBT)	53, 40, 32
Ring quad inner diameter	210-300 mm
No. of sextupole (ring, HEBT, RTBT)	20, 0, 0
Sextupole inner diameter	210-260 mm
No. of corrector (ring, HEBT, RTBT)	61, 18, 17
No. of kicker (injection, extraction)	8, 14
No. of scraper (ring, HEBT, RTBT)	4, 5, 0
No. of absorber (ring, HEBT, RTBT)	3, 3, 2
No. of vacuum pumps (ring, HEBT, RTBT)	50, 18, 12
No. of power supply (ring, HEBT, RTBT)	156, 48, 47
No. of BPM (ring, HEBT, RTBT)	44, 37, 17
No. of loss monitor (ring, HEBT, RTBT)	82, 62, 43
No. of current monitor (ring, HEBT, RTBT)	2, 5, 5
No. of profile monitor (ring, HEBT, RTBT)	4, 13, 8
Vacuum pressure (ring, HEBT, RTBT $\times 10^{-8}$)	5, 1, 10 Torr

- Major systems
  - Magnet
  - Power supply
  - Injection
  - Radio-frequency system
  - Collimation
  - Extraction
  - Vacuum
  - Diagnostics
  - Controls
  - Infrastructure

Controlled beam loss

Mechanism	Location	Fraction	Power
HEBT:			
H^0 from linac	linac dump	10^{-5}	20 W
linac transverse tail	HEBT H/V-collimator	10^{-3}	2 kW
energy jitter/spread from linac	HEBT L-collimator	10^{-3}	2 kW
Ring:			
beam-in-gap	BIG kicker/collimator	10^{-4}	200 W
excited H^0 at foil	collimator	1.3×10^{-5}	26 W
partial ionization at foil	injection dump	10^{-2}	20 kW
foil miss	injection dump	10^{-2}	20 kW
ring beam halo	collimator	1.9×10^{-3}	3.8 kW
energy straggling at foil	collimator	3×10^{-6}	6 W
RTBT:			
kicker misfiring	RTBT collimator	10^{-5}	20 W

SNS beam dump, collimator, target

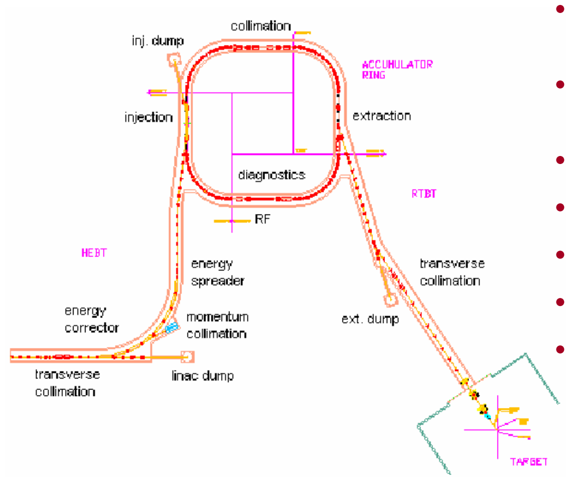

- Linac dump: 7.5 kW
- HEBT momentum dump: ~ 7.5 kW
- HEBT transverse collimator: ~ 2 kW x 2
- Injection dump: 200 kW
- Ring collimator: ~ 2 kW x 3
- Extraction dump: 7.5 kW
- RTBT collimator: ~ 2 kW x 2
- Target: ~ 2 MW

Linac beam dump

Beam stop	steel
Shielding	Fe alloy
Cooling	passive
Maximum	$\leq$ 7.5 kW
Operational	500 h
Maximum	60 mm
beam beam	
Pulse peak	2.3×10^{14} ppp/m^2
density at 60	
Pulse peak	1.4×10^{16} ppp/m^2

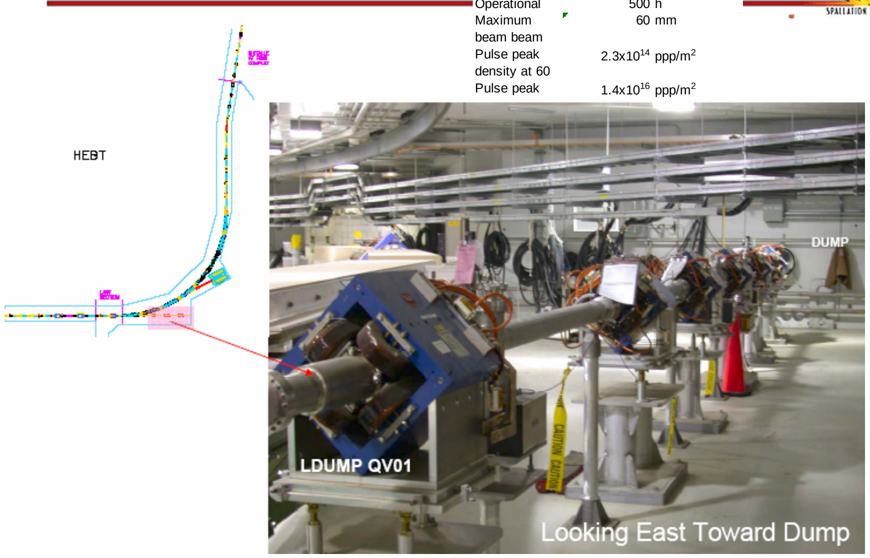

HEBT momentum dump

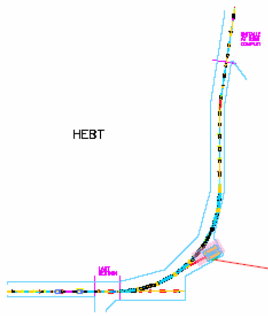

HEBT – Momentum Dump Installed

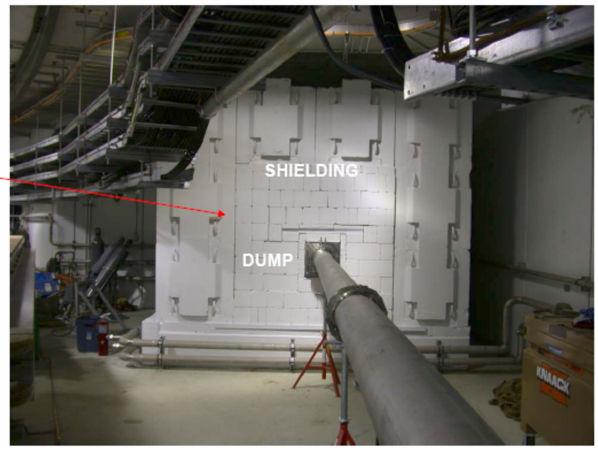

Injection, extraction dump

RING INJECTION DUMP	
Beam stop material	Cu
Shielding material	Fe alloy
Cooling mechanism	forced light water
Maximum power	200 kW
Operational hours per year	5000 h
Maximum beam radius	100 mm
Pulse peak density	5.0×10^{15} ppp/m^2
RING EXTRACTION DUMP	
Beam stop material	steel
Shielding material	Fe alloy
Cooling mechanism	passive
Maximum power	$\leq$ 7.5 kW
Operational hours per year	500 h
Maximum beam radius	100 mm
Pulse peak density at 60 Hz	3.8×10^{13} ppp/m^2
Pulse peak density at 1 Hz	2.3×10^{15} ppp/m^2

HEBT transverse collimator & shielding

HEBT – Betatron Collimators Installed

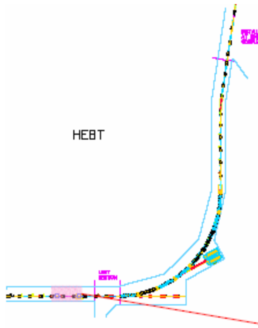

RTBT collimators

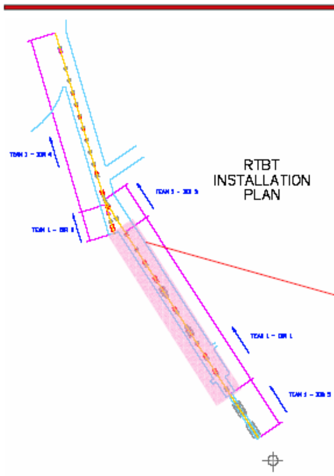

Component Staging
In RTBT

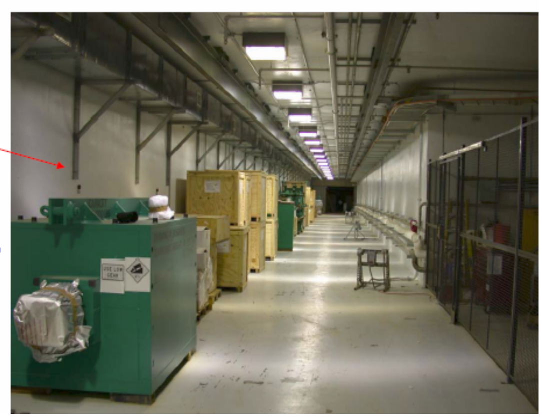

Target

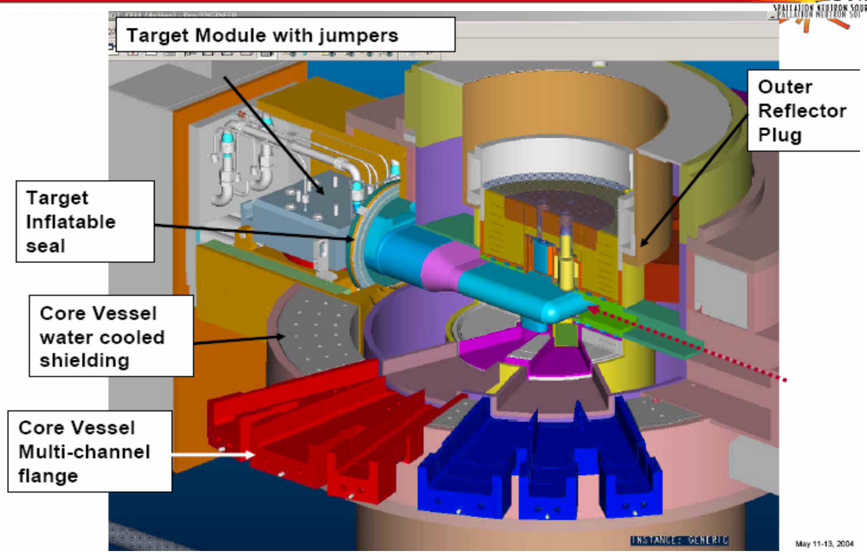

Uncontrolled beam loss

Mechanism	Location	Fraction	Length [m]	Power [W/m]
HEBT:				
H^- magnetic stripping	all HEBT	1.7×10^{-6}	169	0.02
collimator out-scattering	HEBT achromat	7.5×10^{-6}	15	0.1
Ring:				
H^- magnetic stripping	injection dipole	1.3×10^{-7}	1	0.3
nuclear scattering at foil	foil	3.7×10^{-5}	30	2.5
collimation inefficiency	all ring	10^{-4}	218	0.9
RTBT:				
nuclear scattering at window	target window	4×10^{-2}	–	

Spallation Neutron Source II

Accumulator ring & transports

Layout

Jie Wei (BNL)

Yannis Papaphilippou (ESRF)

June 28 – July 2, 2004

Outline

- HEBT layout & function
  - Creation of dispersion region
- Ring layout & function
  - Lattice super-periodicity
  - Dispersive versus non-dispersive injection
- RTBT layout & function

Layout (Frozen Since Aug. 2000)

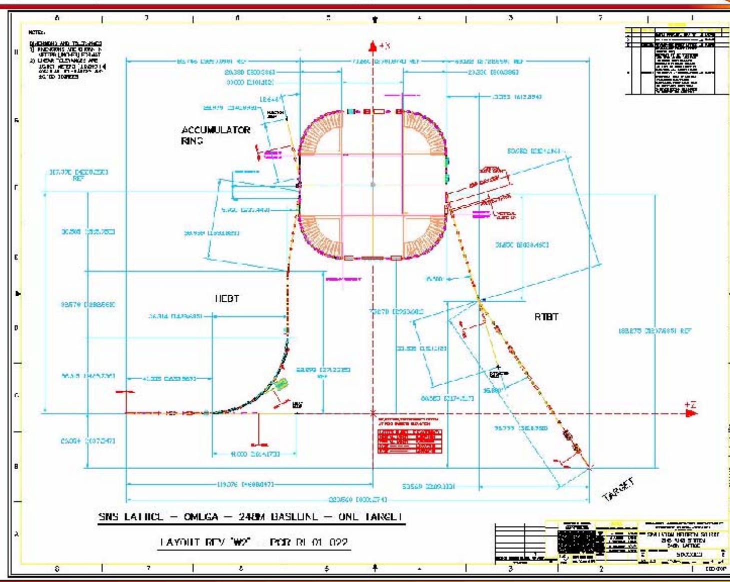

May 7–9, 2002

Geometrical layout guideline

- HEBT
  - Need a high dispersion region for momentum cleaning; created by a bend made of dipole magnets
    - » SNS: 90 degree bend; ESS: 180 degree bend; J-PARC, long debated whether momentum cleaning must be done
  - Need adequate space to prepare beam for ring injection
- Ring
  - Clean geometry; minimize beamline crossing
    - » Design iteration from α to Ω
  - Choice of lattice periodicity
    - » 3 versus 4; separate collimation from injection?
    - » Whether injecting at dispersive region
- RTBT
  - Adequate space to protect the accelerator from target back-shine
  - Geometrically link the accelerator to target(s)

HEBT function

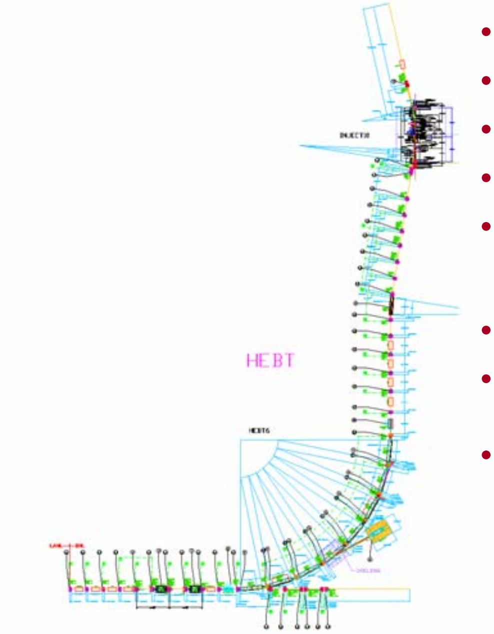

- Match beam from linac
- Diagnose linac beam
- Clean transverse halo
- Reduce linac energy jitter
- Separate linac and ring operation (first dipole a critical device)
- Clean energy tail / halo
- Paint longitudinal phase space by energy painting
- Match beam to ring for zero-dispersion injection

General HEBT/RTBT function

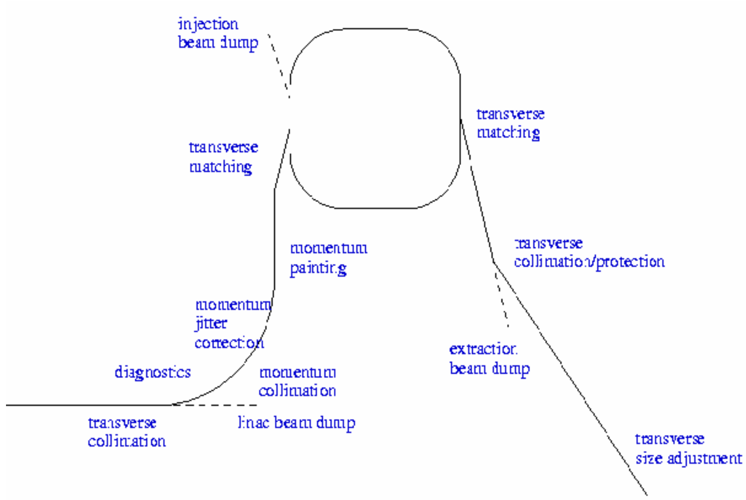

HEBT Beam Instrumentation

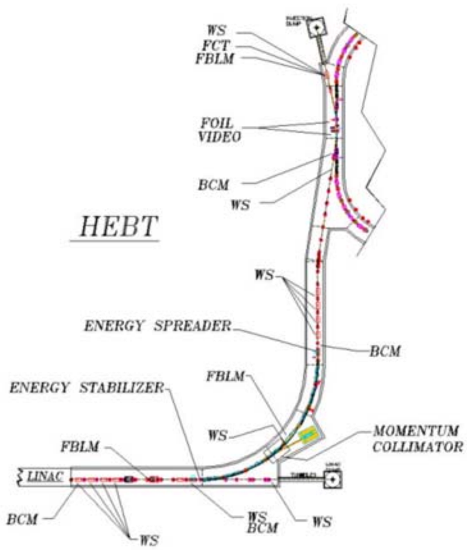

Detectors	BNL	LANL
BPM	36	IFEs
BLM	52	0
FBLM	3	0
BCM	5	0
WS	13	13
Foil Video	3	0

Ring lattice evolution

- From α to Ω (October 1999):
  - ease maintenance
- From all-FODO to hybrid:
  - 50% increase in acceptance
  - uninterrupted straight length increase: from 5.2 m to 12.5 m
  - collimation efficiency increase: from 80% to 95%
  - injection decoupled from tuning
- Ring size increase (March 2000)
  - from 221 to 248 m circumference
  - improved maintainability
  - lower FE peak current, less foil loss
  - compatible with 1.3 GeV (SC linac)

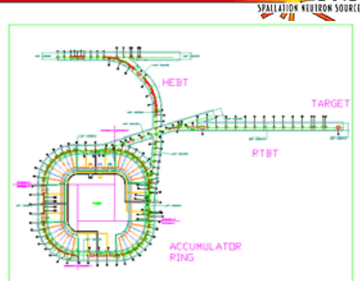

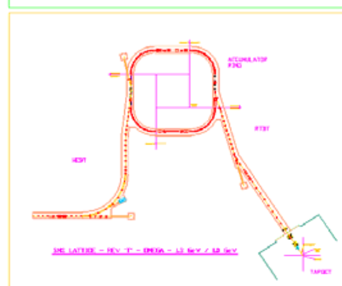

European Spallation Source

ESS layout courtesy RAL

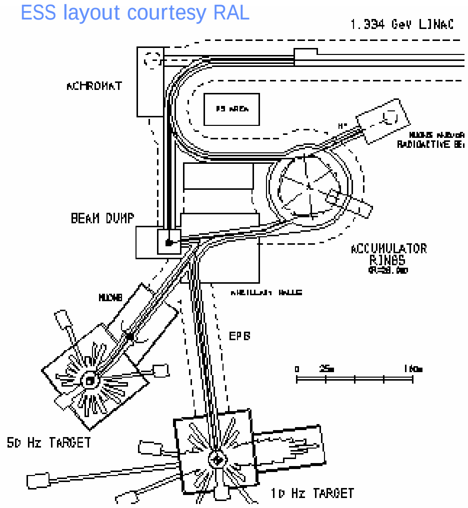

- Linac halo: adjustable foil scraper in HEBT
- Linac energy tail: scraping at high-dispersion location in HEBT
- Linac gap residual: beam-in-gap kicker or momentum collection during initial ramping
- Linac malfunction: scraper in HEBT
- Ring halo: two-stage collimation

Ring: fixed-energy, hybrid lattice

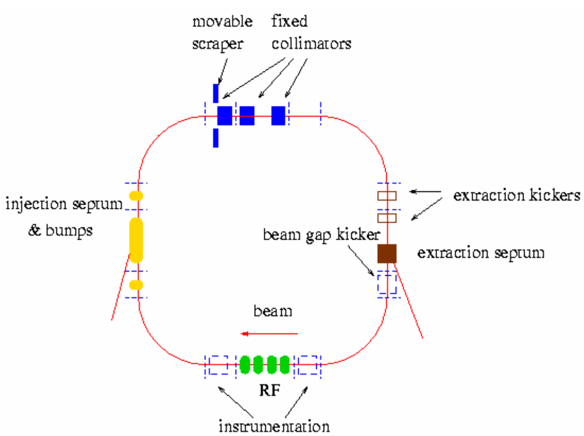

- No energy ramping
- Long straight-section, large aperture
  - Injection flexibility
  - Collimation efficiency
- Four straight-sections for four functions
  - Injection;
  - RF;
  - Collimation;
  - Extraction
  - Diagnostics all-around
- Dispersion-free injection
  - Decoupled H, V, L

J-PARC layout

Japan Proton Accelerator Research Complex

- Similar cost, similar schedule (due 2006 ~ 2007)
- Ring clusters with expandable energy range; multipurpose

(Courtesy J-PARC)

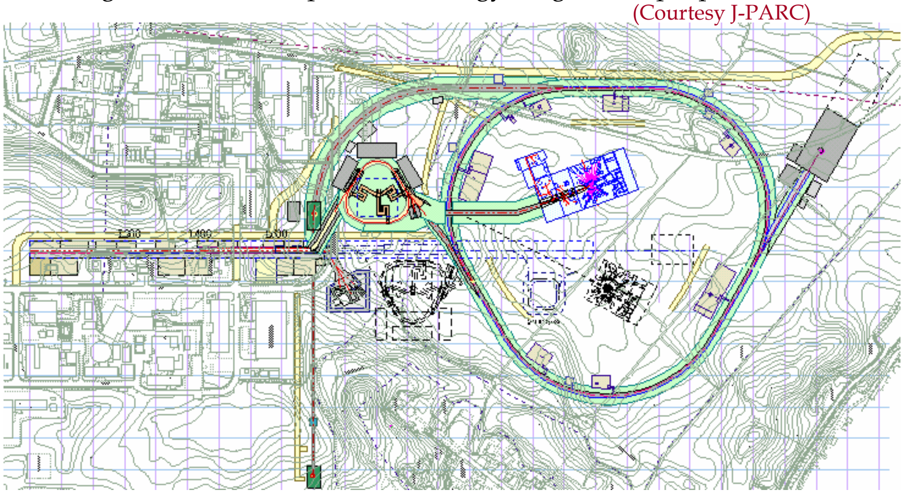

ESS ring layout

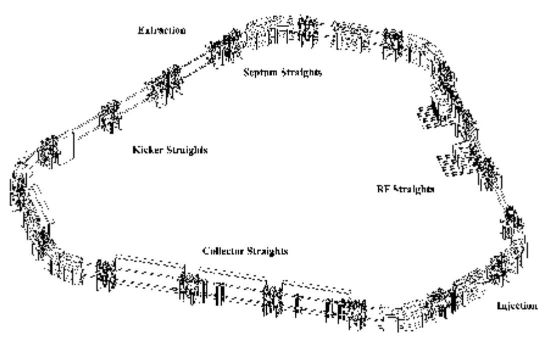

FIG. 6 Schematic layout of the proposed European Spallation Source ring. The ESS accelerator complex consists of two H^- ion sources, a 1.334 GeV linac, and two accumulator rings along with their transport lines. The rings are vertically stacked to achieve a combined 5 MW beam power (Section I, courtesy ESS Council).

A possible RCS ring layout

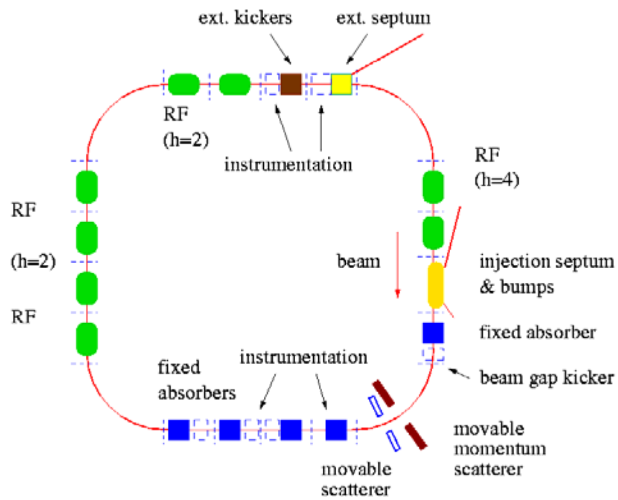

Ring lattice
FODO arcs & doublet straights

- Matched, hybrid lattice
  - FODO arc:
    easy-to-implement correction system, moderate magnet strength
  - Doublet straight:
    long, uninterrupted straight
    - » Improved collimation efficiency
    - » Robust injection
- Zero-dispersion injection
  - Independent painting in the transverse & longitudinal directions

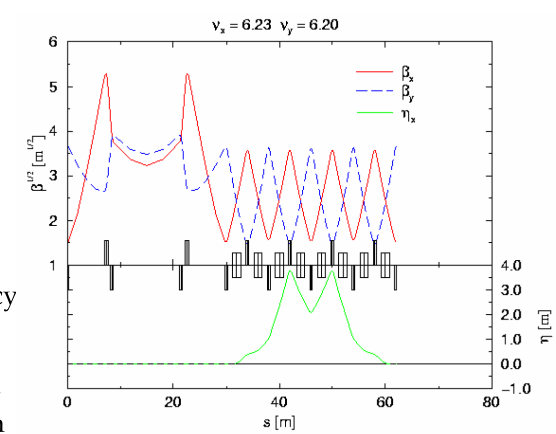

Ring lattice magnets

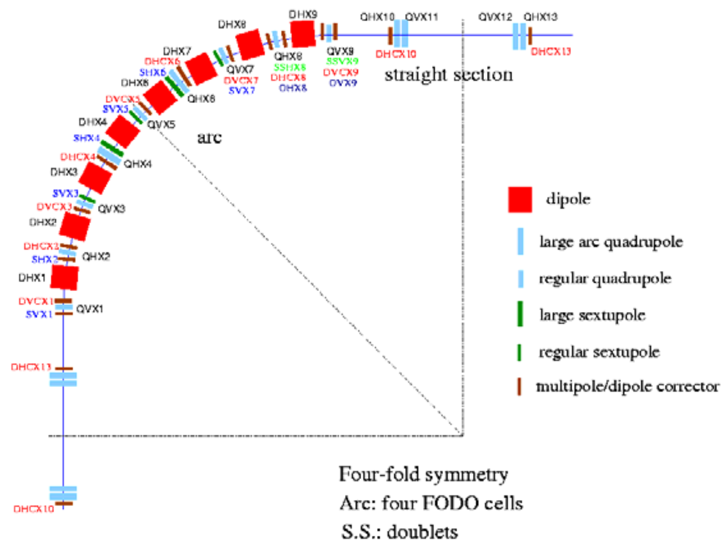

Ring magnet assemblies

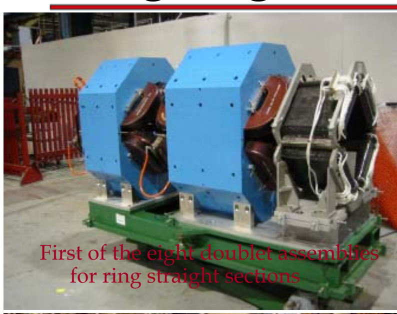
First of the eight doublet assemblies for ring straight sections


Ring arc half-cell assembly in transit


First ring arc half-cell assembly at BNL


First ring quarter cell assembly

ACCUMULATOR RING

WS: 2
QMM : 2
BCM: 1
WCM: 1
Tune :2
E-Det: 5
Damper kicker:2
BIG: 1
IPM :2
BPM:
- 21cm: 28
- 26cm: 8
- 30cm: 8

BLM: 75
FBLM: 12
Foil Video:2

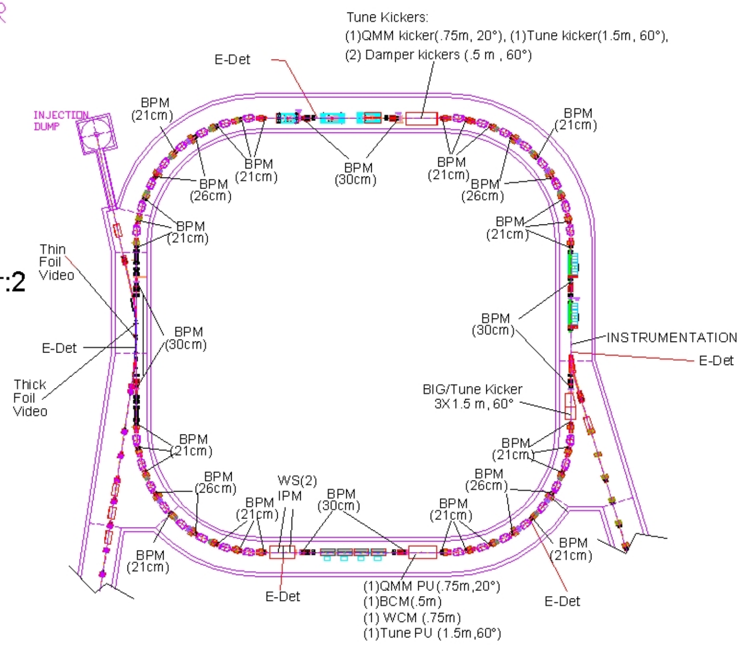

Ring RF straight section example

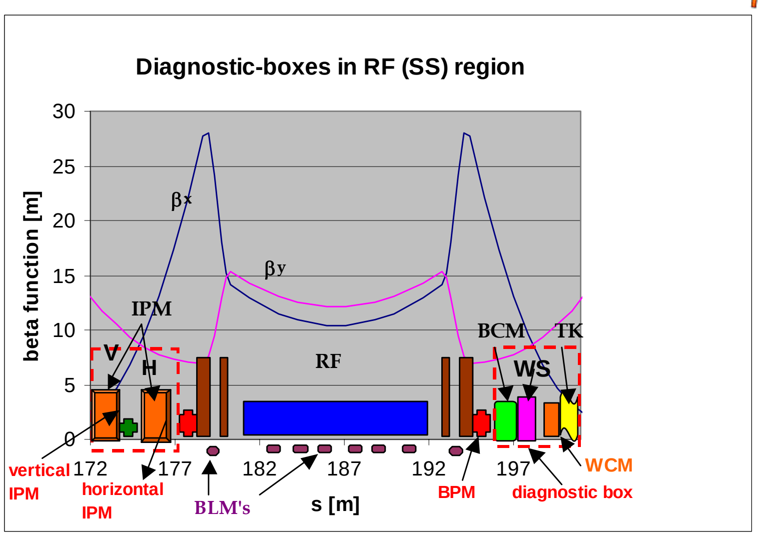

RTBT function

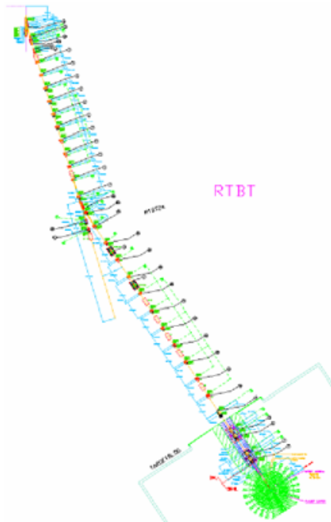

- Matched beam extraction
- Provide beam dumping in case target in not in service
- Collimation to protect device from failure
- Spread the beam transversely for the target
- Beam diagnostics
- Shielding to protect accelerator complex from target back-shine
- Ensure no beam movement on target when kick misfires

RTBT Beam Instrumentation

Detectors	BNL	LANL
BPM	17	0
BLM	40	0
FBLM	3	0
BCM (FCT)	4	0
WS	6	6
HARP	0	1

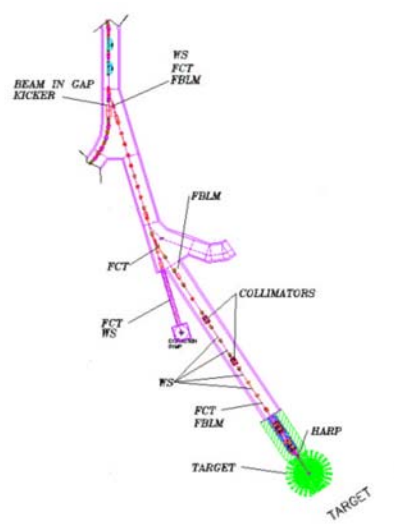

Spallation Neutron Source II

Accumulator ring & transports

Acceptance

Jie Wei (BNL)

Yannis Papaphilippou (ESRF)

June 28 – July 2, 2004

Outline

- Transverse acceptance
  - Emittance and admittance
  - Momentum closed orbit
  - Design closed orbit
  - Closed-orbit deviation
  - Beta beating
  - Dynamic acceptance
- Longitudinal acceptance
  - Bunch area and RF bucket area
  - Momentum acceptance

Transverse acceptance

- Transverse motion

$$x(s) = x_\beta(s) + x_p(s) + x_{c,0}(s) + x_c(s)$$

- Betatron amplitude, off-momentum closed orbit, design closed orbit, closed-orbit deviation

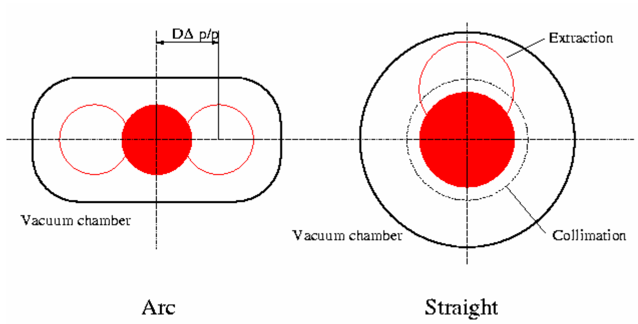

Emittance

- Adiabatic invariant $\oint x dp_x = const$

$$\varepsilon_x = \gamma_x x_\beta{}^2 + 2\alpha_x x_\beta x_\beta' + \beta_x x_\beta'^2 \propto \frac{1}{\beta\gamma}$$

- Injection is most demanding on aperture (given emittance)

$$x_\beta(s) = [\beta_x(s)\varepsilon]^{1/2} \left(\frac{p_{s0}}{p_s}\right)^{1/2} \cos[\psi(s) + \phi_0]$$

- Normalized emittance is an adiabatic invariant

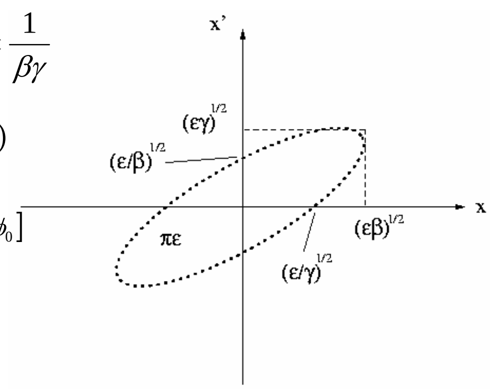

$$\varepsilon_N = \beta\gamma\varepsilon$$

Emittance definition

- Density distribution example -- Gaussian

$$n(x) = \frac{\exp\left(-x^2/\sigma^2\right)}{\sqrt{2\pi}\sigma} \qquad \frac{\varepsilon}{\sigma^2/\beta} = -2\ln(1-F)$$

- Typically convention
  - rms emittance
  - 4-sigma emittance
  - 6-sigma (95%) emittance
  - 99% emittance

ε [σ^2/β]	F [%]
1	15
4	87
6	95
9	99

Off-momentum closed orbit

- Dispersion D is in general a function of location and momentum

$$x_p(\Delta p/p, s) = D(\Delta p/p, s)\frac{\Delta p}{p}$$

- Widen vacuum chamber at high dispersion region (e.g. bending section)
- Eliminate vertical dispersion
- Watch for residual dispersion produced from injection chicane and painting bumps

Design closed orbit

- Injection
  - Single-turn injection: orbit bump
  - Multi-turn painting close-orbit programming
- Extraction
  - Optional orbit bump before kicking
  - Extraction orbit given by kickers
- Diagnostics bump
  - Closed two-bump
  - Closed three-bump
  - Closed four-bump

Dipole error-induced COD

- Single kick effects

COD proportional to sqrt (β) at both source and BPM; maximum:

$$\Delta x(s)\big|_{\max} = \frac{\sqrt{\beta(s)\beta(s_i)}}{2\sin(\pi\nu)}\theta_i \qquad \Delta\phi = \pm\pi(\nu - m), \qquad m = 1,2,\ldots < \nu$$

COD modulation of harmonic close to ν; integer resonance

A symmetric cusp at location of a single steering error

$$\Delta x(s_i) = \frac{\theta_i}{2}\beta(s_i)\cot(\pi\nu); \qquad \Delta x'(s_i^+) = \frac{\theta_i}{2}\left[1 - \alpha(s_i)\cot(\pi\nu)\right]$$

Linear superposition of kicks

$$\Delta x(s)\big|_{rms} = \sqrt{\beta(s)}\frac{\sqrt{N\langle\beta(s_i)\rangle}}{2\sqrt{2}\sin(\pi\nu)}\langle\theta_i\rangle_{rms}$$

Single bump

- Tune notation: ν (US); full Q, fractional q (European)

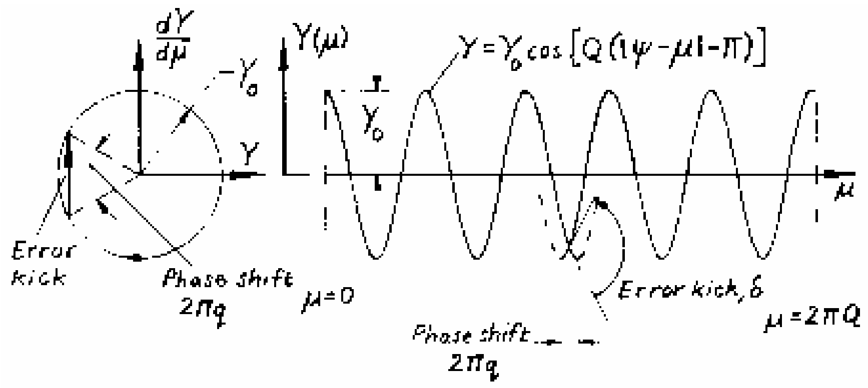

Local closed orbit bumps

- Two-magnet bump

  half-wavelength bump (n=1)

  $\mu_2 - \mu_1 = n\pi \qquad \theta_2\sqrt{\beta_2} = (-)^{n+1}\theta_1\sqrt{\beta_1}$

- Three-magnet bump

  flexible phase closed bump for diagnostics (aperture scan, gradient error measurement, magnet centering, …) & correction

$$\frac{\theta_1\sqrt{\beta_1}}{\sin(\Delta\mu_{32})} = \frac{\theta_2\sqrt{\beta_2}}{\sin(\Delta\mu_{13})} = \frac{\theta_3\sqrt{\beta_3}}{\sin(\Delta\mu_{21})}$$

- Four-magnet bump

  control both amplitude and slope at a location

  (two upstream, two downstream; e.g. for injection, extraction, …)

Two-magnet orbit bump

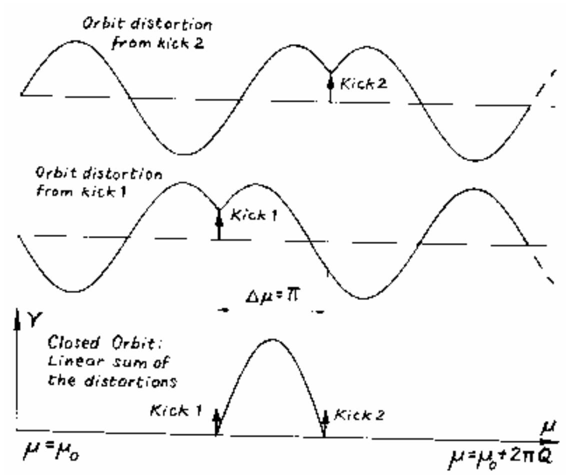

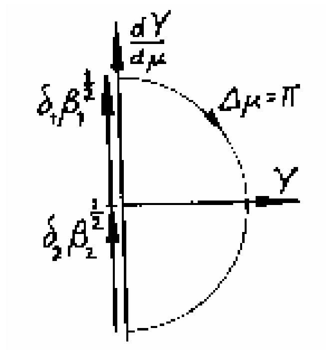

Three-magnet orbit bump

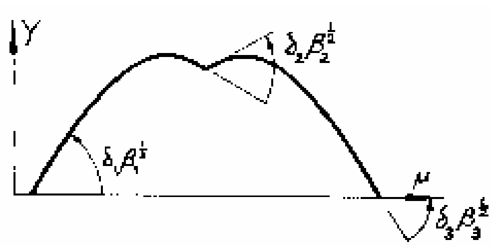

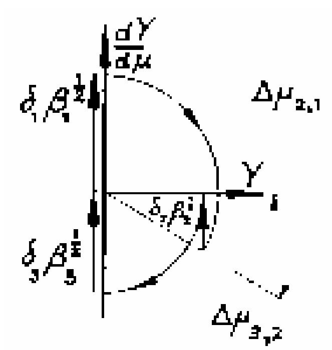

Beta beat

- The increase in peak β is proportional to the reduction in admittance
- Quadrupole gradient error perturbs the amplitude function, generates β wave

$$\frac{\Delta\beta(s)}{\beta(s)} = \frac{1}{2\sin 2\pi\nu}\sum_{i=1}^{N}\beta(s)\Delta K_i L_i \cos[2|\psi(s)-\psi(s_i)|-2\pi\nu]$$

- Off-momentum amplitude deviation

$$\nu = \frac{1}{2\pi}\oint\frac{ds}{\beta} \approx \frac{R}{\langle\beta\rangle} \qquad \langle\frac{\beta(p,s)-\beta(p_0,s)}{\beta(p_0,s)}\rangle \approx -\frac{\Delta\nu}{\nu} = -\frac{\xi}{\nu}\frac{\Delta p}{p} \approx \frac{\Delta p}{p}$$

Dynamic acceptance

- Reduction in acceptance caused by higher-order errors
  - Magnet and powering geometry, systematic
  - Magnet fringe field, systematic
  - Magnet manufacturing imperfection, random
  - Field interference from other devices
- Evaluated in terms of tune shift & resonance crossing
- Evaluated by means of computer tracking

Typical dipole vacuum chamber

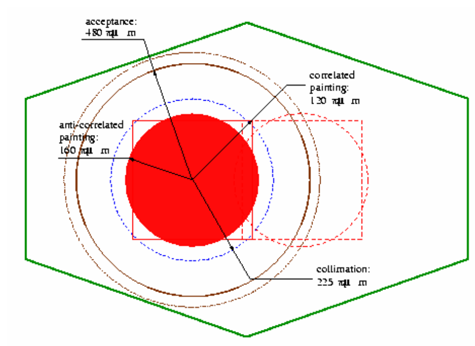

- Dipole chamber: (23x15 cm)
- Acceptance: 480 π mm mr ($\Delta p/p = \pm 1\%$)
- Beam emittance (full) 120-160 π mm mr
- Injection/extraction straight: 480 π mm mr
- Arc: 480-600 π mm mr ($\Delta p/p = \pm 1\%$) depending on working points

Injection straight section example

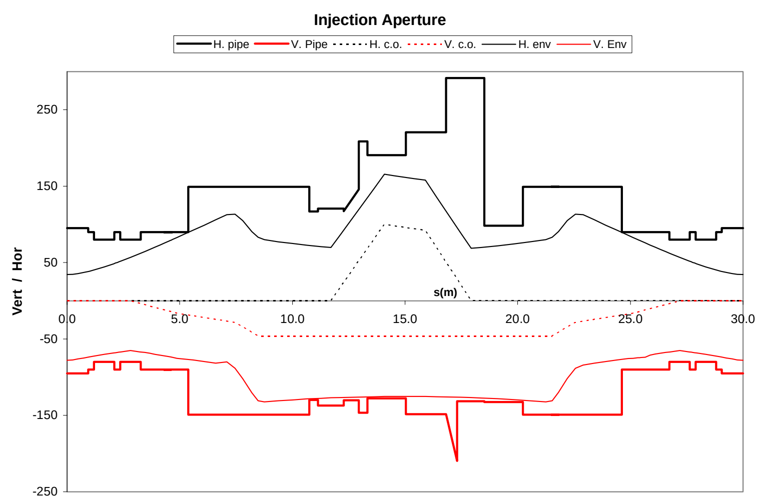

Longitudinal acceptance

- Momentum acceptance from transverse aperture at high-dispersion region
- RF bucket admittance
- Beam gap reserve

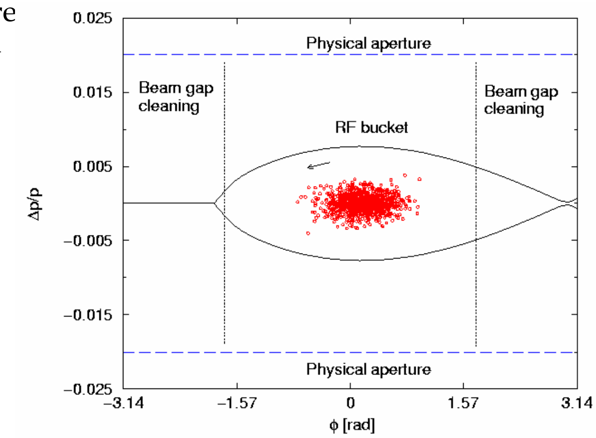

RF bucker admittance

- RF bucket area for a single-harmonic system

$$A_B = \frac{16R}{hc}\sqrt{\frac{eVE_s}{2\phi|\eta|}}\kappa(\phi_s)$$

$$0 \le \kappa(\phi_s) \le 1$$

- κ is 1 for stationary bucket, and decrease quickly as synchronous phase increases
- Dual-harmonic helps

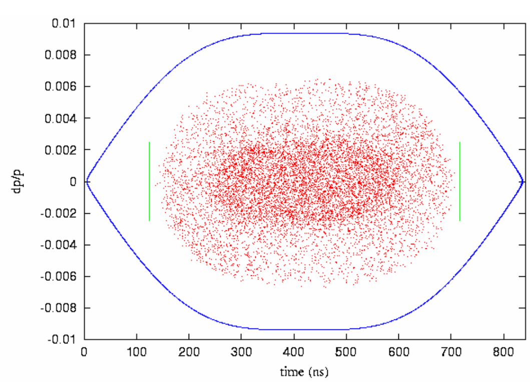

Longitudinal bunch area

- Constant of motion

$$\oint W d\phi = const$$

- Synchrotron motion

$$\Delta\phi = \mp\sqrt{2J/\beta_L}(\sin\varphi + \alpha_L \cos\varphi)$$
$$W = -\sqrt{2J\beta_L}\cos\varphi$$

- Bunch area

$$S = 2\pi\langle J \rangle$$

- Momentum spread peaks at transition energy, when bucket height exceeds physica acceptance

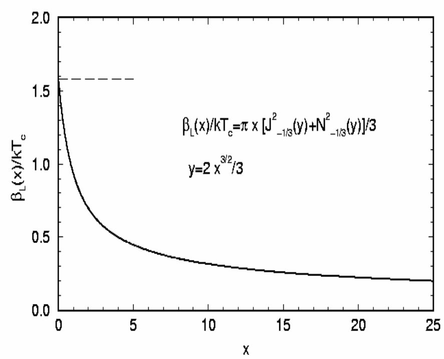

$$\hat{\phi} = \sqrt{2\gamma_L J}, \quad \text{and} \quad \hat{W} = \sqrt{2\beta_L J}$$

Momentum acceptance

- To accommodate large momentum spread, chromaticity often needs to be corrected using sextupole families
  - Natural chromaticity

$$\xi = \frac{d\nu}{d\left(\Delta p / p\right)} \approx -\nu$$

- Non-linear dependence of optics on momentum may cause reduction in acceptance
- Transition needs special attention: linear and chromatic effects

Spallation Neutron Source II

Accumulator ring & transports

Collimation

Jie Wei (BNL)

Yannis Papaphilippou (ESRF)

June 28 – July 2, 2004

Outline

- Transverse collimation
  - H^- beam collimation
  - Proton two-stage collimation
- Longitudinal collimation
  - H^- beam collimation
  - Proton momentum tail collection
  - Beam in gap cleaning
  - Proton momentum collimation

H$^-$ transverse collimation

- Use movable striping foil as scraper, deflect the stripped particle with quadrupole for collection
- For single-pass cleaning, require multi scrapers to enclose different angle of the phase space

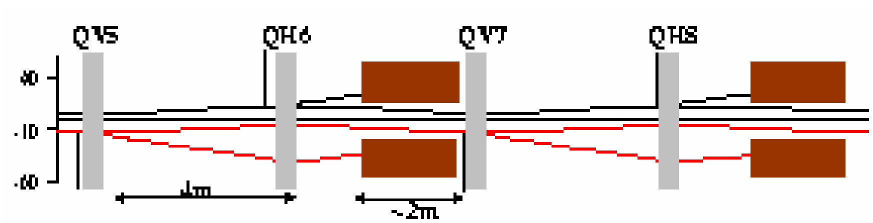

Normalized phase space

- Normalized phase space

$$X \equiv \frac{x}{\sqrt{\beta_x}} \qquad X' \equiv \frac{dX}{d\mu} = \frac{\alpha_x x + \beta_x x'}{\sqrt{\beta_x}} \qquad \mu(s) = \int^s \frac{ds'}{\beta(s')}$$

- Two pairs of scrapers at $\pi/2$ betatron phase advance
  - Escaping radius at $\sqrt{2}$ times scraper radius
  - Channel aperture needs to be larger than the escaping radius

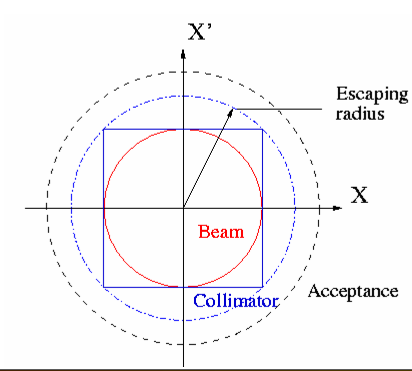

Proton scattering off collimator edge

- Collection efficiency crucially depends on the impact parameter
- To increase overall efficienc use two-stage system
  - Stage 1: movable scraper. Thin material, length optimized between energy loss and scattering angle
  - Stage 2: collector/collimato Thick, usually fixed, self-shielded & cooled, length chosen to be longer than th stopping distance of the particles

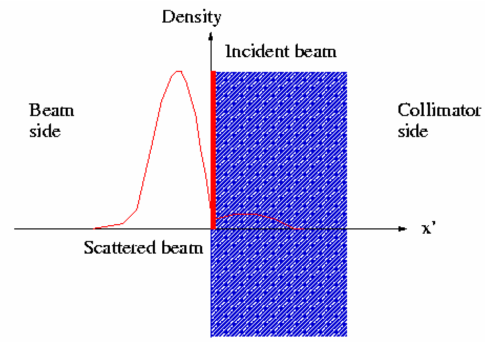

Two-stage collimation

- Comparing with the scraper, the secondary collimator is further away from the primary beam
- Betatron phase advance optimized to minimize escaping

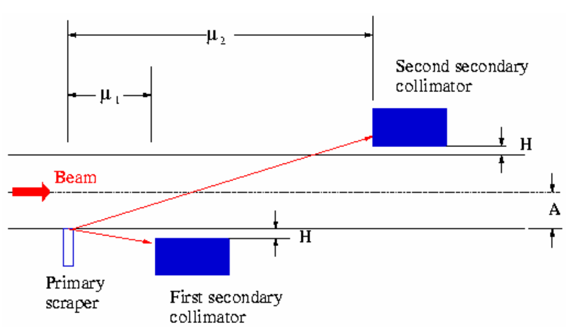

Collimation optimization

- Secondary back-off distance H determined by a balanced consideration
  - Chamber aperture
  - Scraper adjustment range
  - Primary scattering performance
- Phase advance optimized to minimize escaping secondary

$$\mu_1 = \cos^{-1}\left(\frac{A}{A+H}\right)$$

$$\mu_2 = \pi - \mu_1$$

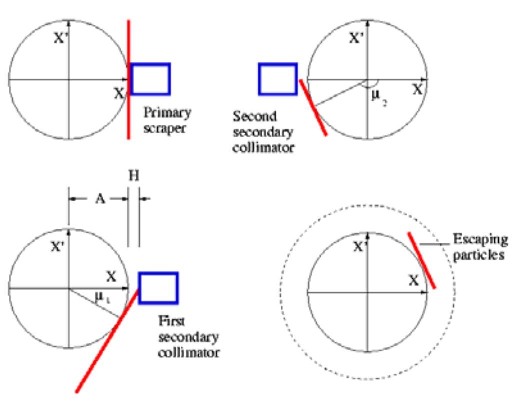

Lattice for transverse collimation

- Dispersion-free region for betatron collimation
- Allow flexible arrangement at optimum phase advance
- Usually prefer doublet/triplet lattice with long drift space

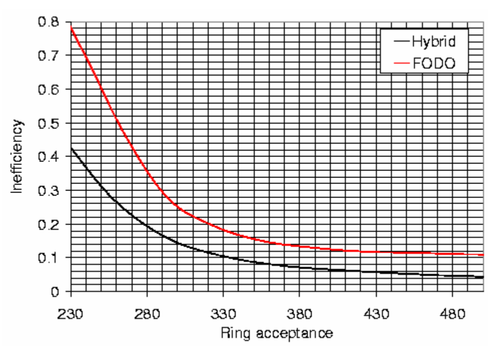

Collimator design

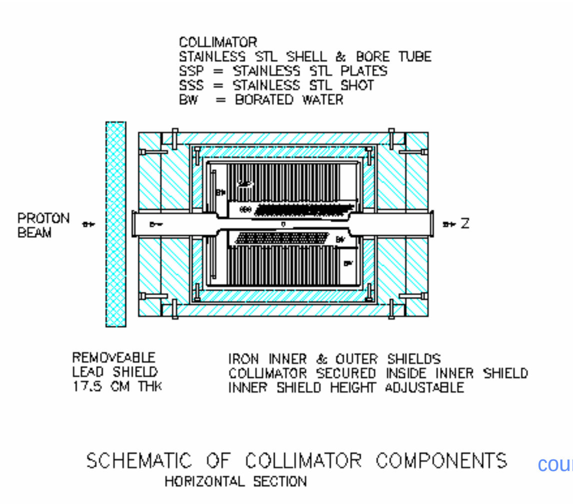

- Stops primary proton
  - Longer length for higher energy
- Contains secondary particles with layered material
  - Neutron
  - γ ray
- Choice of material
  - Vacuum out-gassing
  - Secondary scattering
  - Heat resistance
  - Radiation resistance
  - Stopping capability

courtesy H. Ludewig, N. Catalan-Lasheras

H$^-$ momentum collimation

- Collimate at maximum dispersion region

$$D\left|\frac{\Delta p}{p}\right|_{scraping} >> \sqrt{\beta_x \varepsilon_{x,99\%}}$$

- Use a bending achromat to create high dispersion within a localized region
- The dispersion needed determines the bending angle
- Use movable stripping foils to scrape both positive and negative momentum tails
- Guide the scraped beam to the collectors

Momentum tail collection

- Initial momentum tail (negative energy)
  - Output from linac
  - Developed at injection stripping foil
- Inject at high-dispersion region, collect at π horizontal phase-advance downstream

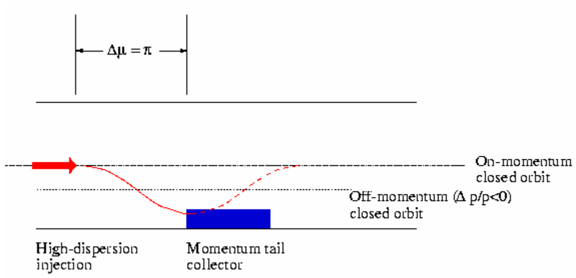

Beam-gap cleaning

- Strip-line kicker at betatron frequency to kick-out particles in tens of turns
- Gated at beam gap, with rise/fall time much shorter that gap length
- Can be used for momentum cleaning if aperture is adequate
- Tune spread may cause complications

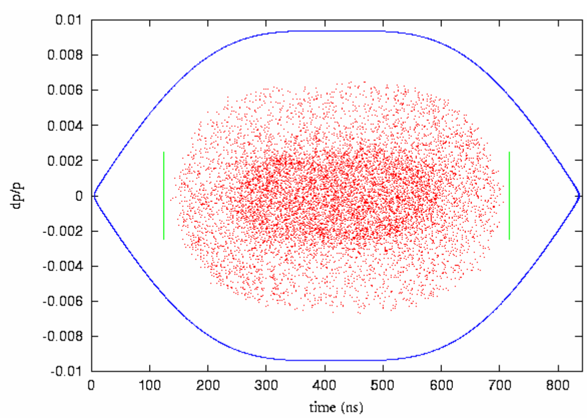

Beam-gap cleaning experimants

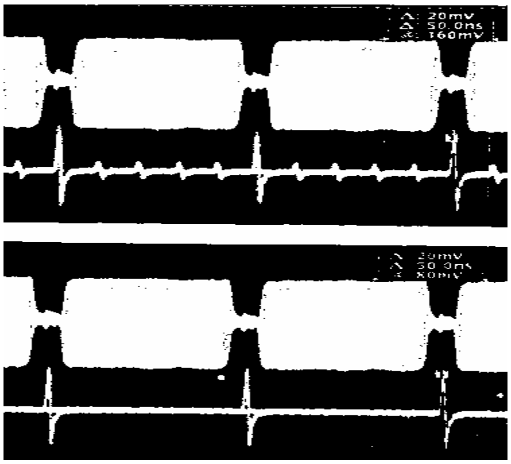

- Used at NSLS and other light sources to kill stray bunches (1993)
- Tested at HERA
  C. Montag J. Klute
- Essential momentum cleaning method for accumulators

courtesy R. Nawrocky et al

Momentum collimation

- Position scraper at high-dispersion region
- Position collimators also at high-dispersion region
- Positive momentum particle may return to core
- Negative momentum particle needs to be collected
- Compact lattice design is challenging; detailed modeling needed

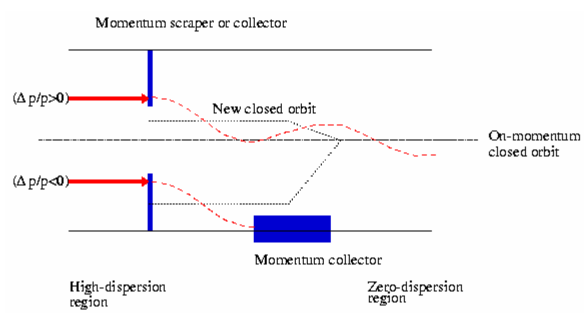

Ring scraper & collimator

- 4 scrapers spaced at 45 degree angle
- 3 collimators; first one to shield scraper shine
- Needs a large vacuum-pipe aperture and a long straight section

(Courtesy H. Ludewig et al)

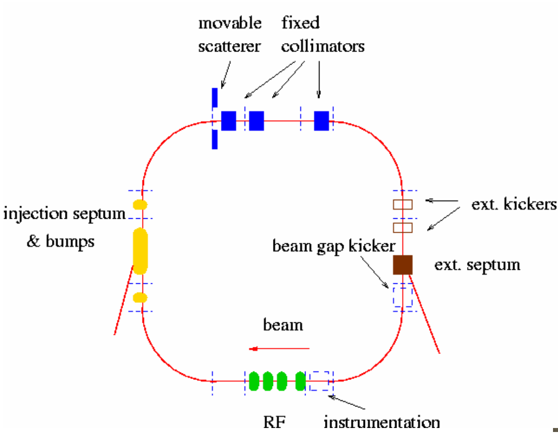

Secondary collector design

- Length enough to stop primary protons (~ 1 m for 1 GeV beam)
- Layered structure (stainless steel particle bed in borated water, stainless steel blocks) to shield the secondary (neutron, γ)
- Fixed, enclosing elliptical-shaped wall for operational reliability
- Double-wall Inconel filled with He gas for leak detection

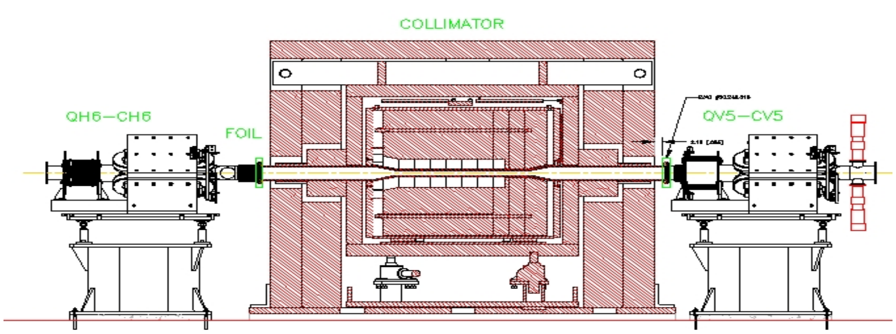

Remote handling

- Overhead, around-the-ring crane
- Quick handling fixtures incorporated into shielding/absorber design
- Remote vacuum clamps; remote water fittings
- Passive dump window & change mechanism

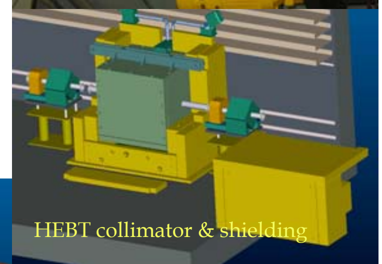
HEBT collimator & shielding

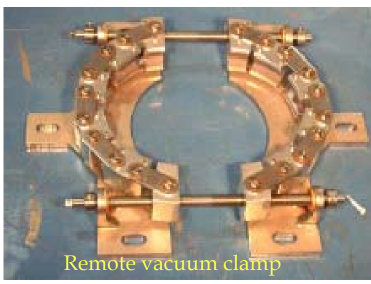
Remote vacuum clamp

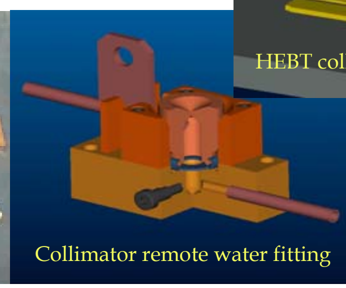
Collimator remote water fitting

(Courtesy
G. Murdoch et al)

Spallation Neutron Source II

Accumulator Ring & Transport Lines

SNS Ring Lattice Design

Jie Wei (BNL)

Yannis Papaphilippou (ESRF)

June 28 – July 2, 2004

Outline

- Basic formalism
  - Betatron Motion
  - Transfer matrices
  - Twiss function parameter evolution
- Arc
  - FODO structure
  - Figure of merit
- Straight
  - Matching
- The SNS design, some history
  - The α-configuration
  - The RCS design
  - The 1.3 GeV hybrid lattice (Ω-Configuration)
- SNS ring design principles
  - Matching
  - Tunability
- Dispersion suppressor
  - Achromat
  - Half-field/missing dipole
- Examples

Betatron motion

- The linear betatron motion of a particle is described by

$$x(s) = \sqrt{(2J_x)\beta_x(s)}\cos\phi_x(s) + D_x(s)\delta$$

with $D_x(s)$ the dispersion function

$\delta = \frac{\delta p}{p}$ the momentum spread

$\alpha,\ \beta,\ \gamma$ the twiss functions $\alpha(s) = -\frac{\beta(s)'}{2},\ \ \gamma = \frac{1+\alpha(s)^2}{\beta(s)}$

ϕ the betatron phase $\phi(s) = \int \frac{1}{\beta(s)}$

- By differentiation, we have that the angle is

$$x'(s) = \sqrt{\frac{2J_x}{\beta_x(s)}}\left(\sin\phi_x(s) + \alpha_x(s)\cos\phi_x(s)\right) + D'_x(s)\delta$$

1-circle transformation

- At some location s, the betatron motion paints an ellipse in phase space which can be transformed into a circle of radius $\sqrt{\epsilon} = \sqrt{2J}$ under the transformation

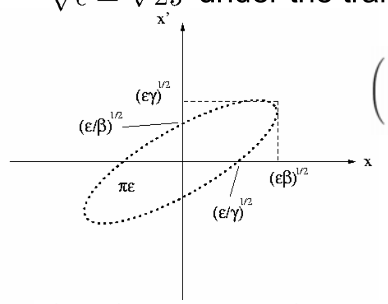

$$\begin{pmatrix}\chi\\ \chi'\end{pmatrix} = T\begin{pmatrix}x\\ x'\end{pmatrix} \quad \text{with} \quad T = \begin{pmatrix}\frac{1}{\sqrt{\beta_x}} & 0\\ \frac{\alpha_x}{\sqrt{\beta_x}} & \sqrt{\beta_x}\end{pmatrix}$$

$$\begin{pmatrix}\chi\\ \chi'\end{pmatrix} = \sqrt{2J_x}\begin{pmatrix}\cos\phi_x\\ \sin\phi_x\end{pmatrix} \qquad \left[+\frac{1}{\sqrt{\beta_x}}\begin{pmatrix}D\\ \alpha_x D + \beta_x D'\end{pmatrix}\cdot\delta\right]$$

Transfer matrix

- Transfer matrix from location a to b

$$M_{a\to b} = T_b^{-1}\begin{pmatrix} \cos\Delta\phi & \sin\Delta\phi \\ -\sin\Delta\phi & \cos\Delta\phi \end{pmatrix} T_a$$

which gives

$$M_{a\to b} = \begin{pmatrix} \sqrt{\frac{\beta_b}{\beta_a}}(\cos\Delta\phi + \alpha_a \sin\Delta\phi) & \sqrt{\beta_a\beta_b}\sin\Delta\phi \\ \frac{(\alpha_a-\alpha_b)\cos\Delta\phi-(1+\alpha_a\alpha_b)\sin\Delta\phi}{\sqrt{\beta_a\beta_b}} & \sqrt{\frac{\beta_a}{\beta_b}}(\cos\Delta\phi - \alpha_b\sin\Delta\phi) \end{pmatrix}$$

One-turn transfer matrix

- One-turn matrix $\begin{pmatrix} x \\ x' \end{pmatrix}_{a+C} = M(a)\begin{pmatrix} x \\ x' \end{pmatrix}_a$

$$M_a = \begin{pmatrix} \cos 2\pi Q + \alpha_a \sin 2\pi Q & \beta_a \sin 2\pi Q \\ -\gamma_a \sin 2\pi Q & \cos 2\pi Q - \alpha_a \sin 2\pi Q \end{pmatrix}$$

or $M = I\cos 2\pi Q_x + J\sin 2\pi Q_x$

with $J = \begin{pmatrix} \alpha & \beta \\ -\gamma & -\alpha \end{pmatrix}$

Transfer matrices

- From point 1 to point 2 $$\begin{pmatrix} x \\ x' \end{pmatrix}_{s_2} = M(1,2)\begin{pmatrix} x \\ x' \end{pmatrix}_{s_1}$$
- Drift: $$M = \begin{pmatrix} 1 & s \\ 0 & 1 \end{pmatrix}$$
- Quadrupole: $$M = \begin{pmatrix} 1 & 0 \\ 1/f & 1 \end{pmatrix} \qquad \frac{1}{f} = Kl = \frac{B'l}{B\rho}$$
- Dipole: $$M(x, x', \Delta p/p) = \begin{pmatrix} 1 & 0 & 0 \\ 0 & 1 & \phi_C/2 \\ 0 & 0 & 1 \end{pmatrix}$$

Courant-Snyder parameter evolution

- Evolution of courant-Snyder parameters $$J_2 = M(1,2)J_1M(2,1)$$
- or $$\begin{pmatrix} \alpha \\ \beta \\ \gamma \end{pmatrix}_{S_2} = \begin{pmatrix} m_{11}m_{22} + m_{12}m_{21} & -m_{11}m_{21} & -m_{12}m_{22} \\ -2m_{11}m_{12} & m_{11}{}^2 & m_{12}{}^2 \\ -2m_{21}m_{22} & m_{21}{}^2 & m_{22}{}^2 \end{pmatrix}\begin{pmatrix} \alpha \\ \beta \\ \gamma \end{pmatrix}_{S_1}$$
- Example: Evolution of β over a drift of distance $$\beta(s) = \beta_0 - 2\alpha_0 s + \gamma_0 s^2$$
- The phase advance of a drift from –L to L with a focus in the center $$\phi = 2\arctan\frac{L}{\beta_o} \xrightarrow{\beta_o \to 0} 180^\circ = \frac{1}{2}2\pi$$

Arc

- FODO is the simplest basic structure
  - Alternating maximum and minimum amplitude function
  - Easy to implement correction
  - Moderate quadrupole strength

$$\beta^{\pm} = \frac{1 \pm \sin \mu_c / 2}{\sin \mu_c} L_c \qquad \alpha^{\pm} = \frac{\mp 1 - \sin \mu_c / 2}{\cos \mu_c / 2} \qquad D^{\pm} = \frac{1 \pm \frac{1}{2} \sin \frac{\mu_c}{2}}{4 \sin^2 \frac{\mu_c}{2}}$$

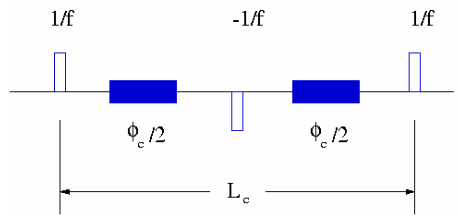

stable motion:

$$\left| \sin \frac{\mu_c}{2} \right| = \frac{L_c}{4f} \le 1$$

Selection of cell phase

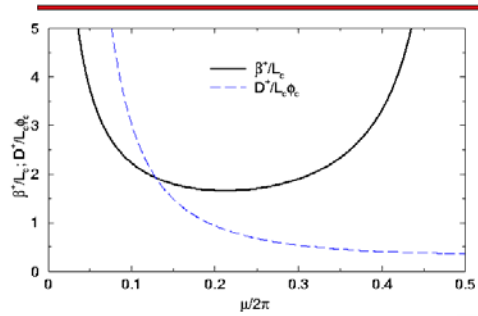

- Given cell length
  - choose lower peak amplitude β^+
  - choose moderate peak dispersion
  - keep moderate β^+/ β^- ratio

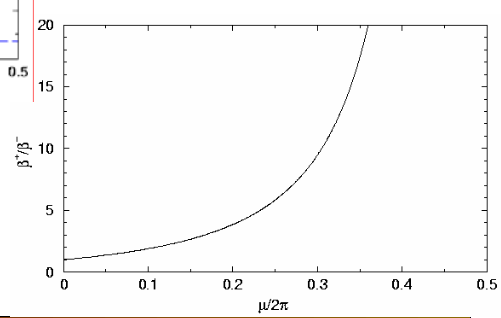

Straight section

- Long, uninterrupted drift space, realized by either quadrupole doublets or triplets
- Matching between arc and straight, without perturbing optics in the arc (not to excite β wave)
- Example: 7 constraint matching
  - Symmetric optics about the middle point of the long drift, I.e.

$$\alpha_x = \alpha_y = 0$$

  - Match to the arc value

$$\alpha_x, \alpha_y, \beta_x, \beta_y$$

  - Adjustable horizontal phase advance
  - Watch for β perturbation in the middle of drift

Straight-arc matching

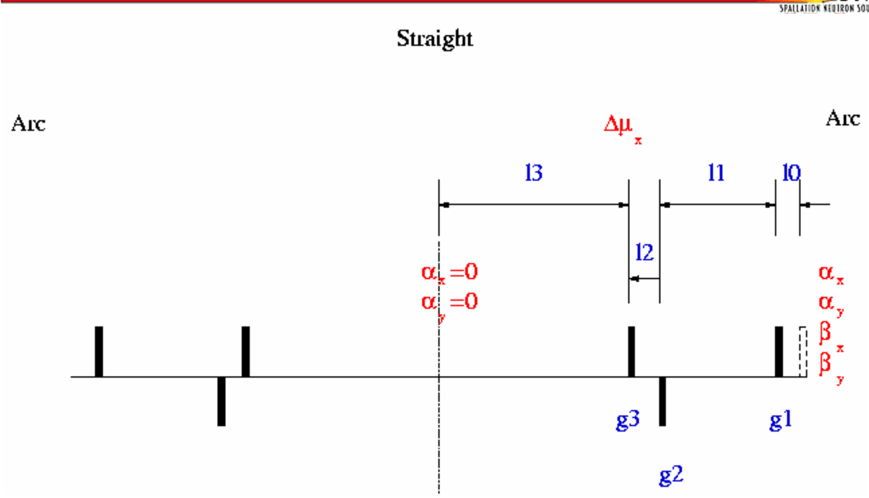

Dispersion propagation

- From a location 0 with D=D'=0

$$\begin{pmatrix} x \\ x' \\ \Delta p/p \end{pmatrix}_s = \begin{pmatrix} C & S & D \\ C' & S' & D' \\ 0 & 0 & 1 \end{pmatrix} \begin{pmatrix} x \\ x' \\ \Delta p/p \end{pmatrix}_0$$

- Solution at location s $D(s) = S(s)\int_0^s \frac{C(s')}{\rho(s')} ds - C(s)\int_0^s \frac{S(s')}{\rho(s')} ds$

- Satisfying the dispersion equation

$$D''(s) + K(s)D(s) = \frac{1}{\rho(s)}$$

Dispersion suppressor: achromat

- Use horizontal achromat for the arc
  - Needs dipole bend to create dispersion
  - Contain all the bending region in integral multiple of 2π betatron phase advance
- Advantage
  - Compact arrangement
- Disadvantage
  - Horizontal phase advance not flexible
  - Dispersion not matched
- Example
  - Arc consists of 4 FODO cells with p/2 phase advance, with either FODO or DOFO quadrupole arrangement; 8 identical dipoles

Dispersion suppressor: half field

- With bending dipoles at half field, excites dispersion oscillation around $D^+/2$ and terminate when D reaches 0
- Advantage
  - Better dispersion matching
- Disadvantage
  - Horizontal phase advance not flexible
- Condition $M\mu_c = \pi$
- Example:
  - M=2 for $\pi/2$ FODO cells

Half-field suppressor examples

- For $\pi/2$ phase advance per FODO cell
- Example 1: half field
- Example 2: missing dipole – modify the last quadrupole to maximize straight section length

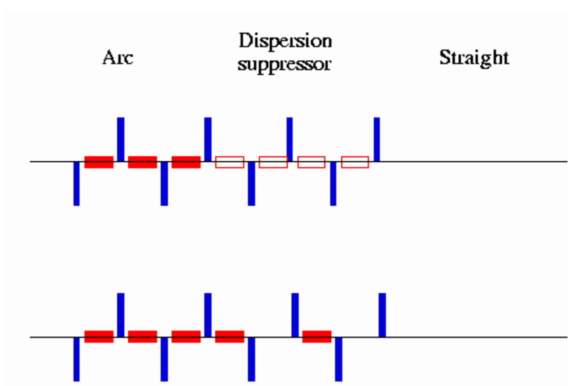

The original α-configuration

or the good old Appleton days (circa 1997)

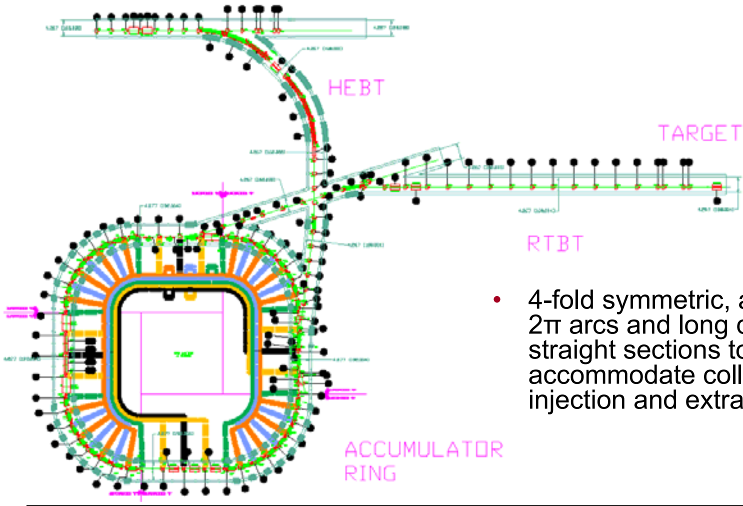

- 4-fold symmetric, all FODO with 2π arcs and long dispersion-free straight sections to accommodate collimation, RF, injection and extraction

The original α-configuration

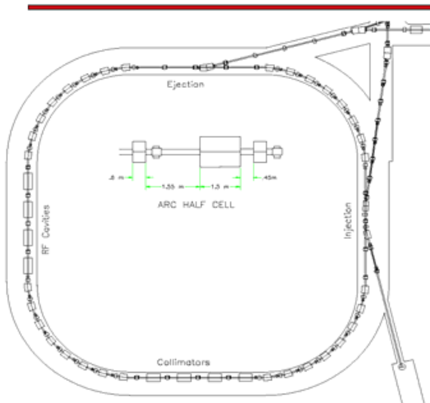

Kinetic Energy	1.0 GeV
Magnetic Rigidity	5.6575 T-m
Circumference	220.688 m
Periodicity	4
Structure	24 FODO
Beam Emittance	120 πmm-mrad
Ring Admittance	312 πmm-mrad
β_{max}(x/y)	19.2/19.2
X_p(max/min)	4.1/0.0 m
$\nu_{x/y}$	5.82/5.80
Natural $\xi_{x/y}$	-6.6/-7.3
γ_t	4.93

- Arc with 4 identical FODO 8m-long-cells
- Straight with 2 identical FODO 11.6m-long-cells without dipole
- Total of 32 dipoles and 48 quadrupoles (but no sextupoles)
- Arcs give 2π-phase advance
- 3 families of quads used for tuning

The original α-configuration

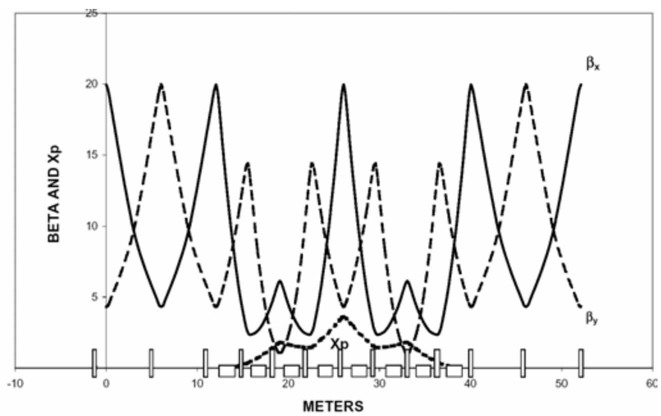

- All FODO lattice chosen for the smoothness of beta function variation around the ring
- Arc quadrupoles set phase advance at 2π
- Two families of straight section quads will adjust the tunes
- But, injection depends on lattice matching, and betas are high in arcs

The Rapid Cycling Synchrotron design

or the glorious Moncton days (circa 1999)

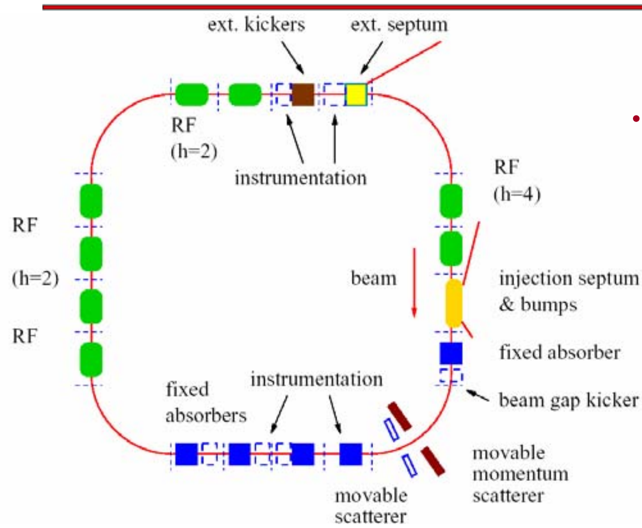

- Two rings vertically stacked with 4-fold symmetric, hybrid structure with FODO arcs and long dispersion-free triplet straight sections to accommodate injection, extraction, RF (a lot of it) and collimation (plus protective absorbers almost everywhere)

The RCS design

number of rings	2
vertical center separation	2 m
circumference	299.2 m
kinetic energy	0.4 – 2 GeV
beam power per ring	1 MW
repetition rate	30 Hz
number of proton	1.04×10^{14}
peak dipole field	0.91 T
peak ramp rate	29.4 T/s
up-ramp period	24 msec
RF harmonic	2, 4
peak RF voltage, $h = 2, 4$	300, 100 kV
RF syn. phase	$0° - 20°$
normalized emittance	264 $\pi\mu$m
betatron acceptance	520 $\pi\mu$m
additional clearance	5 mm
momentum acceptance (full beam)	± 2 %
transverse tunes	7.82, 7.30
transition energy, γ_T	5.91
natural chromaticity	$-9.93, -7.4$
number of superperiod	4
lattice cell length	9.35 m

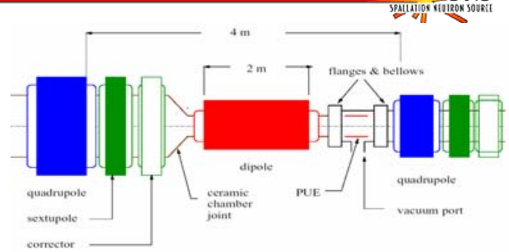

- Arc with 4 identical FODO 8m-long-cells
- Straight with 2 identical 21.4m-long triplet cells
- Total of 32 dipoles, 80 quadrupoles and 20 sextupoles in each ring
- Arcs give 2π-phase advance and tuning is done in the straight sections through a matching quadrupole

The RCS design

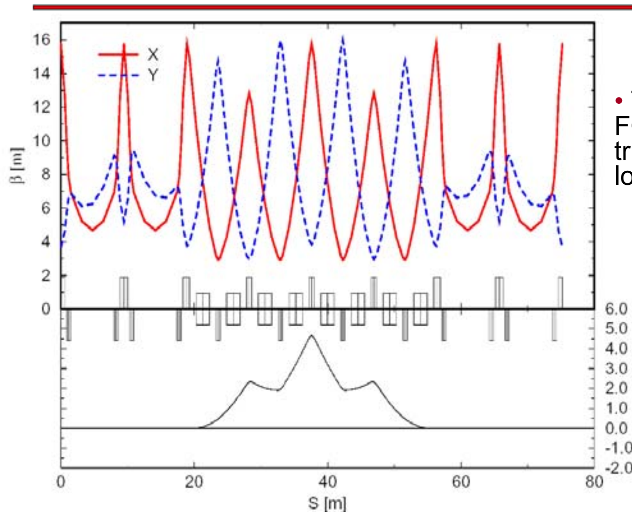

- The lattice combines the FODO simplicity and triplets ability to provide long straight sections

The final Ω-configuration

or the tough Mason days (circa 2000)

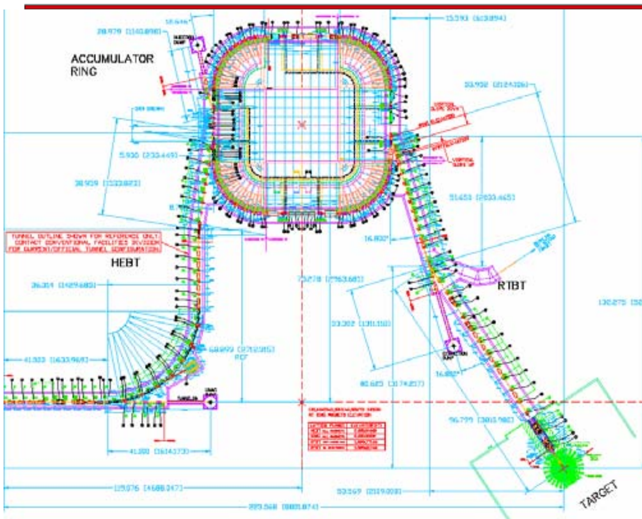

4-fold symmetric, with FODO arcs and doublet dispersion-free straight sections to accommodate collimation, RF, injection and extraction

SNS Ring Schematic

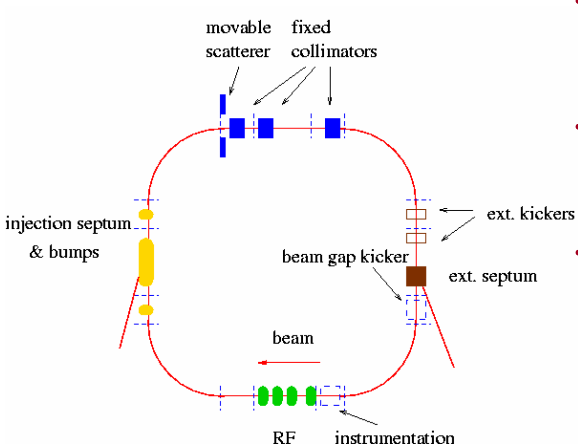

- FODO
  - Modest quad strength
  - Easy for correction (alternating β functions)
- Doublet:
  - Long uninterrupted straights
  - Less joints, bellows, vacuum chambers
- Four straights with separate functions
  - Injection modules
  - Two-stage collimation
  - Extraction & Beam-in-gap kickers
  - 3(h=1)&1(h=2) RF cavities

SNS ring lattice design principles

- Separate-function magnets for robustness
- Each straight section has a separate purpose
  - Collimation section is expected to be radioactively hot
  - Injection section needs frequent access (foil change)
- FODO arc:
  - Modest quad strength
  - Easy for correction (alternating β functions)
  - 2π phase advance for zero dispersion in the straights
- Doublet:
  - Long uninterrupted straights (enough space for collimation optimisation)
  - Less joints, bellows, vacuum chambers
  - Injection independent of lattice tuning (main disadvantage of α-structure)
- Doublet:
  - Long uninterrupted straights (enough space for collimation optimisation)
- Large Acceptance
  - Long uninterrupted straights (enough
- Wide tuneability of "working point"
  - e.g. split tune to suppress coupling from space charge & systematic skew quad
  - Avoid dangerous structure resonances

Ring Lattice

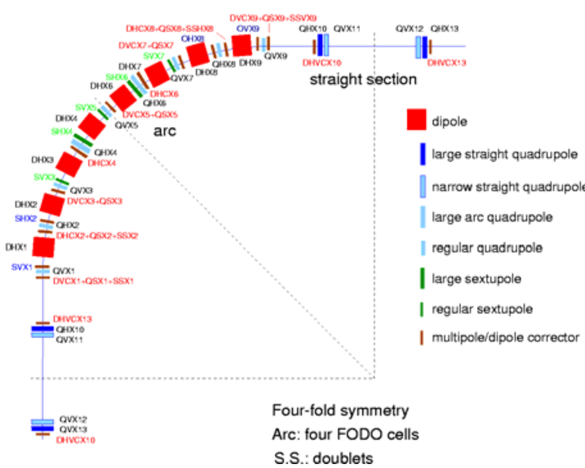

- FODO/Doublet (hybrid) lattice
- 32 dipoles, 52 quadrupoles
- Chromatic correction with 20 arc sextupoles
- Orbit/coupling correction with correctors in the arcs
- Resonance correction in arc and straights

Optics Functions and matching

- First find the strengths of the two arc quadrupole families to get an horizontal phase advance of 2π and using the vertical phase advance as a parameter
- Then match the straight section with arc by using the two doublet quadrupole families and the matching quad at the end of the arc in order to get the correct tune without exceeding the maximum beta function constraints
- Retune arc quads to get correct tunes
- Always keep beta, dispersion within acceptance range and quadrupole strength below design values

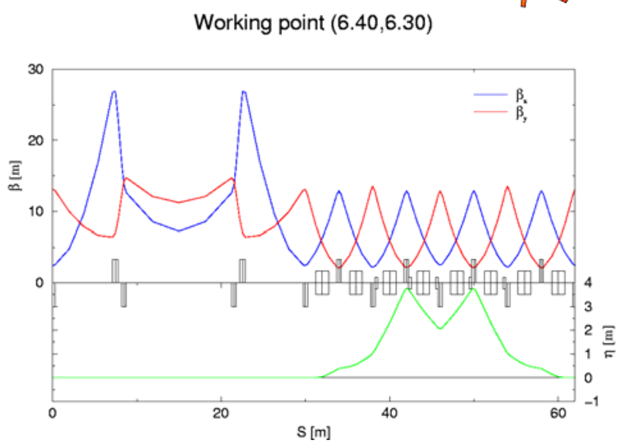

SNS Ring Tuning, β-functions

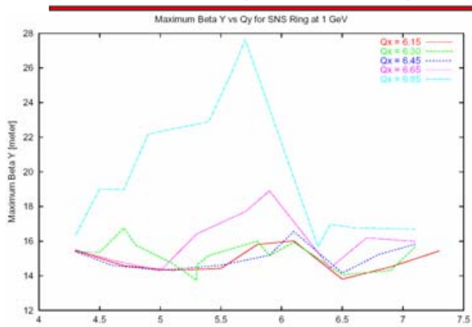

For βy, large values below Qy = 6 for Qx = 6.85 and 6.65

For Qx = 6.15 and 6.85 tend to give large βx values (near 30 m or above).

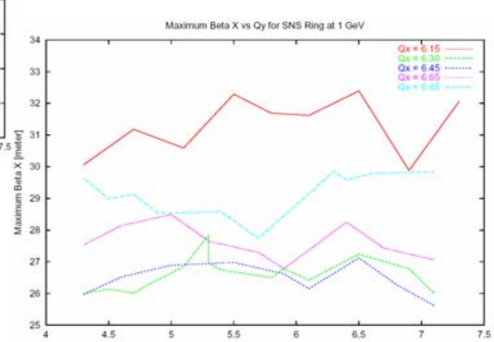

SNS Ring Tuning, dispersion

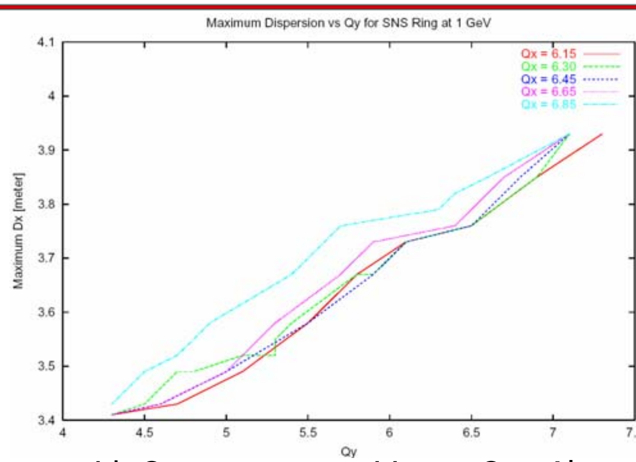

Increases with Qy, not too sensitive to Qx. Always between 3.4 m and 4 m

SNS Ring Tuning, arc quadrupole strengths

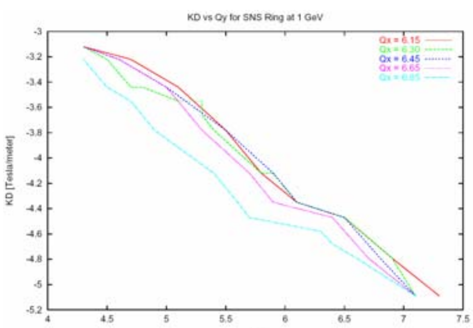

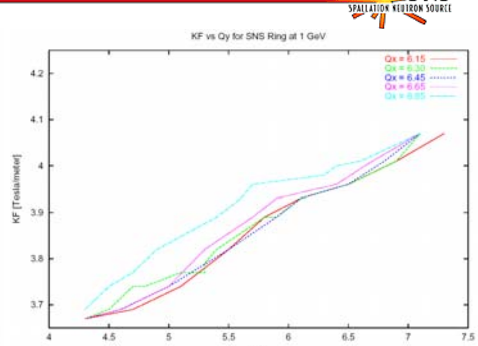

Focusing/Defocusing quad stronger with increasing Qy (almost linear dependence). Defocusing above the limit of 5 Tesla/m for Qy > 7. Lighter dependence with Qx (expected).

SNS Ring Tuning, straight quad. strengths

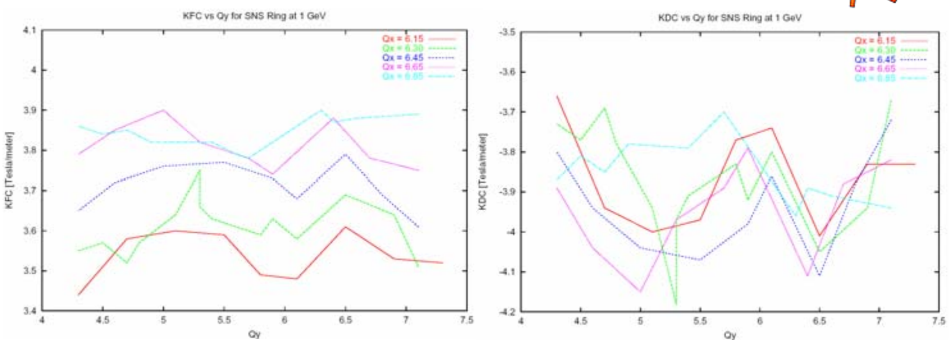

Focusing quad stronger with increasing Qx (almost linear dependence), no systematic behaviour for the defocusing one. Always moderate values.

Working point selection

- Allow flexible tune adjustment (more than one unit)
- Allow split tune for transverse coupling caused by systematic skew quadrupole errors
- Avoid structure resonances
- Avoid known instabilities-sensitive tune values
- Preferably adjustable during injection and ramping, e.g. to accommodate increasing space-charge tune shift during accumulation

SNS Ring Tune Space

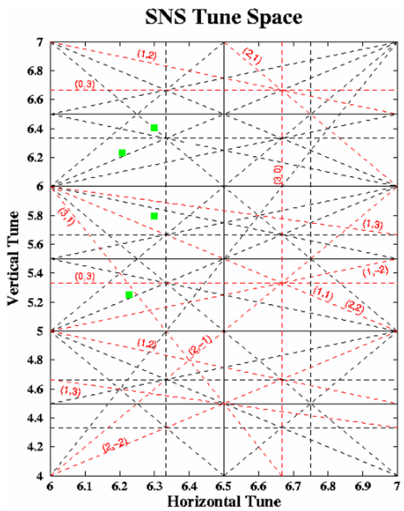

Tunability: 1 unit in horizontal, 3 units in vertical (2 units due to bump/chicane perturbation)

– **Structural resonances (up to 4th order)**
– **All other resonances (up to 3rd order)**

- **Working points considered**
  - **(6.30,5.80) - Old**
  - **(6.23,5.24)**
  - **(6.23,6.20) - Nominal**
  - **(6.40,6.30) - Alternative**

Summary

- Lattice is a key to a low-loss performance
  - Acceptance
  - Straight sections for collimation
  - Correction
- Separated functionality with 4-fold periodicity
  - Compact arc for bending and correction
  - Dispersion free injection
  - Separated sections for injection and collimation for maintenance
- Excellent tunability
- Present lattice is a good choice for an accumulator

Spallation Neutron Source II
Accumulator Ring & Transport Lines

Working point choice

Jie Wei (BNL)
Yannis Papaphilippou (ESRF)
June 28 – July 2, 2004

The ABC of working point choice

During design, impose periodic structure stronger than 1

Resonance condition $n_x Q_x + n_y Q_y = p = mN$, with m the *super-periodicity*

If $p = mN \longrightarrow$ *structural* or *systematic* resonances

If $p \neq mN \longrightarrow$ *non-structural* or *random*

Major design points for high-intensity rings:

- Choose the working point far from structural resonances
- Prevent the break of the lattice supersymmetry

SNS Working point selection

- Allow flexible tune adjustment (more than one unit)
- Quantified all potential effects and evaluate tune-spread
- Allow split tune for transverse coupling caused by systematic skew quadrupole errors
- Avoid structure resonances
- Avoid known instabilities-sensitive tune values
- Preferably adjustable during injection and ramping, e.g. to accommodate increasing space-charge tune shift during accumulation

SNS Ring Tune Space

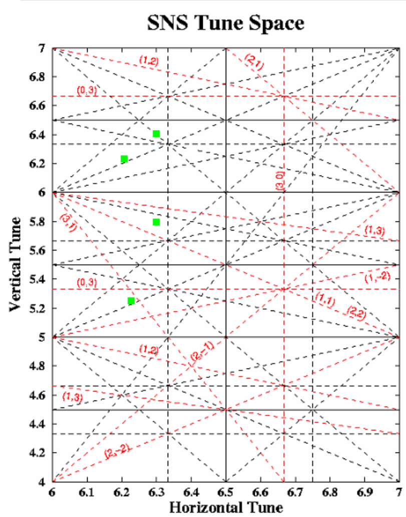

Tunability: 1 unit in horizontal, 3 units in vertical (2 units due to bump/chicane perturbation)

– **Structural resonances (up to 4th order)**
– **All other resonances (up to 3rd order)**

- **Working points considered**
  - **(6.30,5.80) - Old**
  - **(6.23,5.24)**
  - **(6.23,6.20) - Nominal**
  - **(6.40,6.30) - Alternative**

Expected Tune-shifts

Mechanism	Tune-shifts
Space Charge (2MW beam)	0.15-0.20
Chromaticity ($\delta p/p$=1%)	±0.08
Quadrupole fringe-field	0.025
Uncompensated magnet errors	±0.02
Compensated magnet errors	±0.002
Chromatic Sextupoles	±0.002
Fixed injection chicane	0.004
Injection painting bump	0.001

480 π mm mrad

Working Points (6.40,6.30) - (6.23,6.20)

Identification of resonances for new working points

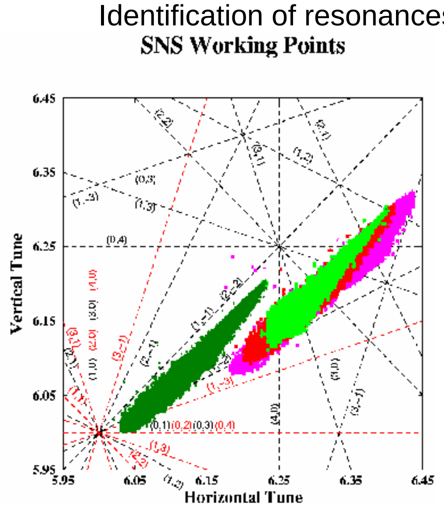

N	Resonances	Type	Perturbation	Correction
2	(2,0) (0,2)	Normal quadrupole	Quadrupole errors & misalignement	Quad TRIMS
2	(1,-1)	Skew quadrupole	Magnet Tilt - Space charge	Skew Quad. round beam
3	(3,0) (1,2) (1,-2)	Normal sextupole	Sextupole errors in dipoles	Sextupoles
3	(2,1) (2,-1) (0,3)	Skew sextupole	Magnet skew sextupole error	Skew Sext.
4	(4,0) (2,2) (2,-2) (0,4)	Normal octupole	Quadrupole fringe-fields, space-charge	Octupoles
4	(3,1) (3,-1) (1,3) (1,-3)	Skew octupole	Magnet errors	None

Linear and non-linear imperfections and correction

Jie Wei (BNL)

Yannis Papaphilippou (ESRF)

June 28 – July 2, 2004

Linear Imperfections and correction

- Steering error and closed orbit distortion
- Gradient error and beta beating correction
- Linear coupling and correction
- Chromaticity

Steering error

- Closed orbit control is a major concern for high-intensity rings (steering error may radio-activate the machine or even destroy components)
- Effect of orbit errors: Consider the vector potential describing a multi-pole magnet

$$A_{n\,z}(x,y) = -B_0 r_0 \Re e \sum_{n=0}^{\infty} \frac{b_n + i a_n}{n} \left(\frac{x+iy}{r_0}\right)^{n+1}$$

- Set $x = x + \delta_x, \quad y = y + \delta_y$, take the normal part

and get multi-pole feed-down

$$A_{n\,z}(x,y) = -\frac{B_0}{r_0^n}\frac{b_n}{n}\sum_{k=0}^{n/2}\sum_{l=0}^{n-2k}\sum_{m=0}^{2k}(-1)^l\binom{n}{2l}\binom{n-2k}{l}\binom{m}{2k}x^{n-2k-l}y^{2k-m}{\delta_x}^l{\delta_y}^m$$

Closed orbit distortion

Horizontal-vertical orbit distortion (Courant and Snyder 1957)

$$\delta_{x,y}(s) = -\frac{\sqrt{\beta_{x,y}}}{2\sin(\pi Q_{x,y})}\int_s^{s+C}\frac{\Delta B(\tau)}{B\rho}\sqrt{\beta_{x,y}}\cos(|\pi Q_{x,y} + \psi_{x,y}(s) - \psi_{x,y}(\tau)|)d\tau$$

with $\Delta B(\tau)$ the equivalent magnetic field error at $s = \tau$.
Approximate errors as delta functions in n locations:

$$\delta_{x,y;i} = -\frac{\sqrt{\beta_{x,y;i}}}{2\sin(\pi Q_{x,y})}\sum_{j=i+1}^{i+n}\phi_{x,y;j}\sqrt{\beta_{x,y;j}}\cos(|\pi Q_{x,y} + \psi_{x,y;i} - \psi_{x,y;j}|)$$

with $\phi_{x,y;j}$ kick produced by jth element:

- $\phi_j = \frac{\Delta B_j L_j}{B\rho} \rightarrow$ dipole field error
- $\phi_j = \frac{B_j L_j \sin\theta_j}{B\rho} \rightarrow$ dipole roll
- $\phi_j = \frac{G_j L_j \Delta x, y_j}{B\rho} \rightarrow$ quadrupole displacement

Closed orbit correction for the SNS ring

- 36 Horizontal/vertical dipole correctors in horizontal and vertical high β's (close to quadrupoles) in the arc. 8 combined horizontal and vertical correctors in the straights. Strings independently powered giving a total of 52, with ability of 1.2mrad kick.
- Simulations by introducing random distribution of errors and other potential orbit distortions (bump, chicane)
- Compute orbit displacement in Beam Position Monitors (placed downstream of the correctors)
- Minimize orbit distortion
  - Globally (harmonic, most efficient steerer)
  - Locally (bumps or SVD)
- Check if there is enough strength for adequate correction

Closed orbit correction for the SNS ring

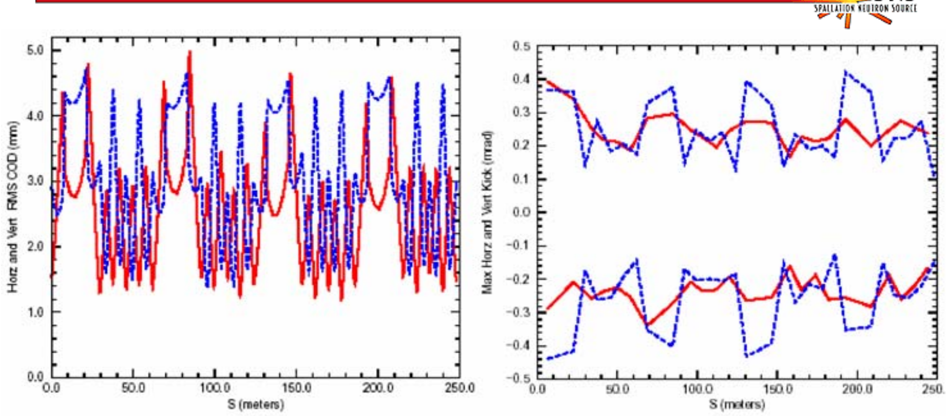

- Horizontal and vertical closed orbit rms displacement (<5mm) for 101 random error distributions in the SNS ring and maximum kicks required for correction (<0.5 mrad)

Gradient error and optics distortion

- Key issue for the performance -> super-periodicity preservation -> only structural resonances excited
- Broken super-periodicity -> excitations of all resonances
- Causes
  - Errors in quadrupole strengths (random and systematic)
  - Injection elements
  - Higher-order multi-pole magnets and errors
- Observables
  - Tune-shift $\delta Q_{x,y} = \frac{1}{4\pi} \oint \beta_{x,y}(s)\delta K_{x,y}(s)ds$
  - Beta-beating

$$\frac{\delta\beta_{x,y}(s)}{\beta_{x,y}(s)} = -\frac{1}{2\sin(2\pi Q_{x,y})}\int_s^{s+C} \beta_{x,y}(\tau)\delta K_{x,y}(\tau)\cos[-2(\pi Q_{x,y} + \psi x, y(s) - \psi x, y(\tau))]d\tau$$

  - Excitation of integer $Q_{x,y} = N$ and half integer resonances $2Q_{x,y} = N$

Gradient error correction in the SNS ring

- TRIM windings on the core of the quadrupoles with ability to provide 1% of their maximum gradient and powered in 16 families
- Simulation by introducing random distribution of quadrupole errors
- Compute the tune-shift and the optics function beta distortion
- Move working point close to integer and half integer resonance
- Minimize beta wave or quadrupole resonance width with TRIM windings
- To correct certain resonance harmonics N, strings should be powered accordingly
- Individual powering of TRIM windings can provide flexibility and beam based alignment of BPM (initial plan)

Gradient error in high dispersion quads

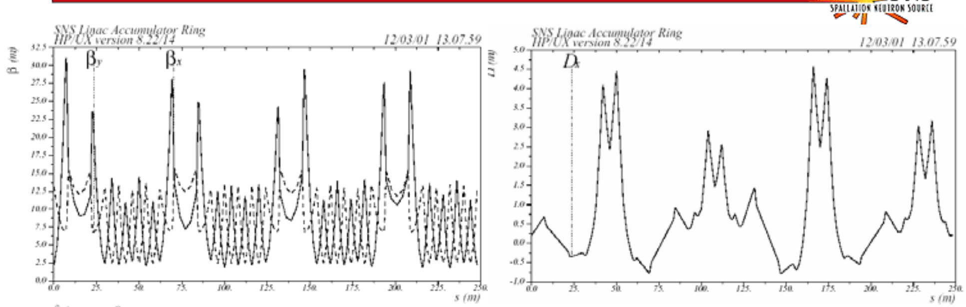

- Optics functions beating of more than 20% by putting random errors (1% of the gradient) in high dispersion quads of the SNS ring
- Justifies the choice of TRIM windings strength

Linear coupling

- Betatron motion is coupled in the presence of skew quadrupoles or solenoids ($|k|xy$ term in the vector potential).
- Motion still integrable with two new eigen-mode tunes, which are always split. In the case of a thin quad: $\delta Q \propto |k|\sqrt{\beta_x\beta_y}$
- On the other hand coupling resonances are excited, with driving terms: $|C_\pm| = \left|\frac{1}{2\pi}\oint ds k(s)\sqrt{\beta_x(s)\beta_y(s)}e^{i(\phi_x\pm\phi_y-(Q_x\pm Q_y-q_\pm)2\pi s/C)}\right|$
- As motion is coupled we can have vertical dispersion and optics function distortion
- Causes:
  – Random rolls in quadrupoles
  – Skew quadrupole errors
  – Off-sets in sextupoles

Linear coupling correction in the SNS ring

- 28 skew quadrupole windings in every low aperture arc dipole corrector placed, powered individual
- Simulation by introducing random distribution of quadrupole errors
- Correct globally/locally coupling coefficient (or resonance driving term) and optics distortion (especially vertical dispersion)
- Move working point close to coupling resonances and repeat
- Evaluate beam losses and correction with multi-particle simulations
  - In particular for the working point (6.3,5.8), extensive losses where observed
  - Less important for (6.23,6.20), and round beams

Coupling correction for the SNS ring

- Local decoupling by super period using 16 skew quadrupole correctors
- Results of Q_x=6.23 Q_y=6.20 after a 2 mrad quad roll
- Additional 8 correctors used to compensate vertical dispersion
- Effect needs to be verified by SC tracking

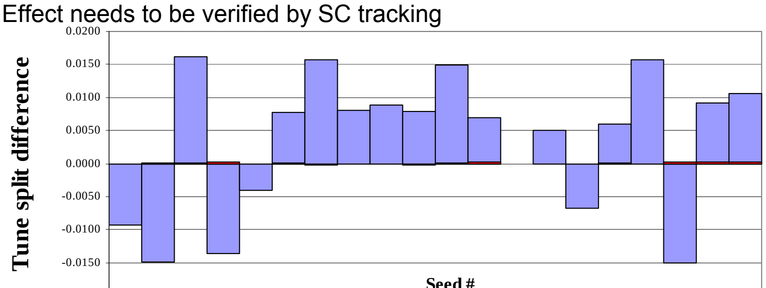

	1	2	3	4	5	6	7	8	9	10	11	12	13	14	15	16	17	18	19	20
Before Correction	-0.009	-0.014	0.016	-0.013	-0.004	0.007	0.015	0.008	0.008	0.007	0.014	0.006	0.000	0.005	-0.006	0.006	0.015	-0.015	0.009	0.010
After correction	0.000	0.000	0.000	0.000	-0.000	0.000	-0.000	0.000	-0.000	-0.000	0.000	0.000	0.000	-0.000	-0.000	0.000	-0.000	0.000	0.000	0.000

Chromaticity

- Linear equations of motion depend on the energy (term proportional to dispersion)
- This leads to dependence of tunes and optics function on energy
- Chromaticity is defined as: $\xi_{x,y} = \frac{\delta Q_{x,y}}{\delta p/p}$
- For a linear lattice the natural chromaticity is:

$$\xi_{x,y} = -\frac{1}{4\pi}\oint \beta_{x,y} K(s) ds$$

- Large momentum spread (up to 2% for the SNS), leads to resonance crossing and excessive beam loss
- By introducing tune-shift with sextupoles, instabilities can be damped down (Landau damping)

Chromaticity correction for the SNS ring

- Off-momentum orbit on a sextupole gives a quadrupole effect and we have a sextupole induced chromaticity:

$$\xi_{x,y} = -\frac{1}{2\pi}\oint \beta_{x,y}(s) b_2(s) D_x(s) ds$$

- Introduce sextupoles in high-dispersion areas and tune them to achieve desired chromaticity
- Two families are able to control only first order chromaticity but not optics functions' distortion and second order chromaticity
- Solutions:
  - Place them accordingly to eliminate second order effects (difficult)
  - Use more families (4 in the case of of the SNS ring)

Two vs. four families chromaticity correction

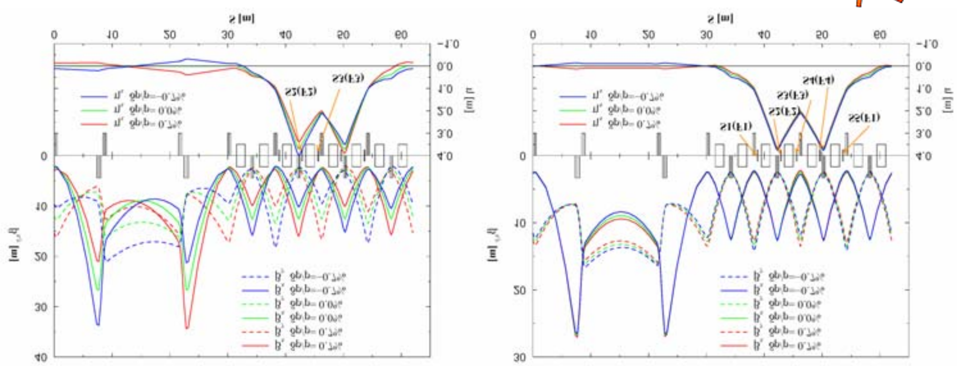

- Large optics function distortion for momentum spreads of +/- 0.7%, when using only two families of sextupoles
- Absolute correction of optics beating with two families

Two vs. four families chromaticity correction

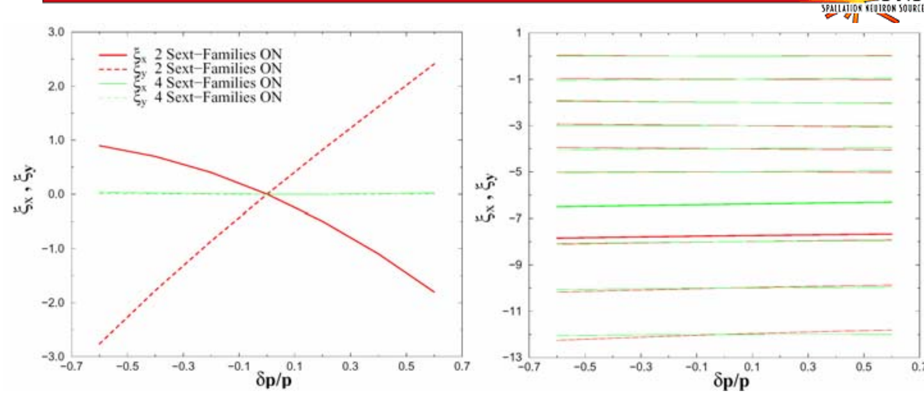

- Chromaticities set to zero (left) and other values (right) are plotted versus momentum spread with two and four sextupole families.
- The second order chromaticity is efficiently corrected with 4 families

Non-linear effects and correction

- Kinematic effect
- Magnet fringe-fields
- Magnet imperfections
- Correction
  - Sextupole correction
  - Skew sextupole
  - Octupole correction
- Singe-particle diffusion
  - Dynamics aperture
  - Frequency maps

Kinematic effect

Kinematic non-linearity $\rightarrow$ high-order momentum terms in the expansion of the relativistic Hamiltonian

- Negligible in high energy colliders
- Noticeable in low-energy high-intensity rings

First-order tune-shift:

$$\delta Q_{x,y} = \frac{1}{2\pi}\sum_{k=2}^{\infty}\frac{(2k-3)!!}{2^k(2k)!!}\times\sum_{\lambda=0}^{k}\lambda\binom{2\lambda}{\lambda}\binom{k}{\lambda}\binom{2(k-\lambda)}{k-\lambda}J_{x,y}^{\lambda-1}J_{y,x}^{k-\lambda}G_{x,y}$$

where $G_{x,y} = \oint_{\text{ring}} \gamma_{x,y}^{\lambda}\gamma_{y,x}^{k-\lambda}ds$

Leading order $\longrightarrow$ octupole-type tune-shift

For the SNS ring, kinematic tune-shift is of the order of 0.001 @ 480 π.mm.mrad

Magnet fringe fields

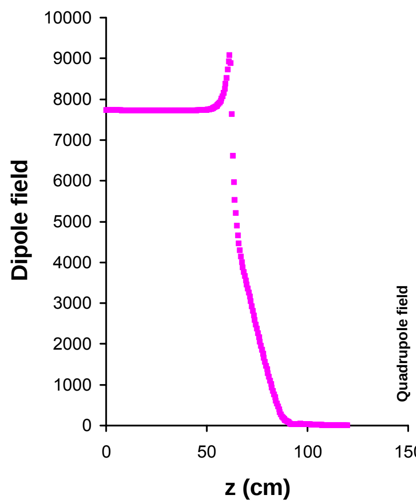

- Up to now we considered only transverse fields
- Magnet fringe field is the longitudinal dependence of the field at the magnet edges
- Important when magnet aspect ratios and/or emittances are big

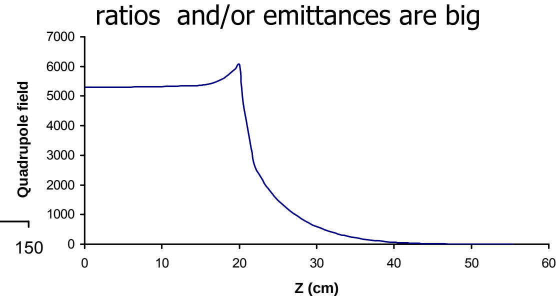

General 3D field expansion

Consider a 3D magnetic field

$$\mathbf{B}(x,y,z) = \nabla\Phi(x,y,z) = \frac{\partial\Phi}{\partial x}\mathbf{x} + \frac{\partial\Phi}{\partial y}\mathbf{y} + \frac{\partial\Phi}{\partial z}\mathbf{z} \ ,$$

where

$$\nabla^2\Phi(x,y,z) = \frac{\partial^2\Phi}{\partial x^2} + \frac{\partial^2\Phi}{\partial y^2} + \frac{\partial^2\Phi}{\partial z^2} = 0 \ .$$

Appropriate expansion:

$$\Phi(x,y,z) = \sum_{m=0}^{\infty}\sum_{n=0}^{\infty} \mathcal{C}_{m,n}(z)\frac{x^n y^m}{n!\,m!} \ ,$$

By Laplace equation: $\mathcal{C}_{m+2,n} = -\mathcal{C}_{m,n+2} - \mathcal{C}_{m,n}^{[2]}$

3D multipole coefficients

The field components:

$$
\begin{aligned}
B_x(x,y,z) &= \sum_{m=0}^{\infty}\sum_{n=0}^{\infty} \mathcal{C}_{m,n+1}(z)\frac{x^n\,y^m}{n!\,m!} \\
B_y(x,y,z) &= \sum_{m=0}^{\infty}\sum_{n=0}^{\infty} \mathcal{C}_{m+1,n}(z)\frac{x^n\,y^m}{n!\,m!} \quad , \\
B_z(x,y,z) &= \sum_{m=0}^{\infty}\sum_{n=0}^{\infty} \mathcal{C}^{[1]}_{m,n}(z)\frac{x^n\,y^m}{n!\,m!}
\end{aligned}
$$

The usual normal and skew multipole coefficients are:

$$
\begin{aligned}
b_n(z) =& \mathcal{C}_{1,n}(z) = \left(\frac{\partial^n B_y}{\partial x^n}\right)(0,0,z) \\
a_n(z) =& \mathcal{C}_{0,n+1}(z) = \left(\frac{\partial^n B_x}{\partial x^n}\right)(0,0,z) \quad .
\end{aligned}
$$

Note that $\mathcal{C}_{m,n} = \sum_{l=0}^{k}(-1)^k\binom{k}{l}\mathcal{C}^{[2l]}_{m-2k,n+2k-2l}$

3D field components

Consider two cases, for $m=2k$ (even) or $m=2k+1$ (odd)

$$
\begin{aligned}
\mathcal{C}_{2k,n} &= \sum_{l=0}^{k}(-1)^k\binom{k}{l}a^{[2l]}_{n+2k-2l-1} \text{ , for } n+2k-2l-1\geq 0 \\
\mathcal{C}_{2k+1,n} &= \sum_{l=0}^{k}(-1)^k\binom{k}{l}b^{[2l]}_{n+2k-2l}
\end{aligned}
\quad ,
$$

and finally the field components are

$$
\begin{aligned}
B_x(x,y,z) &= \sum_{n=0}^{\infty}\sum_{m=0}^{\infty}\sum_{l=0}^{m}(-1)^m\binom{m}{l}\frac{x^n\,y^{2m}}{n!\,(2m)!}\left(b^{[2l]}_{n+2m+1-2l}\frac{y}{2m+1}+a^{[2l]}_{n+2m-2l}\right) \\
B_y(x,y,z) &= \sum_{n=0}^{\infty}\sum_{m=0}^{\infty}(-1)^m\frac{x^n\,y^{2m}}{n!\,(2m)!}\left[\sum_{l=0}^{m}\binom{m}{l}b^{[2l]}_{n+2m-2l}\right. \\
&\qquad \left. -\sum_{l=0}^{m+1}\binom{m+1}{l}a^{[2l]}_{n+2m+1-2l}\frac{y}{2m+1}\right] \quad , \\
B_z(x,y,z) &= \sum_{n=0}^{\infty}\sum_{m=0}^{\infty}\sum_{l=0}^{m}(-1)^m\binom{m}{l}\frac{x^n\,y^{2m}}{n!\,(2m)!}\left(b^{[2l+1]}_{n+2m-2l}\frac{y}{2m+1}+a^{[2l+1]}_{n+2m-1-2l}\right)
\end{aligned}
$$

Dipole fringe field

Using the general z-dependent field expansion, for a straight dipole:

$$B_x = \sum_{m,n=0}^{\infty} \sum_{l=0}^{m} \frac{(-1)^m x^{2n+1} y^{2m+1}}{(2n+1)!(2m+1)!} \binom{m}{l} b_{2n+2m+2-2l}^{[2l]}$$

$$B_y = \sum_{m,n=0}^{\infty} \sum_{l=0}^{m} \frac{(-1)^m x^{2n} y^{2m}}{(2n)!(2m)!} \binom{m}{l} b_{2n+2m-2l}^{[2l]}$$

$$B_z = \sum_{m,n=0}^{\infty} \sum_{l=0}^{m} \frac{(-1)^m x^{2n} y^{2m+1}}{(2n)!(2m+1)!} \binom{m}{l} b_{2n+2m-2l}^{[2l+1]}$$

and to leading order:

$$\begin{aligned} B_x &= b_2 xy + O(4) \\ B_y &= b_0 - \frac{1}{2} b_0^{[2]} y^2 + \frac{1}{2} b_2 (x^2 - y^2) + O(4) \\ B_z &= y\, b_0^{[1]} + O(3) \end{aligned}$$

Dipole fringe to leading order gives a sextupole-like effect (vertical chromaticity)

Quadrupole fringe field

General field expansion for a quadrupole magnet:

$$B_x = \sum_{m,n=0}^{\infty} \sum_{l=0}^{m} \frac{(-1)^m x^{2n} y^{2m+1}}{(2n)!(2m+1)!} \binom{m}{l} b_{2n+2m+1-2l}^{[2l]}$$

$$B_y = \sum_{m,n=0}^{\infty} \sum_{l=0}^{m} \frac{(-1)^m x^{2n+1} y^{2m}}{(2n+1)!(2m)!} \binom{m}{l} b_{2n+2m+1-2l}^{[2l]} \quad .$$

$$B_z = \sum_{m,n=0}^{\infty} \sum_{l=0}^{m} \frac{(-1)^m x^{2n+1} y^{2m+1}}{(2n+1)!(2m+1)!} \binom{m}{l} b_{2n+2m+1-2l}^{[2l+1]}$$

and to leading order

$$\begin{aligned} B_x &= y \left[b_1 - \frac{1}{12}(3x^2 + y^2) b_1^{[2]} \right] + O(5) \\ B_y &= x \left[b_1 - \frac{1}{12}(3y^2 + x^2) b_1^{[2]} \right] + O(5) \\ B_z &= xy b_1^{[1]} + O(4) \end{aligned}$$

The quadrupole fringe to leading order has an octupole-like effect

Scaling law for magnet fringe fields

- Ratio between momentum components produced by fringe field over body contribution

If α small:

$$\frac{(\Delta p_\perp^f)_{rms}}{(\Delta p_\perp^b)_{rms}} \approx \frac{\epsilon_\perp}{L_{\text{eff}}} ,$$

where $\epsilon_\perp$ the rms beam transverse emittance.

When α or α_y large:

$$\frac{(\Delta p_\perp^f)_{rms}}{(\Delta p_\perp^b)_{rms}} \approx \alpha \frac{\epsilon_\perp}{L_{\text{eff}}} ,$$

where α the maximum of α_x or α_y.

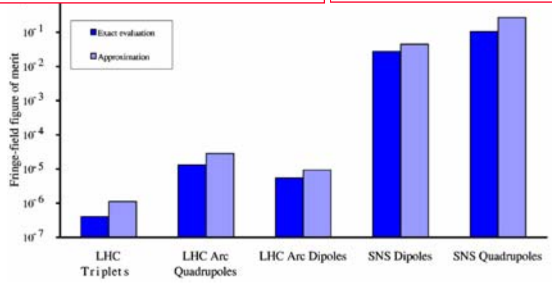

Studying fringe fields effects

- Be sure that they are important for your machine (scaling law)
- Get an accurate magnet model or measurement
- Study dynamics
  - Integrating equations of motion
  - Build a non-linear map
    - » Hard-edge approximation
    - » Integrate magnetic field
    - » Fit magnetic field with appropriate function (Enge function)
- Use your favorite non-linear dynamics tool to analyze the effect

Quadrupole fringe field in the SNS ring

The hard-edge Hamiltonian (Forest and Milutinovic 1988)

$$H_f = \frac{\pm Q}{12B\rho(1+\frac{\delta p}{p})}(y^3 p_y - x^3 p_x + 3x^2 y p_y - 3y^2 x p_x),$$

First order tune spread for an octupole:

$$\begin{pmatrix} \delta\nu_x \\ \delta\nu_y \end{pmatrix} = \begin{pmatrix} a_{hh} & a_{hv} \\ a_{hv} & a_{vv} \end{pmatrix} \begin{pmatrix} 2J_x \\ 2J_y \end{pmatrix},$$

where the normalized anharmonicities are

$$a_{hh} = \frac{-1}{16\pi B\rho}\sum_i \pm Q_i \beta_{xi}\alpha_{xi},$$

$$a_{hv} = \frac{1}{16\pi B\rho}\sum_i \pm Q_i (\beta_{xi}\alpha_{yi} - \beta_{yi}\alpha_{xi}),$$

$$a_{vv} = \frac{1}{16\pi B\rho}\sum_i \pm Q_i \beta_{yi}\alpha_{yi}.$$

Quadrupole fringe field tune spread

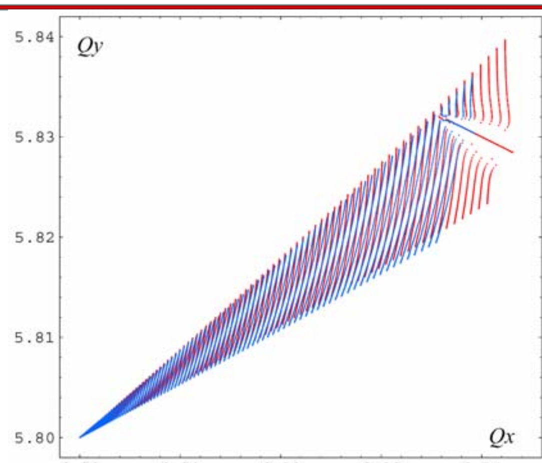

- Tune footprint for the SNS based on hard-edge (red) and realistic (blue) quadrupole fringe-field

Multipole errors

A perfect $2(n+1)$-pole magnet $\rightarrow \Phi(r,\theta,z) = \Phi(r,\frac{\pi}{n+1}-\theta,z)$ which gives $n = (2j+1)(n+1)-1$

- Normal dipole $(n=0) \longrightarrow b_{2j}$
- Normal quadrupole $(n=1) \longrightarrow b_{4j+1}$
- Normal sextupole $(n=2) \longrightarrow b_{6j+2}$

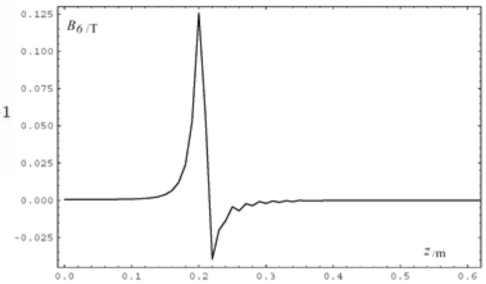

- All multi-pole components give suplementary non-linear effects that have to be quantified and corrected
- Most important the dodecapole component in a 21 cm quadrupole, with un-shaped ends. It is equal to 120.10^{-4} of the main quadrupole gradient.

Sextupole correction for the SNS ring

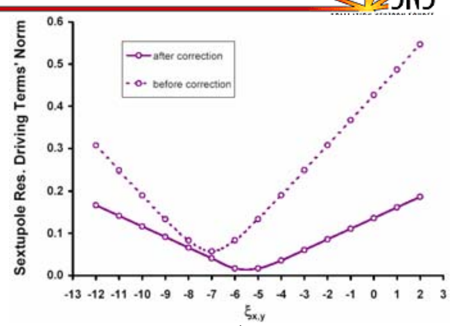

- Causes
  - Chromaticity sextupoles (small effect)
  - Sextupole errors in dipoles (10^{-4} level)
  - Dipole fringe-fields (small effect)
- Effects
  - Zero first order tune-spread, octupole-like (linear in action) 2nd order
  - Excitation of normal sextupole resonances $3Q_x = N$ and $Q_x \pm 2Q_y = N$
- Correction
  - Eight Sextupole correctors in symmetrical non-dispersive areas (beginning of the arc), independently connected
  - Ability to correct resonant lines for all possible working points

Skew Sextupole correction for the SNS ring

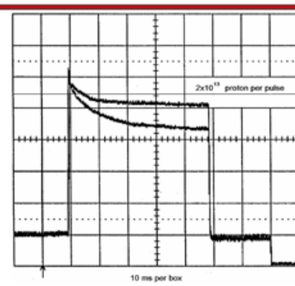

- Causes
  - Chromaticity sextupoles roll
  - Dipole roll
  - Magnet multipoles
- Effects
  - Zero first order tune-spread, octupole-like (linear in action) 2nd order
  - Excitation of skew sextupole resonances $3Q_y = N$ and $2Q_x \pm Q_y = N$
- Correction
  - Skew sextupoles strings in the arc dipole correctors
  - Only connected 16 of them (at the beginning and end of the arc)
  - 8 families formed
  - Ability to correct resonant lines for all possible working points

Octupole correction for the SNS ring

- Causes
  - Quadrupole fringe-fields
  - Kinematic effect (small)
  - Octupole errors in magnets (10^{-4} level)
  - Sextupole, skew sextupole error give octupole-like tune-spread
- Effects
  - Tune-spread linear in action
  - Excitation of normal octupole resonances $4Q_{x,y} = N$ and $2Q_x \pm 2Q_y = N$
- Correction
  - 8 octupole correctors at the end of the arcs, independently powered
  - Tune their strength to minimize resonance driving terms or tune-spread

Octupole tune-spread correction

- The corrected anharmonisities become
- The area for a third octupole family is in the middle of the long straight section

$$A_{hh} = a_{hh} + \frac{3}{16\pi B\rho}\sum_j O_j \beta_{xj}^2,$$

$$A_{hv} = a_{hv} - \frac{6}{16\pi B\rho}\sum_j O_j \beta_{xj}\beta_{yj},$$

$$A_{vv} = a_{vv} + \frac{3}{16\pi B\rho}\sum_j O_j \beta_{yj}^2.$$

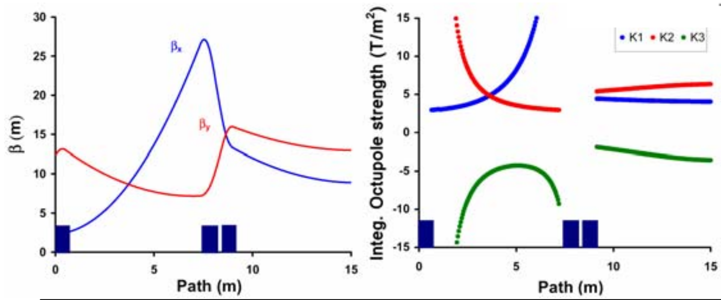

Error compensation in magnet design

Example: dodecapole in quadrupoles

Tune-spread:

$$\begin{pmatrix}\delta\nu_x\\ \delta\nu_y\end{pmatrix} = \sum_i \frac{b_{5i}Q_i}{8\pi B\rho}\mathcal{D}_i \begin{pmatrix}J_x^2\\ J_xJ_y\\ J_y^2\end{pmatrix},$$

where $\mathcal{D}_i$ denotes the 3×2 matrix

$$\begin{pmatrix}\beta_{xi}^3 & -6\beta_{xi}^2\beta_{yi} & 3\beta_{xi}\beta_{yi}^2\\ -3\beta_{xi}^2\beta_{yi} & 6\beta_{xi}\beta_{yi}^2 & -\beta_{yi}^3\end{pmatrix}.$$

i.e. quadratic in the actions.

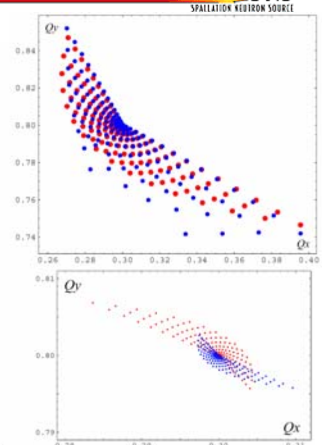

Method of correction $\longrightarrow$ Shape ends of the quadrupoles (local correction)

Magnet sorting

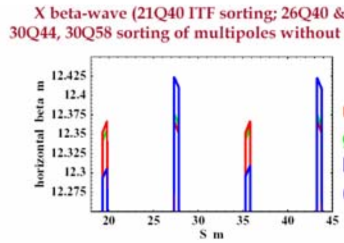

red- ideal
green – sorted 21Q40
blue – beta-wave
(mainly due to 30Q58)

•All measured quads=> 0.5% beta wave for and 10^{-3} tune shift.

•Two string of 8 ,21Q40
• One string of 12, 21Q40
•One string of 8, 26Q40
•One string of 8, 30Q58
•One sting of 8, 30Q44

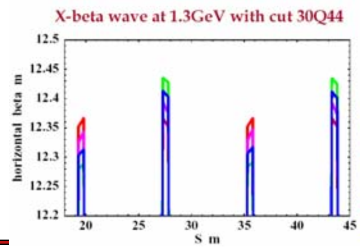

red – ideal
green – 2 magnets cut
blue – 1 magnet compensated
pink – both magnets compensated

All 21Q40 were sorted and 7 were shimmed. Three 26Q40 were shimmed and one re-aligned. All 30Q58 coils were shimmed, three 30Q58 iron was rotated

Sorting quadrupoles to minimize beam loss

- Sort magnets to minimize effects of dangerous resonances for working point (6.4,6.3)
- Balance out multi-pole errors based on a) total field b) phase advance

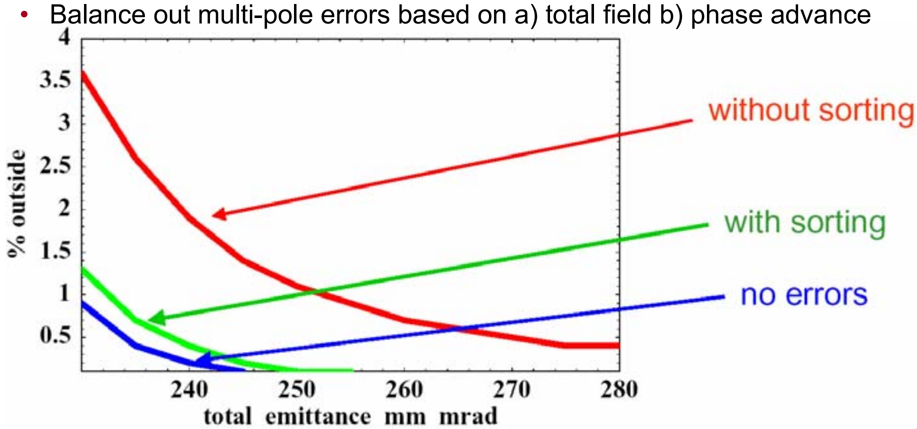

Single particle diffusion process

Three major types of diffusion :

a) Resonance overlapping: particles diffuse across resonance lines.

➔ FAST ~ 10^2 turns

b) Resonance streaming: particles diffuse along resonance lines.

➔ SLOW ~ $\geq 10^4$ turns

c) Arnold diffusion: possibility of diffusion of particles in between the invariant tori of any slightly perturbed dynamical system (n>2).

➔ EXTREMELY SLOW ~ $\geq 10^7$ turns

• With the presence of magnetic errors **only** the machine performance cannot be compromised. BUT: Space-charge + chromaticity + errors + broken super-periodicity enhance particle diffusion

• Important complication:

! The increase of the space-charge force due to beam accumulation shifts the particles in the frequency diagram

Diffusion due to magnet non-linearities for the SNS

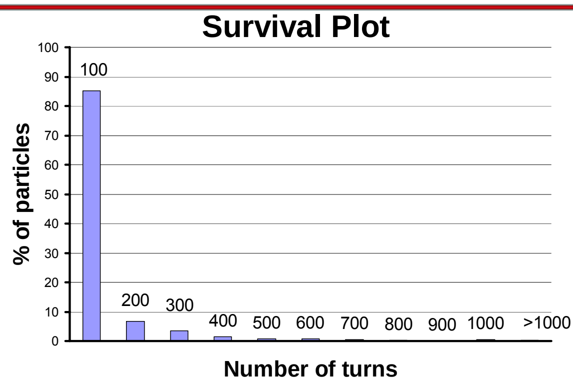

•Tracking ~ 1500 particles with amplitudes near the loss boundary

• 85% of particles are lost within the first 100 turns

• Less than 1% of lost particles survive for more than 1000 turns

• Fast diffusion due to resonance overlapping

Dynamic Aperture

Dynamic aperture tracking for on momentum particles (left) and for $\delta p/p$ = -0.02 (right), without (blue) and with (red) chromatic sextupoles

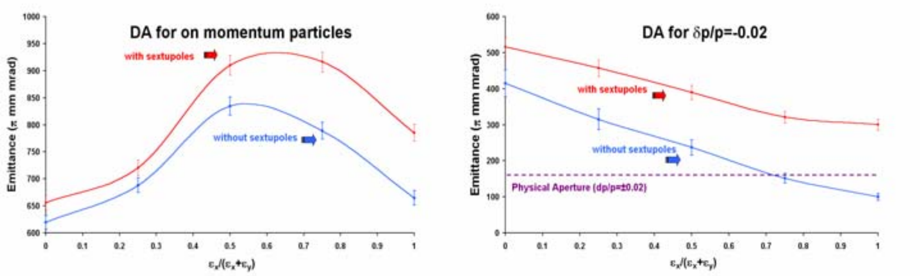

- **Drop of the DA without chromatic sextupoles in both cases**
- **Unacceptable drop below physical aperture for $\delta p/p$ = -0.02 (right)**

Frequency and Diffusion Maps for the SNS Ring

- Model includes
  - Magnet fringe-fields (5^{th} order maps)
  - Magnet systematic and random errors (10^{-4} level)
  - 4 working points, with and without chromaticity correction
  - No RF, no space-charge
- Single particle tracking using FTPOT module of UAL
  - 1500 particles uniformly distributed on the phase space up to 480 π mm mrad, with zero initial momentum, and 9 different momentum spreads (-2% to 2%)
  - 500 turns

$$\boxed{\mathcal{F}_\tau \; : \; \begin{array}{ccc} \mathbb{R}^2 & \longrightarrow & \mathbb{R}^2 \\ (I_x, I_y)|_{p_x,p_y=0}, & \longrightarrow & (\nu_x,\nu_y) \end{array}}$$

Working point (6.4,6.3)

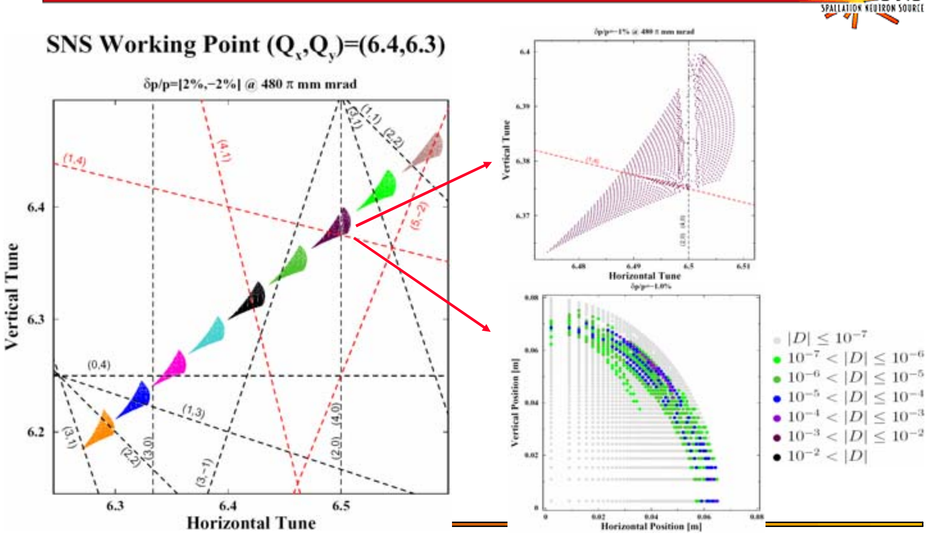

Working point (6.23,5.24)

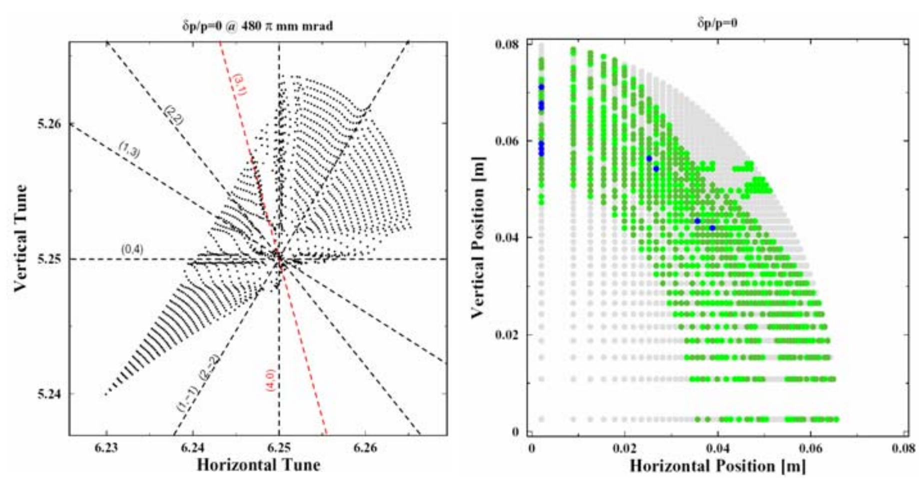

Resonance identification for (6.3,5.8)

Work. Point	δp/p (%)	Resonances	Possible Cause	Correction
(6.3,5.8)	-2.0	(2,-1)	a3 random error	Mag. Qual. + Skew Sext.
	-1.5	(3,3)	b6 error on quads	Mag. Qual.
	-1.0	(3,1) (1,3)	a4 random error	Mag. Qual.
	-0.5	(3,0) (1,2)	b3 error + dipole fringe fields	Mag.Qual. + Sextupole
	0.0			
	0.5			
	1.0	(1,1) (2,2)	Quad. fringe fields	Skew Quad. - Octupole
		(4,0) (2,-2) (0,4)	Quad. fringe fields	Octupole
		(3,-1) (1,-3)	a4 random error	Mag. Qual.
	1.5	(1,1) (2,2)	Quad. fringe fields	Skew Quad. - Octupole
		(4,0) (2,-2) (0,4)	Quad. fringe fields	Octupole
		(1,-3)	a4 random error	Mag. Qual.
	2.0			

Working Point Comparison

Tune Diffusion quality factor $D_{QF} = \left\langle \frac{|\boldsymbol{D}|}{(I_{x0}^2 + I_{y0}^2)^{1/2}} \right\rangle_R$

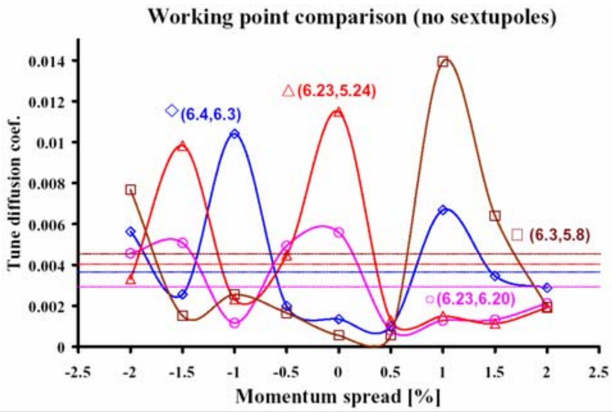

Correction packages

Baseline	Quantity	Powering	Justification
Dipole	52 (+2)	Individual	Injection dump dipoles
TRIM Quadrupoles	52	28 families	Beta beating correction due to lattice symmetry breaking
Skew Quadrupoles	16	Individual	Coupling correction
High-Field Sextupoles	20	4 families	Correction of large chromatic effect
Normal Sextupoles	8	Individual	Sextupole resonance correction due to sextupole errors and octupole feed-down
Skew Sextupoles	16	8 families	Skew sextupole resonance correction (AGS booster)
Octupoles	8	Individual	Octupole resonance correction due to quadrupole fringe-fields

Spallation Neutron Source II

Accumulator Ring & Transport Lines

Magnets

Theory, models and measurements

Jie Wei (BNL)

Yannis Papaphilippou (ESRF)

June 28 – July 2, 2004

SNS magnets

- SNS magnet zoology
- Theory
  - Multi-pole expansion
- Modelisation
  - HEBT magnets
  - Ring magnets
  - RTBT magnets
- Measurements
  - Ring Dipole magnets ITF problem
  - Quadrupoles
  - Injection chicane

The SNS Magnets

REGION	NAME	ELEMENT	MODEL	Deviation of Beam center from magnet center-line	COMMENTS
HEBT	12Q45	QUAD	YES-2D	N/A	
	8D533	DIPOLE	YES-2D	6.55 cm	
	8D406	DIPOLE	YES-2D	3.96 cm	same csect as 8D533
	21Q40	QUAD	YES-3D	N/A	RING & RTBT
INJECTION	7DS297	Septum DIPOLE	YES-2D	2.1 cm	
	24D64 1st Chicane	Septum DIPOLE	YES-3D	0.23 cm	RING
	24D75 2nd Chicane	C-DIPOLE	YES-3D	0.30 cm	RING
	23D64 3rd Chicane	C-DIPOLE	YES-3D	0.30 cm	RING
	24D68 4th Chicane	H-DIPOLE	YES-2D	0.28 cm	RING
	30Q44, 58	QUAD	YES-2D	N/A	RING & RTBT
	20DP64	WF-DIPOLE	YES-3D	N/A	RING
	20DP21	WF-DIPOLE	YES-3D	N/A	RING
RING	17D120	H-DIPOLE	YES-3D	1.5 [cm]	
	21Q40	QUAD	YES-3D	N/A	HEBT & RTBT
	26Q40	QUAD	YES-3D	N/A	
	30Q44, 58	QUAD	YES-2D	N/A	Injection. & RTBT
	21S26	SEXT	YES-3D	N/A	

Magnet parameters

	Type	Location	No.	Field	Aperture	Length
Dipoles	8D533	Achromat	8	0.21 T	8 cm gap	5.43m
	8D406	ARMS	1	0.21 T	8 cm gap	4.13m
	16CDH20	LAMS,ARMS,LDUMP	7	0.03 T	12 cm × 12 cm	0.2 m
	16CDV20		7			
	27CDH20	Achromat	2	0.03 T	20 cm × 20 cm	0.3m
	27CDV20		2			
Quadrupoles	12Q45	LAMS,ARMS	26	4.5 T/m	12 cm ϕ	0.5 m
	21Q40	Achromat	8	2.5 T/m	20 cm ϕ	0.505m
	12Q45	LDUMP	6	3.0 T/m	12 cm ϕ	0.505m

	Type	Number	Field	Aperture	Length
Dipoles	17D244	1	0.67 T	17 cm × 45 cm	2.64 m
	27CD30	15	0.02 T	20 cm × 20 cm	0.3 m
	36CDR30	4	0.02 T	36 cm × 36 cm	0.3
Quadrupoles	21Q45, 36Q85, 30Q44, 30Q58	23	4.7 T/m	20 cm ϕ	0.5 m
		4	2.5 T/m	36 cm ϕ	1.0 m
		3	4.5	30 cm ϕ	0.55 m
		2	4.2	30 cm ϕ	0.70

Ring magnet system

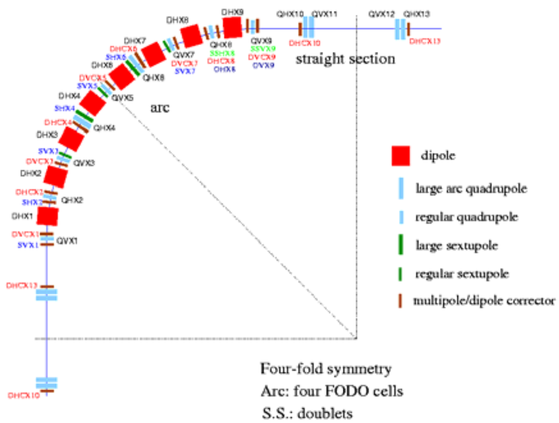

- Dipole: bending
- Quadrupole: focusing
- Sextupole: chromaticity adjustment
- Correctors
  - Normal & skew dipole: orbit bump/correction
  - Normal quadrupole: beta beating correction
  - Skew quadrupole: transverse decoupling
  - Normal and skew sextupole and higher: resonance correction

SNS Ring dipole magnet (17 cm gap)

SNS Ring multipole corrector

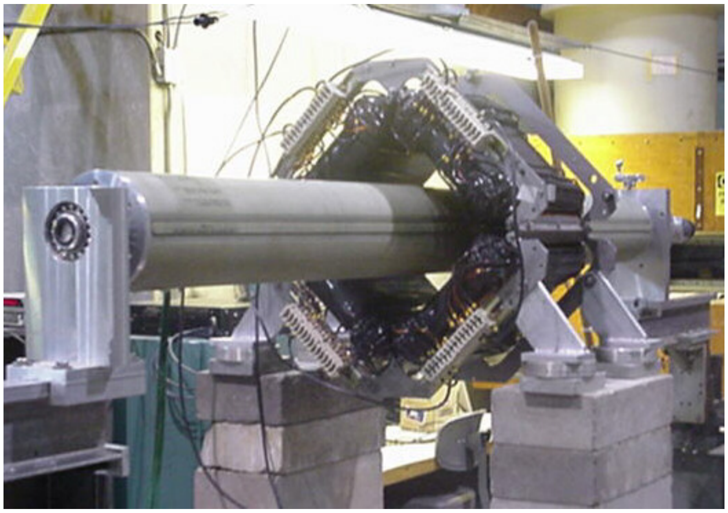

SNS Ring half cell assembly

SNS ring quadrupole doublet and corrector

Typical dipole magnet

- Iron core
- Water-cooled windings
- Good field quality (~10^{-4}) achievable with iron shaping

$$N_{coil} I = gH$$

g [m]: gap size, $N_{coil}/2$: number of turns on each pole, I [A]: current

$$B = \mu_0 N_{coil} I / g \quad \text{[T]}$$

$$\mu_0 = 4\pi 10^{-7}$$

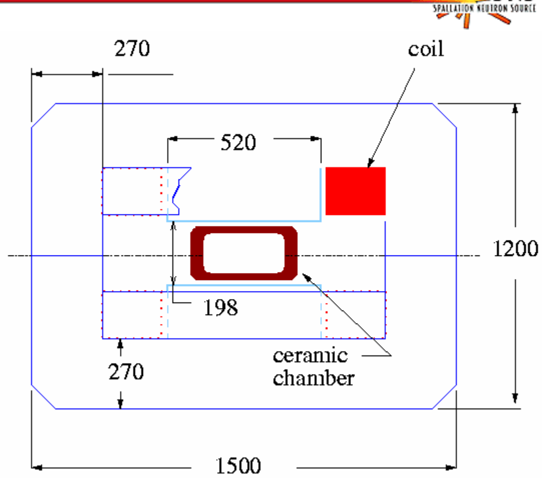

Magnet definitions

- 2m-pole:

dipole quadrupole sextupole octupole decapole …

m: 1 2 3 4 5

- Normal: gap appears at the horizontal plane
- Skew: rotate around beam axis by $\pi/2m$ angle
- Symmetry: rotating around beam axis by π/m angle, the field is reversed (polarity flipped)

Magnetic multipole expression

- 2-D multipole expansion (European convention m->n+1)

$$B_y + iB_x = B_0 \sum_{n=0}^{\infty} (b_n + ia_n)(x+iy)^n$$

- Normalised units (reference radius, main field)

$$B_y + iB_x = 10^{-4} B_0 \sum_{n=0}^{\infty} (b'_n + ia'_n) \left(\frac{x+iy}{R_{ref}}\right)^n$$

- "Allowed multipoles": multipoles allowed by symmetry

$$2m(2k+1), \qquad k = 0,1,2...$$

Magnet, fringe field, compensation

- Dominant error: eddy current (ramp matching), saturation; limit peak field (e.g. 1 T) and ramp rate (e.g. 30 T/s) (e.g. 5%)
- Eased by programmable ramp (IGBT switch etc)
- Dominant field components: allowed multipoles (e.g. 2%); correctable by magnet pole shaping
- Fringe field:
- important for large acceptance, moderate ring circumference (e.g. 0.2%)
- Order of magnitude: **(emittance) / (magnet length)**
- (or (ε/L) β' when β'>>1, e.g. collider IR)
- Correctible with octupole correctors

Superferric magnets

- Saturation
  - Limit ~ 1 T
- Hysteresis
  - Reproducible for given cycle
- Eddy current effects
  - Heating
  - Field distortion (multipoles)
- Ramp rate effects

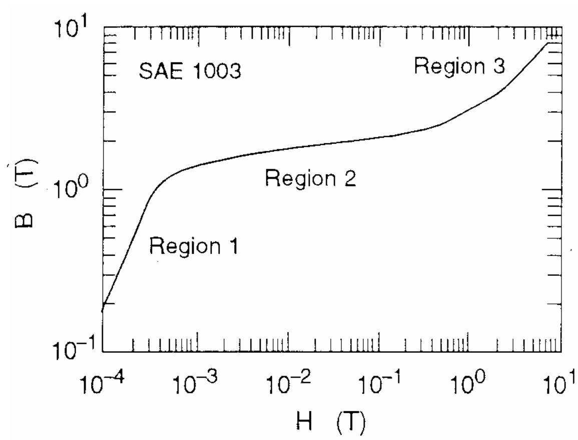

The HEBT quadrupole (12Q45)

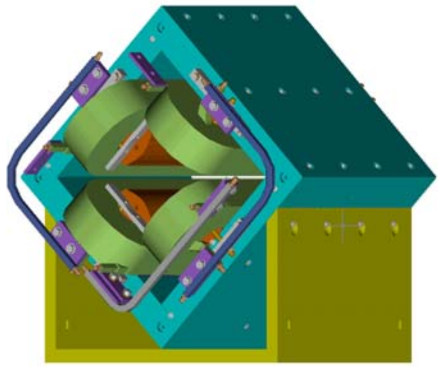

B-field Specifications:

$B_{pole\text{-}tip}$=2.5 kG

$\int b_1 dz/L_{eff}$= 0.42 kG/cm

$B_r=b_1 r\cos(2\theta) + b_5 r^5\cos(6\theta)+\ldots$

$\int(b_5 r^5.dz)/\int(b_1 r.dz) \leq 10^{-3}$ at r=5 cm

Cross section of 1/8th of the 12Q45 Quad

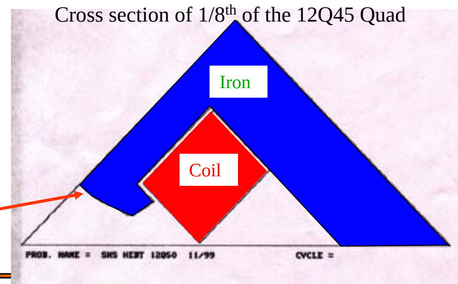

2D-model of 1/8th of quad to minimize the 12th pole mult. inside the magnet by shaping the contour of the pole-face.

HEBT dipoles (8D533 and 8D406)

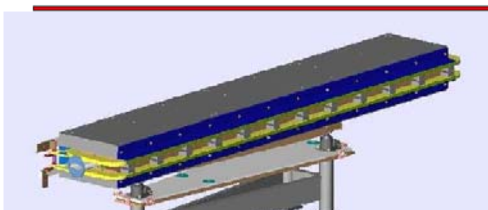

θ = 11.25°, 8.75°

$\int\{b_0\,dz\}$=(1120.1 , 870.2) [kG.cm]

$b_0 \leq 2.10$ kG T=1 GeV H^- (H^- stripping)

$B_y= b_0 + b_1 x + b_2 x^2 + \ldots$

$\int\{b_1 x+b_2 x^2+..\}dz/\int\{b_0\,dz\} \leq \pm 10^{-3}$ r=±8 cm

Δ_{xmax}(displ c-line)= ±(6.55, 3.96) [cm]

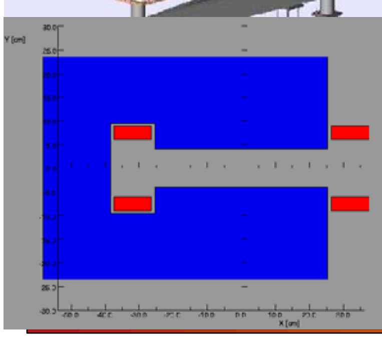

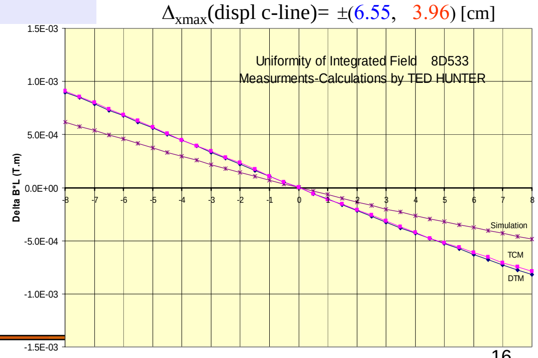

The HEBT and ring arc quad (21Q40)

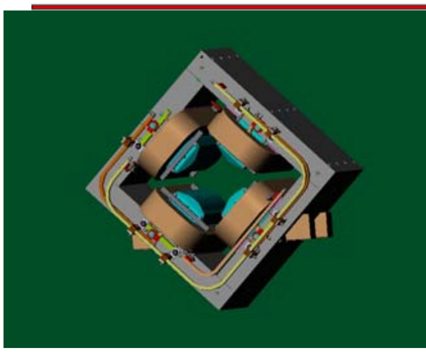

n	a_n	b_n
0	-1.4	-58.1
1	0	10000
2	-0.09	1.64
3	-0.16	1.38
4	0.03	0.08
5	0.1	1.49
6	0.03	-0.09

Integrated Field Meas. r=7 cm I=755 A
Measuring coil 2.1m long and 15.25 cm in diameter

$B_{pole\text{-}tip}$=4.91 kG

$\int b_1 dz/L_{eff}$= 0.468 kG/cm

$\int(b_5(r).dz)/\int(b_1(r)dz) \leq 10^{-4}$ r=7 cm

dz=2.4 cm dr=2.01 cm (r=10cm)

$\int\{b_5(r)dz\}/\int\{b_1(r)dz\} = 2.8\times10^{-4}$ measur.

$\int\{b_5(r)dz\}/\int\{b_1(r)dz\} = 3.7\times10^{-4}$ 3D Calc.

Quadrupole prototype measurements

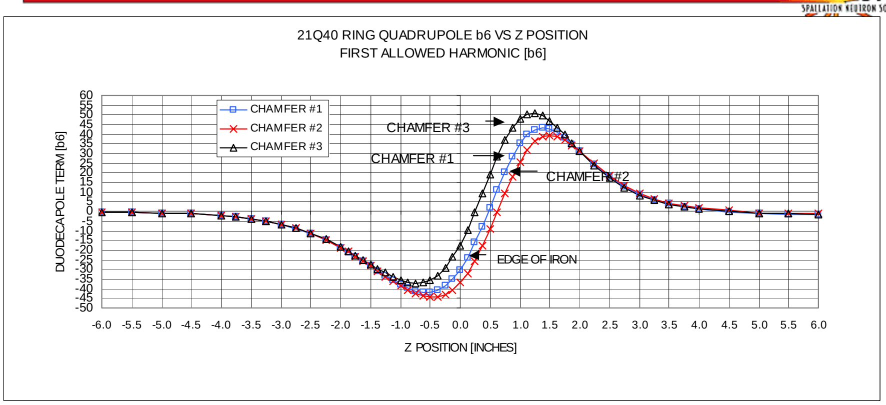

Chamfer optimization for the local correction of the dodecapole harmonic on the 21Q40 quadrupole prototype (final integrated b6 = 1.6 units with chamfer #3)

SNS ring injection layout

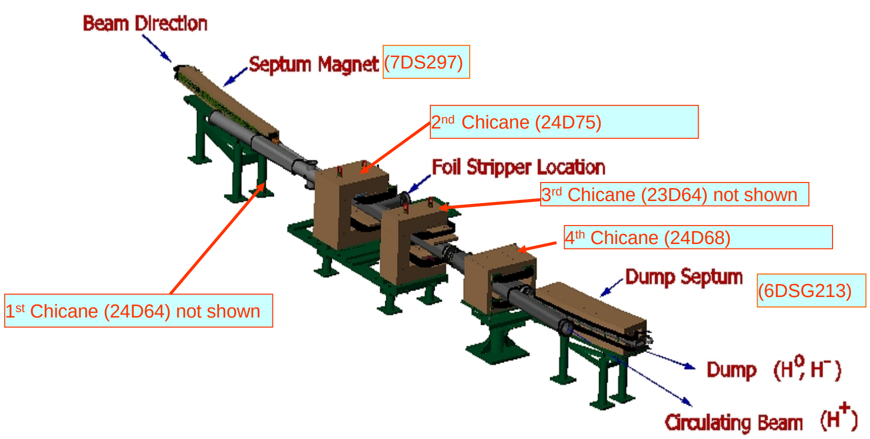

The injection septum (7DS297)

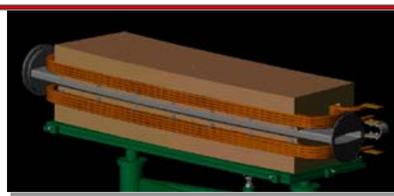

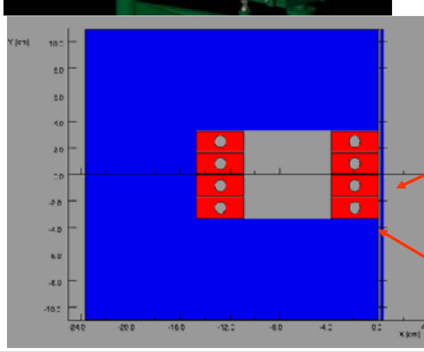

$\theta = 6.3^{o}$ $B_y \le 2.03$ kG for T=1 GeV H^-

$\int\{B_y\, dz\}$=622.0 [kG.cm]

2D Calculations:

$B_y = b_0 + b_1 x + b_2 x^2 + \ldots$

$\{b_1 x + b_2 x^2 + \ldots\}/\{b_0\} \le \pm 1\mathrm{x}10^{-4}$ x={-3,3} [cm] $B_{mod(fringe-field)} < 1$ Gauss

Δx_{max} (max displ from c-line)= ±2.1 [cm]

$B_{mod(fringe-field)} < 1$ Gauss

Magnetic shield

1^{st} chicane dipole (24D64)

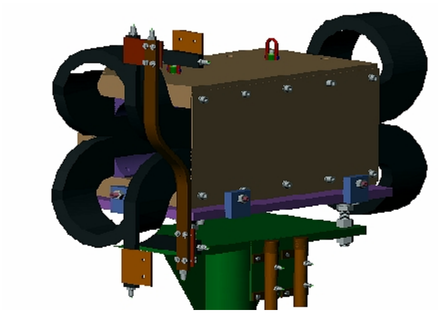

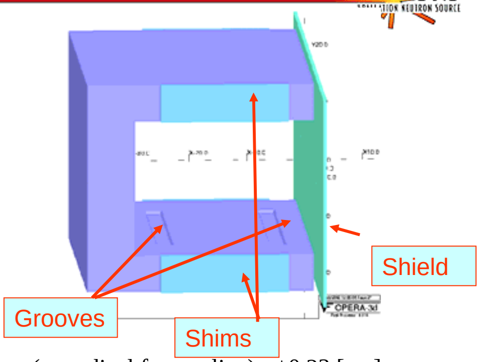

$\theta = 2.4^o$ $b_0 \le 2.72$ kG for T=1 GeV p Δx_{max} (max displ from c-line)= ± 0.23 [cm]

$\int\{b_0\, dz\}$=238 [kG.cm]

$\int\{B1^{st}_y(z) + B2^{nd}_y(z) + B3^{rd}_y(z) + B4^{th}_y(z)\}\, dz \le 10^{-3}$ (over beam)

$\{\int b_1(r) + b_2 r^2 + \ldots\}dz / \{\int b_0\, dz\} \le 10^{-3}$ -7 [cm]$\le r \le$ 7 [cm]   3D-Calc.

The 2^{nd} and 3^{rd} chicane dipoles

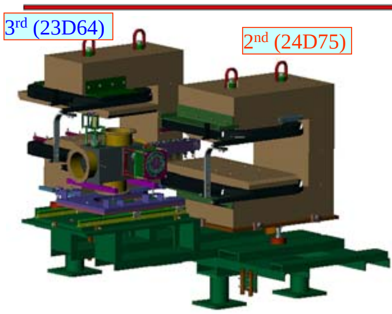

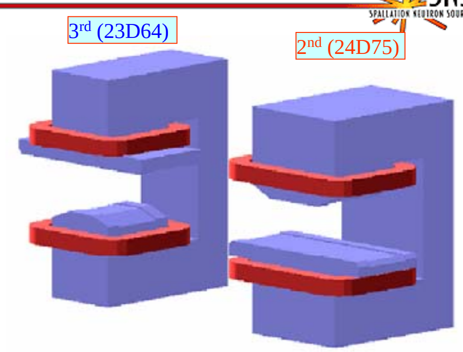

- $B2^{nd}_y(0) \le 3.0$ kG , B_y(foil) $\cong$2.5 kG $B3^{rd}_y(z) \le$2.5 kG (min. $(H^0)^*$ stripping)
- $\int\{B2^{nd}_y(z) + B2^{nd}_y(z)\}dz$=500 [kG.cm]
  - $\theta = \tan^{-1}(B_z(\text{foil})/B2^{nd}_y(\text{foil})) \ge 65$ mrad (minimize hit of foils by e^-)
  - $\int\{B1^{st}_y(z) + B2^{nd}_y(z) + B3^{rd}_y(z) + B4^{th}_y(z)\}\, dz \le \pm 10^{-3}$ (over beam)

The 4th chicane dipole (24D68)

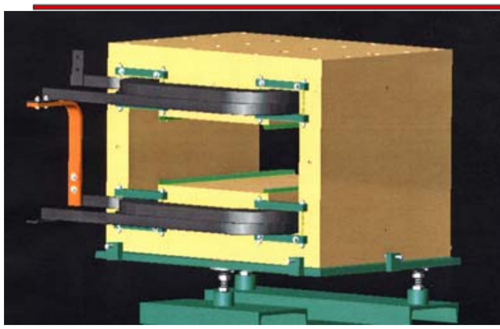

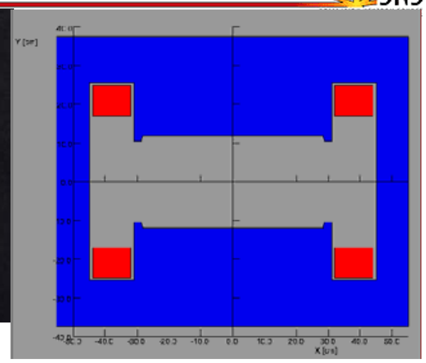

$\theta = 2.75^o$ $B_y \leq 2.95$ kG (T=1 GeV p) $\int\{B_y\, dz\}$=262.0 [kG.cm]

Δx_{max} (max displ from c-line)=±0.28 [cm]

$B_y = b_0 + b_1 x + b_2 x^2 + \ldots$

$\{b_1 x + b_2 x^2 + \ldots\}/\{b_0\} \leq \pm 1\text{x}10^{-5}$ -10 [cm]≤x ≤ 10 [cm] (2D-calc)

The ring dump dipole (6DSG213)

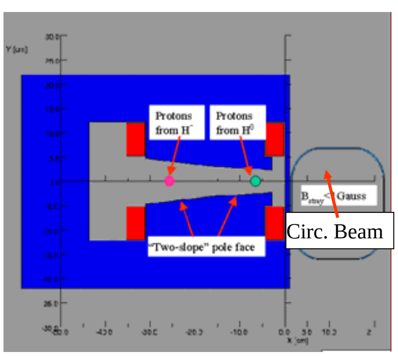

Δx_{max} (max displ from c-line)=±0.0 [cm]

	H^- Location	H^0 Location
B_0 [kG]	3.333	5.226
G[T/m]	1.0515	1.0515
$b_{sext} r^2/b_0$ (at r=1cm)	$\leq 0.5\text{x}10^{-3}$	$\leq 0.5\text{x}10^{-3}$

Doublet quadrupoles (30Q44, 30Q58)

$B_{pole\text{-}tip}$=6.5 kG $\int b_1 dz/L_{eff}$= 0.433 kG/cm $B_r=b_{1(}r)\cos(2\theta)+b_5(r)\cos(6\theta)+..$

$\int(b_5(r)dz)/\int(b_1(r)dz) \leq 3\text{x}10^{-4}$ at r=13 cm

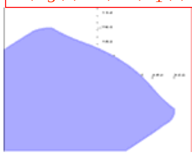

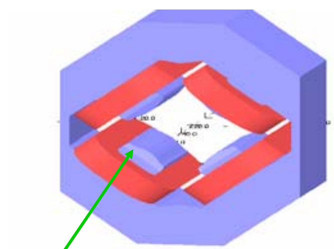

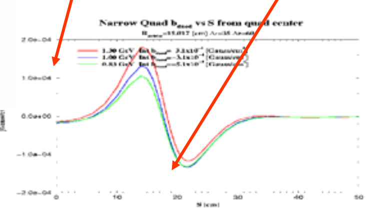

Iron Edge

Magnet center

Using 2-D model shape contour of pole face to min. $(b_5 r^5)/(b_1 r)<2\text{x}10^{-4}$

Using 3-D model chamfer the edge of pole to min. $\int b_5(r)dz/\int b_1(r)dz<3\text{x}10^{-4}$ r=13 cm

Long and Short Kickers for Beam-Painting

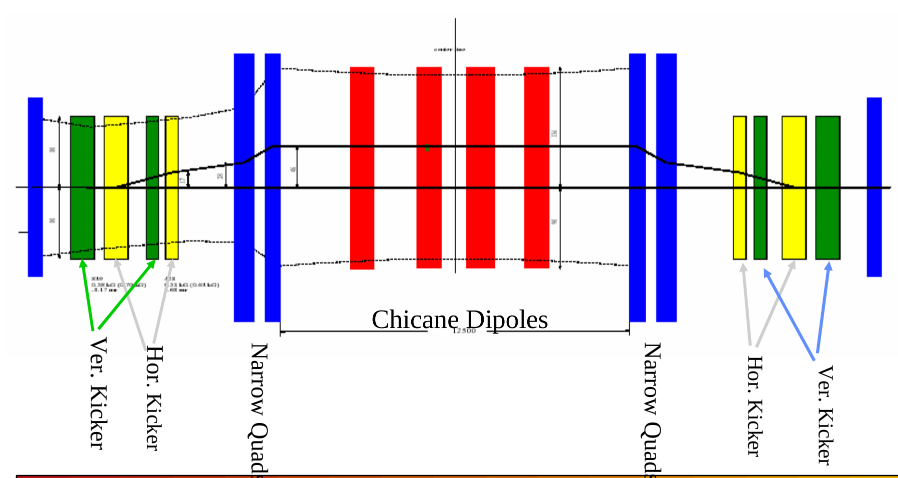

Injection Kickers parameters

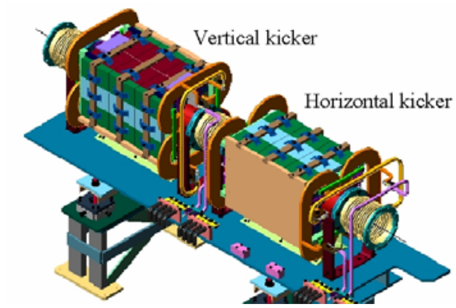

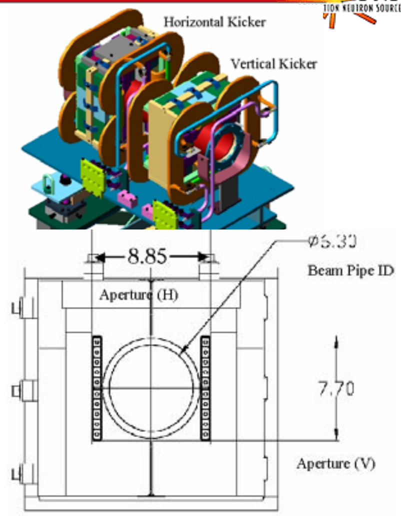

	V [cm]	H[cm]	L [cm]	ID [cm]	Bdl [kGcm]	Trise[nsec]
LONG	19.5	22.5	64	16	65.8	200
SHORT	21.6	24.5	21	18.5	26.9	200

Ring half-cell assembly (17D120, 21Q40, 27CDM30, 21CS30)

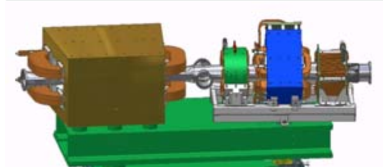

n	b_n (exp)	b_n (std-dev)	b_n 3D Calc
0	10000	0	10000
1	-105.16	0.14	-106.1
2	0.3	0.43	4.2
3	2.11	0.16	1.7

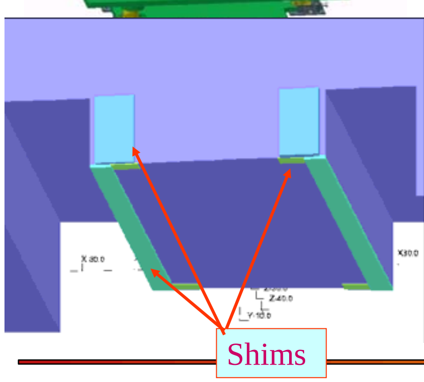

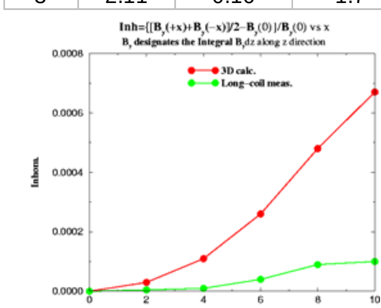

Wide arc Ring Quad (26Q40)

$B_{pole-tip}$=6.10 kG

$\int b_1 dz/L_{eff}$= 0.469 kG/cm

3-D Calc. W. Meng ΔR=5.1 [cm] Δz=2.54 [cm]

$\int(b_5(r)dz)/\int(b_1(r)dz) \leq 1.9\text{x}10^{-4}$ at r=10 cm

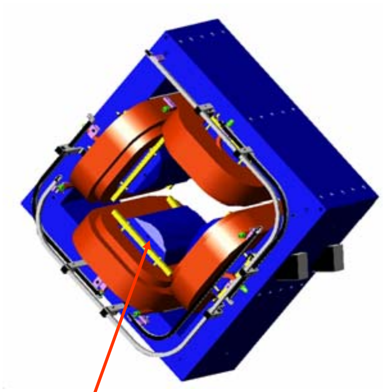

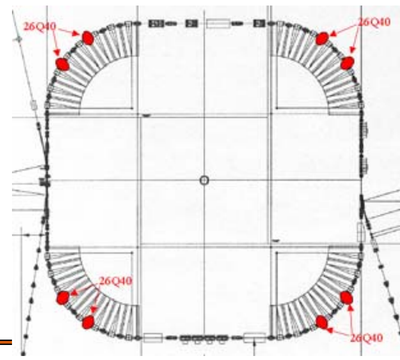

Chamfer ΔR=5.1 [cm] Δz=2.54 [cm]

3-D Calc. W. Meng

Chromaticity Sextupoles (21S26,26S26)

$B_{pole-tip}$=2.6 kG $B_{pole-tip}$ =4.1 kG

$\int b_2 dz/L_{eff}$= 0.705 kG/cm^2

$\int(b_8(r).dz)/\int(b_2 r^2.dz) \leq 5\text{x}10^{-4}$ at r=10 cm

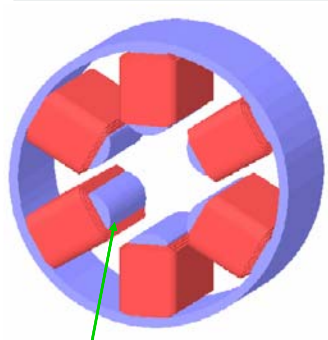

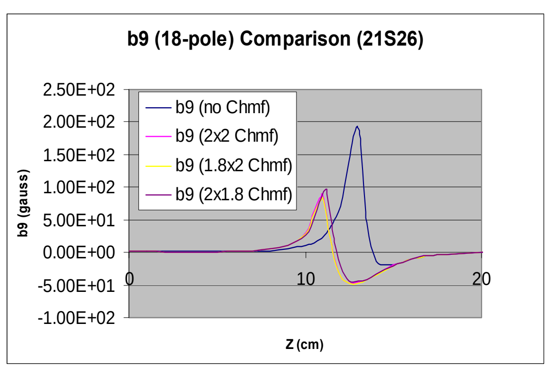

Chamfer ΔR=2.0 [cm] Δz=1.8 [cm]

3-D Calc. W. Meng

The Extraction Region with 14 kickers and Septum

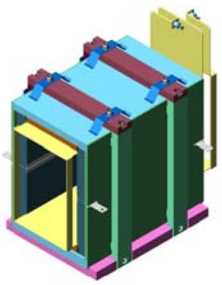

Magnet Type :WF (Ferrite)
Ferrite Length : 0.35 m
$\int Bdl$: 9.5 to 6.5 kGauss.cm
Gap (Hor.) : 13.8 to 19 cm
Width(Vert.): 13.1 to 24.8 cm
Rise time to 95% : 200 nsec
Maintain peak field: 750 nsec

Single kicker 3-D Calc.
$\int Bdl$=7.0 kGauss.cm/kicker
L=0.81 μH/kicker

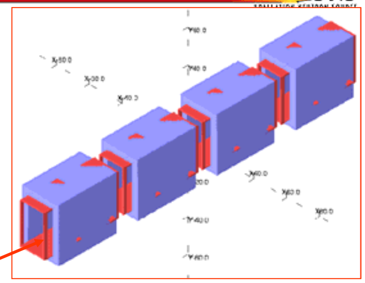

4-Kickers in Tandem
$\int Bdl$=6.75 kGauss.cm/kicker
L=0.87 μH/kicker

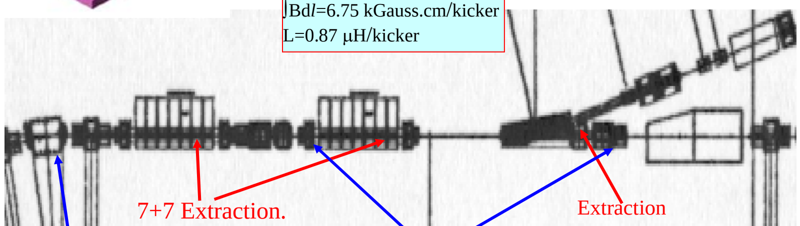

Extraction Septum Magnet (17ELS244)

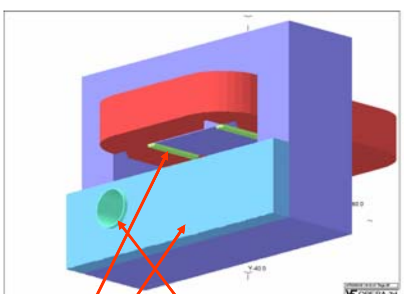

Bend Angle : 16.8^0
Field Un. : $\Delta(\int Bdl)/(B_0 L_{eff}) \leq \pm 1\times10^{-3}$
Iron Length : 2.44 m
$\int Bdl$: 1.58 Tm for 1.0 GeV
Magnet Gap : ~16.5 cm
Septum thickness : 1 cm
Pipe ID Circ Beam : 17.5 cm
$\int Bdl$ at Circ Beam : ≤500 Gauss.cm

“Shims” of the Lambertson Septum

“Field Clam” and “Magnetic-pipe” to reduce stray fields at the circulating beam region

The B_{mod} of the stray fields at the center of the pipe of the circulating beam with and without “Field Clam”

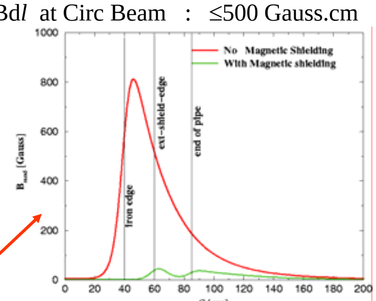

The RTBT (17D244) 16.8^{O} H-Dipole

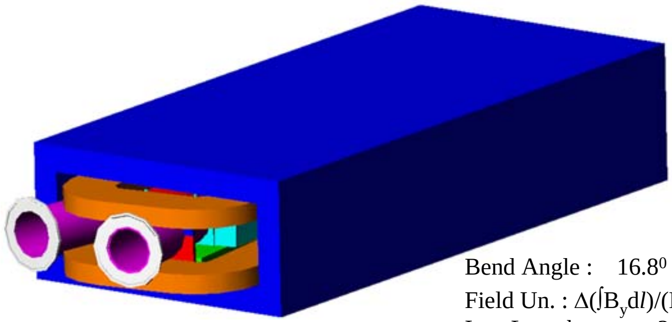

Bend Angle : 16.8^{0}
Field Un. : $\Delta(\int B_y dl)/(B_0 L_{eff}) \leq \pm 1\mathrm{x}10^{-3}$
Iron Length : 2.44 m
$\int Bdl$: 1.58 Tm for 1.0 GeV
Magnet Gap : ~16.5 cm
Septum thickness : 1 cm
Special Vacuum Chamber

The Corrector Multipole 27CDM30

Dipole and Quad windings

Windings for Sextupole

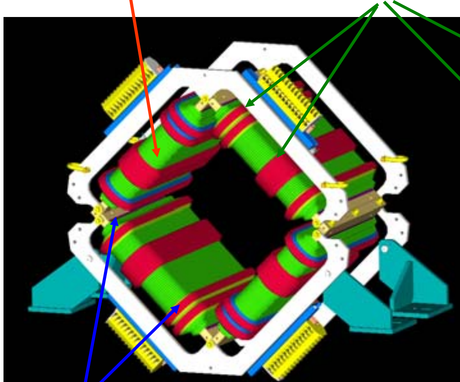

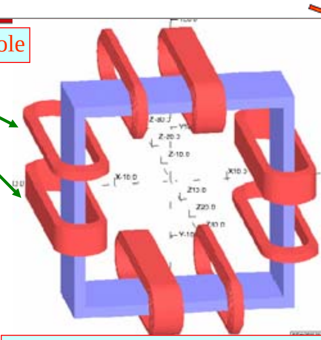

Windings to minimize
Sextupole due to dipole

$B_r = b_0 + a_1(r)\cos(3\theta) + a_2(r)\cos(3\theta)$
dip. sq_quad sq_sext
$\int b_0 dz$ 8.2 [kGcm] at r=10 [cm]
$\int a_1(r)dz$ 0.27 [kG] at r=10 [cm]
$\int a_2(r)dz$ 0.066 [kGcm^{-1}] at r=10 [cm]
The sextupole due to dipole minimized:
$\int b_n(r)dz/\int b_0 dz < \pm 2\mathrm{x}10^{-3}$ r=10cm

Dipole and Skew Quad (36CDM30) Dipole & (16CD20)

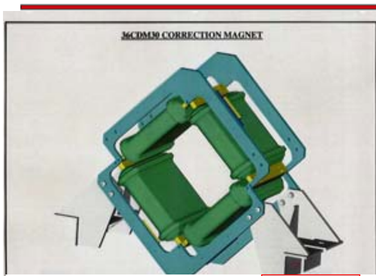

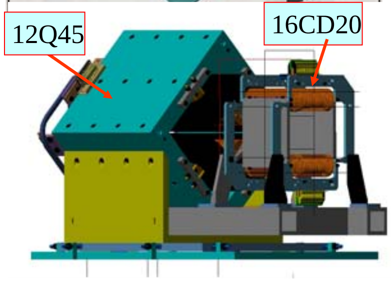

36CDM30

$B_r = b_0 \;+\; a_1(r)\cos(3\theta)$

dip. sq_quad

$\int b_0 dz$ 8.5 [kGcm] at r=10 [cm]

$\int a_1(r) dz$ 0.33 [kG] at r=10 [cm]

The sextupole due to dipole minimized:

$\int b_2(r)dz / \int b_0 dz < \pm 2\times10^{-3}$ r=10cm

16CD20

$\int b_0 dz = 7.5$ [kGcm]

$\int b_2(r)dz / \int b_0 dz < \pm 2\times10^{-3}$ at r=10cm

41CD30 Corrector

41CD30 CORRECTION MAGNET

MATERIALS:

WIRE: AWG #6, Copper .162 dia.
AMIDE-IMID RESIN + A COAT OF POLYAMIDE RESIN
PACKING FACTOR 10% = .178 dia.
WEIGHT OF COPPER: 177 lb./leg
TOTAL MAGNET WEIGHT: 1200 lb.
CURRENT: 13 AMPS

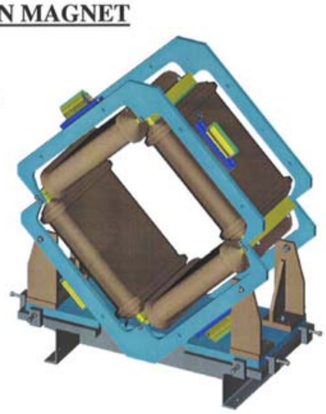

WIRE TURNS:

DIPOLE: 291 + 44 turns/leg FOR CORRECTION COILS
QUADRUPOLE: 374 turns/leg

RESISTANCE:

DIPOLE & CORRECTION COILS – 1.40 ohms
QUADRUPOLE – 1.7 ohms

FIELD:

DIPOLE – 3 LAYERS, INTEGRATED FIELD = 9805 Ga.cm.
QUADRUPOLE – 4 LAYERS, INTEGRATED FIELD @ CENTER = 295 Ga.
DIPOLE CORRECTION COILS (SEXTUPOLE) = 0.052 Ga./cm.

Sextupole corrector (21CS26) and Octupole corrector (21CO26)

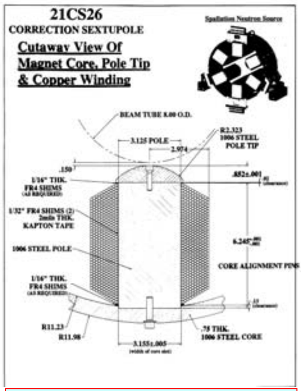

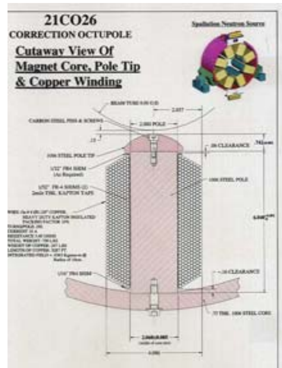

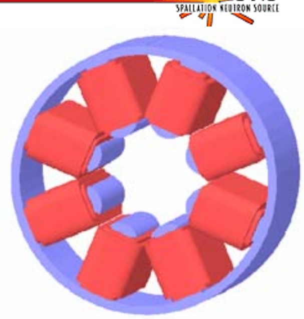

3-D view from the modeling of 21CO26

Pole cs with coil 21CS26
$\int b_2 dz = 0.20$ [$kGcm^{-1}$]
at r=10cm

Pole cs with coil 21CO26
$\int b_3 dz = 0.036$ [$kGcm^{-2}$]
at r=10cm

Quadrupole / corrector interference

- Fringe-field interference studies between adjacent quads and correctors. Steel to steel distance fixed at 20cm.

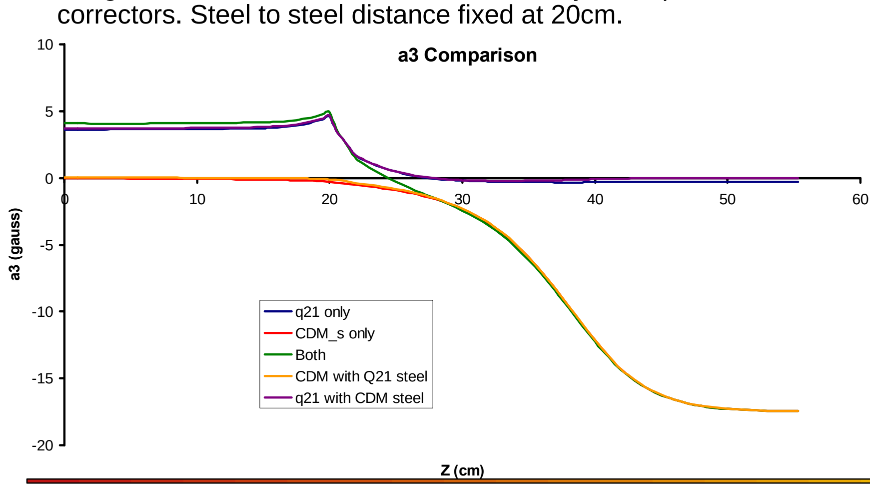

Dipole point coil measurements

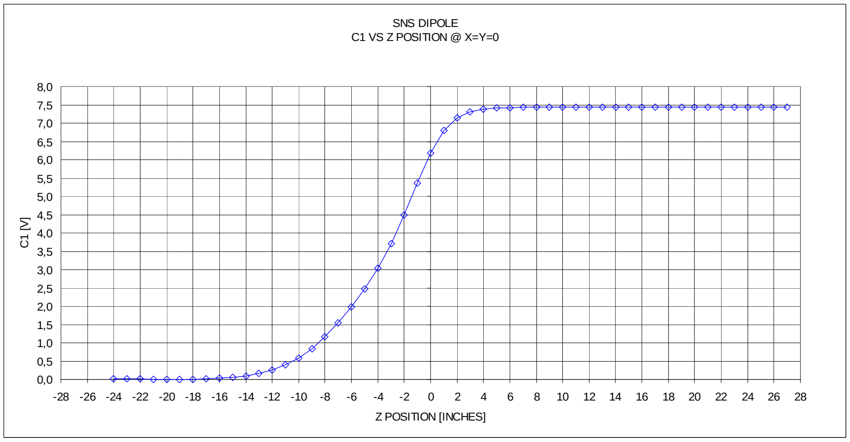

Prototype ring dipole measurements

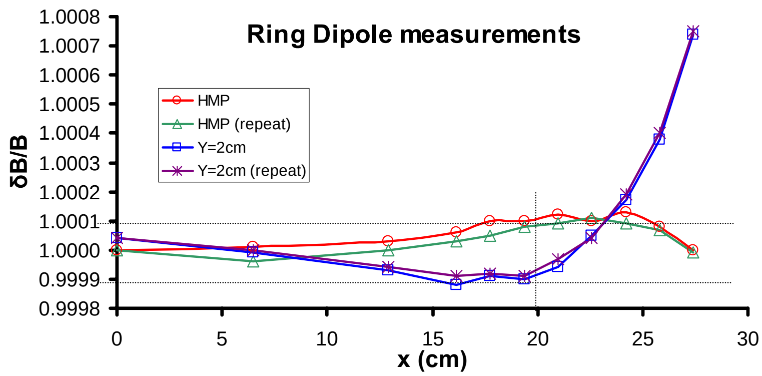

- Normal aperture quadrupole measured and first article purchased
- 1.3 GeV compatible dipole achieved required field non-uniformity level with optimized bumps

Production Dipole measuring equipment

- Rotating coil to measure ***integral*** field harmonics.

(2.49 m long; 163.8 mm diameter; 5 windings)

- Magnet is placed on a level stand.
- Measuring coil is nominally centered axially in the magnet.
- Measuring coil can be moved laterally to scan the entire magnet aperture.
- Measuring coil has survey fiducials to locate its position relative to the magnet.

- Magnet is placed on a level stand.
- Measuring coil is nominally centered axially in the magnet.
- Measuring coil can be moved laterally to scan the entire magnet aperture.
- Measuring coil has survey fiducials to locate its position relative to the magnet.

Field Scans at a Fixed Current

- The entire aperture region is scanned in 5 separate measurements at different lateral positions of the measuring coil (Center, ±2″ and ±4″)

- 5 readings are taken at each position to ensure data quality. Typical noise in integral T.F. is ~0.002%

- Entire scan is done for two currents:
  I = 4395A (1.11 T.m, 1.0 GeV), and
  I = 5409A (1.33 T.m, 1.3 GeV)
- Measurements are done on the down ramp after one cycle to I_{max} (I_{max} = 4834A for 1.0 GeV and 5450A for 1.3 GeV).

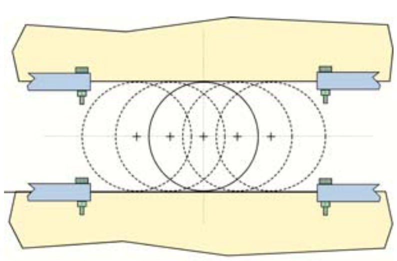

SNS DIPOLE MEASUREMENTS: FIVE HORIZONTAL POSITIONS; 2 INCHES APART

SD1701 Integral dipole field quality @ horizontal center

Integral Transfer Function: 0.25279 T.m/kA

Integrated Dipole Field at 4380 A: 1.1072 T.m (1 GeV)

Integral Normalized Harmonics in "units" of 10^{-4} at 80 mm radius

n	b_n	a_n	n	b_n	a_n
1	–105.21	1.10	8	–0.02	–0.01
2	0.30	–0.53	9	–0.17	–0.01
3	2.10	–0.05	10	–0.32	0.00
4	0.98	0.07	11	0.14	0.01
5	0.08	0.00	12	0.32	0.00
6	–0.27	0.02	13	–0.10	–0.01
7	0.19	0.02	14	–0.32	0.00

SD1701 vertical field profile

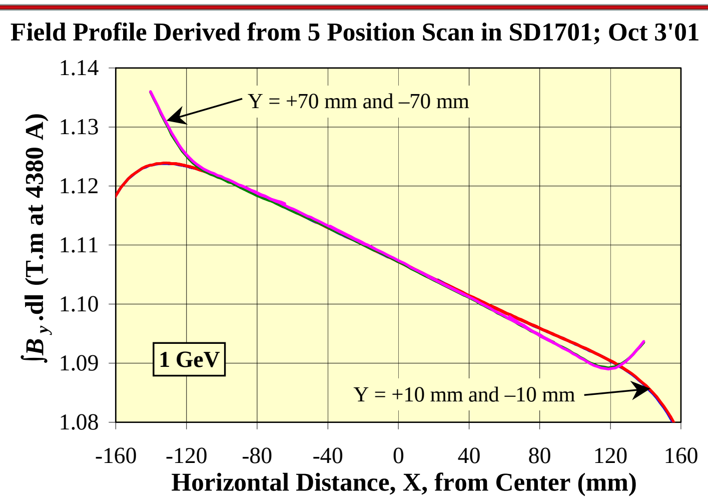

SD1701 horizontal field profile

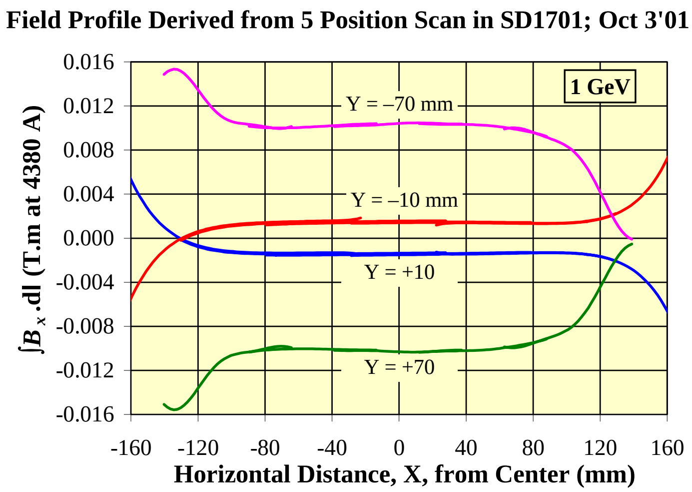

Field Quality as a Function of Current

- The field quality is also measured as a function of current in the central region of the magnet.
- Measurements are done on a down ramp after cycle to (4834A for 1.0 GeV and 5450A for 1.3 GeV).
- Measurements are done at 4395A, 4300A, 4200A, 4100A, 4000A, 3900A and 3770A for 1 GeV cycle.
- Measurements are done at 5409A, 5350A, and 5300A to 4500A in 100A steps, in addition to the I_{max} currents listed above, for the 1.3 GeV cycle.

Integral Transfer Function Problems

Measurement Type	1.0 GeV	1.3 GeV
Positive Polarity, 1st Measurement	0.25178	0.24554
Negative Polarity	0.25177	0.24554
Positive Polarity, 2nd Measurement	0.25178	0.24553
Positive to Negative agreement	0.003%	0.000%
Positive-1 to Positive-2 agreement	0.001%	0.002%
SD1704 relative to current mean	-0.225%	-0.159%

- After the first few magnets were measured, the integral transfer function began to show large magnet to magnet variation (up to ~0.25% from mean).
- Possible sources of measurement errors were ruled out by incorporating redundant current readouts, carrying out NMR measurements and measuring a previously measured magnet again.
- Possible role of remnant magnetization of iron was ruled out by carrying out measurements for negative polarity of current, and then for the positive polarity again. The results were insensitive to the polarity.

Shimming of the Dipoles

- After carefully considering several correction options, it was decided to use iron shims to correct the integral transfer function in all dipoles.
- The transfer function could be either reduced (by adding shims to the return legs) or increased (by adding shims under the pole), without requiring expensive and risky machining operations.
- POISSON (2-D) and TOSCA (3-D) calculations were carried out to verify that no unwanted harmonics were generated by shimming, even for the extreme cases.
- Two dipoles (one low and one high ITF) were shimmed on an experimental basis to verify the effectiveness of the shimming procedure. The results were as expected.

Magnet	Present Status	Measured I.T.F. (T.m/kA)	Deviation from Mean	Shim thickness (mils)	Location	Magnet Offset if not shimmed further
SD1701	+2 mil shims OK to use	0.25238	-0.008%	–0.5	Not Needed	0.622 mm
SD1703	+5 mil shims To be reshimmed	0.25246	0.024%	+1.6	Return Leg	-1.811 mm
SD1704	To be shimmed	0.25178	-0.245%	–16.4	Pole	18.688 mm
SD1705	+10 mil shims OK to use	0.25241	0.004%	+0.3	Not Needed	-0.320 mm
SD1708	To be shimmed	0.25272	0.127%	+8.5	Return Leg	-9.660 mm
SD1709	–15 mil shims To be reshimmed	0.25231	-0.035%	–2.4	Pole	2.687 mm
SD1710	To be shimmed	0.25206	-0.136%	–9.1	Pole	10.363 mm
SD1711	+8 mil shims OK to use	0.25243	0.012%	+0.8	Not Needed	-0.890 mm
SD1714	+7 mil shims To be reshimmed	0.25247	0.029%	+2.0	Return Leg	-2.228 mm
SD1715	To be shimmed	0.25231	-0.034%	–2.3	Pole	2.626 mm
SD1717	OK to use	0.25240	0.000%	–0.0	Not Needed	0.006 mm
SD1718	To be shimmed	0.25262	0.087%	+5.9	Return Leg	-6.659 mm
SD1719	OK to use	0.25240	0.001%	+0.1	Not Needed	-0.109 mm
SD1721	OK to use	0.25238	-0.010%	–0.6	Not Needed	0.731 mm
SD1722	OK to use	0.25241	0.002%	+0.1	Not Needed	-0.157 mm
SD1724	+9 mil shims OK to use	0.25242	0.007%	+0.5	Not Needed	-0.552 mm

Integral transfer function (1 vs 1.3 GeV)

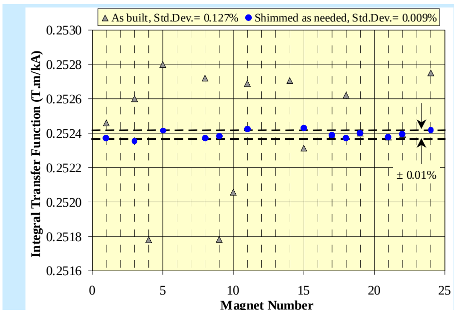

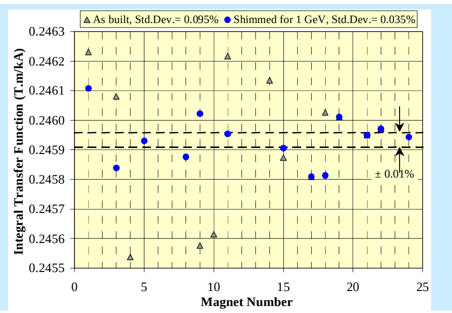

- Shimming is optimized for 1.0 GeV operation (16X reduction in standard deviation).
- Standard deviation at 1.3 GeV operation is also reduced, but only by a factor of ~2.7.

Excitation curves (1.3 GeV cycle)

- After shimming the ITF rms dropped by a factor of two

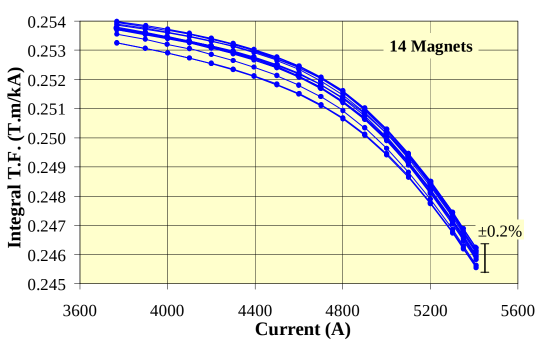

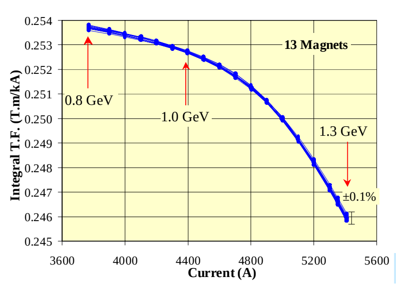

Multi-pole components before and after shimming

	Before	After	Change		Before	After	Change
I.T.F.	0.25280	0.25242	**-0.152%**				
b1	-104.879	-104.850	**0.029**	**a1**	-0.290	-0.302	**-0.012**
b2	-0.415	-0.462	**-0.047**	**a2**	-0.441	-0.473	**-0.032**
b3	2.137	2.146	**0.010**	**a3**	-0.064	-0.080	**-0.015**
b4	1.591	1.557	**-0.034**	**a4**	0.030	0.029	**-0.001**
b5	-0.111	-0.112	**-0.002**	**a5**	-0.061	-0.056	**0.005**
b6	-0.529	-0.531	**-0.002**	**a6**	0.022	0.018	**-0.004**
b7	0.270	0.268	**-0.002**	**a7**	0.106	0.104	**-0.002**
b8	0.017	0.010	**-0.008**	**a8**	-0.016	-0.014	**0.002**
b9	-0.081	-0.084	**-0.003**	**a9**	-0.131	-0.124	**0.007**
b10	-0.237	-0.231	**0.006**	**a10**	-0.009	-0.007	**0.002**
b11	-0.032	-0.028	**0.004**	**a11**	0.142	0.135	**-0.006**
b12	0.151	0.145	**-0.005**	**a12**	0.030	0.027	**-0.004**
b13	0.061	0.057	**-0.004**	**a13**	-0.124	-0.119	**0.005**
b14	-0.117	-0.112	**0.005**	**a14**	-0.037	-0.034	**0.003**

Effective length dependence on shimming

Magnet	I.T.F. (T.m/kA)	T.F. (T/kA)	Leff (m)
SD1701 (shimmed)	0.25237	0.17544	1.4385
SD1705 (shimmed)	0.25242	0.17547	1.4385
SD1709 (1st shims)	0.25231	0.17540	1.4385
SD1710 (unshimmed)	0.25206	0.17526	1.4382
SD1711 (unshimmed)	0.25269	0.17568	1.4384
SD1714 (1st shims)	0.25247	0.17550	1.4386
Mean=	0.25239	0.17546	1.4384
Std. Dev.=	0.082%	0.077%	0.011%

Measured harmonics for the 21Q40

n	a_n	b_n
1	-1.4 †	-58.1 †
2	0	10000
3	-0.1	1.6
4	-0.2	1.4
5	0.0	0.1
6	0.1	1.5
7	0.0	-0.1
8	-0.1	-0.2
9	0.0	0.1
10	0.0	-0.5
11	0.0	0.0
12	0.0	-0.1
13	0.0	0.0
14	0.0	-0.1

- The boxed values are the integrated harmonics allowed by quadrupole symmetry
- All harmonics are on the required within the required level of 10^{-4} of the quadrupole field
- Remark: the large values on the dipole terms are due to errors of the measuring coil location (0.5mm centering error)

26Q40 quadrupole multi-poles

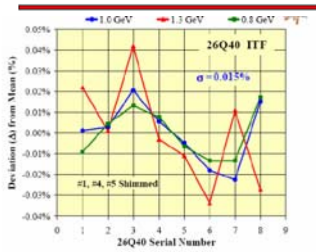

Harmonics at reference radius (480 π mm mrad)

N	RMS (10^{-4})
b_2	1.35
a_2	3.27
a_3	2.53
b_6	0.95
b_{10}	0.36

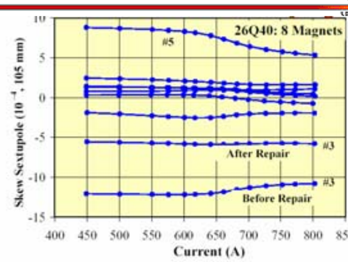

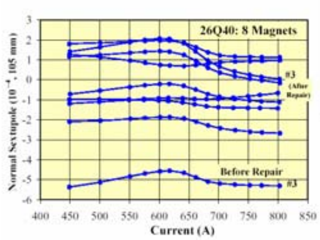

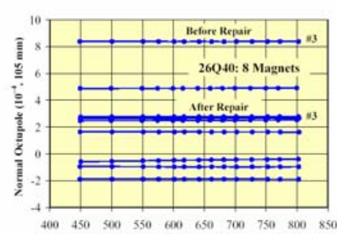

30Q58 quadrupole multi-poles

n	rms (10^{-4})
b_2	3.25
a_2	1.35
b_3	0.87
a_3	0.32
b_9	0.10

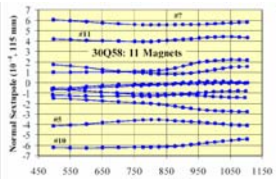

Harmonics at reference radius

Of full acceptance 480 π mm mr

- 30Q58 orientation flip
  - Earlier coil-shimming performed
  - Measurements found outstanding sextupole components
  - Reverse placement orientation of three magnets to compensate
  - Engineering & drawing changes in progress
- 30Q44 edge trimming (for 1.3 GeV)
  - Mechanical interference found with injection and extraction lines
  - Symmetrical edge trim on two quads
  - Negligible change in multipoles; 1.4×10^{-4} change in ITF (1GeV)
  - Compensating re-welding in progress to minimize ITF change at 1.3 GeV
  - Correction not needed; trim coil available

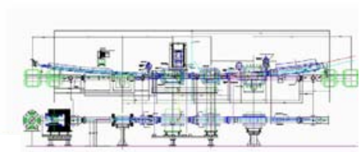

Injection chicane integral measurements

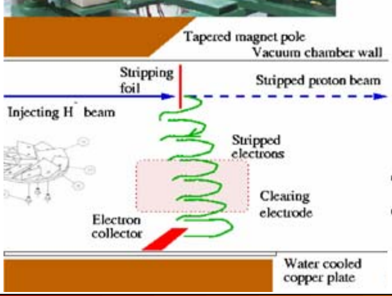

Integral Field Quality Measurements in Chicane #2 & #3

Measurements with a 40.8 mm radius, 4.75 m long coil

Harmonics expressed in 10^{-4} "units" at 80 mm radius

Harmonic	Chicane #2 (2154.8 A)	Chicane #3 (1732.0 A)	Chicane #2 (2154.7 A) + Chicane #3 (1733.2 A)
$\int B.d\ell$ (T.m)	0.3006	0.2016	0.5012
b_1	-1.8	-4.1	-1.9
b_2	-8.2	-9.4	-9.2
b_3	1.2	0.9	1.3
b_4	0.0	-0.4	-0.1
b_5	0.5	-0.7	0.0
b_6	-0.9	0.0	-0.6
a_1	116.0	-158.2	6.2
a_2	-8.0	9.6	-0.9
a_3	8.0	-11.3	0.3
a_4	-0.5	0.4	-0.1
a_5	1.5	-1.3	0.0
a_6	0.1	-0.3	0.0

- Meets integral-field goal (10^{-3})
- Compensation as predicted

Injection chicane field angle measurements

- Single Hall probe mounted on a precise aluminum cube
- Measurement of B_z/B_y
- Angle of electron-guiding field in agreement with 3D modeling

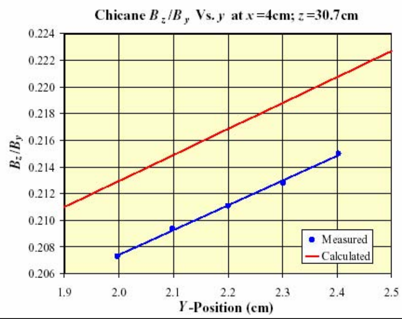

- Trajectory to electron catcher re-confirmed

SNS ring power supplies

Jie Wei (BNL)

Yannis Papaphilippou (ESRF)

June 28 – July 2, 2004

SNS power supply system

PS Function / Technology	Current [A]	Voltage [V]	Power [kW]	HEBT & linac dump	Ring & inj. dump	RTBT & ext. dump	Total
Low field	20	35	0.7	18	98	15	131
corrector /	20	75	1.5		8		8
Switchmode -	40	35	1.4		8		8
linear	40	75	3.0		8		8
	120	35	4.2			4	4
			Total	18	122	19	159
Medium range PS /	185	27	5.0			4	4
	390	24	9.4	15			15
12 pulse phase	700	18	12.6	9		5	14
controlled	900	51	45.9	4		8	12
	1300	95	123.5	1		8	9
	1405	390	548.0	1		6	7
	2400	50	120.0		1	1	2
	4000	18	72.0		6		6
			Total	30	11	28	69
Main dipole PS /	6000	440	2640		1		1
12 pulse phase controlled			**Total**	0	1	0	1
Injection bump PS	1400	800	pulsed		8		8
Switchmode			**Total**	0	8	0	8
Extraction kicker PS	2500	35000	pulsed		14		14
Blumlein PFN			**Total**	0	14	0	14
			Grand total	48	156	47	251

- Conventional for an accumulator / synchrotron
- All DC except injection and extraction.
- Adjustable for tuning and rated up to 1.3GeV operation (except extraction kickers)

Power supplies issues for RCSs

- 3 types
  - Bridge rectifiers connected to the power grid
  - Bridge rectifiers with local energy storage
  - Resonant system with local energy storage in capacitors and chokes
- Large amount of power (MW) and need for local energy storage -> resonant system (disadvantages: not a static injection, Eddy currents, high voltage by the RF)
- Control of flat bottom injection and and flat top extraction with high-frequency ac rectifiers as the Insulated Gate Bipolar Transistors (IGBT) providing maximum flexibility

Low-field corrector power supplies

- All built in a common 20 A module
- Voltage selectable at either 35 or 75 Volts
- Up to 7 of them can be put in parallel, with common reference, common readbacks and control
- The stability of the low-field correctors is of the 10^{-3} order

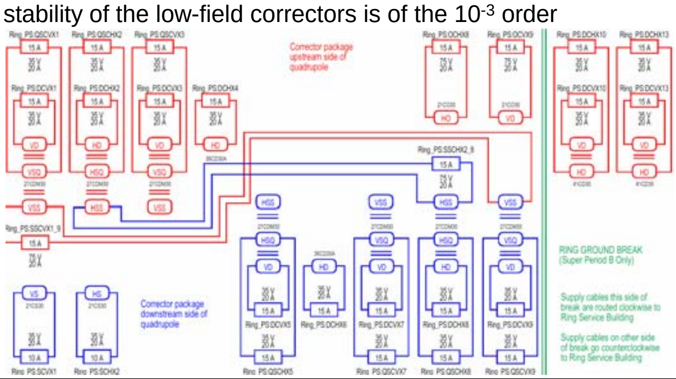

Medium-field power supplies

- Power all main elements in ring and transfer lines apart dipoles
- 69 units grouped at 12 groups to minimize cost (from 185 to 4000A)
- Ripple corrected with passive filters
- Stability requirement of 2×10^{-4} imposes specification of 10^{-4} on current stability (ability to achieve requirement even for half the max current)

5 kW To 550 kW

HEBT Dipole	3
HEBT Quad	22
L Dump Quad	4
Injection Septum	2
Injection DC	4
I Dump Quad	1
Ring Quad	6
Ring Sextupole	4
RTBT Dipole	1
RTBT Quad	19
E Dump Quad	2
Extraction Septum	1

Medium-field power supplies

4000 Amp Unit

700 Amp Unit

Medium-field power supply schedule

Milestone	Estimate/Actual
Release RFP to Procurement	Jun 29, 2001
Contract Award	Oct 31, 2001
Design Review	Feb 15, 2002
Factory Testing Starts	Dec 3, 2002
5040 A, 18V Ships	Mar 1, 2003
First 185A, 27V & 390A, 24V tested	Oct 9, 2003
First 4000A, 18V & 700A, 18V tested	Nov 21,2003
Delivery Complete All 185A, 27V	March 2004
Delivery Complete All 390A, 24V	April 2004
Delivery Complete All 700A, 25V	April 2004
Delivery Complete All 700A, 18V	May 2004
Delivery Complete All 4000A, 18V	July 2004
Last Production Article Ship	Feb 15, 2005

Ring dipole power supply

- One 6000A unit powering 32 ring magnets + reference
- Reference magnet field measured with hall probe and used to regulate ring ring magnets current
- Ripple controled with passive filter
- Regulation of 50ppm tested in low and high voltage

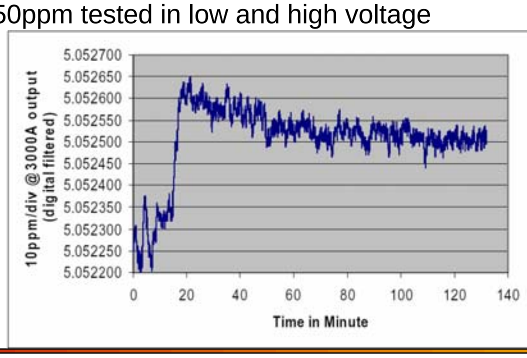

Extraction kickers power supply

- 14 pulsed units
- Repetition rate of 60Hz
- Flat top of 750 ns
- Gap of 250 ns

kicker magnet inductance		0.76 -0.8 uH	
magnet current		2 - 2.5 kA	
blumlein PFN Voltage		35 kV	
pulse current rise time		200nS	
current pulse width		750 nS	
pulse repetition		60 Hz	

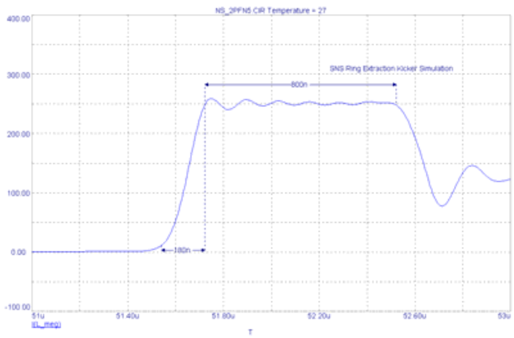

Extraction kickers prototype power supplies

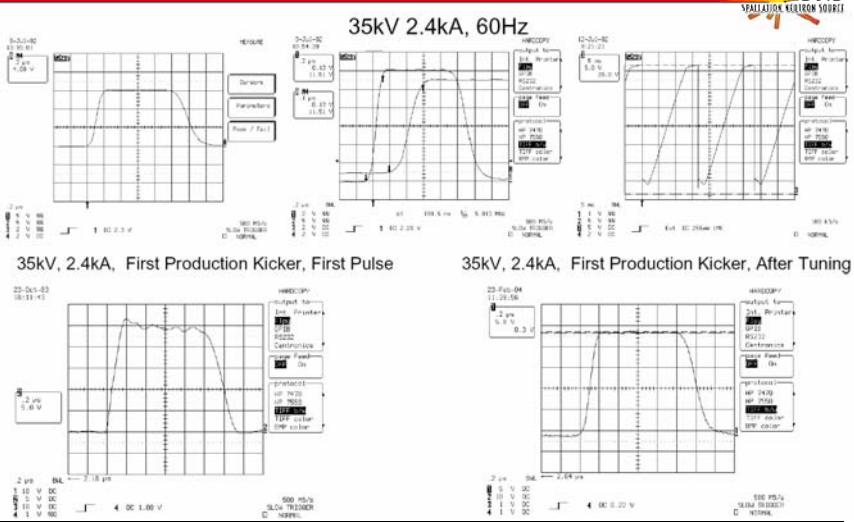

Injection power supplies

DC Voltage	0 to 800V, 0 to –800V
DC Current	0 to 1,400A max. Pulsed (400Arms equivalent)
Pulse Repetition Frequency	60Hz
Switching Frequency	108kHz
Large Signal Current Response	> 2kHz at 45° Shift at 1.4kA
Load Current Tracking	See Figure 2
Load Current Fall time	< 0.5msec. From 1.4kA to 0
Current Stability In Flat Top	< 0.1% (1.4A)
Magnet Load	L= 160μH, R=0.013Ω

- Rise time < 1 ms
- Flat top < 2ms
- Fall time < 500μs
- High frequency switching with IGBT

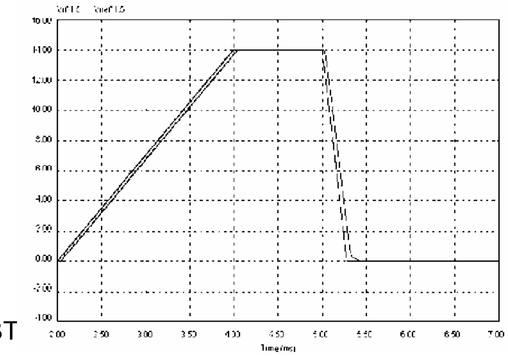

Spallation Neutron Source II
Accumulator ring & transports

Injection

Jie Wei (BNL)
Yannis Papaphilippou (ESRF)
June 28 – July 2, 2004

Outline

- Single-turn injection
- Conventional multi-turn injection
- Charge-exchange multi-turn injection
  - Transverse painting
  - Longitudinal painting
  - Horizontal-longitudinal coupled painting

Injection objective

- Inject the beam into the ring with a minimum uncontrolled beam loss
- Either preserve the emittance, or dilute the emittance in a controlled way
- System requirements
  - Field quality within tolerance
    - » Fringe field of the septum and other magnets
    - » Field profile of the injection kicker
    - » Power supply repeatability
  - Rise and fall time of the kicker within tolerance
  - RF system capable of beam loading transient effects

Single-turn injection

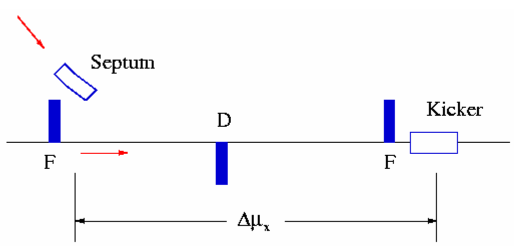

- Septum magnet (dc) and kicker magnet (ac), preferably $\pi/2$ phase advance apart
- Longitudinal matching
  - Usually at "flat-bottom"; upright ellipse
  - Adjust RF frequency for synchronization, and RF voltage for aspect ratio matching

Single-turn transverse matching

- Closed-orbit matching

$$\theta = \frac{x}{\sqrt{\beta_{sep}\beta_{kick}}}, \quad \text{and} \quad x' = -\frac{\alpha_x x}{\beta_x}$$

  - for $\pi/2$ phase advance
  - Choose locations of large β functions to minimize kicker strength
- Optics matching
  - Match $\alpha_x, \beta_x, D_x, D'_x, \alpha_y, \beta_y, D_y, D'_y$
  - Adjustable knobs in the transport line before injection

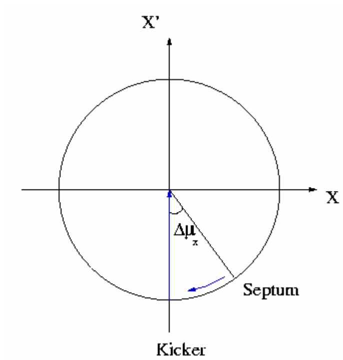

Conventional multi-turn injection

- Used to enhance intensity
- Inject at zero-dispersion region using a septum and programmed orbit bumps (several "slow" kickers)
- For n-turn injection, the final emittance satisfies (Liouville's theorem)

$$\varepsilon \geq n\varepsilon_i$$

- Mismatched injection beam to maximize efficiency

$$\frac{\beta}{\beta_i} = \frac{\alpha}{\alpha_i} = \left(\frac{\epsilon}{\epsilon_i}\right)^{1/2}; \quad \frac{\alpha}{\beta} = \frac{\alpha_i}{\beta_i} = -\frac{x'}{x}$$

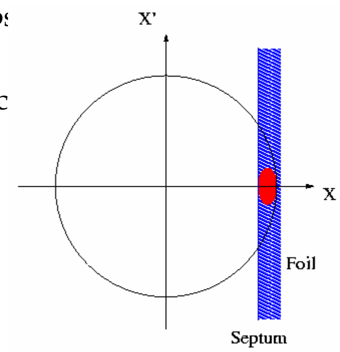

Charge-exchange multi-turn injection

- Painting for desired emittance, desired beam profile
- Stripping of H^- and H^0 requires magnet field selection (< +/-5%)
- Minimize foil hits (e.g. average 6 hits in 1000 turns): "post-stamp" foil
- Long straight for chicane module: decoupled from lattice tuning
- Quick disconnect, easy replacement: multi-foil chain
- Stripped electron collection
  - Water-cooled collector (ISIS);
  - Specially tapered magnets (SNS)
  - Mirror-field coil & magnetized surface (LANL proposal)
- Future proposal: laser stripping -- require high laser power & efficiency

Stripping of H^- and H^0

- General loss criteria for stripping in HEBT and injection:
  - < 10^{-7} per meter beam loss
- Gas stripping sets a limit on vacuum pressure
  - $5\times10^{-8} \sim 10^{-7}$ Torr
- Electro-magnetic Lorentz stripping on H^- beam
  - Mean decay length in laboratory frame

$$\lambda_s = \frac{A_{s1}}{B} \exp \frac{A_{s2}}{\beta\gamma B},$$

$$A_{s1} = (2.47 \pm 0.09) \times 10^{-6} \text{ Tm, and } A_{s2} = 15.0 \pm 0.03 \text{ T}$$

  - Less that 3 kG field for 1 GeV beam
- H^0 stripping
  - Require specific field (<+/-5% error) maintain decay lifetime of certain quantum state (n=5) H^0 from pre-mature stripping
  - Foil residing in a trailing field at 2.4 kG

SNS ring injection layout

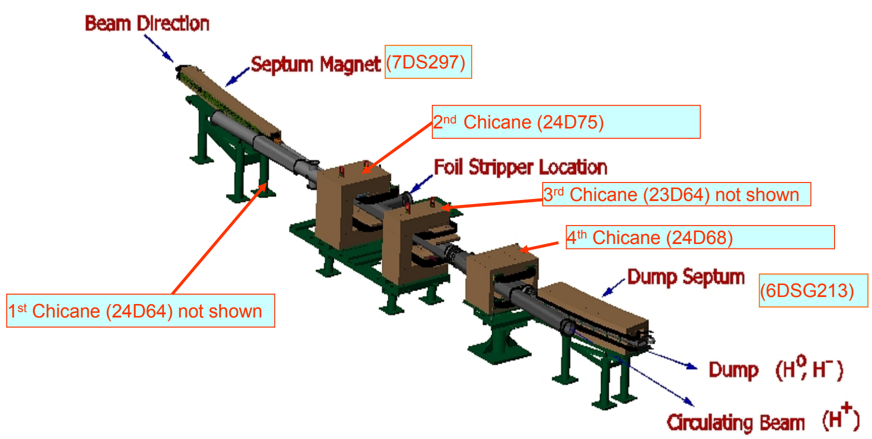

SNS injection

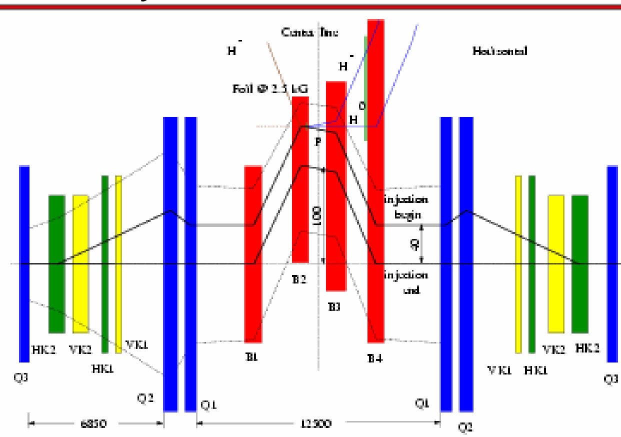

- Horizontal: 2 sets of 4-bumps super-imposed (red and green)
- Green magnets: horizontal 4-bump for painting
- Yellow magnets: vertical 4-bump for painting
- Red: fixed chicane dipoles

SNS injection (zero dispersion)

- Independent H, V, L control
- Circular & square profile both attainable
- Energy corrector & spreader in HEBT
- Tolerable to momentum errors
- Small residual $\Delta\beta/\beta$ & dispersion
- Extra space left for future upgrade to 1.3 GeV (lower field, longer length for chicane 2 & 3

Correlated painting

- Parallel horizontal and vertical orbit bumps, from small to large amplitude

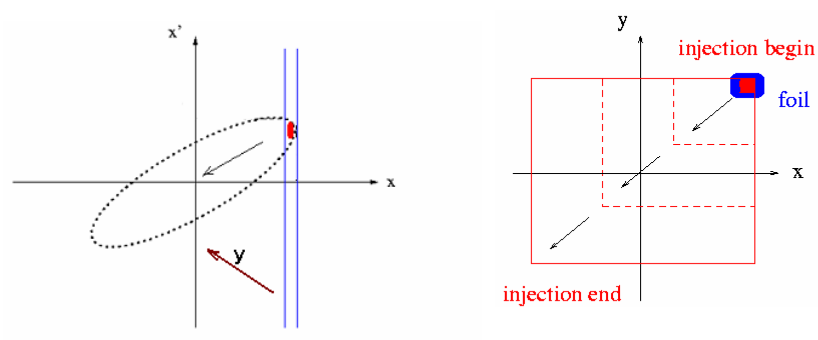

Anti-correlated painting

- Anti-parallel horizontal and vertical orbit bumps

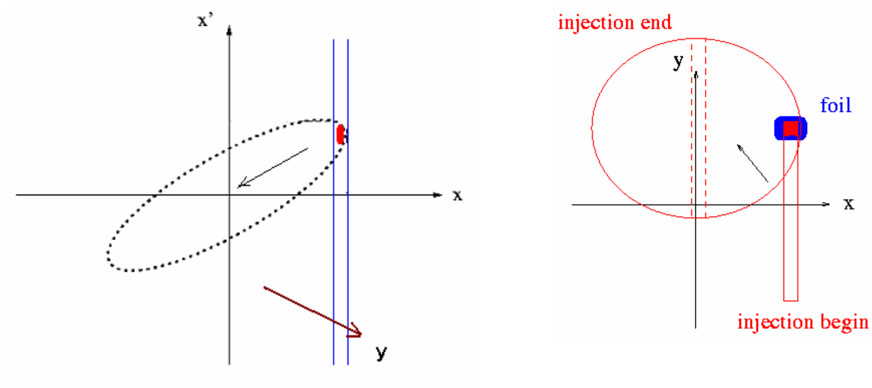

Vertical steering/horizontal painting

- Steer in one direction, painting in the other

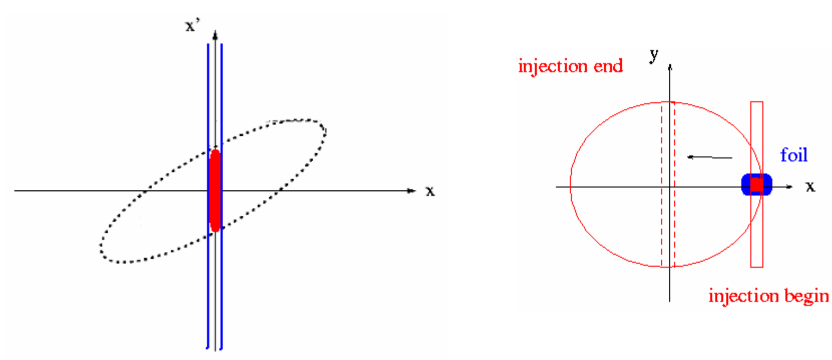

Painting scheme comparison

Scheme	Advantage	Disadvantage
Correlated	Paint over halo (square beam profile)	Singular density Coupling emittance growth
Anti-correlated	Ideal uniform distribution Immune to coupling (circular beam profile)	Halo growth due to space charge Extra 50% aperture
Coupled (correlated)	Paint over halo (diamond beam profile)	Extra acceptance needed
Paint (H) / steer (V)	Similar to anti-corr. Paint Less fast kickers	Foil support difficult suscep. to operational error
Paint (V) / steer (H)	Similar to anti-corr. Paint Less fast kickers	Vertical injection suscep. to operational error
Oscillating bump	Uniform distribution Paint over halo	Fast power supply switch Extra 50% aperture (H&V)

Space charge & halo formation

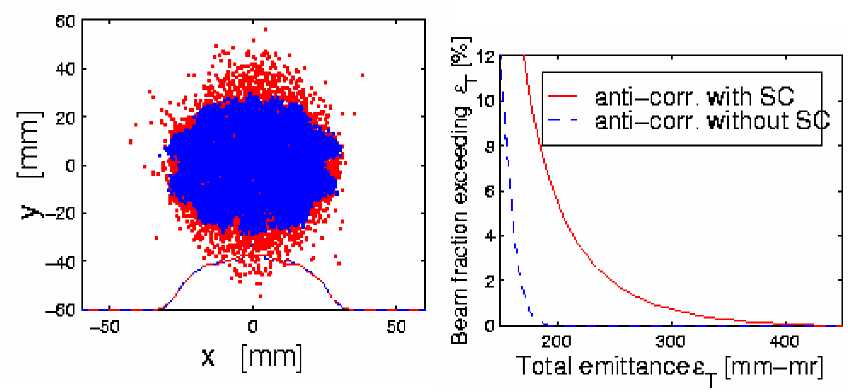

- Disadvantage of not painting over halo (vertical direction)

Collection of stripped electrons

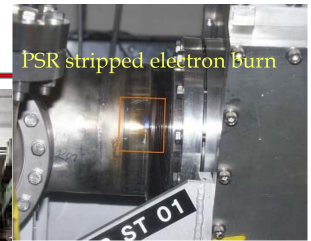

(Courtesy W. Meng, J. Brodowski, YY Lee, D. Abell, R. Macek et al)

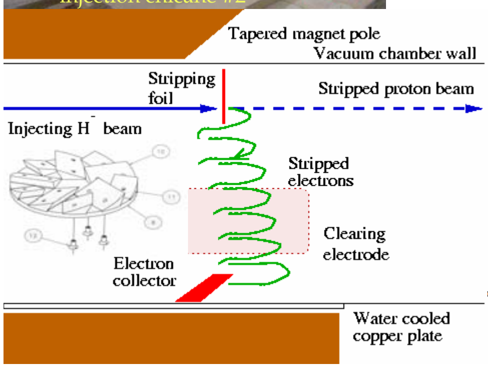

- Tapered magnet to guide stripped electrons (~ 2 kW), compensated for the circulating beam
- Carbon-carbon collector on water-cooled copper plate
- Clearing electrode (~ 10 kV) to reduce scattered electrons
- Video monitors on foil & collector

Collector material test

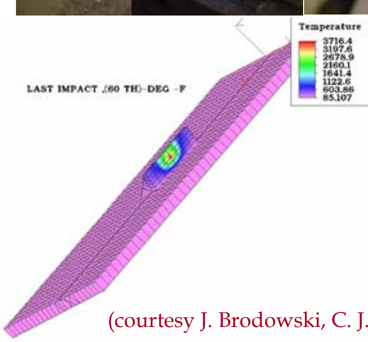

(courtesy J. Brodowski, C. J. Liaw)

- SNS electron collection
  - Special magnetic field to guide stripped electrons
  - Collector of carbon-carbon block on water-cooled Cu plate
  - Tested with touch-gun and electron welder
  - Confirmed with computer modeling of stress, heating, fatigue under pulsed mode

SNS injection foil device

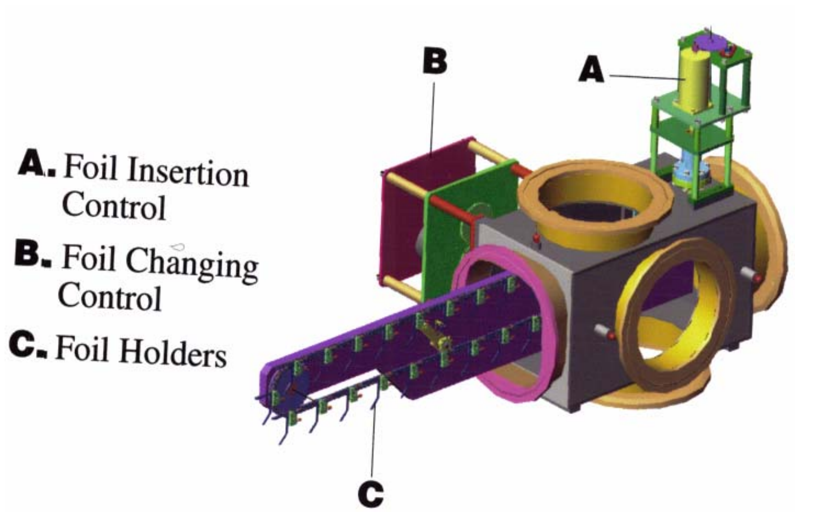

Test of ORNL/UT diamond foil at BNL

- Newly developed diamond foil tested on AGS linac with 750 keV H- beam
- Foil duration test
  - Four-side supported foil withstands an equivalent power beyond 2 MW
  - No observable damage during each 5-day testing periods
- Foil support test
  - Two-edge foil tested
  - Three-edge free-hang foils under development


(ORNL/UT diamond foil test at BNL)

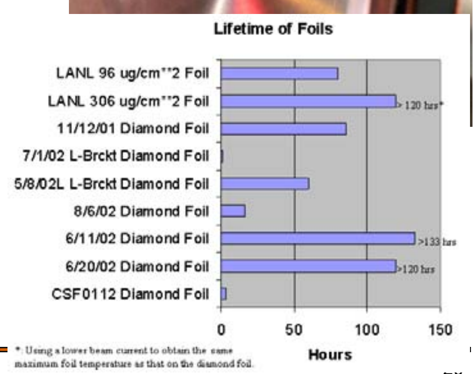

*: Using a lower beam current to obtain the same maximum foil temperature as that on the diamond foil.

(foil from ORNL/UT; C.-J. Liaw et al on test)

2^{nd} and 3^{rd} chicane dipoles

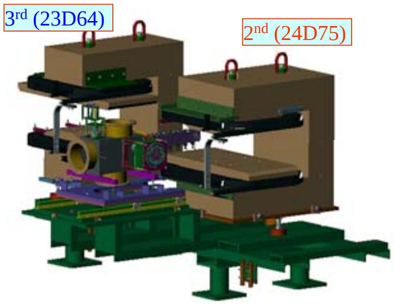

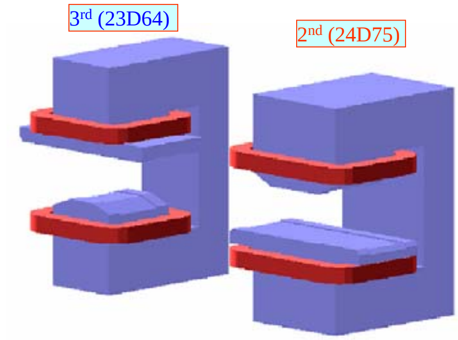

- $B2^{nd}_y(0) \leq 3.0$ kG , $B_y(\text{foil}) \cong 2.5$ kG $B3^{rd}_y(z) \leq 2.5$ kG (min. $(H^0)^*$ stripping)
- $\int \{B2^{nd}_y(z) + B2^{nd}_y(z)\}dz = 500$ [kG.cm]
  - $\theta = \tan^{-1}(B_z(\text{foil})/B2^{nd}_y(\text{foil})) \geq 65$ mrad (minimize hit of foils by e^-)
  - $\int\{B1^{st}_y(z) + B2^{nd}_y(z) + B3^{rd}_y(z) + B4^{th}_y(z)\}\,dz \leq \pm 10^{-3}$ (over beam)

Injection chicane field-angle measurement

Wanderer, Jackson, Jain, Hoey, Meng, Lee

- Single Hall probe mounted on a precise aluminum cube
- Measurement of B_z/B_y
- Angle of electron-guiding field in agreement with 3D modeling

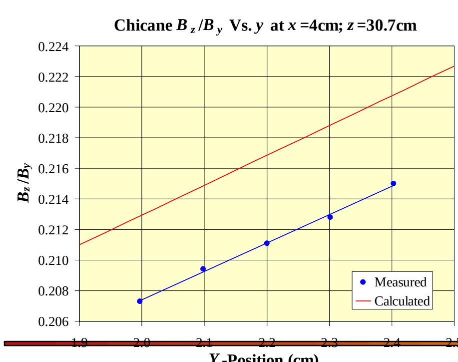

- Trajectory to electron catcher re-confirmed

Injection dump combined-function magnets

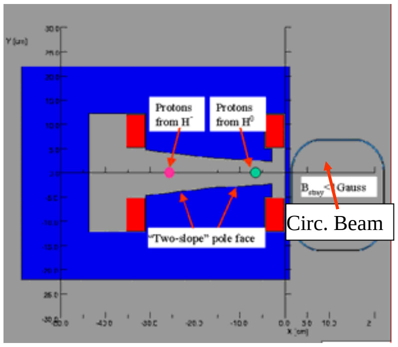

Δx_{max} (max displ from c-line)=±0.0 [cm]

	H^- Location	H^0 Location
B_0 [kG]	3.333	5.226
G[T/m]	1.0515	1.0515
$b_{sext}r^2/b_0$ (at r=1cm)	$\leq 0.5\times10^{-3}$	$\leq 0.5\times10^{-3}$

Injection kickers parameters

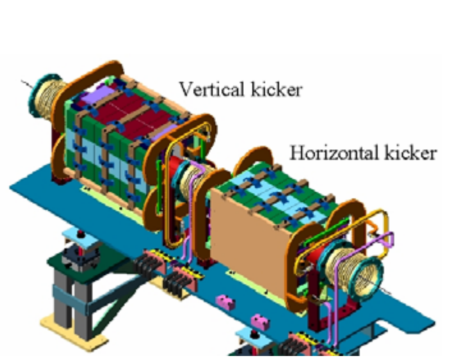

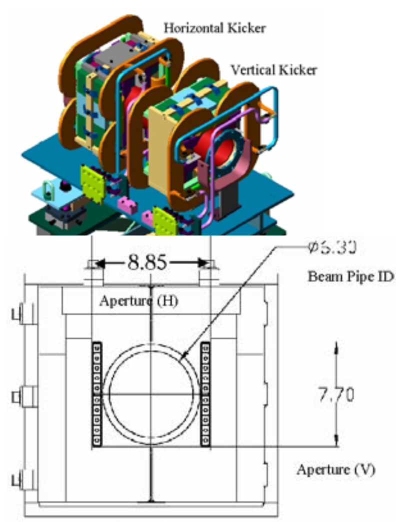

	V [cm]	H[cm]	L [cm]	ID [cm]	Bdl [kGcm]	Trise[nsec]
LONG	19.5	22.5	64	16	65.8	200
SHORT	21.6	24.5	21	18.5	26.9	200

Injection vacuum chamber coating

(Hseuh, He, Todd …)

- Injection kicker ceramic chamber double coating
  - Cu (~ 0.7 μm) for image current
  - TiN (0.1 μm) for electron cloud
  - Meets requirement: conductive coatings w/ end-to-end resistance of ~0.04Ω ± 50% (Henderson, Davino)
  - Thickness uniformity < ± 30%

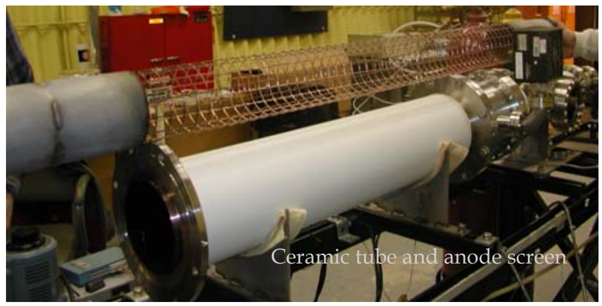

Injection kicker time response measurement

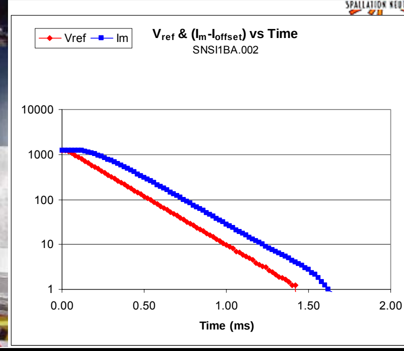

Expected time constant [ms]	0.15	0.2	0.25	0.3	0.4
Measured time constant [ms]	0.171	0.213	0.260	0.307	0.402

- Satisfactory time response (< 0.2 ms)
- Interference from vacuum chamber/coating not noticeable
  - 700 nm Cu and 100 nm TiN
- Need to verify magnet-to-magnet matching

Injection power supplies

DC Voltage	0 to 800V, 0 to –800V
DC Current	0 to 1,400A max. Pulsed (400Arms equivalent)
Pulse Repetition Frequency	60Hz
Switching Frequency	108kHz
Large Signal Current Response	> 2kHz at 45° Shift at 1.4kA
Load Current Tracking	See Figure 2
Load Current Fall time	< 0.5msec. From 1.4kA to 0
Current Stability In Flat Top	< 0.1% (1.4A)
Magnet Load	L= 160μH, R=0.013Ω

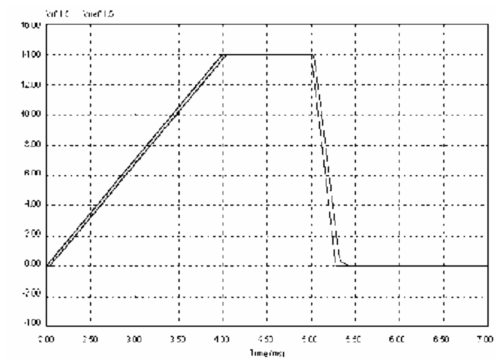

- Rise time ~ 0.2 ms
- Flat top < 2ms
- Fall time < 500μs
- High frequency switching with IGBT

Longitudinal painting

- Momentum painting
- “sharpen” the painting pen by reducing momentum spread before injection (correcting energy jitter, e.g.)
- Paint the momentum space by modulating the injecting beam energy

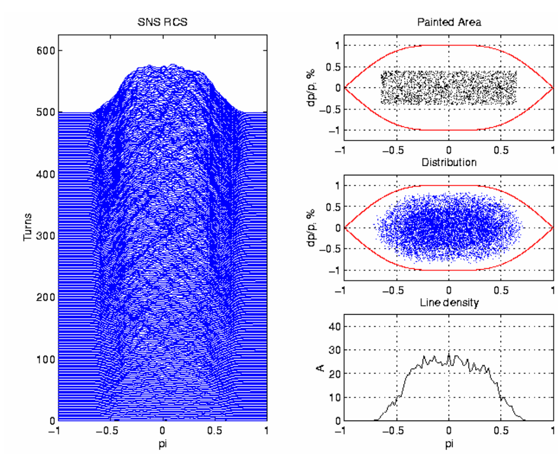

Figure 7: Longitudinal bunch evolution during injection with a dual ($h = 2$ and $h = 4$) RF system. The full injection momentum spread at the end of HEBT line is $\Delta p/p = \pm 0.4\%$, the peak current is 26 A, and the bunching factor is 0.46.

Painting vs spreading

- Momentum painting: create momentum spread without enhancing momentum tail – in controlled way

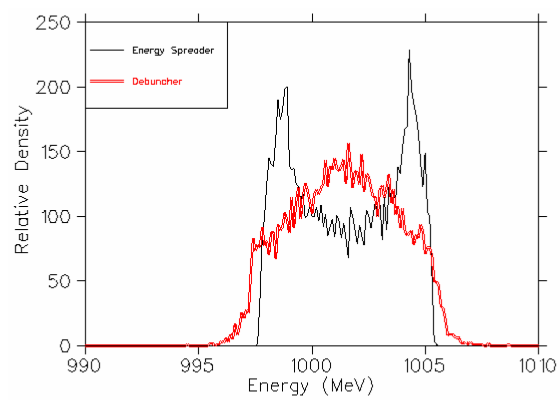

H-L coupled painting (ESS injection)

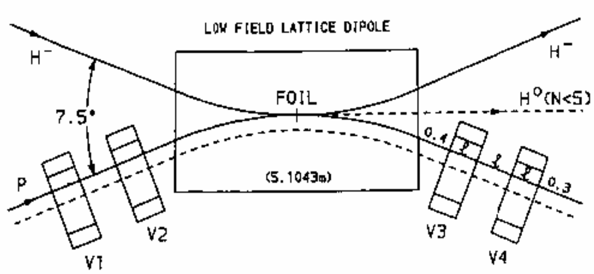

courtesy G. Rees, C. Prior

- Inject at high dispersion region
- Simple magnet layout, less no. of septum
- Avoid horizontal kickers
- Facilitates momentum tail collection
- Same long dipole every superperiod perfect symmetry

Spallation Neutron Source II

Accumulator ring & transports

Extraction

Jie Wei (BNL)

Yannis Papaphilippou (ESRF)

June 28 – July 2, 2004

BROOKHAVEN NATIONAL LABORATORY

Outline

- Fast, single-turn extraction
- Extraction layout
- Power supply
- Coating & impedance

Extraction (single-turn)

- A reversed process of injection
- Typical high-activation area
- Measures to control beam loss
  - Clean beam gap before extraction
  - Wide extraction channel, tolerable to 1 kicker failure
  - Beam position on target immune to kicker failure
- Impedance control
  - Kickers often reside inside vacuum chamber – needs to minimize coupling impedance and to perform special coating
- Maintainability
  - Remove device (pulse forming network, etc.) outside of tunnel

Extraction layout

- A reversed process of single-turn injection

$$\theta = \frac{x}{\sqrt{\beta_{sep}\beta_{kick}}\sin\Delta\mu}$$

- Example
  - Multiple (14) kickers vertically deflect beam
  - Horizontal bending beam away with a septum (e.g. Lambertson dipole)
  - Single-turn, no pre-bumps

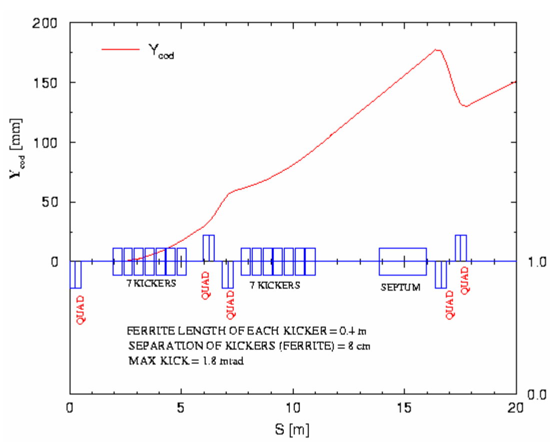

The Extraction Region with 14 kickers and Septum

Magnet Type :WF (Ferrite)
Ferrite Length : 0.35 m
∫Bd*l* : 9.5 to 6.5 kGauss.cm
Gap (Hor.) : 13.8 to 19 cm
Width(Vert.): 13.1 to 24.8 cm
Rise time to 95% : 200 nsec
Maintain peak field: 750 nsec

Single kicker 3-D Calc.
∫Bd*l*=7.0 kGauss.cm/kicker
L=0.81 μH/kicker

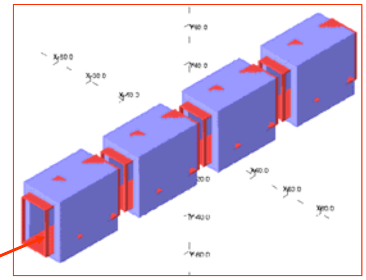

4-Kickers in Tandem
∫Bd*l*=6.75 kGauss.cm/kicker
L=0.87 μH/kicker

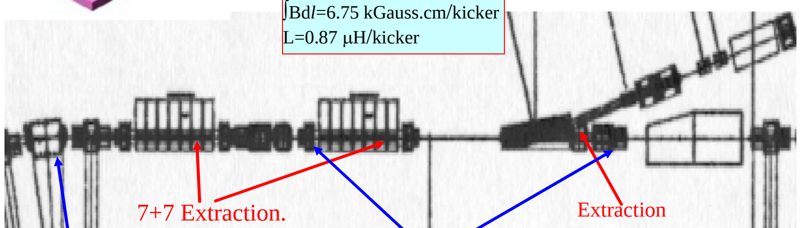

Extraction chamber

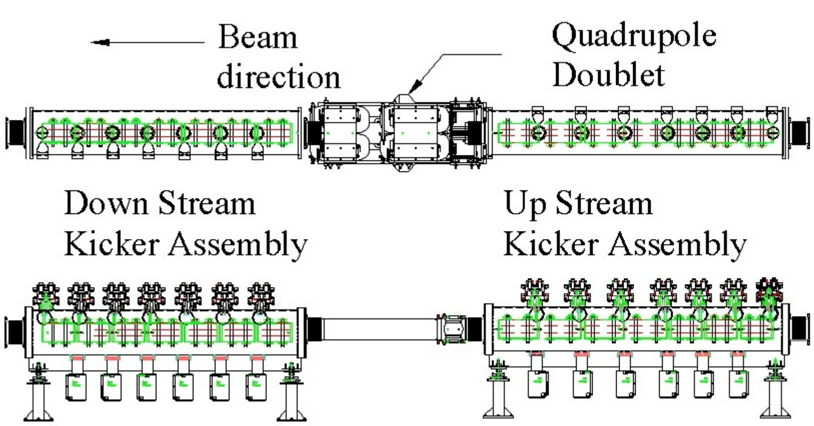

Pulse-forming network

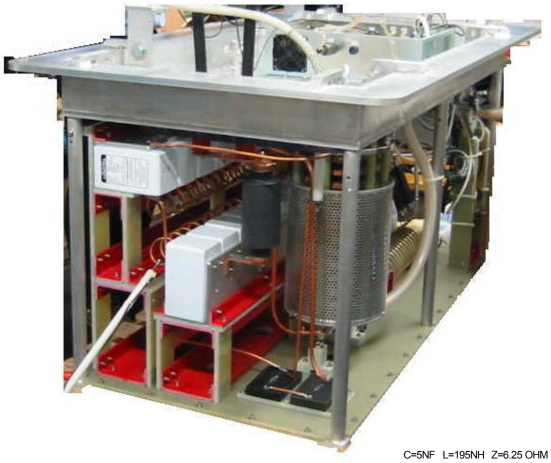

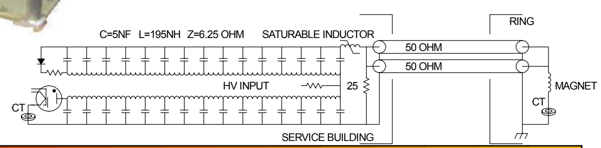

Extraction Septum Magnet (17ELS244)

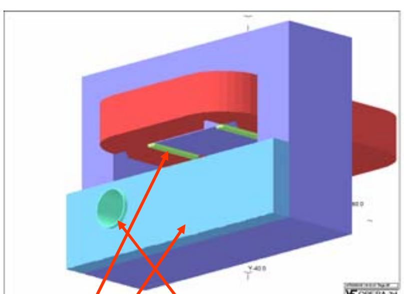

Bend Angle : 16.8^0

Field Un. : $\Delta(\int Bd\mathit{l})/(B_0L_{eff})\leq\pm1\times10^{-3}$

Iron Length : 2.44 m

$\int Bd\mathit{l}$: 1.58 Tm for 1.0 GeV

Magnet Gap : ~16.5 cm

Septum thickness : 1 cm

Pipe ID Circ Beam : 17.5 cm

$\int Bd\mathit{l}$ at Circ Beam : ≤500 Gauss.cm

“Shims” of the Lambertson Septum

“Field Clam” and “Magnetic-pipe” to reduce stray fields at the circulating beam region

The B_{mod} of the stray fields at the center of the pipe of the circulating beam with and without “Field Clam”

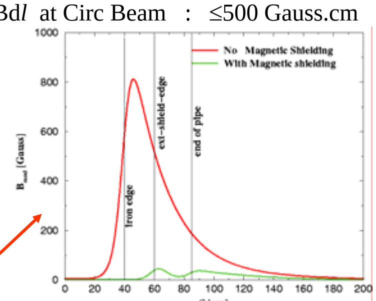

Ring vacuum chamber coating

(Hseuh, He, Todd …)

- Injection kicker ceramic chamber double coating
  - Cu (~ 0.7 μm) for image current
  - TiN (0.1 μm) for electron cloud
  - Meets requirement: conductive coatings w/ end-to-end resistance of ~0.04Ω ± 50% (Henderson, Davino)
  - Thickness uniformity < ± 30%
- Extraction kicker ferrite patterned TiN coating
  - 0.1 μm TiN on ≥ 90% inner surface, with good adhesion

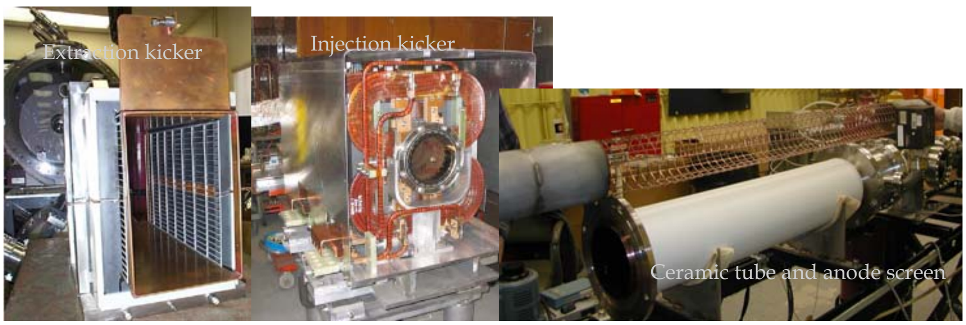

Extraction kicker rise-time & impedance minimization

(J. Mi, J. Sandberg, D. Davino, H. Hahn, V. Danilov, Y. Y. Lee, S. Kurennoy …)

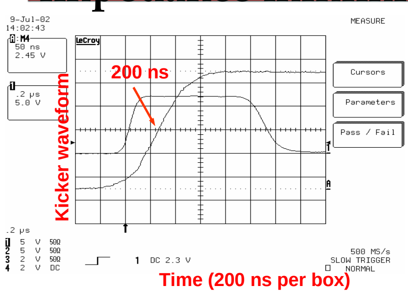

- Ferrite kicker inside vacuum pipe
- Optimize saturable inductor to effectively "shorten" rise time (200ns)
- Improved flat-top flatness (1%)
- PFN termination: lower impedance
- Increase magnet height to halve coupling impedance (same drive)
- Shield the terminating resistance, reducing cable reflection

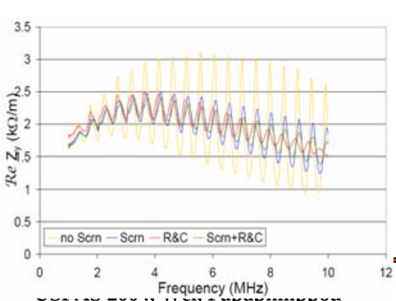

Extraction kickers power supply

- 14 pulsed units
- Repetition rate of 60Hz
- Flat top of 750 ns
- Gap of 250 ns

kicker magnet inductance	0.76 -0.8 uH
magnet current	2 - 2.5 kA
blumlein PFN Voltage	35 kV
pulse current rise time	200nS
current pulse width	750 nS
pulse repetition	60 Hz

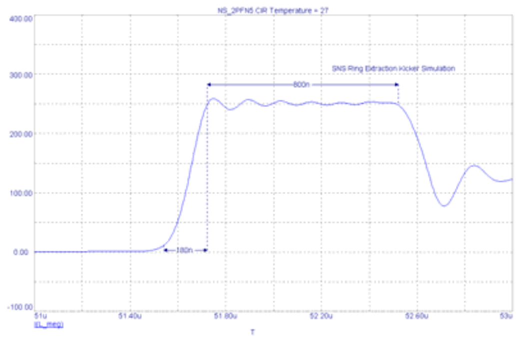

Extraction parameters

Beam Rigidity	5.6575 T-M
Extraction Energy	1.0 GeV
Extraction type	Single-turn
Magnet window	Full aperture
Beam revolution period	945.4 ns (at 1.0 GeV) 911.1 ns (at 1.3 GeV)
Beam gap during extraction	250 ns
Bunch length (full)	695 ns
Maximum extraction rate	60 Hz
Pulse flat-top length	> 700 ns
Pulse Flat-top tolerance	+/- 3%
Pulse rise time	200 ns (1% - 95%)
Pulse fall time	< 16.6 ms
Kicker strength	1.276 to 1.775 mrad per section
Total deflection strength	20.344 mrad
Kicker horizontal aperture	120 mm to 211.3 mm
Kicker vertical aperture	166 mm to 243 mm
Kicker length	390 mm to 505 mm per section
Kicker magnet inductance	695 nH to 789 nH per section
Operating voltage	~ 35 kV per section
Operating current	~ 2.5 kA per section
Beam Impedance Termination	~ 25 Ω

Spallation Neutron Source II
Accumulator ring & transports

Radio-frequency System

Jie Wei (BNL)

Yannis Papaphilippou (ESRF)

June 28 – July 2, 2004

Outline

- Ramping and acceleration
- SNS Radio Frequency system
  - Cavity
  - Power amplifier and tuning supply
  - Wall current
- New developments
  - J-PARC RF cavity with magnetic alloy

Ramping

- Typical injection "flat-bottom" and extraction "flat-top"
- Possibly slower up-ramp and faster down-ramp
- Smooth variation of longitudinal parameters

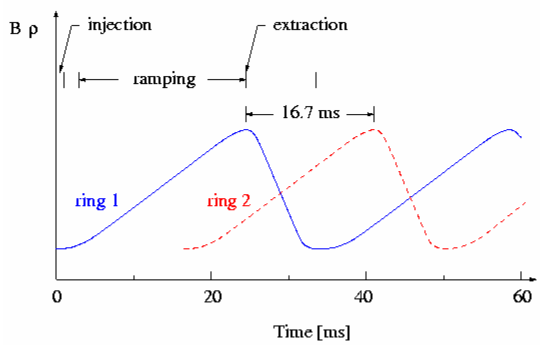

Condition of adiabatic motion

- Adiabatic condition

$$\frac{1}{\Omega_s^2}\frac{d\Omega}{dt} << 1 \qquad\qquad \Omega_s = \omega_s\sqrt{\frac{eVh\eta_0\cos\phi_s}{2\pi E_s\beta^2}}$$

- Continuous function of both synchronous phase ϕ_s , its derivative $\dot{\phi}_s$ and voltage V
- Transition crossing is intrinsically non-adiabatic
- In principle, adiabatic capture is possible but in reality, beam loss is often excessive when ramping cycle is fast – beam pre-chopping is usually performed at low energy

Examples of RF ramping

- Single RF system

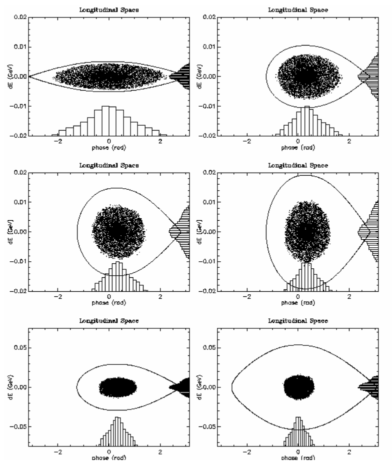

- Dual RF system

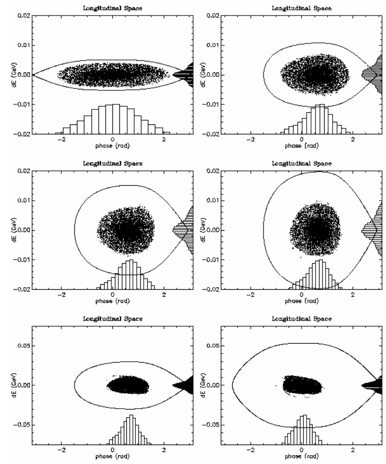

Program of RF voltage & phase

- Beam loss often occurs at initial ramping due to reduction in bucket area when the synchronous phase is increased
- Careful program of voltage and phase to ensure monotonic increase of bucket area
- Keep the process adiabatic

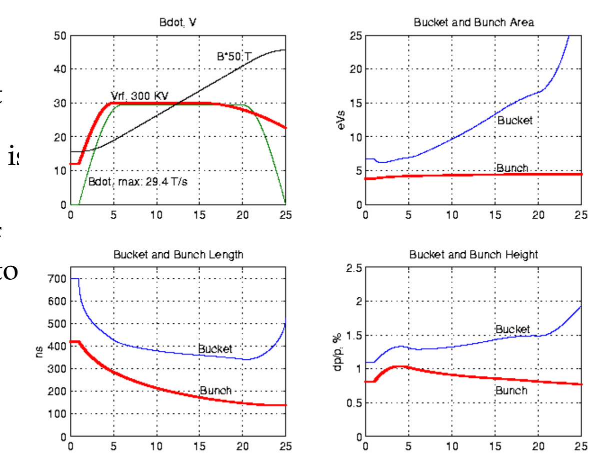

Figure 8: Programming of RF voltage and magnetic field, and the evolution of momentum spread, bunch area and bunch width in comparison with the $(h = 2)$ RF bucket.

RF system components

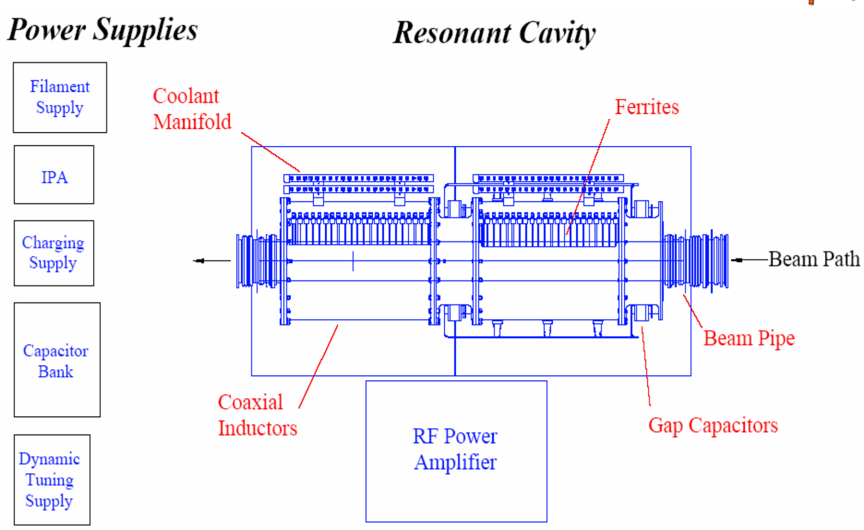

Ferrite-loaded cavities

- Frequently used when variable resonance frequency is needed to follow the change of beam speed
- Cavity acts as a resonance transformer with the beam as the secondary winding
- Ferrite serves two purposes
  - Enhances the magnetic field for given current, allowing a small cavity size
  - Allow dynamic tuning of the cavity

SNS ring RF cavities

Ring RF power supply

(Ring RF power amplifier)

(RF tuning power supply)

SNS RF system at ORNL

RF Labview control system

- **Purpose**

  Allows stand-alone
  control and monitor

- **Features**

  - LabView System
  - Analog Circuitry
  - PID loops
  - Dynamic tuning control
  - PLC monitor and control

Wall current monitor

- **Features**
  - Ferrite-loaded cavity
  - Balanced gap resistors
  - High current handling

- **Measurements**
  - Beam revolution frequency
  - Longitudinal profiles
  - Injection phase error

Wall current monitor profiles

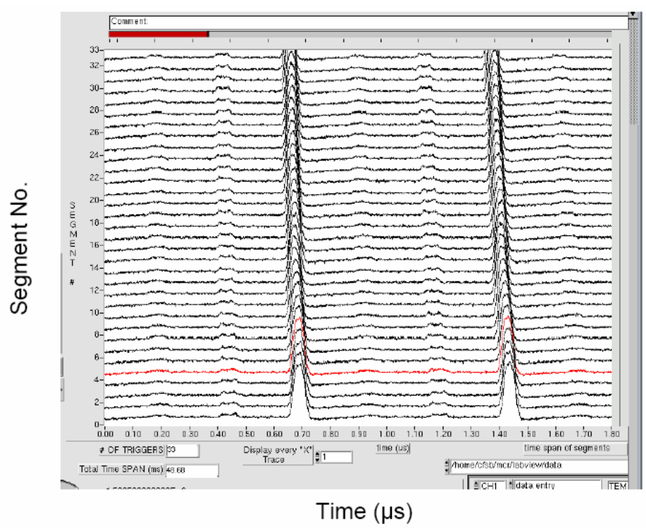

RF cavity gradient upgrade at J-PARC

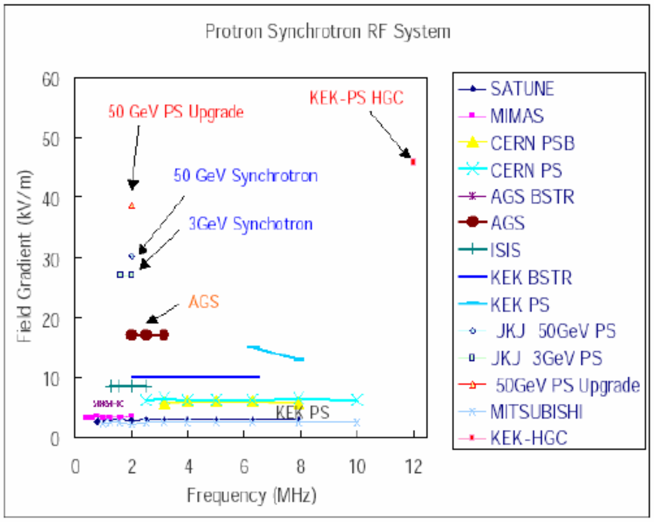

J-PARC layout with RF cavities

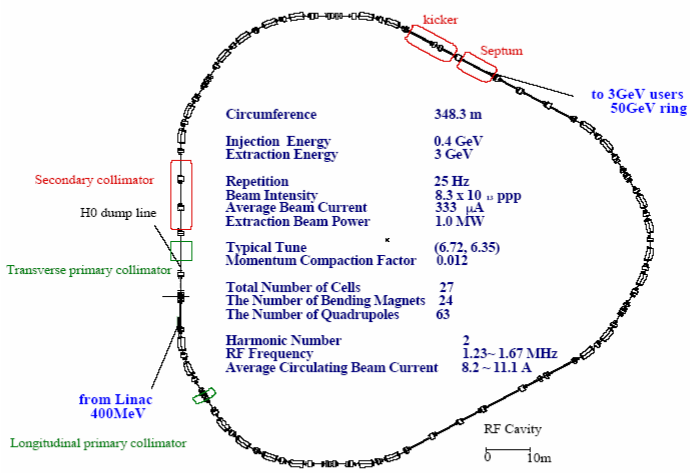

J-PARC Magnetic-Alloy cavities

High Gradient RF system for 50GeV MR
Indirect Cooling Type:

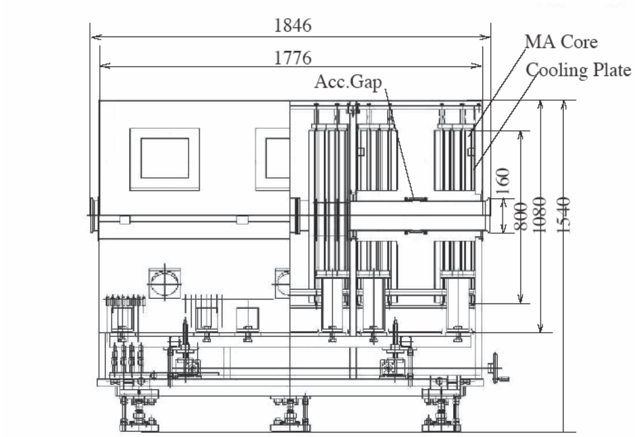

Spallation Neutron Source II
Accumulator ring & transports

Vacuum & Electron cloud

Jie Wei (BNL)

Yannis Papaphilippou (ESRF)

June 28 – July 2, 2004

Outline

- Vacuum chamber
  - Chamber layout
  - RCS chamber and shielding
  - SNS chamber
  - Chamber coating
- Electron cloud
  - Impact to the beam and accelerator
  - Sources of electron cloud
  - Mitigation measures

Typical RCS half-cell layout

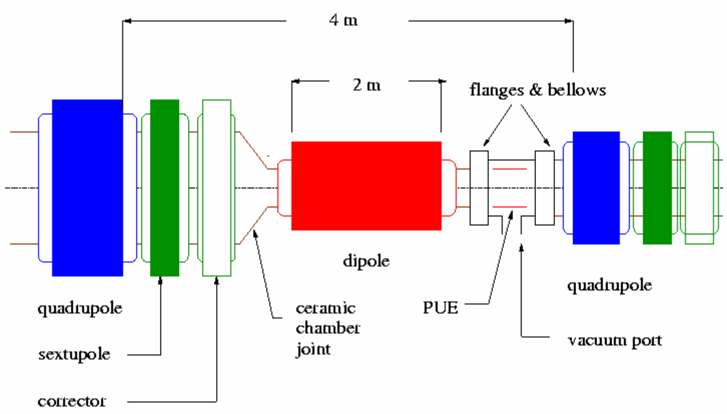

Eddy current effects

- Eddy current induced sextupole field

$$\frac{\partial^2 B_y}{\partial x^2} = \frac{\mu_0}{\rho_r}\frac{d_w}{g}\dot{B}$$

  - Inversely proportional to resistivity, gap height
  - Proportional to ramp rate, chamber width

Leading sources of field imperfections are ramping Eddy-current and saturation. Variation in the level of saturation contributes to the tracking errors between different types of magnet. Eddy-currents induced in the vacuum chamber under the changing magnetic field distort and delay the field and generate multipole errors. For a wide chamber of thickness d_w inside a dipole magnet of gap g, the sextupole field is given by (Edwards , 1993; Rice , 1998)

Thermal heating

Consider a pipe of thickness d_w and volume resistivity ρ_r. As an example, for a resistive loop of width w_r and height h_r penetrated by a magnetic field B, the instantaneous power per unit length is given by

$$\frac{dP_r}{ds} = \frac{\dot{B}^2 w_r^2 h_r d_w}{2\rho_r}. \tag{15}$$

For a circular pipe of radius b, the average power is proportional to the repetition rate, the field-variation rate, the magnetic-field amplitude squared, and the pipe's radius, b, cubed. It also is inversely proportional to the sheet-resistivity ρ_r/d_w.

J-PARC RCS vacuum chamber

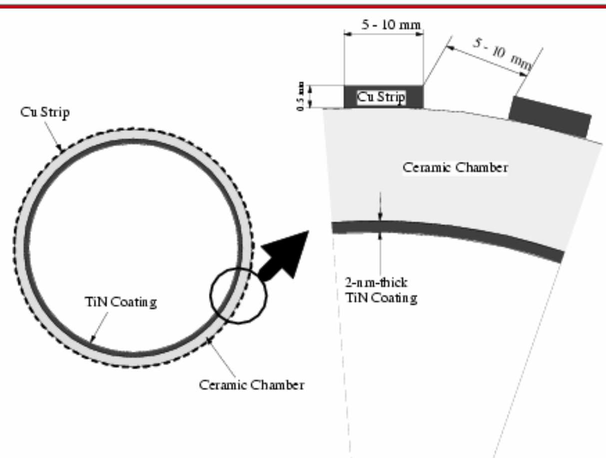

FIG. 35 Schematic view of the ceramic vacuum-chamber and the RF shield of the 3 GeV synchrotron of the J-PARC project (Section III.H) (courtesy M. Kinsho). The 5-6 mm thick chamber wall is made of 99.8% high-purity alumina.

Vacuum chamber candidates

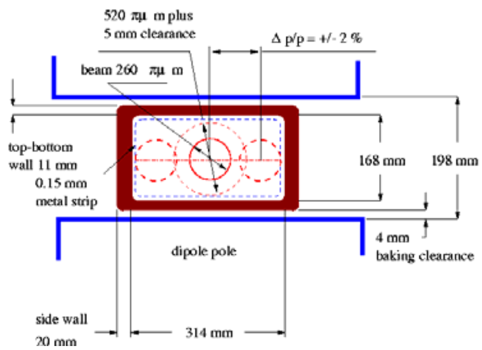

- Conventional:
  - metal pipe
  - connected to magnets (FNAL Booster)
- Development for RCS:
- Ceramic chamber w/ sustained shield following beam contour (ISIS)
- Ceramic w/ printed wires (KAON study, SNS/RCS)
- Ceramic w/ external shield & internal coating (JKJ)
- Thin Inconel pipe (FNAL PD)

Typical quadrupole chamber

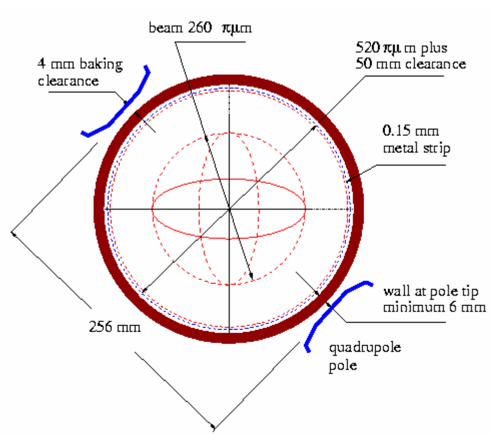

SNS vacuum chamber example

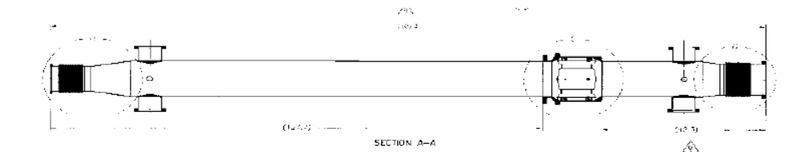

Fig. 2 Schematics of typical SNS ring straight section doublet chambers for 30cm quadrupole doublets.

- Number of vacuum chamber type minimized
- Stainless steel pipe, inconel bellows for radiation resistance
- Inner surface coated with TiN to suppress electron cloud

Ring vacuum chamber

(electron detector)

Electron-cloud phenomena: RHIC

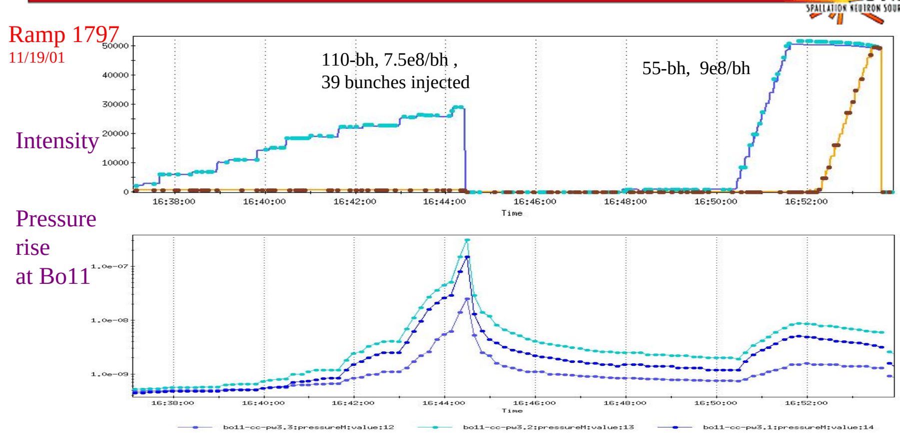

- Pressure rise & interlock when the bunch spacing is halved
- Total intensity reaching only 60% before pressure rise occurs

(courtesy RHIC crew; S.Y. Zhang)

Electron-cloud phenomena: PSR

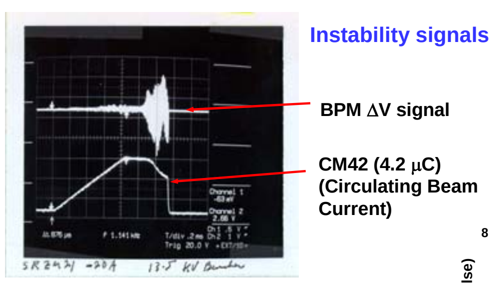

Control by rf buncher voltage

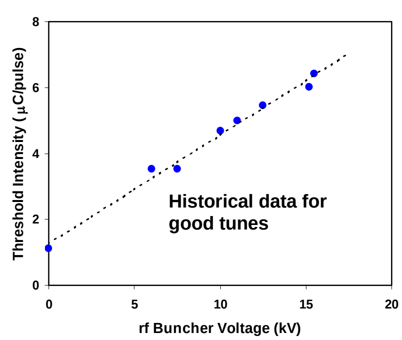

- Growth time ~ 75 μs or ~200 turns
- High frequency ~ 70 – 200 MHz
- Controlled primarily by rf buncher voltage
- Requires electron neutralization of ~ 1% (from centroid model)

Effects of electron clouds

- Electron neutralization, tune shifts, and resonance crossing
- Transverse (horizontal or vertical) instability
- Associated emittance growth and beam loss
- Vacuum pressure rise
- Heating & damage of vacuum chamber
- Interferences with diagnostics system

Electron generation

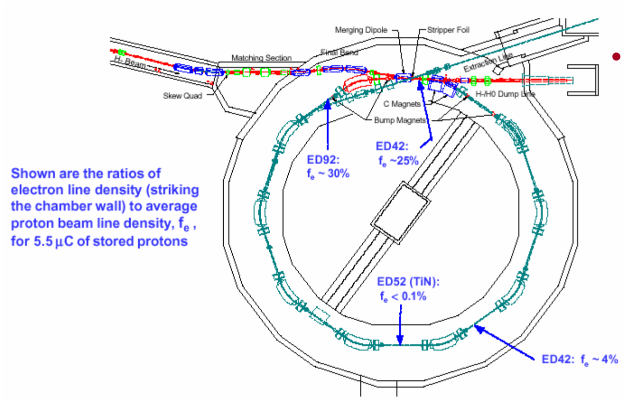

- PSR e-flux measure
  - High electron concentration near injection & extraction
  - Electron wall-striking level to be distinguished from electron neutralization level in the bunch

- Major sources of electrons in a high-intensity ring
  - From stripping foil (H^-, H^0)
  - Proton striking collimators or aperture bottleneck
  - Gas ionization, ion desorption, electron desorption
  - Beam-induced electron multipacting

Electron generation: H^- (H^0) injection

- Stripping-foil generated electrons
  - Stripped electrons
    - » 100% (H^0) – 200% (H^-); same γ and emittance as injecting beam
    - » Intense, localized high-energy electrons
  - Foil-secondary and knock-on electrons
    - » Low one-pass yield
    - » Proportional to number of foil traversal (SNS: average 6 hits)
  - Thermionic electrons
- Back-scattered electrons

Electron source	No. per injected H^0	Kinetic energy	Ave. current
Stripped electron	1.0	430 keV	75μA
Secondary electron	3.6	up to 20 eV	μA
Knock-on electron	1.2	up to 2.4 MeV	μA
Thermionic electron	< 0.002	~0.24 eV	μA
Residual-gas ionization	0.0037	up to 2.4 MeV	μA

PSR H0 injection with average 300 foil traversal

(courtesy M. Plum)

Collection of stripped electrons (SNS)

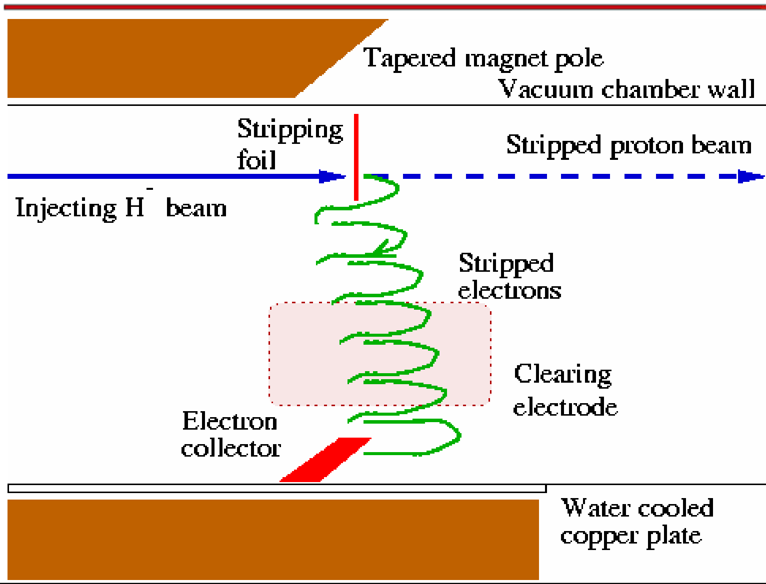

Electrons from collimator surface

(courtesy H. Ludewig, N. Simos)

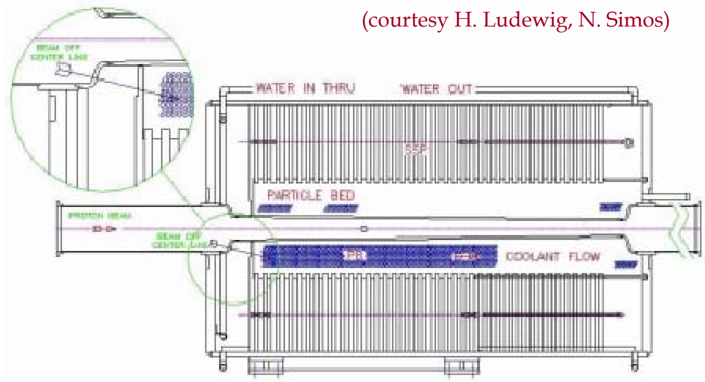

- Designed to absorb 2 – 10 kW (0.1% -- 0.5%) proton beam loss
- Beam halo at large grazing angle enhances electron production
- Possible saw-tooth surface complicated by proton stopping distance
- Possible magnetized surface proposed at LANL
- Rely on two-stage collimation for a large impact distance

BNL's Tandem study on grazing angle

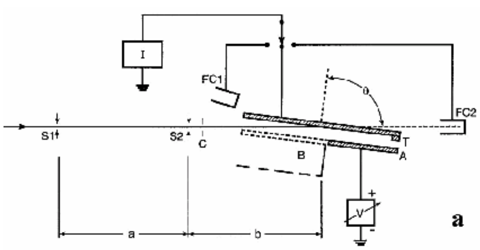

$$Y_{ep} = \frac{1.11 Y_{ep}^{max}\left\{1-\exp\left[-2.3\left(\frac{E_s}{E_s^{max}}\right)^{1.35}\right]\right\}}{\left(\frac{E_s}{E_s^{max}}\right)^{0.35}\cos\theta_g}$$

a

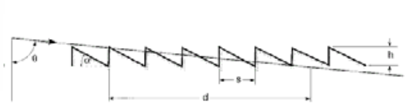

(courtesy P. Thieberger et al)

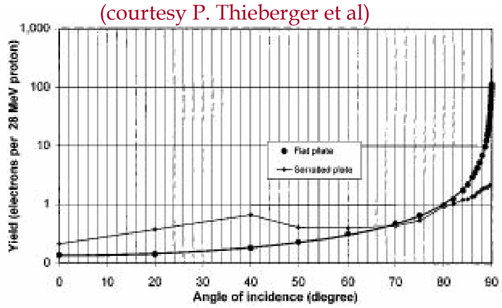

Measured at BNL's Tandem for 3 ion species

- Confirmed dependence on grazing angle (0 – 89°)
- Confirmed benefit of saw-toothed surface
- Energy dependence not verified; expecting peaked at E_{max}~0.7 MeV

Ionization and desorption

- Electron production due to ionization is proportional to vacuum pressure, average beam current, and ionization cross section

$$\frac{d^2\lambda_e}{dtds} = \frac{\rho_m \beta I \sigma_{ion} P}{e}$$

  - Molecular density ρ_m=3.3x10^{22} m^{-3} at 300 K
  - Ionization cross section σ_{ion}=2 Mbarn = 2x10^{-22} m^2
  - Pressure P [Torr]
- Rate of ion or electron desorption is proportional to the number of ion or electron hitting surface – resulting in pressure run-away

Beam-induced electron multipacting

- Multi-bunch multipacting
  - Sensitive to bunch spacing and parameter configuration

(e.g., O. Grobner, 1998)

  - **Short-bunch regime** $\quad \frac{b}{\beta_e} \geq \frac{\sqrt{2\pi}\sigma_s}{\beta_p} \qquad \beta_e \approx \frac{1}{2}\sqrt{\frac{2e\Delta V_p}{m_e c^2}} \qquad \Delta V_p \approx \frac{I_{peak} Z_0}{2\pi\beta_p}$
  - $R_l \equiv \frac{b\beta_p}{\sqrt{2\pi}\sigma_s \beta_e}$ RHIC: $R_l \approx 1$ SNS: $R_l \approx 0.015$
- Single-bunch regime "trailing-edge" multipacting
  - Insensitive to bunch spacing (e.g., R. Macek, 1999; V. Danilov, 1999)
  - PSR and SNS
  - **Long-bunch regime** $\quad \frac{b}{\beta_e} << \frac{\sqrt{2\pi}\sigma_s}{\beta_p}$
  - Maximum gain in e$^-$ energy: $\Delta V_e \approx \left(\frac{I_{peak} Z_0 b}{4\pi^2 R_0 B_f} \sqrt{\frac{m_e c^2}{2e}} \right)^{2/3}$ SNS: 50 [V]

Trailing-edge electron multipacting

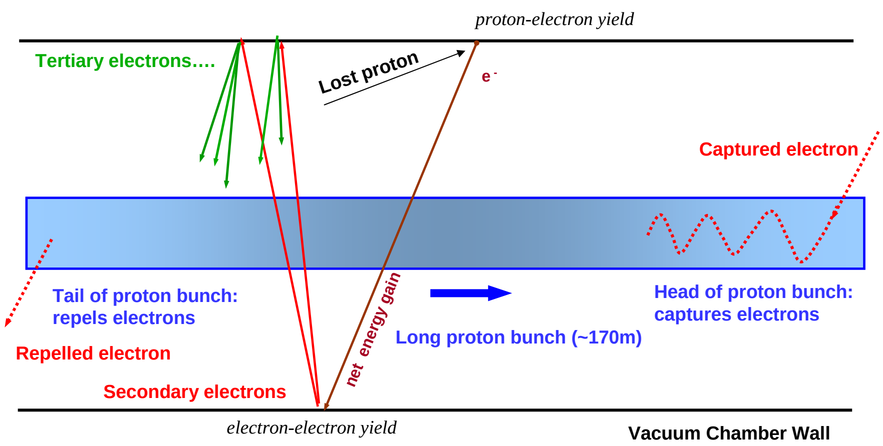

PSR wall-electron spectrum

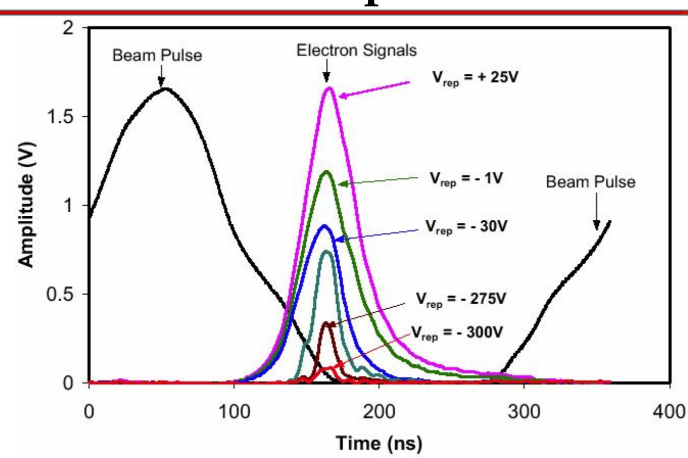

- Trailing-edge multipacting
- Total electrons striking the wall is ~ 25% of the proton number
- Actual neutralization level much lower (swept electron)

Secondary electron yield vs. primary electron energy

(courtesy N. Hilleret, O. Grobner,)

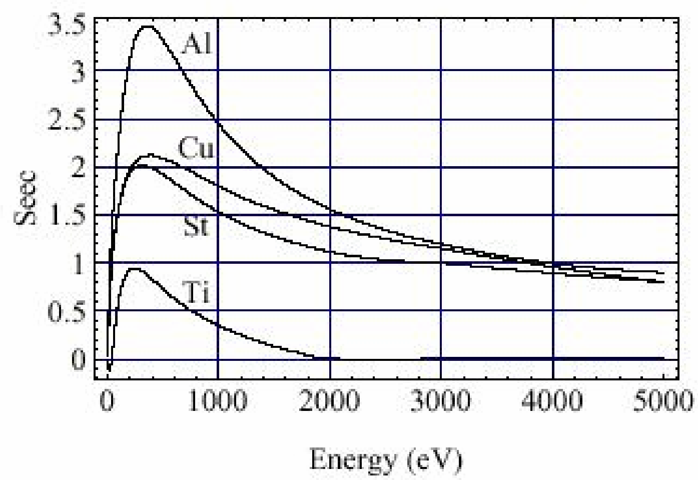

Secondary emitted-electrons model

(courtesy M. Pivi, M. Furman)

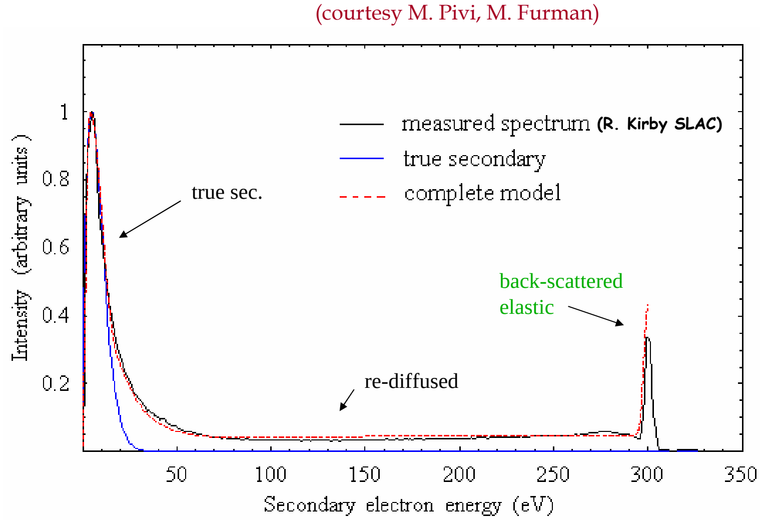

Electron concentration & neutralization

- Trapped electrons
  - Bouncing frequency proportional to square-root of proton intensity

$$\omega_e = c\sqrt{2\pi r_e n_p}$$

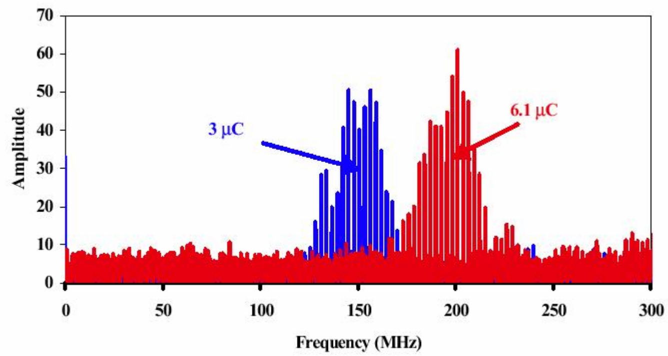

Tune-shift & the Pacman effect

$$\Delta\nu_{x,y} = -\frac{f_{sc} N r_p R_0}{2\pi B_f \nu_{x,y} \beta^2 \gamma}\left(\frac{1}{\sigma_{x,y}(\sigma_x+\sigma_y)}\left(\frac{1}{\gamma^2}-\eta_e\right)+A_{image}\right)$$

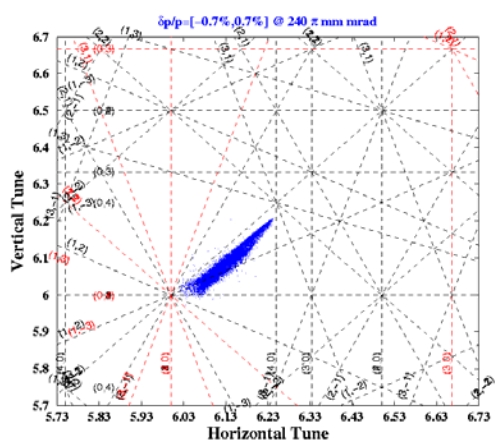

(courtesy A. Fedotov)

- Electron neutralization causes positive tune shifts on trailing-edge particles
- For given space-charge tune spread at injection (typically 0.2), the electron tune-shift if enhanced by factor γ^2 -- may be important at a high injection energy
- May keep on losing trailing-edge particle upon resonance crossing – the Pacman effect
- Require detailed evaluation of neutralization level in proton beam

Simulation of electron production

(courtesy M. Pivi, M. Furman)

within vacuum pipe

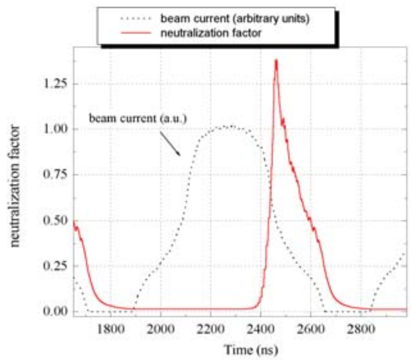

within beam

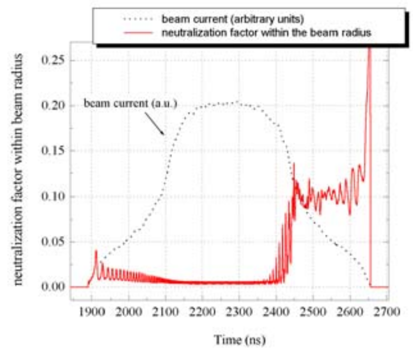

- SNS: electron-cloud tune-shift ~ 0.4 $\eta_{e,peak}$: +0.04 (~ 0.4?)

Electron-cloud instabilities

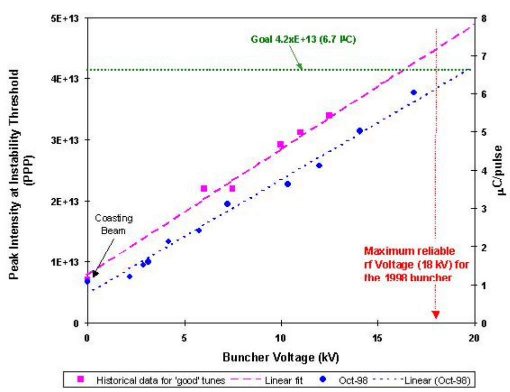

- PSR observed fast, transverse instability with both coasting and bunched beam
- Linear stability threshold scaling with RF voltage
- All cures are related to enhancement of Landau damping

Instability-threshold scaling

- Motion is stable if the coherent growth-rate or mode shift is less than the incoherent tune-spread providing Landau damping

$$|Z_\perp| \le F_\perp \frac{4B_f E_s}{e\beta\langle\beta_\perp\rangle I_0}\left(\frac{\Delta E}{E_s}\right)_{FWHM} |(n-\nu_\perp)\eta + \xi_\perp|$$

- Instability occurs only near electron bouncing frequency

$$\frac{\omega_e}{\omega_0} \gg \nu_\perp; \quad |\eta|\omega_e \gg \xi_{x,y}\omega_0$$

- Threshold intensity proportional to momentum-spread squared

$$|Z_{\perp x,y}| \le F_\perp \frac{4|\eta|E_s}{\sqrt{\pi}e^2\omega_0 a\langle\beta_\perp\rangle}\sqrt{\frac{B_f R_0 r_e}{N_0}}\left(\frac{\Delta p}{p}\right)_{FWHM}$$

- What is the dominant coupling-impedance?
  - Space-charge (M. Blaskiewicz): gives questionable scaling on the bunch length
  - Electron-cloud impedance?

Theoretical approaches on e-p instability

- Coasting-beam centroid model (Neuffer, 1992)
  - Provides estimates of instability modes and their intensity dependency for a given average neutralization
  - Provides plausible instability threshold (PSR)
  - Poor estimate on growth rates and behavior beyond threshold
- Bunched-beam centroid model (M. Blaskiewicz, T. Wang, …)
  - Use trailing-edge electron concentration
  - With momentum-spread & damping
  - Space-charge as part of simulation (scaling with bunch length?)
- Fully kinematics simulation based on self-consistent Maxwell-Vlasov solution (PPPL)
  - Confirmed Landau-damping due to momentum spread
  - Coasting-beam, smooth-focusing
  - Perturbation-method, disallow large change of distribution

Preventive measures

- Suppress electron production
  - Tapered magnets for electron collection near injection foil; back-scattering prevention
  - TiN coated vacuum chamber to reduce multipacting
  - Striped coating of extraction kicker ferrite (TiN)
  - Beam-in-gap kicker to keep a clean beam gap (10^{-4})
  - Good vacuum ($5x10^{-9}$ Torr or better)
  - ports screening, step tapering; BPMs as clearing electrodes
  - Install electron detectors around the ring
  - Two-stage collimation; winding solenoids in the straight section
- Enhance Landau damping
  - Large momentum acceptance with sextupole families; high RF voltage; momentum painting
  - Inductive inserts to compensate space charge
  - Reserve space for possible wide band damper system

Electron detectors

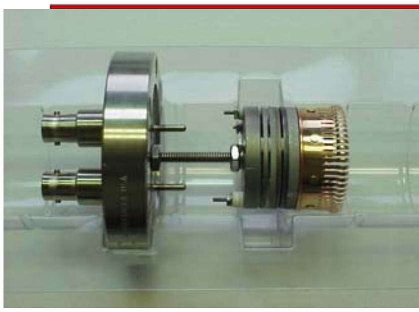

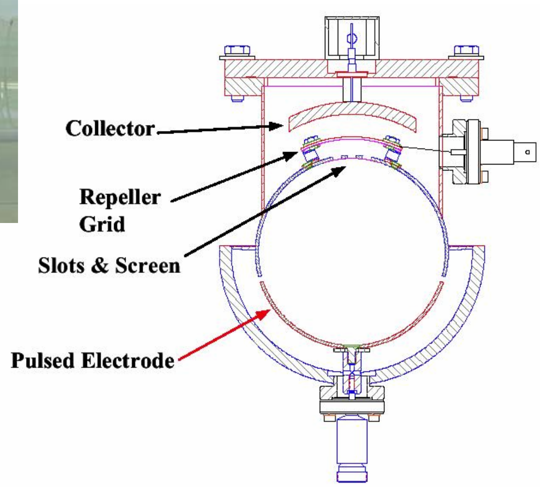

Retarding Field Analyzer (R. Macek courtesy)

- Described in R. Rosenberg and K. Harkay, NIM A 453 (2000) p507-513.
- LANL augmentation is fast electronics (~80 MHz) on the collector output
- Minimal perturbation of beam/wall environment
- Use of repeller permits collecting a cumulative energy spectrum
- Measures electrons striking the wall, not electrons remaining in the pipe

Simplified RFA Installation Sketch

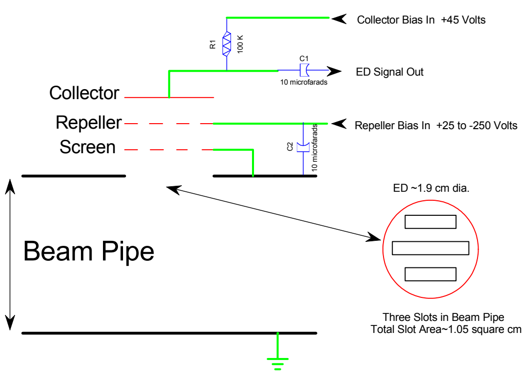

Electron-cloud mitigation

- Inner surface of vacuum chambers coated with TiN to reduce secondary electron emission
- Solenoids used in collimation region to confine scattered electrons
- Beam-position-monitors act as clearing electrodes
- Beam-in-gap kicker to clear residuals
- Extra vacuum ports for beam

(Courtesy H. Hseuh, P. He, M. Blaskiewicz, L. Wang, SY Zhang et al)

SEY= 2.4, as-received condition

SEY= 1.1 after air and vacuum bake

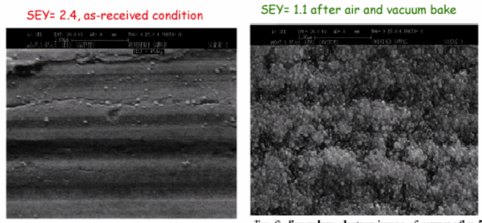

FIG. 8. Secondary electron image of copper as-received (magnification = 15 000).

FIG. 9. Secondary electron image of copper after 5 min air exposure at 350 and 350 °C bakeout under vacuum (magnification = 15 000).

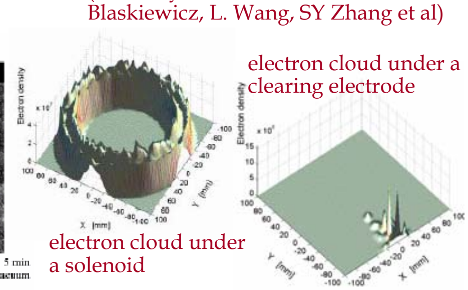

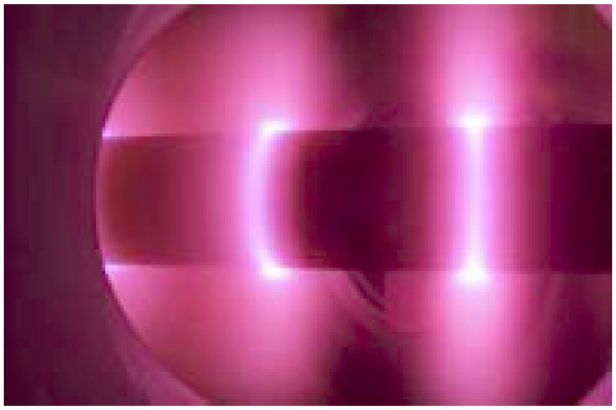

Fig. 4 The discharge plasma during TiN coating of the SNS ring vacuum chambers. The brighter rings are the locations of the spacers between the permanent magnets.

Ring vacuum chamber coating

(Hseuh, He, Todd …)

- Injection kicker ceramic chamber double coating
  - Cu (~ 0.7 μm) for image current
  - TiN (0.1 μm) for electron cloud
  - Meets requirement: conductive coatings w/ end-to-end resistance of ~0.04Ω ± 50% (Henderson, Davino)
  - Thickness uniformity < ± 30%
- Extraction kicker ferrite patterned TiN coating
  - 0.1 μm TiN on ≥ 90% inner surface, with good adhesion

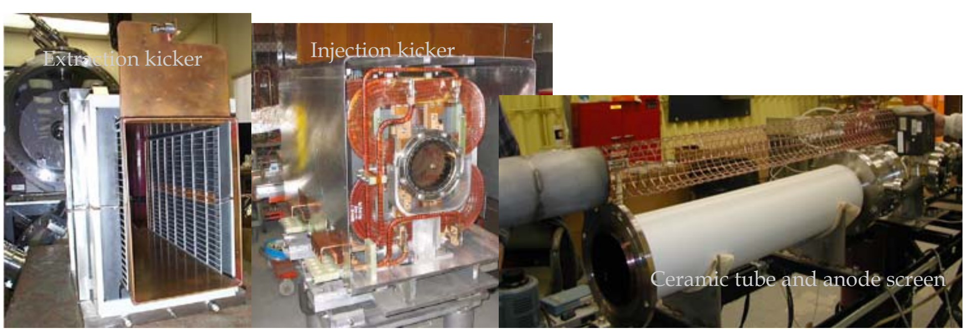

Sample secondary emission yield

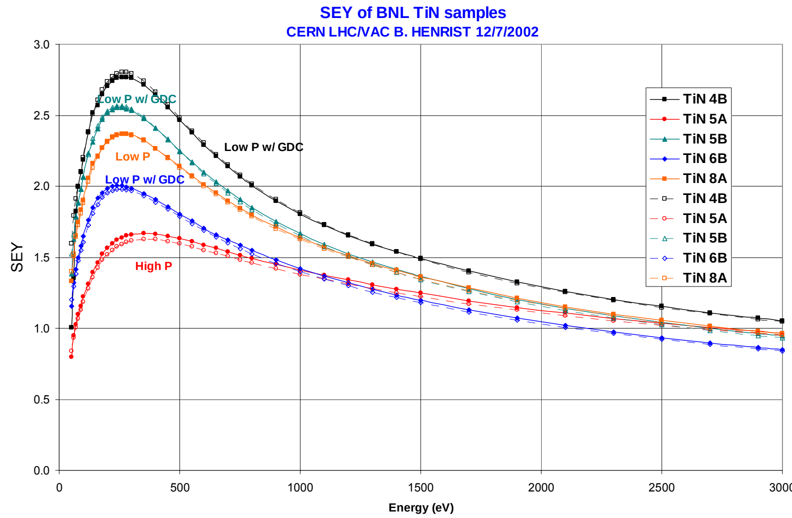

Solenoids

- Electrons confined in small radius comparing with beam pipe radius

$$r_e = \frac{m_e v_e}{eB_\phi} \qquad B_\phi = \frac{\mu_0 N_\phi I_\phi}{L_\phi}$$

  - SNS: 200 turn/m; 20 A current; 50 G field; r_e~1.1 cm
- Minimum impact on the proton beam
  - Alternating polarity to minimize impact
  - Global decoupling with skew quadrupoles

$$-\sum_{sq} \frac{\sqrt{\beta_x\beta_y}}{f_{sq}} \begin{pmatrix} \cos(\phi_x - \phi_y) \\ \sin(\phi_x - \phi_y) \end{pmatrix} = \sum_{sol} g_\phi \theta_\phi \begin{pmatrix} \cos(\phi_x - \phi_y + \omega_\theta) \\ \sin(\phi_x - \phi_y + \omega_\theta) \end{pmatrix}$$

$$g_\theta = \sqrt{\gamma_x\beta_y + \gamma_y\beta_x + 2(1-\alpha_x\alpha_y)} \qquad \tan(\omega_\phi) = \frac{\beta_x + \beta_y}{\alpha_x\beta_y - \alpha_y\beta_x} \qquad \theta_\phi = \frac{B_\phi L_\phi}{B_0\rho}$$

Solenoid effects (L. Wang, M. Blaskiewicz, et al)

- 30G Solenoid field can reduce the e-cloud density with a factor 2000 !
- Zero density within beam
- Solenoid winding in the collimator straight section

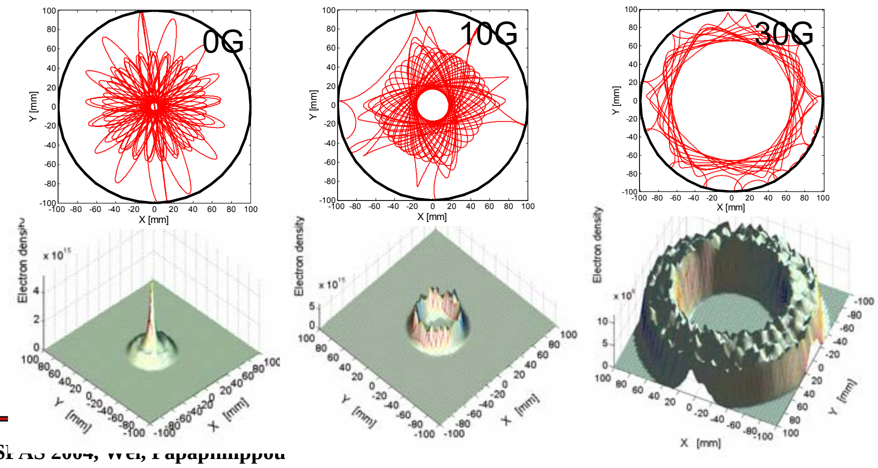

BPM as clearing electrodes

(courtesy P. Cameron)

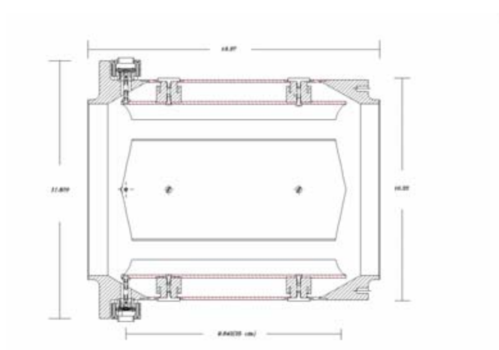

- Floating-ground BPM serve dual purpose
- Moderate voltage needed
  - SNS one-pass energy gain ~ 50 eV

$$\Delta V_e \approx \left(\frac{I_{peak} Z_0 b}{4\pi^2 R_0 B_f} \sqrt{\frac{m_e c^2}{2e}} \right)^{2/3}$$

- 48 BPM, each 25 cm long, holding up to +/- 1 kV
- More clearing electrodes at special locations
  - Inside injection foil assembly

Electrode clearing (L. Wang, M. Blaskiewicz, et al)

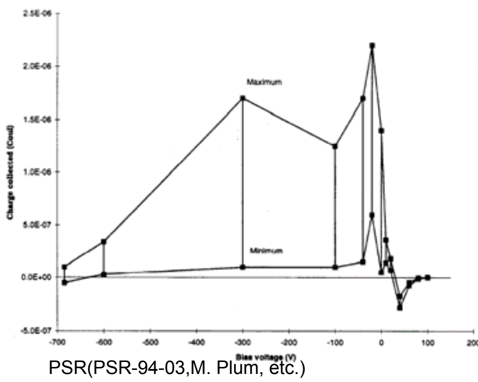

PSR(PSR-94-03,M. Plum, etc.)

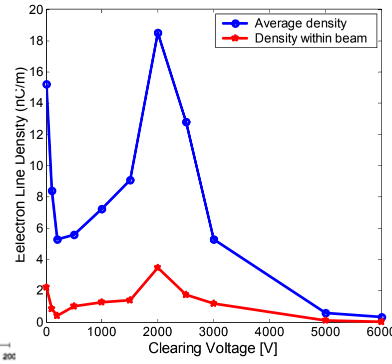

e-cloud density vs clearing fields

- **Weak field(~200V) is very helpful**
- **Strong Multipacting at 2kV, which could be stronger than zero field case**
- **Clearing electrode in injection (10 kV), and BPM +/- 1kV**

Electron cloud, diagnostics interference, mitigation (Wang, Connolly, Blaskiewicz, Zhang, Cameron …)

- Implementing solenoid windings in collimation straight, clearing electrode hardware in injection assembly (10kV) and BPMs (+/- 1 kV)
- Particle-in-cell study of e-cloud generation and mitigation mechanisms & hardware design
- RHIC run-4 confirmed SNS Ionization Profile Monitor (IPM) design
  - Multi-channel plates recessed from beam pipe, shielded from spray
  - Clearing electrodes reduce electron cloud interference
  - Profile broadening understood: non-uniformity of sweeping electric field

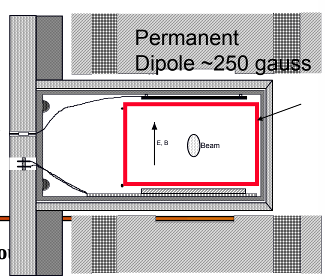

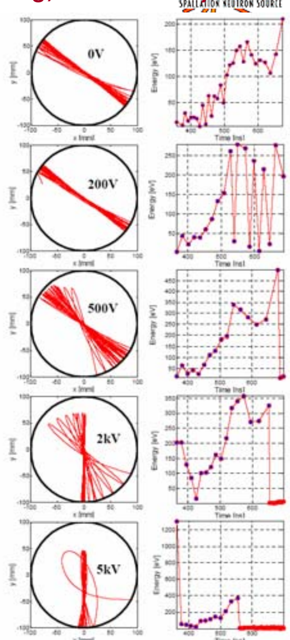

Spallation Neutron Source II

Accumulator ring & transports

Space charge, Impedances
Collective effects

Jie Wei (BNL)

Yannis Papaphilippou (ESRF)

June 28 – July 2, 2004

Outline

- Impedance budget
- Space charge
  - Tune spread
  - Induced halo
- Impedance minimization

SNS impedance budget (below 10 MHz)

Key impedances were bench measured, as recommended.

	Z_ℓ/n [Ω]	Z_T [kΩ/m]
Space charge	-j196	j(-5.8+0.45)[1] x10^3
Extraction kicker[2]	0.6n+j50	33+j125[3]
Injection kicker[4]	≈0.5, at w_0	17.5 (lowest tune 200 kHz)
RF cavity	**Resonances:** (7.48 MHz,Q≅136, 4.1Ω);(12.24, 54, 5.0); (16.88, 71, 8.33); (18.3, 129, 3.94);(20.60, 61, 3.2); (25.50, 38, 3.08); (33.35, 52, 9.5).[5]	18 (at resonance)[6]
Injection foil assembly	j0.05[7]	j4.5
Resistive wall	(j+1)0.71, at w_0	(j+1)8.5, at w_0
Broadband		
BPM	j4.0	j18
BIG and TK	j1.1	j7
Bellows	j1.3	j11
Steps	j1.9	j16
Ports	j0.49	j4.4
Valves	j0.15	j1.4
Collimator	j0.22	j2.0
Total BB	j9	j60

[1] incoherent and coherent part
[2] 25 Ω termination at PFN
[3] measured inside vacuum vessel
[4] ceramic pipe coated with 0.7 μm of copper and 0.1 μm of TiN
[5] modes will be damped (peak values per cavity without damping)
[6] without damping (at 17.8 MHz, contribution from 3 cavities), damping with glow bar
[7] based on MAFIA simulations

Impedance budget (at 50 MHz)

	Z_ℓ/n [Ω]	Z_T [kΩ/m]
Space charge	-j196	j(-5.8+0.45)[8] x10^3
Extraction kicker, 25 Ω termination	19.4[13]+j12	12.5 + j65[9]
RF cavity	**See before**	≅ 0 [10]
Injection foil assembly	j0.05	j4.5[11]
BPM	2 + j3.5	9+j16
BIG and TK	0.7+j0[12]	5.0+j0[12]
Broadband		
Bellows	j1.3	j11
Steps	j1.9	j16
Ports	j0.49	j4.4
Valves	j0.15	j1.4
Collimator	j0.22	j2.0
Total BB	j4.1	j35

[8] incoherent and coherent parts
[9] measured inside vacuum vessel without feed-through
[10] damped resonance at 17,6 MHz
[11] possible high impedance around 170MHz (can be damped with lossy material)
[12] resonant frequency around 50MHz
[13] peak value 35Ω at 35MHz

Space charge tune shift

- Transverse tune shift: $$\Delta\nu_{sc} \approx \frac{f_{sc} N_0 r_0}{4\pi B_f \epsilon_{rms} \beta^2 \gamma^3}$$

$$\epsilon_{rms} = \sigma_\perp^2/\beta_\perp \qquad \beta_\perp \approx R_0/\nu_0.$$

  - Based on cancellation between electric and magnetic field for relativistic particles
  - Strong dependence on energy

- General Laslett tune shift

$$\Delta\nu_{x,y} = -\frac{f_{sc} N_0 r_0 R_0}{2\pi B_f \nu_{x,y,0} \beta^2 \gamma} \left[\frac{1}{\sigma_{x,y}(\sigma_x + \sigma_y)} \left(\frac{1}{\gamma^2} - \eta_e\right) + A_{im}^e \left(\gamma^{-2} - \eta_e\right) + A_{im}^m\right]$$

Combined tune spread: various intensities

w.p. (6.23,6.20) – combined tune spreads at the end of accumulation:
N=0.1*10^{14} - red
(mainly chromatic spread and resulting loss due to resonances above- chromaticity correction with sextupoles or slight w.p. adjustment)
N=1*10^{14} - pink
(depressed by space charge)
N=2*10^{14} - green
(depressed by space charge)

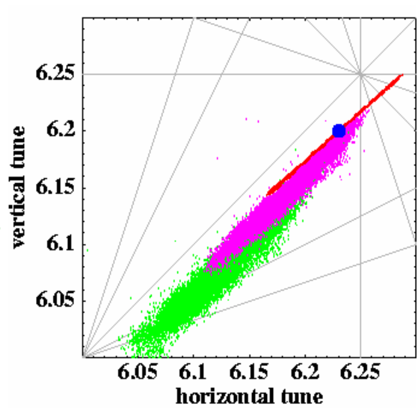

Space charge & halo formation

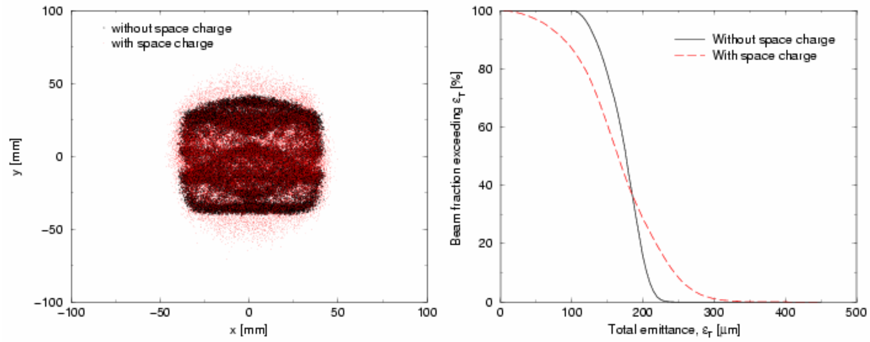

FIG. 41 Vertical emittance growth due to space charge if anti-correlated painting is used during SNS beam accumulation. The transverse tunes are (6.23, 6.20). For the data shown in black, space-charge was neglected; for the data shown in red, the space-charge force for a 2 MW beam was included. Space charge produces a significant beam tail (Section IV.C.1, courtesy A. Fedotov).

Beam tail from space charge & field error

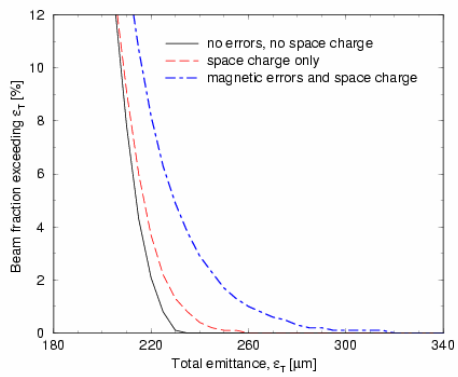

FIG. 42 Beam tail driven by space charge and magnet errors. The development of beam tail is noticeably enhanced by the combination of these two driving sources (Section IV.C.1). A non-standard working point, (6.40, 6.30), is chosen to illustrate the effect. The noimnal working point, (6.23, 6.20), is chosen to avoid resonances that lead to the development of such enhanced beam tail (Section IV.C.1, courtesy A. Fedotov).

Loss model: comparison for two working points

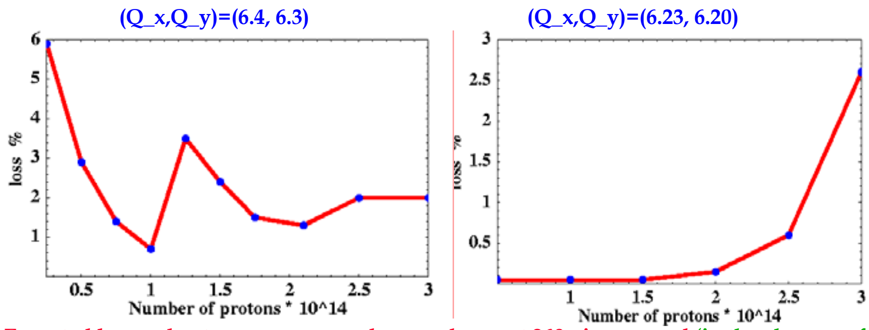

•Expected losses due to resonances and space charge at 260 pi mm mrad (in the absence of resonance correction and collective instabilities) – September'01.

•First-turn "background" losses (foil scattering and excited states of H^0) are not included in simulation. At LANL PSR they account for 0.3-0.5% loss. In the SNS their contribution is expected to be below 0.1%

Transverse space-charge impedance

- Space-charge impedance is by far the largest contribution to impedance budget (Z_{sc}= -j (5.8 - 0.45) MΩ/m)

Transverse Impedance – coherent part of the force: force generated by motion of beam center

Space-charge impedance – difference between coherent and incoherent parts, so that the largest self-field term does not contribute to coherent force (incoherent space-charge force does not directly influence coherent motion of the beam, in the absence of synchrotron motion); remaining part is still significant – pure imaginary and contributes only to the tune shift.

Space charge influences stability condition but does not lead to instability in the absence of Re(Z). However, its combined effect with Re(Z) can make beam more unstable.

Space charge impedances

$$Z_{\parallel}^{\text{sc}}(\omega) = -j\frac{ng_0 Z_0}{2\beta\gamma^2}; \quad Z_{\perp}^{\text{sc}}(\omega) = -j\frac{g_0 Z_0}{\beta^2\gamma^2}\left(\frac{1}{a^2} - \frac{1}{b^2}\right)$$

$$n = \omega/\omega_s, \; Z_0 = (\varepsilon_0 c)^{-1} = 377 \; \Omega \qquad g_0 \approx 1/2 + 2\ln(b/a)$$

- Longitudinal
  - Defocuses the beam longitudinally (below transition)
  - Capacitive
  - Cancellation between electric and magnetic forces results in strong energy dependence
- Transverse
  - Strong dependence on energy
  - Strong dependence on vacuum chamber size
  - ISIS: wire cage tapered according to beam envelope

Space-charge compensation with inductive inserts

 courtesy R. Macek, W. Chou

Resistive wall impedance

- Resistive wall impedance

$$Z_{\parallel}^{\mathrm{rw}}(n\omega_s) = n(1+j)\frac{\beta Z_0 \delta_s}{2b}; \quad Z_{\perp}^{\mathrm{rw}}(n\omega_s) = (1+j)\frac{R_0 Z_0 \delta_s}{b^3}$$

- Skin depth

$$\delta_s = \sqrt{\frac{2\rho_r}{\mu\omega}}$$

  - Larger radius vacuum chamber is preferred
  - Image passage thought RF shielding with thickness larger than the skin depth
  - Conductive coating with thickness thinner than skin depth is often used; complicated analysis

Extraction kicker impedance minimization

(J. Mi, J. Sandberg, D. Davino, H. Hahn, V. Danilov, Y. Y. Lee, S. Kurennoy …)

- Ferrite kicker inside vacuum pipe
- Optimize saturable inductor to effectively “shorten” rise time (200ns)
- Improved flat-top flatness (1%)
- PFN termination: lower impedance
- Increase magnet height to halve coupling impedance (same drive)
- Shield the terminating resistance, reducing cable reflection

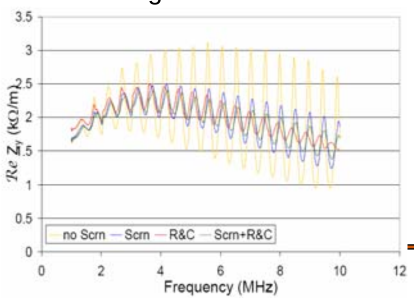

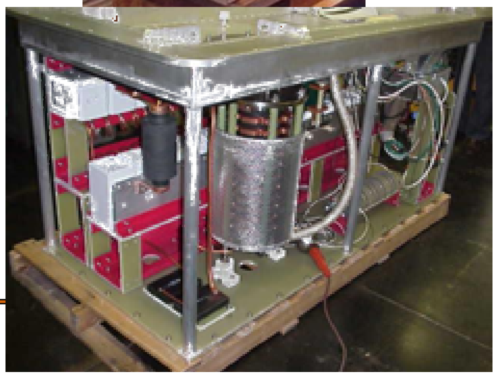

Extraction kicker impedance iterations

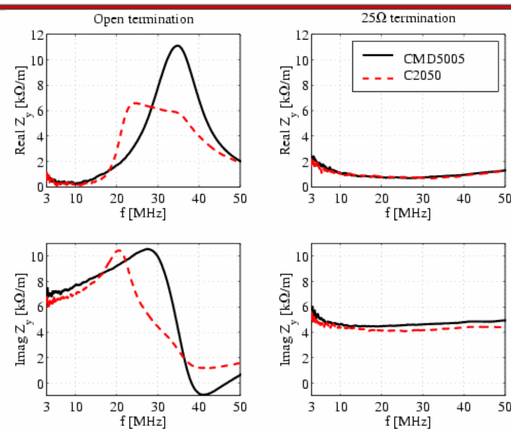

FIG. 43 Comparison of bench-measured coupling impedance for open and 25 Ω PFN termination, and high (1600) and medium (100) permeability ferrite of the SNS ring extraction-kicker assembly. The extraction kickers, residing inside the vacuum chamber of the SNS ring, are a major source of beam-coupling impedances (Section IV.C.2, courtesy D. Davino and H. Hahn).

Extraction Kicker offset

(A.Fedotov,M.Blaskiewicz,J.Wei,Y.Y.Lee,D.Davino,A.Shishlo,S.Danilo)

- In reality Extraction Kickers are offset from the center to save on mechanical dimensions when the full-size accumulated beam is extracted.
- Due to longitudinal current distribution along the bunch center of the beam will experience a kick different from the head and tail which results in a "banana-shape" distortion.
- Emittance growth associated with this effect was explored.
- Largest offset is in second 7-kicker module after the doublet (from 2.9 cm to 4.3 cm). In simulations we assume a single impedance node with offset of 35 mm.

Kicker offset – effect on beam distribution

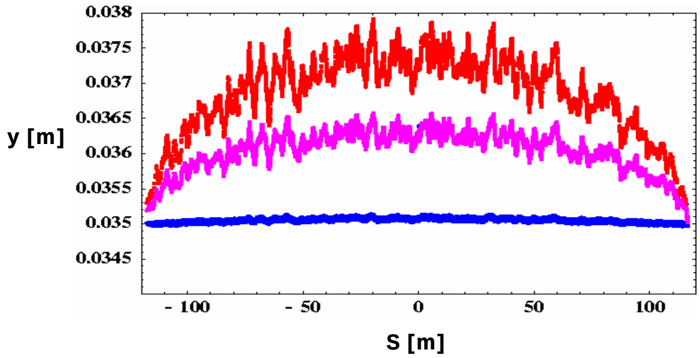

Pencil beam – y distribution along the bunch after turns 1, 2 and 3.

SNS ring diagnostics

Jie Wei (BNL)

Yannis Papaphilippou (ESRF)

June 28 – July 2, 2004

Installation an Integration Overview

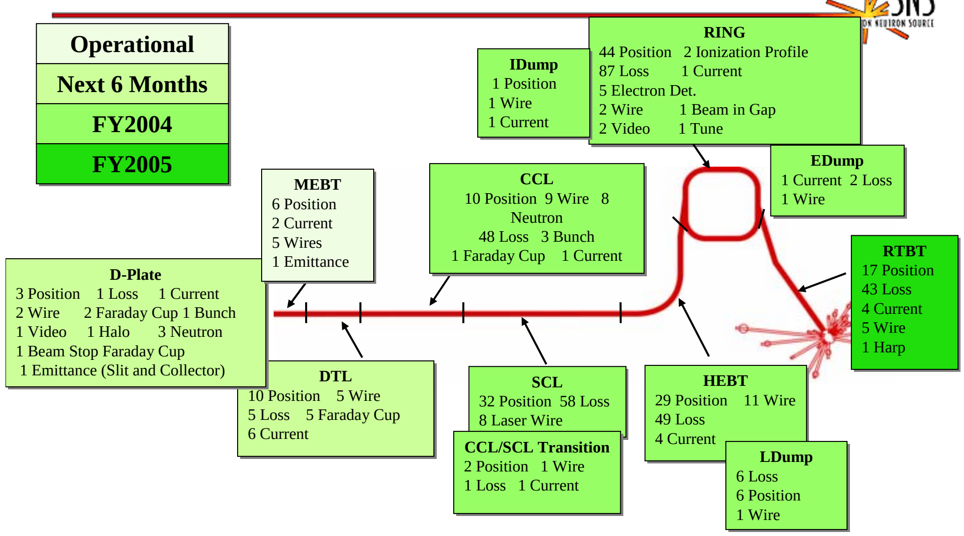

Diagnostics Requirements Table

Ring System Diagnostics AP Requirements (11/2002)

Device	Location	Intensity [ppp]	Range	Accuracy	Resolution	Data structure	Comments
BPM (position)	Ring, HEBT,RTBT	5e10 - 2e14	+/- pipe radius	+/-1%	0.5/1.0%	aver./turn-by-turn	dual plane/high frequency correction for non-linear region average < 1.5e11
BPM (phase)	HEBT	5e10 - 2e14	+/- 180 deg	+/-2 deg	0.1 deg		402.5MHz
IPM	Ring	5e10 - 2e14	+/- 64mm	2.2mm	2.2 mm	few per turn	H,V; pressure bump early
BLM (0.1 HZ)	Linac-HEBT Ring,RTBT	2e8 - 2e14	1-2.5e5 rem/h 1-2.5e5 rem/h	1%	0.5 r/h	10 s averaging	1% of 1 W/m
BLM (35 kHZ)	Linac-HEBT Ring,RTBT	2e10 - 2e14	1-2.5e5 rem/h 1-2.5e5 rem/h	1%	50 rem/h	at 6Hz rate, sel. 10 BLMs at 10Hz	
FBLM	Linac-HEBT Ring		1-1000 rem/h 1-1000 rem/h			inside mini pulse intra turn	fast; not calibrated
BCM	MEBT-to-HEBT Ring-RTBT	 5e10 - 2e14	15mA - 52 mA 15mA - 100A	1% 1%	.5% .5%	inside mini pulse turn-by-turn	 All are Fast Current Transf.
Tune	Ring			+/- 0.001 +/- 0.005	+/- 0.0005 +/- 0.001	req. averaging req. averaging	tune kicker/pick-up - coherent BTF and QM - incoherent
Wire	HEBT Ring RTBT	5e10 - 2e11 5e10 - 2e14 2e12 - 2e14	+/- pipe radius +/- pipe radius +/- pipe radius	10%rms width 10%rms width 10%rms width	5%rms width 5%rms width 5%rms width	40KHz 40KHz 40KHz	SEM SEM+FBLM SEM+FBLM
Beam-in-gap	Ring		0 - 0.1 A	20%			BIG kicker/mon., relative acc.
Foil Video	Ring	5e10 - 2e14	Visible - near IR	+/- 1mm	+/- 1mm	standard video data	2 systems (primary, secondary), phosphor screen
e - detectors	Ring		2e8 - 2e11 (e-)	5%	1e8 (e-)	turn-by-turn	5 locations: Inj.,Coll., Ext, IPM and in the arc; MCPs?
Luminescence	Ring						vacuum chambers,É

HEBT Beam Instrumentation

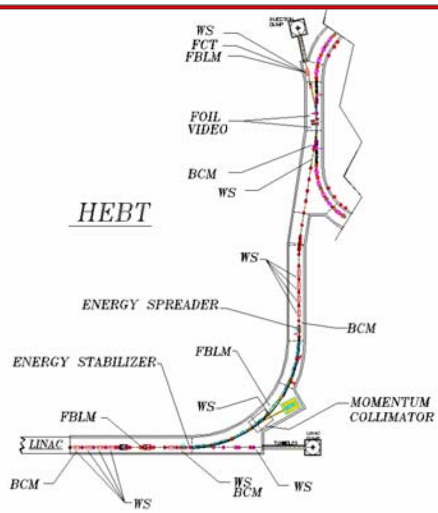

Detectors	BNL	LANL
BPM	36	IFEs
BLM	52	0
FBLM	3	0
BCM	5	0
WS	0	13
Foil Video	2(3)	0

SNS Ring Instrumentation

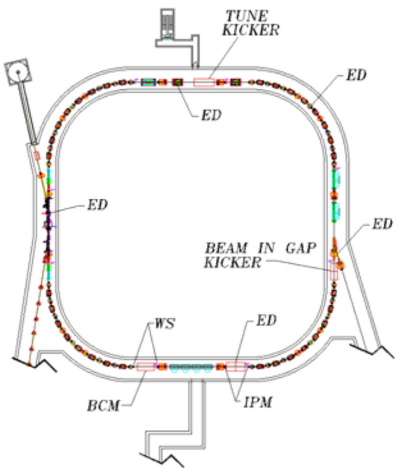

Detectors	Qty	Comments
BPM	44	dual plane
IPM	2	H+V
e-detector	5	ANL style
BLM	75	ion chamber
FBLM	12	PMT
BCM	1	
WCM	1	RF
Coh Tune	1	kick/PU
Incoh Tune	2	BTF, QMM
WS	2	H+V
BIG	1	kicker+PMT
Scraper	2	H+V

SNS Ring Instrumentation

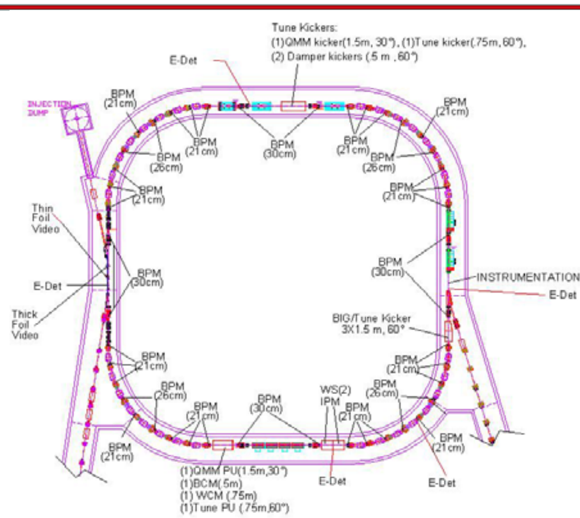

RTBT diagnostics

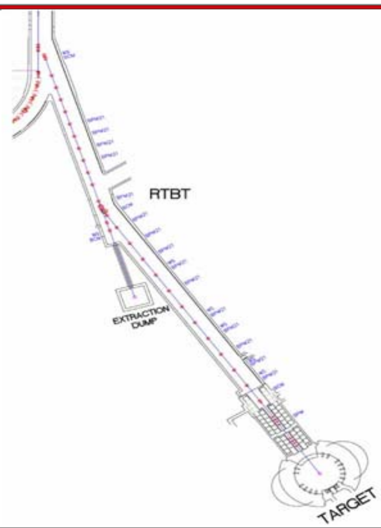

Detectors	BNL
BPM	16
BLM	40
FBLM	3
BCM	5
WS	7

Loss Monitor Detector Types

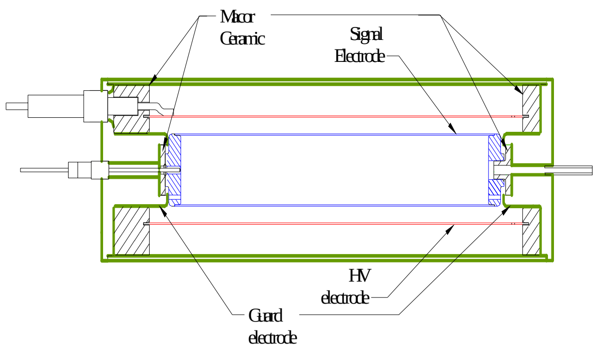

- Upper end loss limit: Response up to 0.5 % fast single point (Linac, HEBT), 0.1% in Ring, RTBT
- Lower end loss limit: 1% resolution of 1 W/m loss over 10 sec average

- Ion Chambers
  - Main array
- Neutron Detectors
  - Photo-multipliers
  - In lower energy Linac
  - Provided by INR
- FBLMs
  - For observing sub mini-bunch losses
  - HEBT, Ring, RTBT

Neutron Detectors

- **Slow Loss: 1 W/m limit**
  - Corresponds to ~10^{-4} loss distributed around Ring
  - Beam-off activation approximately 100 mrem/hr at 1 ft (~1 W/m)
  - "Rule of thumb": Multiply by 1000 to get beam-on dose rate
  - Need to resolve 2 decades below 1 W/m = 324 pA
- Low-end resolution limited by noise, upper end by detector and/or electronics saturation
  - Scaling noise observed in RHIC for the BW difference gives a noise equivalent to 550 pA
- **What is maximum high-end loss?**
  - 0.5% local loss gives total range of almost 6 decades or approximately 20-bits + sign
- Machine Protect System (MPS) signal derived from loss integrated over macropulse.
  - Same signal used for RTBT data logging.
  - Computer settable gain does not affect MPS input signal

Location	Installed units	Stroke	Spares
HEBT	**11**	**8 inch**	**2**
Ring	**2 (1 ea. H & V)**	**8 inch**	**1**
RTBT	**5**	**TBD**	**1**

Location	Method	Wires*
HEBT*	**SEM**	**3 ea. 32 u dia. C**
Ring	**Beam loss** **SEM backup method**	**1 ea. 32 u dia. C**
RTBT	**SEM**	**3 ea. 32 u dia. C, or** **3 ea. 100 u dia. SiC**

Wire scanner

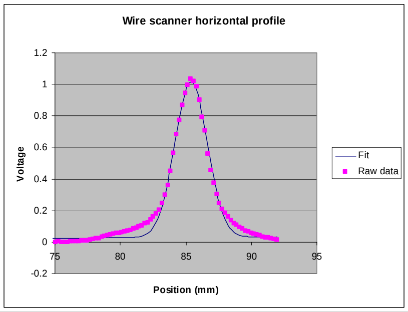

Beam Current Monitors

- MEBT to HEBT 0.3 - 1000 us,
  - » 15 to 52mA
  - » Accuracy < 1%
  - » Resolution 0.5%
  - » Detail within mini-pulse

•Ring to RTBT 5e10 to 2e14 Protons

»0.015A to 100A

»Accuracy < 1%

»Resolution 0.5%

»Turn-by-turn data

LOCATION	DIAM.	NUMBER OF BCMS
Front End	5.5cm ID 13.5cm OD	2
Linac	2.5cm,3.0cm,8cm ID	DTL=6 CCL=2 SCL=1
HEBT	13cm ID	5
Ring	22cm ID	1
RTBT	22cm ID	5
	TOTAL	22

250 μs MEBT Pulse

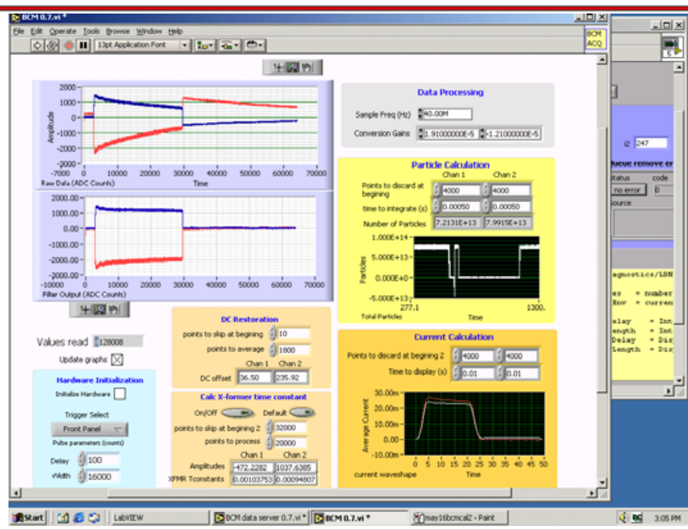

Beam Position Monitors

PUE	Required units	Machined parts	Completed units	Delivered units
21 cm ring	28	100%	33	32 (complete)
26 cm ring	8	100%	10	9 (complete)
30 cm ring	15	67%	10	0
12 cm HEBT	31	100%	34	11
21 cm HEBT /RTBT	19	100%	21	9
36 cm RTBT	2	100%	3	0

BPM Processing Linearity to Displacement

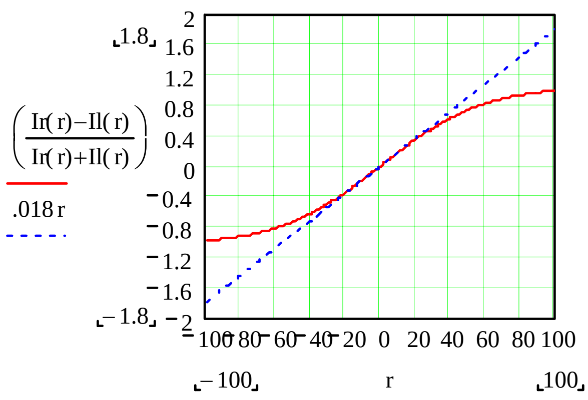

A plot of sensitivity along the axis of a pair of pick-up elements for a 70 degree stripline designed BPM with a half aperture of 105mm. The sensitivity is shown to be 0.018 per mm. Linearity is shown to be "reasonable" over a range of +/- 20mm.

SNS BPM signals

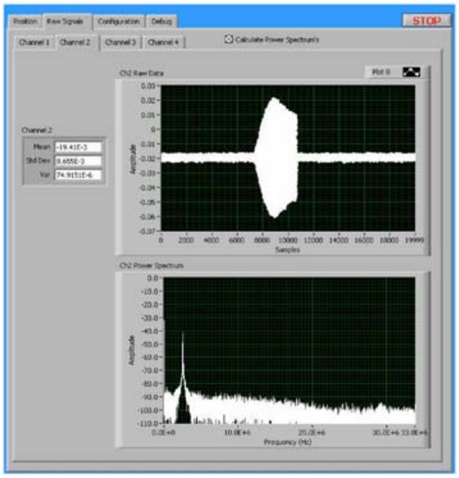

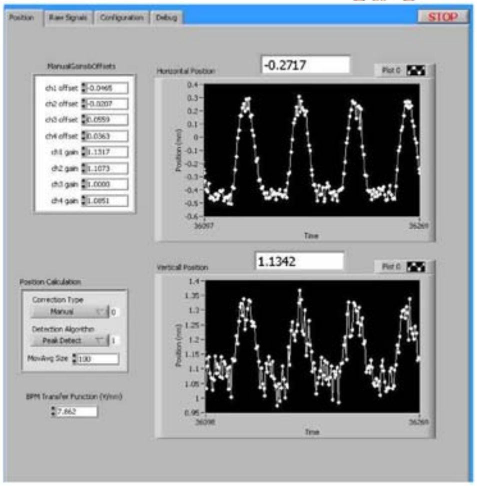

Tune Measurements

- •Coherent tune
  - •accuracy .001
  - •Resolution .0005
- •Incoherent tune
  - •accuracy .005
  - •Resolution .0025
- •Hardware used: pulser, kicker, BPM & associated DAQ/processing electronics
- •Initial processing executed in BPM PCI card
- •Tune calculations performed in a LabVIEW program
- •Measured one or more times during accumulation cycle for 1-10 turns
- •AP required measurement accuracy = +/- 0.001
- •AP required measurement resolution = +/- 0.0005
- •Measurement requires averaging

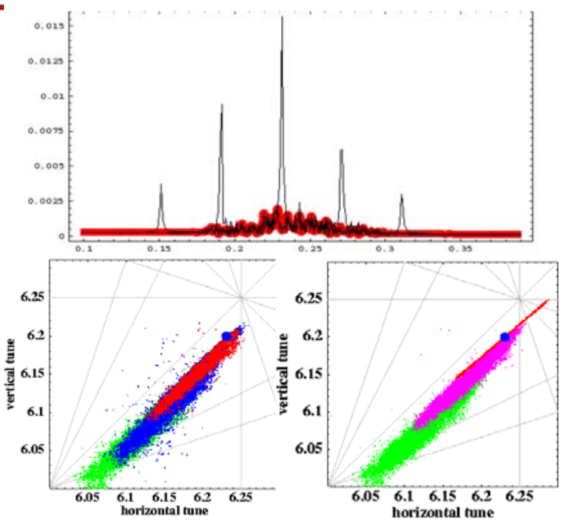

Beam In Gap kicker

- Should be no beam in the gap from linac
  - Chopper should be 100% efficient
  - Linac team claims nothing can make it from one end of the Linac to the other, and at the same time find its way from the mini-bunch to the gap
- However, nuclear scattering, foil losses, RF noise, collimation inefficiency, etc. exist
- Loss budget is 10^{-4}. Don't use it up in the gap!

•Hardware used: pulser, kicker, FBLM (gated PMT or MCP) & Gap/Halo calculations performed in LabVIEW

- AP range = 0-0.1A
- AP required accuracy = 20%
- Operated during last 100 turns of accumulation
- Kick the gap beam onto collimators/scraper
- Measure with fast loss monitors (PMT or MCP)
- Function as both gap monitor and gap cleaner
- Scraper will be located at wire scanner location

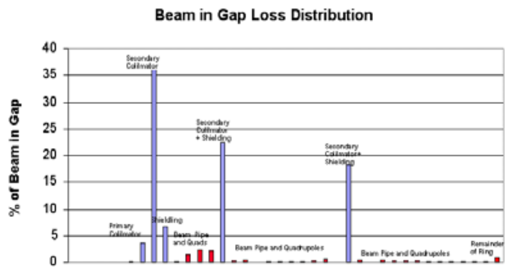

Collimator loss monitor

- Limiting apertures are the collimators
  - Locate detector near collimators (Further study needed)
  - Collimators designed to intercept controlled losses
  - Beam cleaned from gap will be lost in collimators
  - In place all the time – allows measurement during normal operation
  - Will be "warm" area – possible high background which may make fine measurement difficult
- Beam Halo measurement scraper can be used for higher resolution BIG measurement
  - Becomes temporary limiting aperture
  - Lower background region
  - Cannot be used continually – losses to high
- Use both approaches

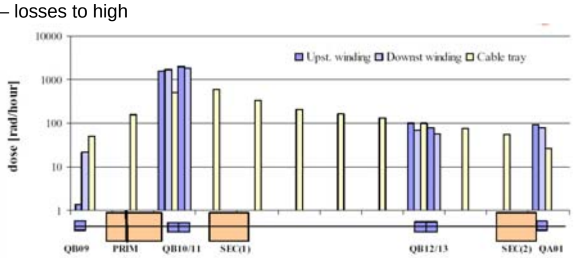

Electron detector

Side View

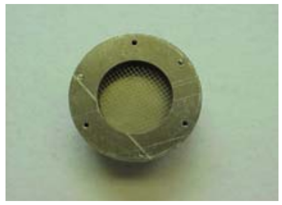

Figure 2: View of Mesh Grid

Top View

Range:
100pC/cm^2/turn minimum collected current
10nC/cm^2/turn is expected to interfere with beam

We will design for the range, 5×10^{-11}C/cm^2/turn – 10^{-6}C/cm^2/turn

Data Structure:
Digitize at 400MS/s, using standard PCI scope card

Foil video cameras

Goals:

Provide general diagnostic for SNS injection stripping foil (weak link).

Provide beam profiles at primary & secondary locations using phosphor screens.

Ring System Diagnostics AP Requirements (11/05/2002)							
Device	Location	Intensity [ppp]	Range	Accuracy	Resolution	Data structure	Comments
Foil Video	Ring	5e10 - 2e14	Visible - near IR	+/-1mm	+/-1mm	standard video data	2 systems (primary & secondary) Each with phosphor screens

Spectral response defined by Newvicon® video tube, 300-800nm.

Phosphor screens inserted:
- Beam intensity reduced
- Beam Loss Monitors masked

Foil/phosphor motion control interface within PC & to MPS.

SNS Video Foil Layout

Secondary (thick) Foil Camera Cubby **Primary (thin) Foil Camera Cubby**

Camera to foil distance 5 meters

HEBT Beam

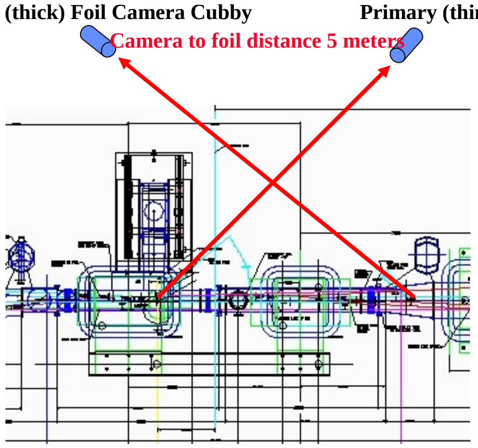

Estimated Radiation levels
The main cause of loss at injection will be nuclear scattering at the thin carbon foil.
Uncontrolled loss = 2.5W/m
Produces about 250 R/hr at 1 ft.

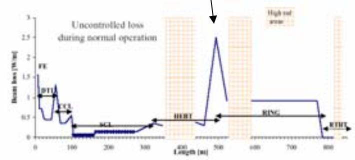

SNS/AP Tech note 7

Paraffin or boron type neutron shield in cubbies.

Est. Camera Dose 10's kR/year

SNS Video Camera Assembly

Dage 70RV camera, ND filter, lens assembly on rails inside cubby recessed in nearby wall.

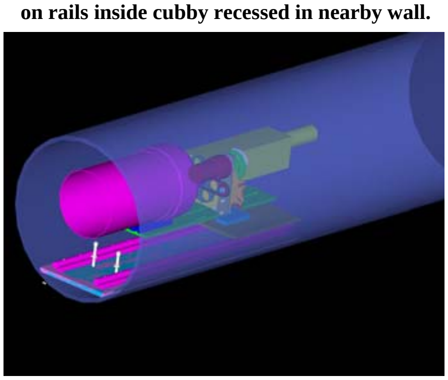

The cubby hole, camera mount, with drawer slides.

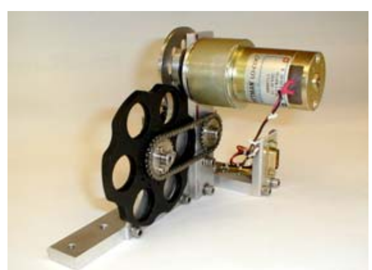

Neutral density filter assembly (C-AD):
- **DC motor drive**
- **Geneva gear with chain**
- **6 positions (blank, 1, 2, 3, 4, 5)**

Response & Timing

SNS injected beam properties [1,2]

Kinetic energy	1 GeV
Beam pulse length	1 ms
Repetition rate	60 Hz
Ave. beam current (1 MW)	18.2 mA
RMS emittance (x & y dir.)	0.14 π mm-mr
Beta function	17.4 m (x dir.) 4.56 m (y dir.)
Beam current density distribution on the foil	2-D Gaussian distribution
Beam size @ 1-σ	3.1 mm (x dir.) 1.6 mm (y dir.)

Response Characteristics:

Video Camera - Newvicon Tube:

- **Time constant = 10's of ms**
- **Saturation recovery = 100's of ms**
- Standard RS-170 Video, interlaced:
  - **1 frame every 1/30 second (33ms)**
  - **1 field every 1/60 second (16.6ms)**
- May need to phase shift camera synch to line synch.

Phosphor Screen:

- **Time constant = 10's of ms**
- **Fluorescence wavelength 700 – 900 nm**
- **Radiation Resistance about 1 x 10^{20} p/cm^2**

(C Johnson, CERN)

Stripping Foil Response:

Design & testing continues.

Diamond film or Carbon foil.

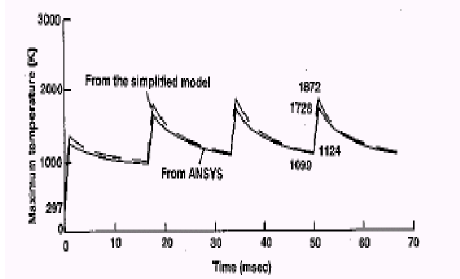

Fig. 3: The maximum temperatures on the carbon foil verse time in SNS (area density: 400 μg/cm^2)

Video Image Processing

- Personal Computer based
  - Shared with stripping foil motion control
  - Rack mounted in Ring Service Building
- NI PCI 1409 Image Acquisition board
  - 8 bit digitizer
  - 16MB onboard memory (about 75 frames)
  - External trigger, RTSI (Real Time System Integration) bus
  - Digital I/O (ND Filter control, Lamp, etc..)
  - NI-IMAQ driver, & LabView Software

Ionization Profile monitor

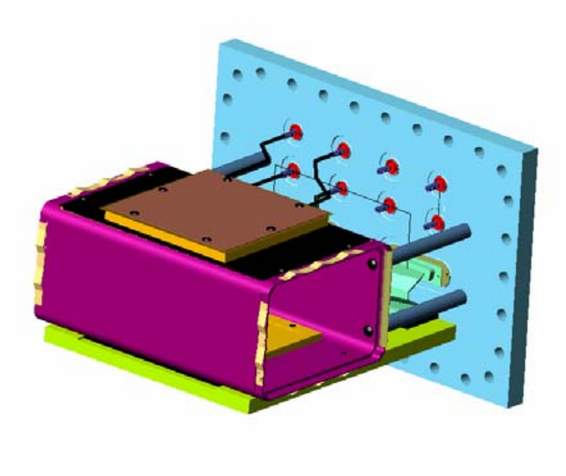

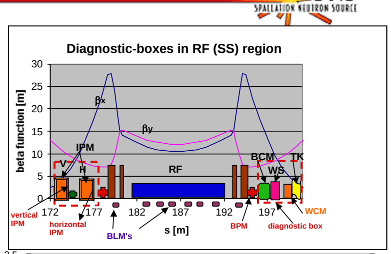

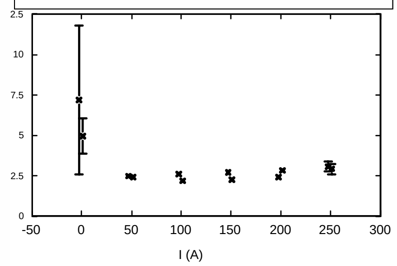

Spallation Neutron Source II
Accumulator Ring & Transport Lines

SNS Commissioning

Jie Wei (BNL)

Yannis Papaphilippou (ESRF)

June 28 – July 2, 2004

Outline

- Orbit
  - Error source and effects
  - Measurements & diagnostics: closed bumps & difference orbit
  - Corrections: local & global
- Tunes and optics
  - Error source and effects
  - Measurements: kick method, swept freq. & Schottky method
  - Corrections: main quads & trim quads
- Chromaticity
  - Source, effects, measurements
  - Correction & adjustment
- SNS commissioning plan

Orbit error sources

- Sources:

dipole field error: $\theta_i = \dfrac{B_i L_i}{B_0 \rho}$

quadrupole feed-down:

$$B_i = \left(\frac{\partial B}{\partial x}\right)_i [x_{c,i} + D_{xi}(\Delta p / p)]$$

$$\Delta x(s) = \frac{\sqrt{\beta(s)}}{2\sin(\pi\nu)} \sum_{i=1}^{N} \theta_i \sqrt{\beta(s_i)} \cos\left[\left|\phi(s) - \phi(s_i)\right| - \pi\nu\right]$$

Orbit error effects

- Single kick effects:

COD proportional to sqrt (β) at both source and BPM; maximum:

$$\Delta x(s)\big|_{\max} = \frac{\sqrt{\beta(s)\beta(s_i)}}{2\sin(\pi\nu)}\theta_i \qquad \Delta\phi = \pm\pi(\nu - m), \qquad m = 1,2,\ldots < \nu$$

COD modulation of harmonic close to ν; integer resonance
A symmetric cusp at location of a single steering error

$$\Delta x(s_i) = \frac{\theta_i}{2}\beta(s_i)\cot(\pi\nu); \qquad \Delta x'\left(s_i^{\ +}\right) = \frac{\theta_i}{2}\left[1 - \alpha(s_i)\cot(\pi\nu)\right]$$

Linear superposition of kicks

$$\Delta x(s)\big|_{rms} = \sqrt{\beta(s)}\,\frac{\sqrt{N\langle\beta(s_i)\rangle}}{2\sqrt{2}\sin(\pi\nu)}\langle\theta_i\rangle_{rms}$$

Single-bump orbit error

- Tune notation: ν (US); full Q, fractional q (European)

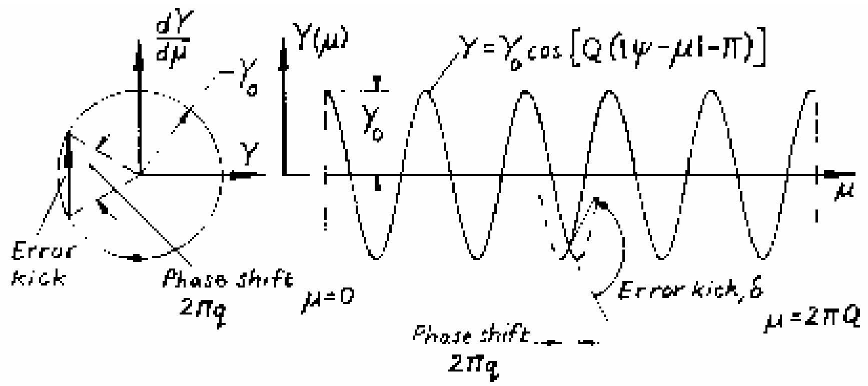

Position & orbit measurement

- Beam position & orbit

  Beam Position Monitor; single & dual plane

$$\frac{V_R - V_L}{V_R + V_L} = \frac{x}{b}\frac{4\sin(\phi_e/2)}{\phi_e}$$

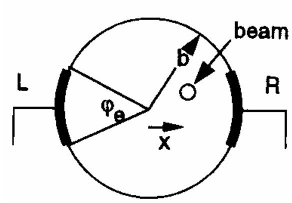

- Orbit centering in magnets

  Dipole: aperture scan

  Quadrupole: difference orbit for feed-down kick $\Delta\theta_Q = -\Delta x \Delta K L_Q$

  Sextupole: feed-down tune shift & minimum tune split

- Dispersion $\Delta\nu_{x,y} = \mp \frac{\beta_{x,y}(s)}{4\pi}\Delta x \Delta SL_s \quad \Delta\nu_{\min} = -\frac{\sqrt{\beta_x\beta_y}}{4\pi}\Delta y \Delta SL_s$

  Difference orbit at rf frequency

$$\Delta x(s) = -\frac{D(s)}{\eta}\frac{\Delta f_{rf}}{f_{rf}}$$

Local closed orbit bumps

- Two-magnet bump

  half-wavelength bump (n=1)

  $$\mu_2 - \mu_1 = n\pi \qquad \theta_2\sqrt{\beta_2} = (-)^{n+1}\theta_1\sqrt{\beta_1}$$

- Three-magnet bump

  flexible phase closed bump for diagnostics (aperture scan, gradient error measurement, magnet centering, …) & correction

  $$\frac{\theta_1\sqrt{\beta_1}}{\sin(\Delta\mu_{32})} = \frac{\theta_2\sqrt{\beta_2}}{\sin(\Delta\mu_{13})} = \frac{\theta_3\sqrt{\beta_3}}{\sin(\Delta\mu_{21})}$$

- Four-magnet bump

  control both amplitude and slope at a location

  (two upstream, two downstream; e.g. for injection, extraction, …)

Orbit correction

- Difference orbit to identify source
- Local correction

  local bumps for correction

- Global correction (orbit response matrix & singular value decomposition)

  matrix method: using N correctors optimizing M BPM readings

  $$\mathbf{A\theta} = \mathbf{d}$$

  $$A_{mn} = \frac{\sqrt{\beta_{m\beta}\beta_{nm}}}{2\sin\pi\nu}\cos\left(\left|\phi_m - \phi_n\right| - \pi\nu\right)$$

  when M=N: unique solution

  when M > N, minimizing quantity $\left|\mathbf{A\theta} - \mathbf{d}\right|^2$

  start with largest eigenvalue vectors

Tune & gradient error source & effect

- Sources:

  quadrupole field error: $\Delta K_i = \left(\frac{\partial B}{\partial x}\right)_i \Big/ B_0\rho$

  sextupole feed-down: $B'_i = \left(\partial^2 B \big/ \partial x^2\right)_i [x_{c,i} + D_{xi}(\Delta p / p)]$

$$\Delta\nu = -\frac{1}{4\pi}\sum_{i=1}^{N}\beta_i \Delta K_i L_i$$

$$\Delta\beta(s) = \frac{\beta(s)}{2\sin(2\pi\nu)}\sum_{i=1}^{N}\Delta K_i L_i \beta(s_i)\cos\left[2|\phi(s)-\phi(s_i)| - 2\pi\nu\right]$$

- Effects:

  Tune shift and tune spread, resonance crossing

  Ring β-function modulation of harmonic 2ν from each kick

  Non-linear superposition of kicks due to β-function modulation

Tune measurement & diagnostics

- Fractional tune by monitor sampling at a single azimuth
- Integral tune by global orbit analysis and lattice analysis
- Kick method:

  transverse kicker $\quad y\lambda(t) = A\sum_{i=-\infty}^{\infty} e^{in\omega_0 t} +_i B\sum_{i=-\infty}^{\infty} e^{i\omega_0(n+\nu)t}$

  longitudinal RF phase modulation

  subject to de-coherence
- RF knockout, RF dipole sweeping, swept-frequency:

  destructive or non-destructive
- Schottky signal measurement:

  coasting beam and bunched beam signal

Tune measurement illustration

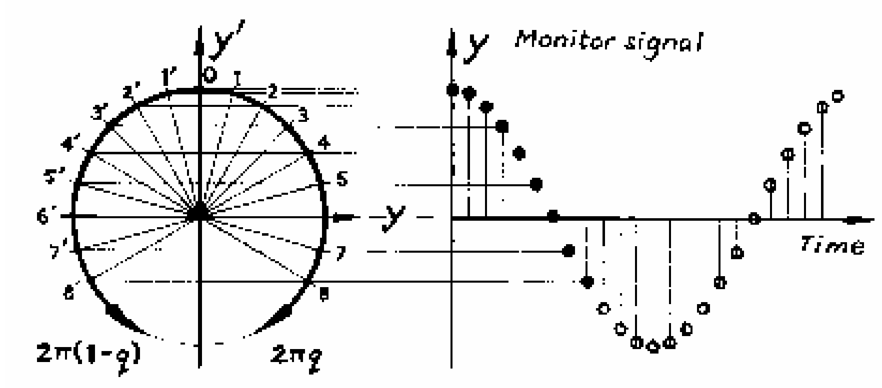

Beam frequency spectrum (longitudinal)

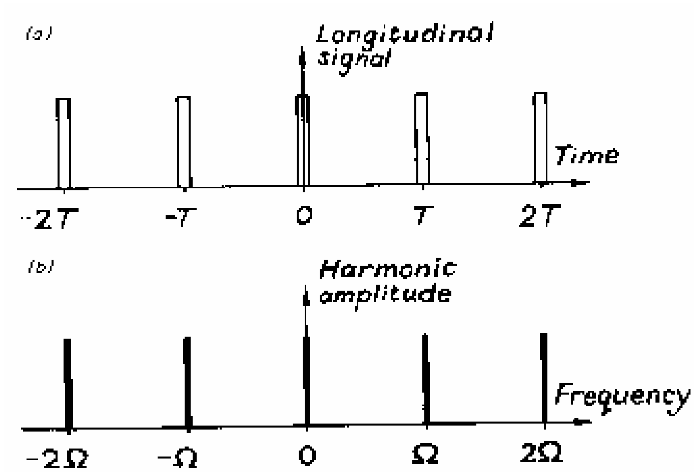

Beam frequency spectrum (transverse)

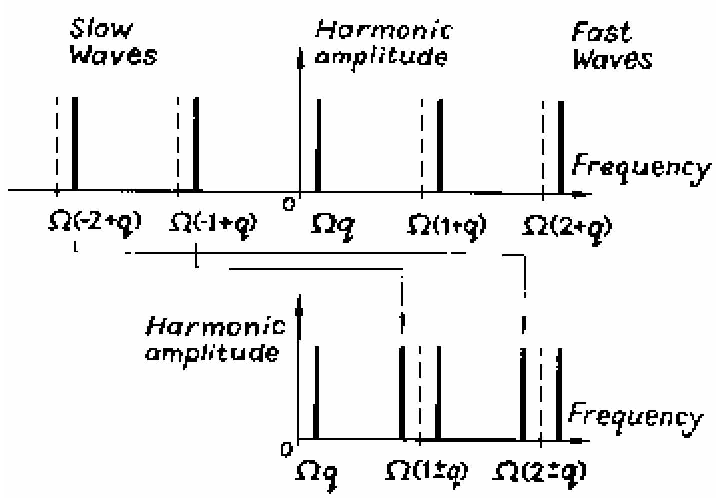

Schottky signal

- Incoherent signal from finite number of charges in beam
- Signal location, band width, band overlapping
- Coasting beam:

longitudinal: $\Delta\Omega = n\Delta\omega = n\omega_0|\eta|\Delta p/p \qquad n < \left(|\eta|\Delta p/p\right)^{-1}$

transverse: $\Delta\Omega = (n \pm \nu)\Delta\omega \pm \omega_0 \Delta\nu$

linearly increasing width, constant power at each harmonic

- Bunched beam:

longitudinal & transverse: ``fine structure'' of synchrotron bands

$$\Delta\Omega = \quad \ldots \quad + m\Omega_s$$

Schottky signal (longitudinal)

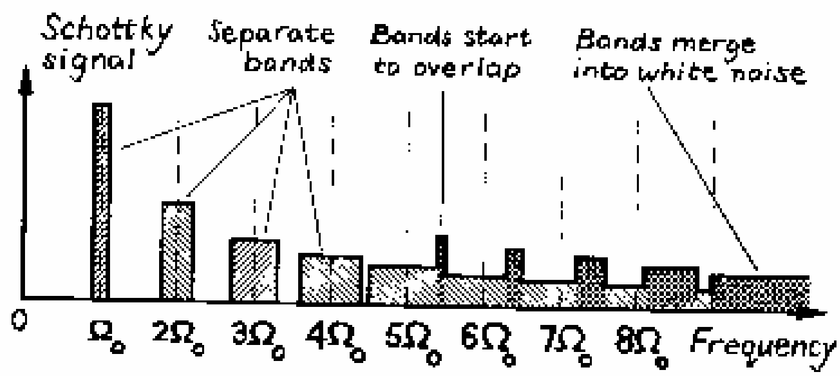

Schottky signal (transverse)

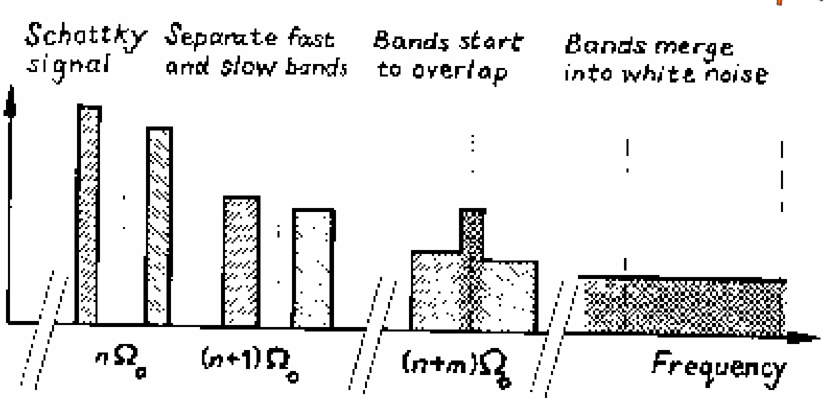

Amplitude function measurement

- Direct quadrupole pulsing $\Delta\nu = -\frac{\beta}{4\pi}\Delta K\ L$
  - Sensitive only to large β quad location
  - Susceptible to magnet hysteresis and coupling
- Betatron envelope measurement from kicking
  - Envelope proportional to $\sqrt{\beta}$
- Phase detection
  - Beam shaking at betatron freq. & phase detection at BPM's
  - Especially useful at small β locations

$$\phi(s) - \phi(s_0) = \int_{s_0}^{s_1} \frac{ds}{\beta(s)}$$

Tune & optics correction

- Adequate tuning flexibility at machine design
  - Typical range of 1 unit in both transverse directions
  - Prepare for the unexpected $\Delta\nu = -\frac{1}{4\pi}\sum_{i=1}^{N}\beta_i \Delta K_i L_i$
- Trim quad families for fast & flexible adjustment
  - Flexible, fast response (rapid cycling synchrotrons, super-conducting magnet machines, hysteresis, …)
  - Optimized power supply arrangement
- Independently powered quad correctors
  - Half-integer stop-band correction

    β wave correction

Chromaticity: errors, effects, measurement

- Sources:

  quadrupole chromatic abbreviation

  magnetic error of sextupole symmetry (eddy current, dipole fringe…)

$$\xi = -\frac{1}{4\pi}\oint K\beta(s)ds \pm \frac{1}{4\pi}\sum_{i=1}^{N}\beta_i D_i S_i L_i \qquad S_i = {B''_i}/{B\rho}$$

- Effects:

  Chromatic tune spread and resonance crossing

  Off-momentum optical mismatch

  Head-tail instability (negative ξ above transition)

- Measurement:

  Measuring tunes at various orbits of different RF frequency

Chromaticity correction & adjustment

- Minimum compensation
  - Two-family sextupole: SF & SD
  - Inadequate for non-local compensation
- Off-momentum optical function matching
  - Typical four-family for the two transverse planes
  - Located in arc region for global chromatic compensation
- Resonance excitation compensation
  - Proper location of chromatic sextupoles
  - Additional resonance correction sextupoles in zero-dispersion region

Commissioning Timeline

- Testing of all components is complete before commissioning
- HEBT/Ring Commissioning: Dec. 22, 2004 – June 17, 2005
  - Commission HEBT to Injection Dump
  - Commission Accumulator Ring
  - Commission RTBT to Extraction Dump
- Integrate and test Target Safety Systems: June 17 – Oct. 31, 2005
- RTBT to Target Commissioning: Dec. 1, 2005 – Dec. 30, 2005
  - Commission RTBT to Target
  - Commission Target

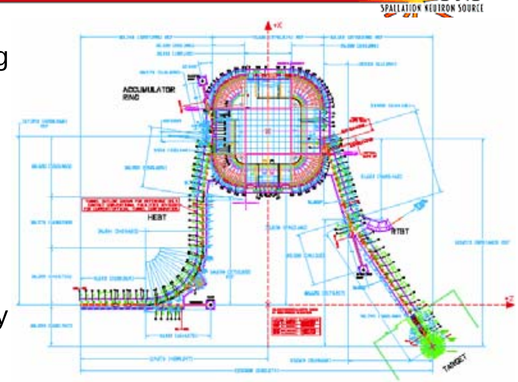

Commissioning Goals

Primary Goal:

→ Reach CD-4: 10^{13} protons/pulse on target

- Deliver CD-4 beam to the extraction dump within the allotted HEBT/Ring Commissioning period.
- Make use of the remaining time to accomplish additional goals:

Secondary Goals:

1. Measurements aimed at more detailed understanding of the machine: linear optics, HEBT/Ring/RTBT optics matching, chromaticity, resonance structure
2. Explore performance of the machine with high-intensity bunches (> 10^{13} protons/pulse): beam stability, dynamic RF tuning, impedance, e-p, space-charge

   → advanced warning on collective effects

Commissioning Philosophy: Diagnostics

- Many diagnostic devices require beam to be "timed-in"
- Assumptions about functioning diagnostics on day one:
  - Beam Loss Monitors (BLMs) and their display program
  - Raw digitized BPM signals available in the control room
- The diagnostics are commissioned and software debugged (with beam) at the earliest possible moment.
- Diagnostics commissioned in this order:
  - Beam loss monitors
  - Beam current monitors: "timed-in", display programs
  - Beam position monitors: "timed-in", display and analysis
  - Profile measuring devices: data acquisition, display, analysis

HEBT Commissioning Sequence

- Transport minimum pulse-length beam to Linac Dump
- Transport beam to Injection Foil
  - Use BLM/BPMs to track progress
  - Minimize losses with H,V correctors
  - Commission BCMs as encountered
  - Tuneup efficiency with BCMs
  - Observe beam on phospor
- Transport beam to Injection Dump
- Measure/Correct Trajectory
  - Commission BPM/Aps Soft
  - Check corrector polarities

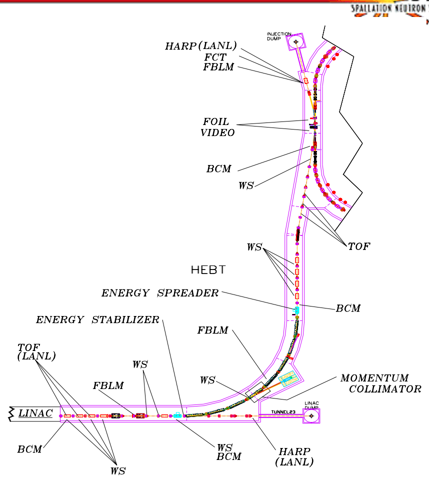

HEBT Commissioning Sequence

- HEBT Optics Measurement and Correction
  - Measure dispersion/correct achromaticity
  - Commission wire scanners, measure beam profiles
  - Obtain emittance, twiss parameters at WS arrays
  - Match linac to achromat optics and achromat to ring optics
- Verify Injection Dump Performance
  - Confirm beam profile, dump and bulk shielding, cooling system
- Measure Linac Beam Parameters
  - Emittance, energy, energy spread and jitter

- Commission ECC and ESC
  - Establish phase and amplitude setpoints
  - Measure energy jitter in arc
- Optimize HEBT collimation
  - Optimize transverse foils to minimize losses
  - Optimize momentum scrapers
- Transport 10^{13} protons/pulse to injection dump
  - Increase pulse-length, minimize losses
  - Verify dump performance at higher power

Ring Commissioning Sequence

- Transport beam to Injection Dump
- Transport minimum practical pulse-length in ring:
  - Setup dynamic bumps
  - Track progress with BLM/BPMs
  - Minimize losses with H,V correctors
  - Commission BCM
- Multi-turn transport:
  - Optimize injection bumps/fixed chicane
- Closed-orbit measurement and correction:
  - Commission BPM System
  - Measure orbit
  - Check corrector polarities
  - Close injection bumps/chicane
  - Correct closed orbit

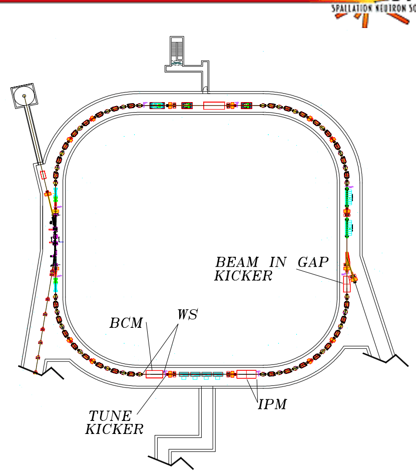

Ring Commissioning Sequence

- Transport beam 1 msec
  - Minimize losses, optimize injection conditions and closed-orbit
- Commission RF System
  - Set cavity resonant frequencies
  - Establish phase and amplitude of h=1 and h=2 cavities
- Measure and Correct Linear Optics
  - Commission and calibrate tune adjustment controls
  - Correct tunes
  - Measure linear optics and dispersion
  - Correct optics
- Measure and Correct Chromaticity
  - Measure chromaticity, commission and calibrate chromaticity controls
- Resonance Correction
  - Explore tunes, measure and minimize stopbands

Ring Extraction and Dump Commissioning

- Verify Extraction Kicker Operation
  - Check polarity/strength by exciting beam in ring
- Establish Extraction Conditions
- Transport beam to Extraction Dump
  - Track progress with BLMs
  - Minimize losses with H,V correctors
- Measure/Correct Extracted Beam Trajectory
- Commission Extraction Dump
  - Measure beam profile
  - Verify dump performance
  - Verify dump and bulk shielding
- Measure and Correct Extracted beam parameters
  - Measure beam profiles
  - Tune Ring/RTBT matching

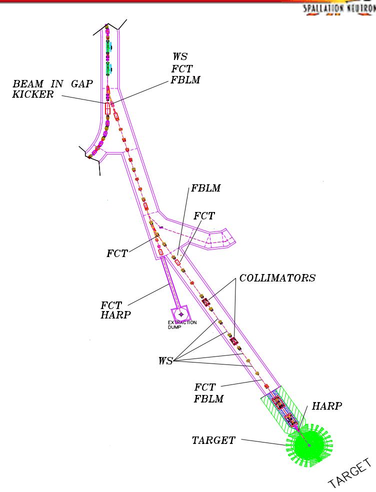

Ring Commissioning – Phase Space Painting and Collimation

- Injection Painting:
  - Characterize Injected Beam Conditions
  - Establish Injected Beam Controls (x, x′, y, y′)
- Achieve multi-turn injection of 10^{13} protons/pulse:
  - Increase pulse-length
  - Optimize losses/transmission by tuning injection conditions, tunes, chromaticity, momentum spread, extraction conditions, …
  - Measure painted-beam parameters (beam profile at Ext. Dump)
- Ring Collimation and Beam in Gap:
  - Explore Ring Aperture
  - Establish Primary Collimator Settings
  - Investigate Orbit Bumps in Collimators
  - Setup BIG Kicker System
- At this point, we have transported 10^{13} protons/pulse to Extraction Dump

High-Intensity Studies

- If time permits, we will explore machine performance with high-intensity bunches during HEBT/Ring Commissioning period with beam taken to the extraction dump:
  - Establish high-intensity conditions – increase pulse length, reoptimize injection/collimation/beam-in-gap/extraction
  - Test Dynamic RF Tuning and Feedforward Beam-loading Compensation
  - Ring loss study (losses vs. intensity/working point/chromaticity/energy spread/painting conditions)
  - Beam Stability (delay extraction and hunt for unstable modes, measure mode frequencies and growth rates)
  - E-p (commission e- detectors, measure electron production)
  - Space-charge: beam-profiles vs. intensity, working point
  - Prototype transverse feedback system tests

RTBT to Target Commissioning Sequence

- Transport minimum practical pulse-length beam to extraction dump
- Transport beam to target
  - Track progress with BLM/BPMs
  - Minimize losses with H,V
- Measure and correct trajectory
  - Commission BPM System
- Measure/Correct RTBT Optics
  - Commission Wire Scanners and Harp
  - Measure emittance and twiss parameters
  - Measure dispersion
  - Measure/verify target beam profile
  - Correct as necessary

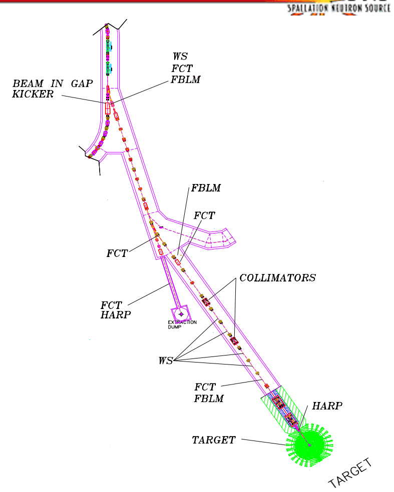

RTBT to Target Commissioning

- Investigate Fault Scenarios
  - Extraction kicker failures
  - Injection kicker failures
- Transport 10^{13} protons/pulse to the Target
  - Increase pulse-length
  - Optimize injection painting conditions, extraction
  - Optimize collimation and BIG to minimize losses

$\rightarrow$CD-4 Accelerator Goal Reached!

- Deliver beam as needed for Target/Instrument CD-4

Machine Protection, Fault Studies, Shielding

- An essential part of the Commissioning Plan involves verifying MPS functionality, conducting fault studies and verifying bulk shielding.
- Establish MPS inputs
  - Set BLM thresholds, check BLMs with local controlled losses
  - Check Harp calibration/outputs
  - Check MPS response time
- Check Fault Scenarios at Low Power (described in SNS-OPM)
  - Extraction, injection kicker, Ring RF failures
- Verify bulk shielding performance with controlled losses
  - e.g. at 1st HEBT dipole, extraction septum, 1st ring dipole, collimators
  - Verify bulk shielding performance of dumps, dump lines and collimators
- Repeat MPS and shielding tests whenever beam intensity increased.

Spallation Neutron Source II

Accumulator Ring & Transport Lines

Computer lab exercises

Jie Wei (BNL)

Yannis Papaphilippou (ESRF)

June 28 – July 2, 2004

FODO cell matched

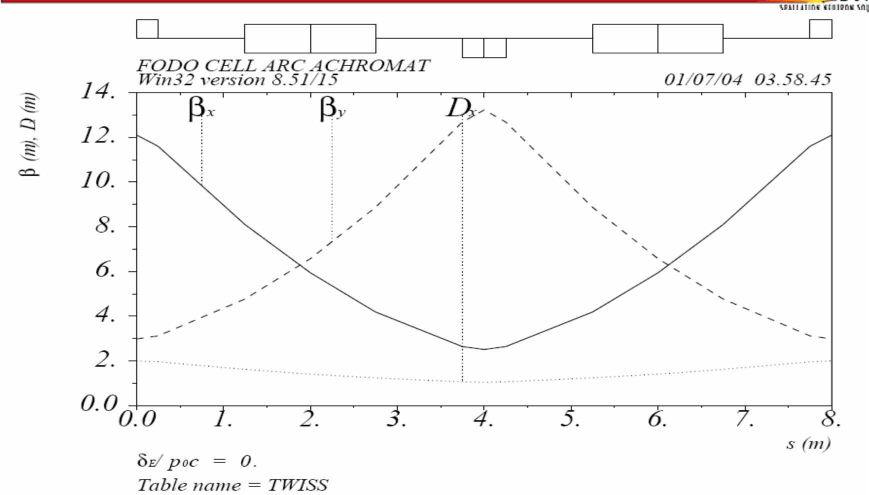

FODO cell with dispersion suppression

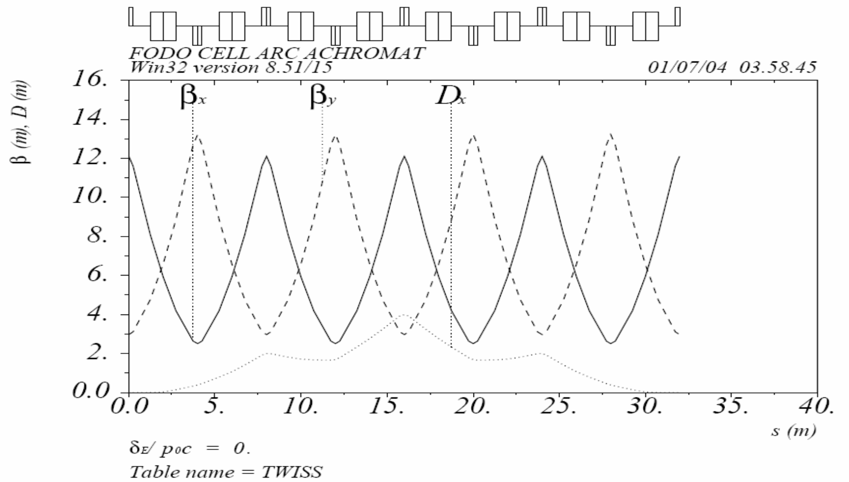

DOFO cell matched

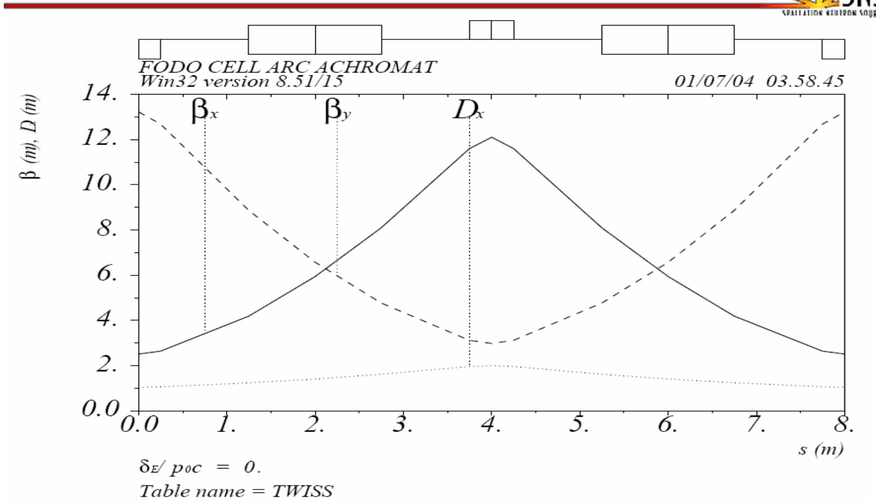

DOFO cell with dispersion suppression

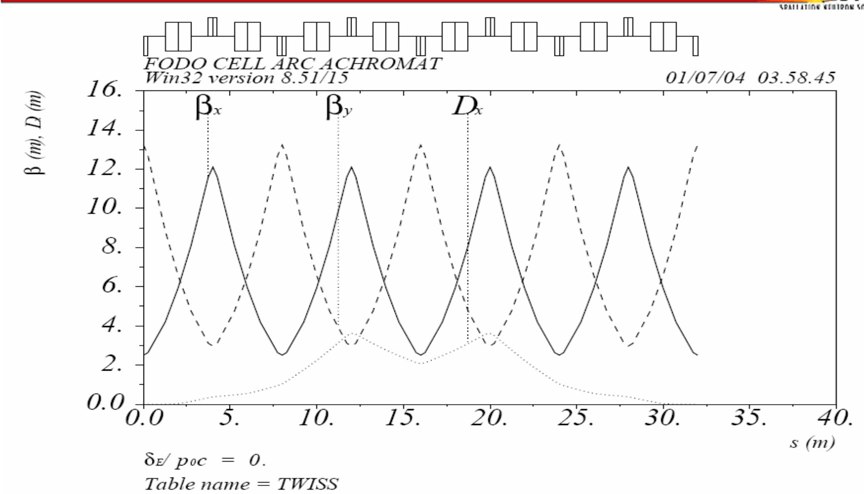

Half-field dispersion suppression using missing dipoles

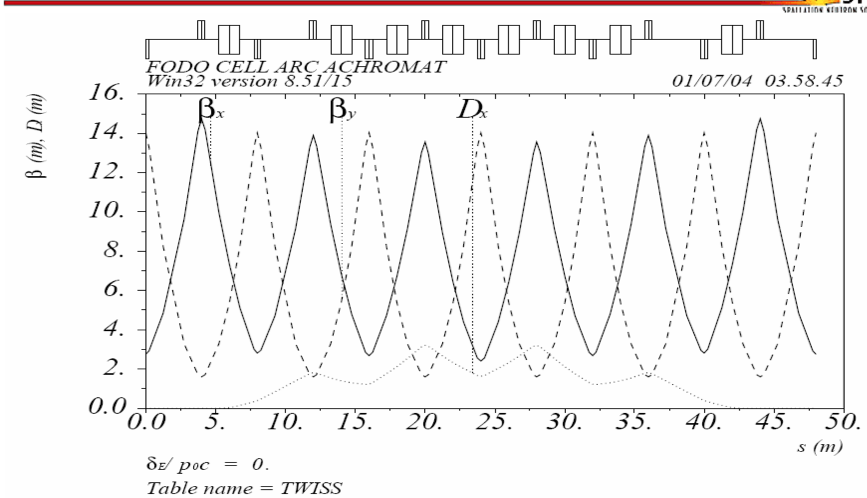

Half-field dispersion suppression using half field

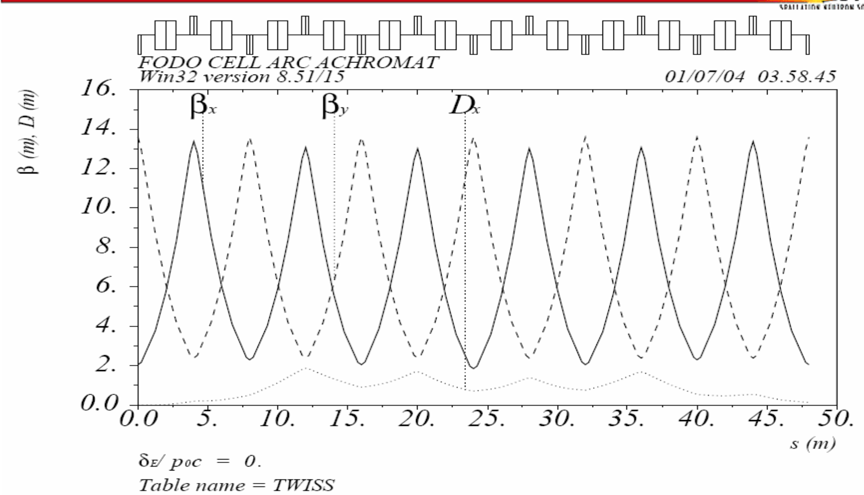

```
   Title, "FODO CELL ARC ACHROMAT"
!-------------------------------------------------------------
!------------Physical costants------------------------------
  E0    := 0.938272310   !proton mass [GeV]
  C     := 2.99792458e8  !speed of light [m/sec]
  PI    := 3.141592654
  DTR   := PI/180.

  EK    := 1.00          ![GeV] injection kinetic Energy

  PC    := sqrt(EK*(EK+2*E0))       ;  Value PC
  BRHO  := 1.e9*PC/C                ;  Value BRHO
  GAMMA := 1+EK/E0                  ;  Value GAMMA
  BETA  := sqrt(1-1/(GAMMA*GAMMA))  ;  Value BETA
!
!-------------------------------------------------------------
! Half Dipoles
!-------------------------------------------------------------
  ANG:= 2*PI/32
  EE := ANG/2
  LBEND := 1.5
  BL:  Sbend, L=LBEND/2, Angle=EE, E1=0., E2=0.
  BL2:  Sbend, L=LBEND/2, Angle=EE/2, E1=0., E2=0.

  RHOB:=LBEND/ANG ; Value RHOB
  BBND:=Brho/RHOB ; Value BBND

!-------------------------------------------------------------
! Half-Quads
!-------------------------------------------------------------
   LF:=0.25
   LD:=0.25
  LDC:=0.275
  LFC:=0.35
   QF:  Quad,  L=LF,   K1=KF/Brho
   QD:  Quad,  L=LD,   K1=KD/Brho
  QDC:  Quad,  L=LDC,  K1=KDC/Brho
  QFC:  Quad,  L=LFC,  K1=KFC/Brho


!-------------------------------------------------------------
! Drift lengths
!-------------------------------------------------------------
   SDS:  Drift, L=1
   SDS0: Drift, L=1.5

!-------------------------------------------------------------
! FODO cells
!-------------------------------------------------------------
FODO: Line =(QF,SDS,BL,BL,SDS,QD,QD,SDS,BL,BL,SDS,QF)

DOFO: Line =(QD,SDS,BL,BL,SDS,QF,QF,SDS,BL,BL,SDS,QD)

DISP: Line = (QD,SDS,BL,BL,SDS,QF,QF,SDS,SDS0,SDS,QD)

DISPH: Line = (QD,SDS,BL2,BL2,SDS,QF,QF,SDS,BL2,BL2,SDS,QD)
```

```
!-------------------------------------------------------------
! ARC cells
!-------------------------------------------------------------
ARC: Line =(4*FODO)

ARC2: Line =(4*DOFO)

ARCDISP: Line = (-2*DISP,2*DOFO,2*DISP)

ARCDISPH: Line = (-2*DISPH,2*DOFO,2*DISPH)

!-------------------------------------------------------------
!Phase advances
!-------------------------------------------------------------
  CMUX:=0.25
  CMUY:=0.22
!-------------------------------------------------------------



!-------------------------------------------------------------
! FODO CELL
!-------------------------------------------------------------
  Use, FODO
  KF = 3E+00
  KD = -4E+00
  Cell
  Vary, KF, step=.00001, lower=0, upper=6.0
  Vary, KD, step=.00001, lower=-6.0, upper=0.0
  Constraint, Range=#E, MUX=CMUX, MUY=CMUY
  Simplex, calls=2000, Tolerance=1.0E-10
  Endmatch

  PRINT, FULL
  SELECT, FLAG=FIRST, RANGE=#S/E
  TWISS, SAVE, DELTAP=0.00,TAPE=twiss
  setplot post=2 xsize=24 ysize=16 ascale=1.5 rscale=1.5
  PLOT, HAXIS=S, VAXIS1=BETX,BETY,DX, RANGE=#S/#E, STYLE=100


  SELECT, OPTICS, RANGE = #S/#E
  OPTICS,FILENAME = "optics.FODO",&
  COLUMNS = NAME, KEYWORD, S, L, K1L, BETX, ALFX, DX, BETY, ALFY, DY

!-------------------------------------------------------------
! FODO ARC
!-------------------------------------------------------------
  USE, ARC
  PRINT, FULL
  SELECT, FLAG=FIRST, RANGE=#S/E
  TWISS, SAVE, DELTAP=0.00, DX=0,DPX=0,TAPE=twiss
  setplot post=2 xsize=24 ysize=16 ascale=1.5 rscale=1.5
  PLOT, HAXIS=S, VAXIS1=BETX,BETY,DX, RANGE=#S/#E, STYLE=100


  SELECT, OPTICS, RANGE = #S/#E
  OPTICS,FILENAME = "optics.ARC",&
```

```
  COLUMNS = NAME, KEYWORD, S, L, K1L, BETX, ALFX, DX, BETY, ALFY, DY


!------------------------------------------------------------
! DOFO CELL
!------------------------------------------------------------

  Use, DOFO
  KF = 3E+00
  KD = -4E+00
  Cell
  Vary, KF, step=.00001, lower=0, upper=6.0
  Vary, KD, step=.00001, lower=-6.0, upper=0.0
  Constraint, Range=#E, MUX=CMUX, MUY=CMUY
  Simplex, calls=2000, Tolerance=1.0E-10
  Endmatch

  PRINT, FULL
  SELECT, FLAG=FIRST, RANGE=#S/E
  TWISS, SAVE, DELTAP=0.00,TAPE=twiss
  setplot post=2 xsize=24 ysize=16 ascale=1.5 rscale=1.5
  PLOT, HAXIS=S, VAXIS1=BETX,BETY,DX, RANGE=#S/#E, STYLE=100


  SELECT, OPTICS, RANGE = #S/#E
  OPTICS,FILENAME = "optics.DOFO",&
  COLUMNS = NAME, KEYWORD, S, L, K1L, BETX, ALFX, DX, BETY, ALFY, DY


!------------------------------------------------------------
! DOFO ARC
!------------------------------------------------------------
  USE, ARC2
  PRINT, FULL
  SELECT, FLAG=FIRST, RANGE=#S/E
  TWISS, SAVE, DELTAP=0.00, DX=0,DPX=0,TAPE=twiss
  setplot post=2 xsize=24 ysize=16 ascale=1.5 rscale=1.5
  PLOT, HAXIS=S, VAXIS1=BETX,BETY,DX, RANGE=#S/#E, STYLE=100


  SELECT, OPTICS, RANGE = #S/#E
  OPTICS,FILENAME = "optics.ARCD",&
  COLUMNS = NAME, KEYWORD, S, L, K1L, BETX, ALFX, DX, BETY, ALFY, DY

!------------------------------------------------------------
! Missing dipole dispersion suppression
!------------------------------------------------------------

  USE, ARCDISP
  Cell
  Vary, KF, step=.00001, lower=0, upper=6.0
  Vary, KD, step=.00001, lower=-6.0, upper=0.0
  Constraint, Range=#E, DX=0,DPX=0
  Simplex, calls=2000, Tolerance=1.0E-10
  Endmatch

  PRINT, FULL
```

```
  SELECT, FLAG=FIRST, RANGE=#S/E
  TWISS, SAVE, DELTAP=0.00, DX=0,DPX=0,TAPE=twiss
  setplot post=2 xsize=24 ysize=16 ascale=1.5 rscale=1.5
  PLOT, HAXIS=S, VAXIS1=BETX,BETY,DX, RANGE=#S/#E, STYLE=100


  SELECT, OPTICS, RANGE = #S/#E
  OPTICS,FILENAME = "optics.misdip",&
  COLUMNS = NAME, KEYWORD, S, L, K1L, BETX, ALFX, DX, BETY, ALFY, DY

!-------------------------------------------------------------
! Half dipole dispersion supression
!-------------------------------------------------------------
  Use, DOFO
  KF = 3E+00
  KD = -4E+00
  Cell
  Vary, KF, step=.00001, lower=0, upper=6.0
  Vary, KD, step=.00001, lower=-6.0, upper=0.0
  Constraint, Range=#E, MUX=CMUX, MUY=CMUY
  Simplex, calls=2000, Tolerance=1.0E-10
  Endmatch

 USE, ARCDISPH
  Cell
  Vary, KF, step=.00001, lower=0, upper=6.0
  Vary, KD, step=.00001, lower=-6.0, upper=0.0
  Constraint, Range=#E, DX=0,DPX=0
  Constraint, Range=#S/E, BETY<13.5
  Simplex, calls=2000, Tolerance=1.0E-10
  Endmatch



  PRINT, FULL
  SELECT, FLAG=FIRST, RANGE=#S/E
  TWISS, SAVE,  DX=0,DPX=0, TAPE=twiss

 setplot post=2 xsize=24 ysize=16 ascale=1.5 rscale=1.5
 PLOT, HAXIS=S, VAXIS1=BETX,BETY,DX, RANGE=#S/#E, STYLE=100
STOP

  SELECT, OPTICS, RANGE = #S/#E
  OPTICS,FILENAME = "optics.halfdip",&
  COLUMNS = NAME, KEYWORD, S, L, K1L, BETX, ALFX, DX, BETY, ALFY, DY


STOP





!
!------------------ Chromaticity correction ------------------
!
CHRM3=0
CHRM4=0
```

```
CHRM5=0
CHRM6=0

HARMON

HCHROMATICITY

HVARY, NAME=CHRM3,STEP=0.001
HVARY, NAME=CHRM4,STEP=0.001
HVARY, NAME=CHRM5,STEP=0.001
HVARY, NAME=CHRM6,STEP=0.001
HWEIGHT, QX'=1.0,QY'=1.0,BX'I=1.0,BY'I=1.0
HCELL, QX'=0,QY'=0,BX'I=0.0,BY'I=0.0


ENDHARMON

PRINT, RANGE=#E
!PRINT, FULL
TWISS, CHROM, TAPE="chrom0.twiss",TUNES,DELTAP=-0.01:0.01:0.005
!
SELECT, OPTICS, RANGE = #S/#E
OPTICS,FILENAME = "chrom0.optics",deltap=0, &
        COLUMNS = NAME, KEYWORD, S, L, K1L, BETX,ALFX,DX, BETY,ALFY,DY


USE, RNG
SELECT, OPTICS, RANGE = #S/#E
OPTICS,FILENAME = "all_elementsdp_p1.optics",deltap=0.01, &
        COLUMNS = NAME, KEYWORD, S, L, K1L, BETX,ALFX,DX,BETY,ALFY,DY

  Stop
```

```
  Title, "SNS Linac Accumulator Ring "
!-------------------------------------------------------------
!------------Physical costants--------------------------------
  E0    := 0.938272310   !proton mass [GeV]
  C     := 2.99792458e8  !speed of light [m/sec]
  PI    := 3.141592654
  DTR   := PI/180.

  EK    := 1.00          ![GeV] injection kinetic Energy

  PC    := sqrt(EK*(EK+2*E0))       ;  Value PC
  BRHO  := 1.e9*PC/C                ;  Value BRHO
  GAMMA := 1+EK/E0                  ;  Value GAMMA
  BETA  := sqrt(1-1/(GAMMA*GAMMA))  ;  Value BETA
!
!--------------Select Nominal Tunes---------------------------
  QH:=6.230
  QV:=6.200
  MUH:=QH/4.0
  MUV:=QV/4.0
!-------------------------------------------------------------
!  Call file='chicane.lat'
  Call file='SNSring.v.1.-1'
!  Call file='HKICKS'
!  Call file='VKICKS'
!-------------------------------------------------------------
  SET, SDL, 0.0
  SET, DSO, 0.0
  SET, DSOO, 0.0
  SET, DUU, 0.0
!-------------------------------------------------------------
  CMUX:=0.25
  CMUY:=0.272
  SCMUH:=MUH-4.0*CMUX
  SCMUV:=MUV-4.0*CMUY
  BHMAX:=27.0
  BXMCH:=2.374
  BYMCH:=13.182
!-------------------------------------------------------------
  Use, AC
  KF = 3.933999E+00
  KD = -4.353047E+00
  Cell
  Vary, KF, step=.00001, lower=0.0, upper=6.0
  Vary, KD, step=.00001, lower=-6.0, upper=0.0
  Constraint, Range=#E, MUX=CMUX, MUY=CMUY
  Simplex, calls=2000, Tolerance=1.0E-10
  Endmatch
!-------------------------------------------------------------
  Use, SC
  KDE = -1.6E+00
  KFC = 3.5E+00
  KDC = -3.8E+00
  Match, Line=AC, ALFX=0.0, ALFY=0.0, DX=0.0, DY=0.0
  Vary, KDE, step=.00001, lower=-8.0, upper=0.0
  Vary, KFC, step=.00001, lower=0.0, upper=8.0
  Vary, KDC, step=.00001, lower=-8.0, upper=0.0
```

```
  Constraint, Range=QFC, BETX < BHMAX
  Constraint, Range=#E, BETY=BYMCH, BETX=BXMCH
  Constraint, Range=#E, MUX=SCMUH, MUY=SCMUV
  Simplex, calls=2000, Tolerance=1.0E-10
  Endmatch
!------------------------------------------------------------
  Use, SPP
  Cell
  Vary, KDE, step=.00001, lower=-8.0, upper=0.0
  Vary, KFC, step=.00001, lower=0.0, upper=8.0
  Vary, KDC, step=.00001, lower=-8.0, upper=0.0
  Constraint, Range=#E, MUX=MUH, MUY=MUV
  Constraint, Range=QFC, BETX < BHMAX
  Constraint, Range=#E, BETY=BYMCH, BETX=BXMCH
  Simplex, calls=2000, Tolerance=1.0E-10
  Endmatch
!------------------------------------------------------------
  SET, KDEE, 0.5*(KDE+KD)
  Use, SP
  Cell
  Vary, KDEE, step=.00001, lower=-8.0, upper=0.0
  Vary, KFC, step=.00001, lower=0.0, upper=8.0
  Vary, KDC, step=.00001, lower=-8.0, upper=0.0
  Constraint, Range=#E, MUX=MUH, MUY=MUV
  Constraint, Range=QFC, BETX < BHMAX
  Constraint, Range=#E, BETY=BYMCH, BETX=BXMCH
  Simplex, calls=2000, Tolerance=1.0E-10
  Endmatch
!------------------------------------------------------------
  Use, SP
  Cell
  Vary, KFC, step=.00001, lower=0.0, upper=8.0
  Vary, KDC, step=.00001, lower=-8.0, upper=0.0
  Constraint, Range=#E, MUX=MUH, MUY=MUV
  Simplex, calls=2000, Tolerance=1.0E-10
  Endmatch
!------------------------------------------------------------
  Use, RINGSX
!  Use, RNG
!  Call file='Dalnerr'
!  Call file='Qalnerr'
  Cell
  Vary, KFC, step=.00001, lower=0.0, upper=8.0
  Vary, KDC, step=.00001, lower=-8.0, upper=0.0
  Constraint, Range=#E, MUX=QH, MUY=QV
  Simplex, calls=2000, Tolerance=1.0E-10
  Endmatch
!  Eprint
!
  SELECT, OPTICS, RANGE = #S/#E
  OPTICS,FILENAME = "optics",&
  COLUMNS = NAME, KEYWORD, S, L, K1L, BETX, ALFX, DX, BETY, ALFY, DY

  PRINT, FULL
  SELECT, FLAG=FIRST, RANGE=#S/E
  TWISS, SAVE, DELTAP=0.00, TAPE=twiss
```

```
 setplot post=2 xsize=24 ysize=16 ascale=1.5 rscale=1.5
 PLOT, HAXIS=S, VAXIS1=BETX,BETY, RANGE=#S/#E, STYLE=100
 PLOT, HAXIS=S, VAXIS1=BETX, RANGE=#S/#E, STYLE=100
 PLOT, HAXIS=S, VAXIS1=BETY, RANGE=#S/#E, STYLE=100
 PLOT, HAXIS=S, VAXIS1=DX,DY,   RANGE=#S/#E, STYLE=100
 PLOT, HAXIS=S, VAXIS1=DX,   RANGE=#S/#E, STYLE=100
 PLOT, HAXIS=S, VAXIS1=DY,   RANGE=#S/#E, STYLE=100
 PLOT, HAXIS=S, VAXIS1=X,Y,   RANGE=#S/#E, STYLE=100
 PLOT, HAXIS=S, VAXIS1=X,   RANGE=#S/#E, STYLE=100
 PLOT, HAXIS=S, VAXIS1=Y,   RANGE=#S/#E, STYLE=100

!
!------------------ Chromaticity correction ------------------
!
CHRM3=0
CHRM4=0
CHRM5=0
CHRM6=0

HARMON

HCHROMATICITY

HVARY, NAME=CHRM3,STEP=0.001
HVARY, NAME=CHRM4,STEP=0.001
HVARY, NAME=CHRM5,STEP=0.001
HVARY, NAME=CHRM6,STEP=0.001
HWEIGHT, QX'=1.0,QY'=1.0,BX'I=1.0,BY'I=1.0
HCELL, QX'=0,QY'=0,BX'I=0.0,BY'I=0.0


ENDHARMON

PRINT, RANGE=#E
!PRINT, FULL
TWISS, CHROM, TAPE="chrom0.twiss",TUNES,DELTAP=-0.01:0.01:0.005
!
SELECT, OPTICS, RANGE = #S/#E
OPTICS,FILENAME = "chrom0.optics",deltap=0, &
        COLUMNS = NAME, KEYWORD, S, L, K1L, BETX,ALFX,DX, BETY,ALFY,DY


USE, RNG
SELECT, OPTICS, RANGE = #S/#E
OPTICS,FILENAME = "all_elementsdp_p1.optics",deltap=0.01, &
        COLUMNS = NAME, KEYWORD, S, L, K1L, BETX,ALFX,DX,BETY,ALFY,DY

  Stop
```

Spallation Neutron Source II
Accumulator Ring & Transport Lines

MAD crash course

Jie Wei (BNL)

Yannis Papaphilippou (ESRF)

June 28 – July 2, 2004

Methodical Accelerator Libraries

(Hans Grote and Chris Iselin)

- Basic design tool for circular machine and beam lines, including
  - Linear lattice optics calculation
  - Optics matching
  - Transverse matrix matching
  - Survey calculations
  - Error definition
  - Correction (closed orbit, coupling non-linear)
  - Tracking
  - Chromatic effects and resonances
  - Intrabeam scattering
- Basic structure input for many other computer tools (UAL, MaryLie, Accelerator Toolbox, COSY, etc.)
- MAD versions:
  - 8: FORTRAN based code, actually frozen
  - 9: C++ based code, still to be debugged
  - X: FORTRAN and C based code, in development

Commands and statements

Name	Meaning	Section
HELP	Help on command names	2.2.1
SHOW	Help on defined names	2.2.2
TITLE	Define page header for output	2.5
STOP	End program run	2.6
OPTION	Set command options	2.7
:=	Define parameter dependencies	2.8.1
SET	Set parameter value	2.8.2
VALUE	Show parameter values	2.8.3
SYSTEM	Execute operating system command	2.10

`keyword` Identifies the action desired.

`attribute` Most commands require attributes for their operation. These are normally entered in the form

`attribute-name=attribute-value`

The `attribute-name` selects the attribute, and `attribute-value` gives it a value.

General command format

`label: keyword {,attribute}`

It has three parts:

`label` Gives a name to the stored command. A `label` is required for a definition statement.

`keyword` Identifies the action desired.

`attribute` Most commands require attributes for their operation. These are normally entered in the form

`attribute-name=attribute-value`

The `attribute-name` selects the attribute, and `attribute-value` gives it a value.

When a command is entered with a `label`, MAD keeps it in memory. This allows repeated execution of the same command by just entering its label. If the label of such a command appears together with new attributes, the attributes will be replaced first:

```
QF: QUADRUPOLE,L=1,K1=0.01    ! first definition of QF
QF,L=2                        ! redefinition of QF, new length
TW1: TWISS,BETX=1,BETY=1      ! first execution of TW1
                              ! with BETX=1, BETY=1
TW1,BETX=2,BETY=3             ! second execution of  TW1
                              ! with BETX=2, BETY=3
```

Parameter statement

A relation is established between variables by the statement

```
parameter-name:=expression
```

It creates a new parameter parameter-name and discards any old parameter with the same name. Its value depends on all quantities occurring in expression on the right-hand side. Whenever an operand in expression changes, a new value is calculated. The definition may be thought of as a mathematical equation; but MAD is not able to solve the equation for a quantity on the right-hand side. Example:

```
GEV:=100
BEAM,ENERGY=GEV
```

Circular definitions are not allowed (but see Section 2.8.2):

```
X:=X+1     ! X cannot be equal to X+1
A:=B
B:=A       ! A and B are equal, but of unknown value
```


Assignment of parameters

```
SET,VARIABLE=parameter-name,VALUE=expression
```

This statement acts like a FORTRAN assignment. If the parameter parameter-name does not yet exist, it is created. Then the expression is evaluated, and the result is assigned to the parameter parameter-name. Finally the expression is discarded. Therefore a sequence like the following is permitted:

```
...                        ! some definitions
USE,line
X:=0                       ! create parameter X with value zero
                           ! could also use "SET,X,0"
DO,TIMES=10                ! repeat ten times
  TWISS                    ! uses X=0, 0.01, ..., 0.10
  SET,X,X+.01              ! increment parameter X by 0.01
ENDDO
```

Output of parameters

The `VALUE` statement

```
VALUE,VALUE=expression{,expression}
```

evaluates up to five expressions using the most recent values of any operands and prints the results on the `ECHO` file. Example:

```
P1:=5
P2:=7
VALUE,P1*P2-3
```

After echoing the command, this prints:

```
AAVALU.  Value of expression "P1*P2-3" is     32.00000000
```

The main use of this commands is for printing a quantity which depends on matched attributes. It allows use of MAD as a programmable calculator. One may also tabulate functions.

Comments

Commands bracketed between `COMMENT` and `ENDCOMMENT` are not executed, but skipped. These commands may be nested. Example:

```
EMIT       ! executed
COMMENT
SURVEY     ! not executed (nesting level 1)
COMMENT
SURVEY     ! not executed (nesting level 2)
ENDCOMMENT
TWISS      ! still not executed (nesting level 1)
ENDCOMMENT
TWISS      ! executed again
```

Physical elements and markers

Name	Meaning	Section
MARKER	Marker for beam observation	3.2
DRIFT	Drift space	3.3
SBEND	Sector bending magnet	3.4
RBEND	Rectangular bending magnet	3.4
QUADRUPOLE	Quadrupole	3.5
SEXTUPOLE	Sextupole	3.6
OCTUPOLE	Octupole	3.7
MULTIPOLE	Thin multipole	3.8
SOLENOID	Solenoid	3.9
HKICKER	Horizontal orbit corrector	3.10
VKICKER	Vertical orbit corrector	3.10
KICKER	Corrector for both planes	3.10
RFCAVITY	RF cavity	3.11
ELSEPARATOR	electrostatic separator	3.12
HMONITOR	Horizontal orbit position monitor	3.13
VMONITOR	Vertical orbit position monitor	3.13
MONITOR	Orbit position monitor (both planes)	3.13
INSTRUMENT	Space for beam instrumentation	3.13
ECOLLIMATOR	Elliptic collimator	3.14
RCOLLIMATOR	Rectangular collimator	3.14
YROT	Rotation about vertical axis	3.15
SROT	Rotation about longitudinal axis	3.15
BEAMBEAM	Beam-beam interaction	3.16
MATRIX	Arbitrary matrix	3.17
LUMP	Concatenation of elements	3.20

Input format

All physical elements are defined by statements of the form

`label: keyword [,TYPE=name] {,attribute}`

Example:

`QF: QUADRUPOLE,TYPE=MQ,L=1.8,K1=0.015832`

where

`label` A name to be given to the element (in the example `QF`),

`keyword` An element type keyword (in the example `QUADRUPOLE`),

`TYPE` A label to be attached to the element. It denotes the "engineering type" as defined document-labelin earlier versions of MAD, and may be used for selection of elements in various commands like error definitions. (in the example `MQ`).

`attribute` Normally has the form

`attribute-name=attribute-value`

`Attribute-name` selects the attribute, as defined for the element type keyword (in the example `L` and `K1`), and `attribute-value` gives it a value (in the example 1.8 and 0.015832).

Markers and drift spaces

```
label: MARKER,TYPE=name
```

The simplest element which can occur in a beam line is the `MARKER`. It has no effect on the beam, but it allows one to identify a position in the beam line, for example to apply a matching constraint. A marker has only the `TYPE` attribute: Example:

```
M27: MARKER,TYPE=MM}
```

```
label: DRIFT,TYPE=name,L=real
```

A `DRIFT` space has one real attribute:

`L` The drift length (default: 0 m)

Examples:

```
DR1: DRIFT,L=1.5
DR2: DRIFT,L=DR1[L],TYPE=DRF
```

The length of `DR2` will always be equal to the length of `DR1`. The reference system for a drift space is shown in Figure 3.1.

Bending magnets

`RBEND` Rectangular bending magnet

`SBEND` Sector bending magnet

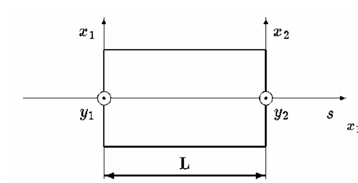

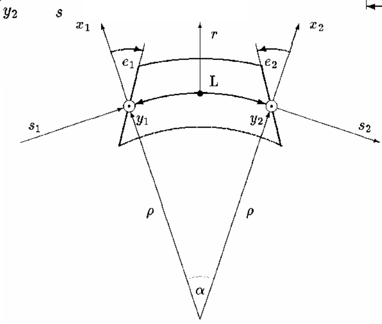

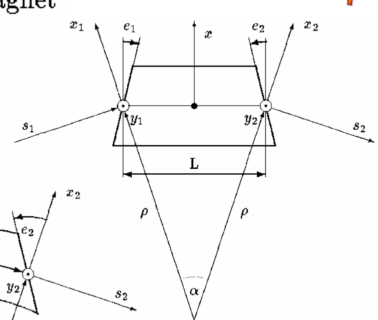

Bending magnet definition

```
SBEND, TYPE=name,L=real,ANGLE=real,K1=real,E1=real,E2=real,&
       TILT=real,K2=real,H1=real,K2=real,HGAP=real,FINT=real,&
       K3=real
RBEND, TYPE=name,L=real,ANGLE=real,K1=real,E1=real,E2=real,&
       TILT=real,K2=real,H1=real,K2=real,HGAP=real,FINT=real,&
       K3=real
```

For both types, the following first-order attributes are permitted:

`L` The length of the magnet (default: 0 m). For a rectangular magnet the length is measured along a straight line, while for a sector magnet it is the arc length of the reference orbit.

`ANGLE` The bend angle (default: 0 rad). A positive bend angle represents a bend to the right, i.e. towards negative x values.

`K1` The quadrupole coefficient $K_1 = (1/B\rho)(\partial B_y/\partial x)$. The default is 0 m^{-2}. A positive quadrupole strength implies horizontal focussing of positively charged particles.

`E1` The rotation angle for the entrance pole face (default: 0 rad).

`E2` The rotation angle for the exit pole face (default: 0 rad).

`FINT` The field integral, see [8] and below. The default value is 0.

Bending magnet definition

`TILT` The roll angle about the longitudinal axis (default: 0 rad, a positive bend angle then denotes a bend to the right). A vertical bend is defined by entering `TILT` with no value; this implies a roll of $\pi/2$ rad, i.e. a positive bend angle denotes a deflection down. A positive angle represents a clockwise rotation. The following second-order attributes are permitted:

`K2` The sextupole coefficient $K_2 = (1/B\rho)(\partial^2 B_y)/(\partial x^2)$ (default: 0 m^{-3}).

`H1` The curvature of the entrance pole face (default: 0 m^{-1}).

`H2` The curvature of the exit pole face (default: 0 m^{-1}). A positive pole face curvature induces a negative sextupole component; i.e. for positive `H1` and `H2` the centres of curvature of the pole faces are placed inside the magnet.

```
BR: RBEND,L=5.5,ANGLE=+0.001              ! Deflection to the right
BD: SBEND,L=5.5,ANGLE=+0.001,TILT         ! Deflection down
BL: SBEND,L=5.5,ANGLE=-0.001              ! Deflection to the left
BU: SBEND,L=5.5,ANGLE=-0.001,TILT         ! Deflection up
```

Quadrupoles

```
label: QUADRUPOLE,TYPE=name,L=real,K1=real,TILT=real
```

A `QUADRUPOLE` has three real attributes:

`L` The quadrupole length (default: 0 m).

`K1` The quadrupole coefficient $K_1 = (1/B\rho)(\partial B_y/\partial x)$. The default is 0 m^{-2}. A positive quadrupole strength implies horizontal focussing of positively charged particles.

`TILT` The roll angle about the longitudinal axis (default: 0 rad, i. e. a normal quadrupole). A skewed quadrupole is defined by entering `TILT` with no value; this implies a roll of $\pi/4$ rad about the s-axis. A positive angle represents a clockwise rotation.

Example:

```
QF: QUADRUPOLE,L=1.5,K1=0.001
```


Sextupoles

```
label: SEXTUPOLE,TYPE=name,L=real,K2=real,TILT=real
```

A `SEXTUPOLE` has three real attributes:

`L` The sextupole length (default: 0 m).

`K2` The sextupole coefficient $K_2 = (1/B\rho)(\partial^2 B_y/\partial x^2)$ (default: 0 m^{-3}).

`TILT` The roll angle about the longitudinal axis (default: 0 rad, i. e. a normal sextupole). A skewed sextupole is defined by entering `TILT` with no value; this implies a roll of $\pi/6$ rad about the s-axis. A positive angle represents a clockwise rotation.

Example:

```
S: SEXTUPOLE,L=0.4,K2=0.00134
```

Octupoles

```
label: OCTUPOLE,TYPE=name,L=real,K3=real,TILT=real
```

An OCTUPOLE has three real attributes:

L The octupole length (default: 0 m).

K3 The octupole coefficient $K_3 = (1/B\rho)(\partial^3 B_y/\partial x^3)$ (default: 0 m^{-4}).

TILT The roll angle about the longitudinal axis (default: 0 rad, i. e. a normal octupole). A skewed octupole is defined by entering TILT with no value; this implies a roll of $\pi/8$ rad about the s-axis. A positive angle represents a clockwise rotation.

Example:

```
O3: OCTUPOLE,L=0.3,K3=0.543
```


Beam lines

Name	Meaning	Section
LINE	Beam line definition	4.1
SEQUENCE	Beam line sequence	4.2
LIST	Replacement list definition	4.6

The simplest beam line consists of single elements:

```
label: LINE=(member{,member})
```

Example:

```
L:      LINE=(A,B,C,D,A,D)
        USE,L
```

The USE command tells MAD to perform all subsequent calculations on the sequence

A,B,C,D,A,D

Sub-lines lines

Instead of referring to an element, a beam line member can refer to another beam line defined in a separate command. This provides a shorthand notation for sub-lines which occur several times in a beam line. Lines and sub-lines can be entered in any order, but when a line is expanded, all its sub-lines must be known. Example:

```
L:      LINE=(A,B,S,B,A,S,A,B)
S:      LINE=(C,D,E)
        USE,L
```

This example produces the following expansion steps:

1. Replace sub-line S:

   `(A,B,(C,D,E),B,A,(C,D,E),A,B)`

2. Omit parentheses:

   `A,B,C,D,E,B,A,C,D,E,A,B`

Repetition and reflection

An unsigned repetition count and an asterisk indicate repetition of a beam line member. A minus prefix causes reflection, i.e. all elements in the subsequence are taken in reverse order. Sub-lines of reflected lines are also reflected, but physical elements are not. If both reflection and repetition are desired, the minus sign must precede the repetition count. Example:

```
R:      LINE=(G,H)
S:      LINE=(C,R,D)
T:      LINE=(2*S,2*(E,F),-S,-(A,B))
        USE,T
```

Proceeding step by step, this example produces

1. Replace sub-line S:

   `((C,R,D),(C,R,D),(E,F),(E,F),(D,-R,C),(B,A))`

2. Replace sub-line R:

   `((C,(G,H),D),(C,(G,H),D),(E,F),(E,F),(D,(H,G),C),(B,A))`

3. Omit parentheses:

   `C,G,H,D,C,G,H,D,E,F,E,F,D,H,G,C,B,A`

Note that the inner sub-line R is reflected together with the outer sub-line S.

Action commands

Name	Meaning	Section
USE	Select working beam line	5.1
COGUESS	Enter guess for initial closed orbit	5.2
BEAM	Beam data: particle energy and charge, emittances etc.	5.3
PRINT	Select print positions	5.4
SELECT	Select output positions	5.4
SURVEY	Print geometry of machine	5.6
TWISS	Print lattice functions	5.7
IBS	Intra-beam scattering	5.8
EMIT	Equilibrium emittances	5.9.1
EIGEN	Eigenvectors for normal modes	5.9.2
ENVELOPE	Beam envelopes in 3 degrees of freedom	5.9.2
TWISS3	Mais-Ripken lattice functions	5.9.2
DYNAMIC	Dynamic normal form analysis	5.10
STATIC	Static normal form analysis	5.10
SPLIT	Interpolate within element for OPTICS command	5.5
OPTICS	Output lattice functions and element strengths for control system	5.11
SECTORMAP	TRANSPORT map for sectors of the ring	5.13

USE statement

The USE statement specifies the beam line and its range to be used in subsequent commands. It must be entered before any physics computation is requested. It has the form

```
USE,PERIOD=line,RANGE=range,SYMM,SUPER=integer
```

The USE statement has four attributes:

PERIOD The beam line to be expanded (see Section 4.5). If omitted, the previous line is used without a new expansion.

RANGE The range of the beam line to be used. If PERIOD is given and RANGE is omitted, the range is the complete line. If PERIOD and RANGE are both omitted, the previous line and range are assumed. If RANGE is given, but PERIOD omitted, a new range is selected from the previous line.

SYMM A logical flag. If set, subsequent calculations are made as if the mirror image had been appended to the range.

SUPER An integer. Specifies the number of superperiods desired in the calculations. Quantities like tunes, chromaticities, and the like which refer to the machine circumference will be scaled with the value of SUPER (default: 1).

Example:

```
OCT: LINE=(...)              ! one octant of the machine
     USE,OCT,SYMM,SUPER=4
```

PRINT and SELECT statement

Each position in the beam line carries several associated selection flags. They are initially cleared by the USE command when the beam line is expanded. Output is selected by setting some of these flags by one of the commands

```
PRINT,RANGE=range,CLASS=name,PATTERN=string,FULL,CLEAR
SELECT,FLAG=name,RANGE=range,CLASS=name,PATTERN=string,FULL,CLEAR
```

```
USE,OCT                ! print at beginning and end only
PRINT,#35/37           ! print at positions number 35 to 37
SELECT,TWISS,FULL      ! set all print flags
PRINT,CLEAR            ! clear all print flags
PRINT,OCT              ! set all print flags
PRINT,CELL[3],CLEAR    ! clear all flags,
                       ! then set flags for all of third CELL
```


SPLIT statement

The OPTICS command writes one table line for each element selected by SELECT,OPTICS. The output line contains the element parameters and the lattice functions for the element centre or its exit. The command

```
SPLIT,NAME=name,FRACTION=real&
      [,RANGE=range][,CLASS=name][,PATTERN=string][,FULL][,CLEAR]
```

selects additional positions for output of the lattice functions only. The positions are given the name NAME, and element parameters in those positions are output as zero. The elements are selected as by SELECT, and FRACTION specifies a fraction of the length of the element where output is desired. Any number of points can be selected in the same element; output occurs in order of increasing s. Example:

```
SPLIT,NAME=B1,FRACTION=0.25,CLASS=B
SPLIT,NAME=B2,FRACTION=0.5,CLASS=B
SPLIT,NAME=B3,FRACTION=0.75,CLASS=B
```

Gives three lines for each B, at 1/4, 1/2, and 3/4 of its length respectively and assigns the names B1,B2,B3 to the three positions.

TWISS Statement

The simplest form of the TWISS command is

```
TWISS, DELTAP=real{,value},CHROM,COUPLE,&
       TAPE=file-name,SAVE=table-name
```

It computes the periodic solution for the specified beam line for all values of DELTAP entered (or for DELTAP = 0, if none is entered). Example:

```
USE,OCT,SYMM,SUPER=4
TWISS,DELTAP=0.001,CHROM,TAPE=OPTICS
```

This example computes the periodic solution for the linear lattice and chromatic functions for the beam line OCT, made symmetric and repeated in four superperiods. The DELTAP value used is 0.001. Apart from saving computing time, it is equivalent to the command sequence

```
RING: LINE=(4*(OCT,-OCT))
      USE,RING
```

As from Version 8.19 of MAD the following variables are accessible after calling TWISS:

```
QX, QY, QX', QY',
ALFX, ALFY, BETX, BETY,
X0, PX0, Y0, PY0, T0, PT0.
```

The first five are global variable denoting horizontal and vertical tunes, horizontal and vertical chromaticities respectively, while the local Twiss parameters and closed orbit coordinates refer to the beginning of the beam line being USEd.

TWISS Output

When DATAVRSN=TWISS, the third to fifth lines of the position records have the format

```
(5E16.9/5E16.9/5E16.9)
```

and contain the quantities

```
ALFX    BETX    MUX    DX    DPX
ALFY    BETY    MUY    DY    DPY
X       PX      Y      PY    SUML
```

in this order. The trailer record has three lines in the format

```
(3E16.9/5E16.9/5E16.9)
```

and contains

```
DELTAP  GAMTR   C
COSMUX  QX      QX'    BXMAX    DXMAX
COSMUY  QY      QY'    BYMAX    DYMAX
```

in this order. If the COUPLE option was given, the output has the same format, but the quantities given refer to the two possible modes (1,2) instead of referring to the two planes (x, y).

OPTICS Statement

Control system applications often require tables with arbitrary selections of element data and/or lattice functions. Such tables can be generated by the command

```
OPTICS, BETX=real,ALFX=real,MUX=real,&
        BETY=real,ALFY=real,MUY=real,&
        DX=real,DPX=real,DY=real,DPY=real,&
        X=real,PX=real,Y=real,PY=real,T=real,PT=real&
        WX=real,PHIX=real,DMUX=real,&
        WY=real,PHIY=real,DMUY=real,&
        DDX=real,DDY=real,DDPX=real,DDPY=real,&
        LINE=beam-line,BETA0=name,CENTRE,&
        FILENAME=file-name,DELTAP=real:real:real,&
        COLUMNS=name{,name}
```

CENTRE Normally output occurs at the exit of each selected element. If the CENTRE flag is on, output occurs at the centre of each selected element;

FILENAME The output is written on the file file-name (default: optics). Note that the resulting table is written on this file and erased from the computer's memory. In order to plot it, it must be read back by an RETRIEVE command.

COLUMNS Up to 50 table columns may be selected by name for output. All optical and chromatic functions listed in Sections 1.5.1, 1.5.3, and 1.5.4 are accepted. Further possibilities are:

OPTICS Output

```
@ GAMTR          %f     64.3336
@ ALFA           %f    0.241615E-03
@ XIY            %f    -.455678
@ XIX            %f     2.05279
@ QY             %f    0.250049
@ QX             %f    0.249961
@ CIRCUM         %f     79.0000
@ DELTA          %f    0.000000E+00
@ COMMENT        %20s "DATA FOR TEST CELL"
@ ORIGIN         %24s "MAD 8.01     IBM - VM/CMS"
@ DATE           %08s "19/06/89"
@ TIME           %08s "09.47.40"
* NAME           S              BETX           BETY
$ %16s           %f             %f             %f
  B1               36.6600        24.8427        126.380
  SF1              37.6200        23.8830        130.925
  QF1              39.5000        23.6209        132.268
  B2               75.8000        124.709        25.2153
  SD1              77.1200        130.933        23.8718
  QD1              79.0000        132.277        23.6098
```

File Handling

Name	Meaning	Section
ASSIGN	Assign standard streams to files	7.2
SAVE	Save machine structure in MAD format	7.3
CALL	Read alternate input file	7.3
RETURN	Return to calling file	7.3
EXCITE	Read element excitations	7.4
INCREMENT	Increment element excitations	7.4
ARCHIVE	Archive an internal table	7.5
RETRIEVE	Retrieve an internal table	7.5
PACKMEMORY	Garbage removal	7.6
STATUS	Show status of files	7.7
POOLDUMP	Dump data pool to disk	7.8
POOLLOAD	Reload data pool from disk	7.8

SAVE and CALL commands

The SAVE command

```
SAVE, FILENAME=string, PATTERN=string
```

causes all beam element, beam line, and parameter definitions to be written on the named file. The output format is similar to the normal input format. The file may be read again in the same run. The attributes are

FILENAME The name of the file to be written (default: save).

The CALL command

```
CALL, FILENAME=string
```

serves to read an alternate input file. Input continues on that file until a RETURN statement or end of file is encountered. The attribute is

FILENAME The name of the file to be read (default: save).

Example:

```
CALL, FILENAME=STRUCT
```

PLOT command

The SETPLOT command allows to specify parameters common to all subsequent plots:

```
SETPLOT, FONT=integer,LWIDTH=real,XSIZE=real,YSIZE=real,&
         ASCALE=real,LSCALE=real,SSCALE=real,TSCALE=real,POST=integer
```

The PLOT command produces one or several frames (pictures) at a time:

```
PLOT,VAXIS=name,VAXIS1=name,VAXIS2=name,VAXIS3=name,VAXIS4=name,&
     HAXIS=name,BARS=integer,STYLE=integer,SYMBOL=integer,&
     MAXPLOT=integer,SORT=logical,SPLINE=logical,MULTIPLE=logical,&
     FFT=logical,HMIN=real,HMAX=real,VMIN=real,VMAX=real,&
     TABLE=name,TITLE=string,PARAM=name,RANGE=range,DELTAP=real,&
     PARTICLE=integer,TURNS=integer
```


Matching modules

Name	Function	Section
CELL	Initialise cell matching	12.1
MATCH	Initialise insertion matching	12.1
WEIGHT	Set matching weights	12.2
CONSTRAINT	Impose matching constraint	12.3
COUPLE	Impose periodicity between two points	12.3
GLOBAL	Constraint on global quantities	12.4
GWEIGHT	Weights for Global Constraints	12.4
VARY	Vary parameter	12.2
FIX	Fix parameter value	12.2
RMATRIX	Constraint on linear matrix	12.3
TMATRIX	Constraint on second-order terms	12.3
LEVEL	Set print level	12.5
LMDIF	Minimisation by gradient method	12.6
MIGRAD	Minimisation by gradient method	12.6
SIMPLEX	Minimisation by simplex method	12.6
ENDMATCH	Leave matching mode	12.1

Matching a periodic cell

In the first mode, called cell matching, a periodic cell is adjusted. The periodicity is enforced exactly, and constraints are fulfilled in the least squares sense. Cell matching mode is initiated by the CELL command:

```
CELL,DELTAP=real,ORBIT
```

It has two attributes:

DELTAP The value of the momentum error $\Delta p/p_0c$ for which the match should be performed (default: 0).

ORBIT If this flag is true, the closed orbit is also matched.

Examples:

```
! Match a simple periodic cell
USE,PERIOD=OCTANT,RANGE=CELL1
CELL,ORBIT
!
! Match a symmetric and periodic cell with repetitions
USE,HALFCELL,SYMM,SUPER=5
CELL
```


Matching an insertion

In the second mode, called insertion matching, a beam line is matched with given initial values for the optical functions. Constraints may be imposed in other places, i.e. intermediate or end values can be requested. In this case the initial values are assumed as exact, and constraints are fulfilled in the least squares sense. The insertion matching mode is initiated by the MATCH command. In the simplest form the initial values for the optical functions are taken from the periodic solution of another beam line. In this case, all of $(\beta_x, \beta_y, \alpha_x, \alpha_y, D_x, D_y, D_{p_x}, D_{p_y})$ are transmitted to be used as initial values. If there is a constraint on the orbit, the values (x, p_x, y, p_y) of the orbit are also transmitted. Such a condition is entered in the form

```
MATCH,LINE=beam-line,MUX=real,MUY=real,DELTAP=real,ORBIT
```

The initial phases angles may be specified by:

MUX The initial horizontal phase μ_x,

MUY The initial vertical phase μ_y.

DELTAP The value of the momentum error $\Delta E/p_0c$ for which the match should be performed (default: 0).

ORBIT If this flag is true, the closed orbit is also matched.

Matching insertion example

```
CELL1:  LINE=(...)
INSERT: LINE=(...)
        USE,INSERT
        MATCH,LINE=CELL1,MUX=9.345,MUY=9.876,ORBIT
```

This matches the beam line INSERT. Initial conditions are given by the periodic solution for the beam line CELL1.

It is also possible to enter numerical initial values. The MATCH command then has the form

```
MATCH, BETX=real,ALFX=real,MUX=real,&
       BETY=real,ALFY=real,MUY=real,&
       X=real,PX=real,Y=real,PY=real,&
       DX=real,DY=real,DPX=real,DPY=real,&
       DELTAP=real,ORBIT
```

The ENDMATCH command terminates the matching section and deletes all tables related to a tracking run:

```
ENDMATCH
```


Variable parameters

A parameter to be varied is specified by the VARY command:

```
VARY,NAME=variable,STEP=real,LOWER=real,UPPER=real
```

It has four attributes:

NAME The name of the parameter or attribute to be varied (see Section 2.4.10),

STEP The approximate initial step size for varying the parameter. If the step is not entered, MAD tries to find a reasonable step, but this may not always work.

LOWER Lower limit for the parameter (optional),

UPPER Upper limit for the parameter (optional).

Examples:

```
VARY,PAR1,STEP=1.0E-4       ! vary global parameter PAR1
VARY,QL11[K1],STEP=1.0E-6   ! vary attribute K1 of the QL11
VARY,Q15[K1],STEP=0.0001,LOWER=0.0,UPPER=0.08 ! vary with limits
```

Constraints

Simple constraints are imposed by the CONSTRAINT command. It can take three forms. The first form is

```
CONSTRAINT,[RANGE=range,][CLASS=name,][PATTERN=string,]&
           LINE=beam-line,MUX=real,MUY=real
```

The second form of the CONSTRAINT command is

```
CONSTRAINT,[RANGE=range,][CLASS=name,][PATTERN=string,]&
           BETA0=beta0-name,MUX=real,MUY=real
```

The third form

```
CONSTRAINT,[RANGE=range,][CLASS=name,][PATTERN=string,]&
           BETX=real,ALFX=real,MUX=real,&
           BETY=real,ALFY=real,MUY=real,&
           X=real,PX=real,Y=real,PY=real,T=real,PT=real,&
           DX=real,DPX=real,DY=real,DPX=real
```

allows one to enter numerical values for any optical function(s) in place.

Weights

```
WEIGHT, BETX=real,ALFX=real,MUX=real,&
        BETY=real,ALFY=real,MUY=real,&
        X=real,PX=real,Y=real,PY=real,T=real,PT=real,&
        DX=real,DPX=real,DY=real,DPY=real
```

Default Matching Weights

name	weight	name	weight	name	weight	name	weight
BETX	1.0	ALFX	10.0	MUX	10.0		
BETY	1.0	ALFY	10.0	MUY	10.0		
X	10.0	PX	100.0	Y	10.0	PY	100.0
T	0.0	PT	0.0				
DX	10.0	DPX	100.0	DY	10.0	DPY	100.0

LMDIF Matching method

The `LMDIF` command minimises the sum of squares of the constraint functions using their numerical derivatives:

```
LMDIF,CALLS=integer,TOLERANCE=real
```

It is the fastest minimisation method available in MAD. The command has two attributes:

`CALLS` The maximum number of calls to the penalty function (default: 1000).

`TOLERANCE` The desired tolerance for the minimum (default: 10^{-6}).

Example:

```
LMDIF,CALLS=2000,TOLERANCE=1.0E-8
```


MIGRAD Matching methods

The `MIGRAD` command minimises the penalty function using its numerical derivatives of the sum of squares:

```
MIGRAD,CALLS=integer,TOLERANCE=real,STRATEGY=1
```

The command has three attributes:

`CALLS` The maximum number of calls to the penalty function (default: 1000).

`TOLERANCE` The desired tolerance for the minimum (default: 10^{-6}).

`STRATEGY` A code for the strategy to be used (default: 1). The user is referred to the MINUIT manual for explanations [23].

Example:

```
MIGRAD,CALLS=2000,TOLERANCE=1.0E-8
```

SIMPLEX Matching methods

The `SIMPLEX` command minimises the penalty function by the simplex method:

`SIMPLEX,CALLS=integer,TOLERANCE=real`

Details are given in the description of the MINUIT program [23]. The command has two attributes:

`CALLS` The maximum number of calls to the penalty function (default: 1000).

`TOLERANCE` The desired tolerance for the minimum (default: 10^{-6}).

Example:

`SIMPLEX,CALLS=2000,TOLERANCE=1.0E-8`